VLÁKNA a TEXTIL

2

Volume 25.
June
2018

FIBRES AND TEXTILES

STU FCHPT

TECHNICAL UNIVERSITY OF LIBEREC
Faculty of Textile Engineering

Trenčianska univerzita Alexandra Dubčeka v Trenčíne
Fakulta priemyselných technológií v Púchove

VÚCHV

VÚTCH CHEMITEX

Spoločnosť priemyselnej chémie ZSVTS

CHEMOSVIT FIBROCHEM

Indexed in:
SCOPUS
Chemical Abstracts
World Textiles

ISSN 1335-0617
print version

ISSN 2585-8890
online version

Fibres and Textiles
Vlákna a textil

Published by	*Vydáva*
• Slovak University of Technology in Bratislava, Faculty of Chemical and Food Technology	• Slovenská technická univerzita v Bratislave, Fakulta chemickej a potravinárskej technológie
• Technical University of Liberec, Faculty of Textile Engineering	• Technická univerzita v Liberci, Fakulta textilní
• Alexander Dubček University of Trenčín, Faculty of Industrial Technologies	• Trenčianska univerzita Alexandra Dubčeka v Trenčíne, Fakulta priemyselných technológií
• Slovak Society of Industrial Chemistry, Bratislava	• Slovenská spoločnosť priemyselnej chémie, Bratislava
• Research Institute of Man-Made Fibres, JSC, Svit	• Výskumný ústav chemických vlákien, a.s. Svit
• VÚTCH – CHEMITEX, Ltd., Žilina	• VÚTCH – CHEMITEX, spol. s r.o., Žilina
• Chemosvit Fibrochem, JSC, Svit	• Chemosvit Fibrochem, a.s., Svit

Editorial office and distribution of the journal
(Redakcia a distribúcia časopisu)

Ústav prírodných a syntetických polymérov
Fakulta chemickej a potravinárskej technológie
Slovenská technická univerzita v Bratislave
Radlinského 9, 812 37 Bratislava, SK
Tel: 00 421 2 59 325 575
e-mail: marcela.hricova@stuba.sk

Order and advertisement of the journal
(Objednávka a inzercia časopisu)

Slovenská spoločnosť priemyselnej chémie,
člen Zväzu vedecko-technických spoločností
Radlinského 9, 812 37 Bratislava, SK
Tel: 00 421 2 59 325 575
e-mail: marcela.hricova@stuba.sk

Order of the journal from abroad – excepting Czech Republic
Objednávka časopisu zo zahraničia – okrem Českej Republiky

SLOVART G.T.G, s.r.o. EXPORT-IMPORT
Krupinská 4, P.O.Box 152, 852 99 Bratislava, SK
Tel: 00421 2 839 471-3, Fax: 00421 2 839 485
e-mail: info@slovart-gtg.sk

Typeset and printing *(Sadzba a tlač)*

FOART, s.r.o., Bratislava

Journal is published 4x per year
Subscription 60 EUR

Časopis vychádza 4x ročne
Ročné predplatné 60 EUR

Evidenčné číslo MKCR SR Bratislava EV 4006/10

Fibres and Textiles (2) 2018
Vlákna a textil (2) 2018
June 2018

Content

LIQUID MOISTURE TRANSPORT PERFORMANCE OF TEXTILES

Svitlana Arabuli[1], Viktoriia Vlasenko[1] and Lenka Martinkova[2]

[1]Kyiv National University of Technologies & Design, N.-Danchenko srt. 2, 01011 Kyiv, Ukraine
[2]INOTEX Ltd, Dvur Kralove, Czech Republic
arabuli.si@knutd.edu.ua

Abstract: *The main purpose of this study is the data base creation of different textiles moisture management performance for design multilayer textile composites with predicted liquid moisture transport properties. In this paper are the results of studies the influence of fabrics structure and its raw composition on the liquid moisture transport performance of textiles. Moisture management property of the textiles was examined using MMT instrument.*

Keywords: *textiles, multilayer textiles, liquid moisture transfer.*

1 INTRODUCTION

The multilayer textile composites can be obtained by bonding the individual textiles in one multilayer structure. Such composites consist of textiles with various functional properties of different structure and different fibrous composition [1].

The main purpose of this study was the data base of moisture management performance of the modern technical textiles creation. These textiles can be used for design of multilayer textile composite with predicted liquid moisture transport properties, for example, quick absorbing of moisture and quick transport, distribution; reliable accumulating in textile composite volume. At the same time these liquids do not have to penetrate in external environment. Some test methods are known to measure liquid water absorbency and water vapor transport in textiles. These methods characterize by different aspects of moisture management characteristics, namely: diffusion ability, wicking, water vapor permeability, drying time etc. However, these methods are unable to characterize the behavior of dynamic liquid transfer in to textiles [2, 3].

In this work the liquid moisture transport properties were characterized by using the Moisture Management Tester (MMT). The method allows to measure quantitatively liquid moisture transfer in one step in a fabric in multidirections, where liquid moisture spreads on both surfaces of the fabric and transfers from one surface to the opposite. The essence of this method is described in detail in works [4, 5].

2 EXPERIMENTAL

2.1 Materials

In previous investigations, we have studied 31 textiles using more than 35 indicators, with the help of which we can evaluate the ability of textile materials to interact with moisture, heat, vapor, etc [6]. According to these results we chose 6 textiles with different structures, compositions and physical properties (Table 1, Figure 1). Before investigation, the samples were put into the condition room with controlled temperature (T) 21±1°C and relative humidity (RH) 65±2% (refer to ASTM D1776) for at least 24 hours.

2.2 Methods

Structural characteristics of textiles were determined by standard methods in accordance with ISO 3932–76, ISO 3933–76, ISO 3801–77.

Hygroscopic and water-repellent properties of textiles were determined by methods in accordance with Ukrainian standard DSTU GOST 3816 2009 (ISO 811 81).

Moisture Management Tester (SDL Atlas) was chosen as testing equipment for textile dynamic wicking process visualizations. This method allows to quantitatively measuring liquid moisture transfer in one step in a textile in multidirections, where liquid moisture spreads on both surfaces of the textile and transfers from one surface to the opposite. Ten moisture management indexes are using to characterize the moisture management properties of textile [4, 5].

Table 1 Basic structural parameters and physical performance of textiles

Properties		Sample code					
		S	***Pq***	***E***	***A***	***L***	***BA***
Type of textile		knitted fabric			two-layer knitted fabric	woven fabric	
Pattern		tuck	tuck	plain	double	twill 3/3	twill 2/3
Linear density [tex]	warp	12.0	19.1	35.2	Cotton 12.6	12.4	20,4
	weft				PP 14.8	17.2	13.3
Density of weave (knitting)	warp	230	245	315	132	800	650
	weft	135	120	230	90	340	430
Fiber type [%]		PP-100	Cotton-100	Viscose-100	PP-40/Cotton-60	PES-100	PES-100
Surface density [g/m^2]		95	207	330	183	160	180
Thickness [mm]		0.7	0.8	0.8	1.6	0.3	0.3
Hygroscopicity *H* [%]		1.1	14.5	15.5	8.9	1.5	1.4
Water absorption *Wa* [g/m^2]		270	315	650	1060	185	0
Vertical capillarity *C* [mm]		158/136	177/175	143/139	23/148 // 22/131	197/177	0/0
Water resistance W_R [Pa]		–	–	–	–	–	4310

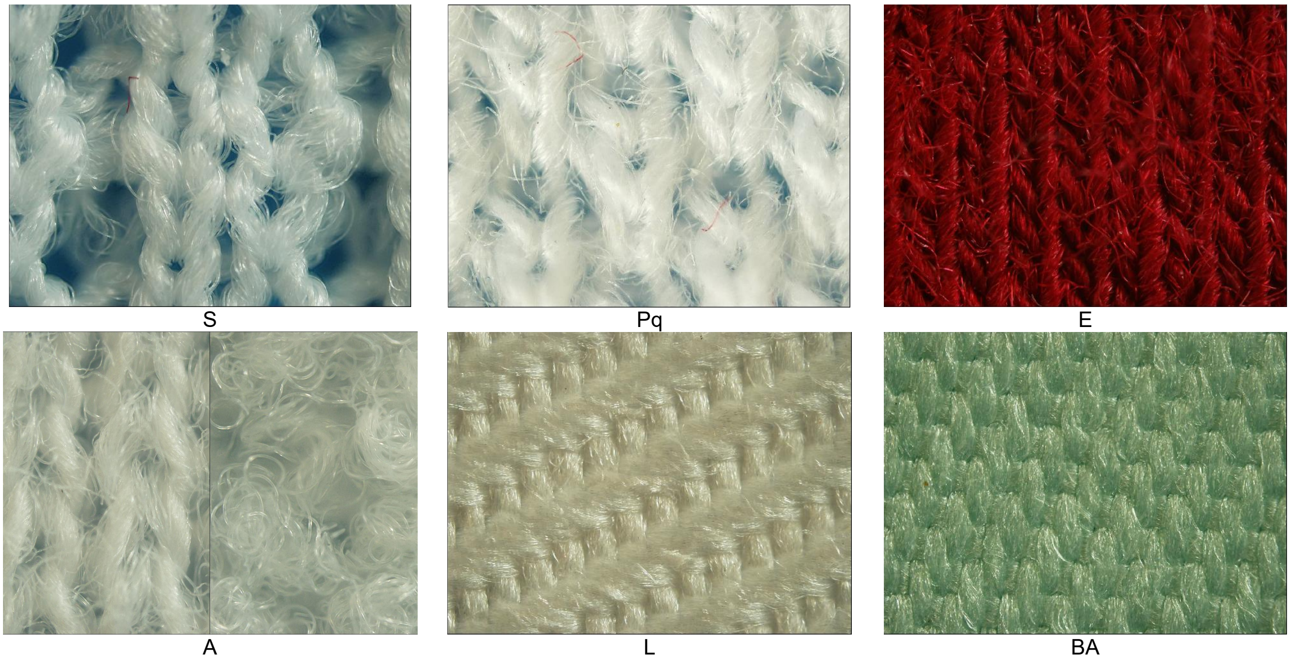

Figure 1 The structure of textiles (Scale x 50)

3 RESULTS AND DISCUSSION

The liquid moisture transport performance of textiles and water content curves for the top (UT) and bottom (UB) surfaces of the individual textiles are shown in Figure 2 and Table 2.

Sample "BA" has a water repellent finishing so water did not spread out over the top surface and did not penetrate through the fabric

Table 2 Liquid moisture transport performance of textiles

Properties		Fabrics sample code										
		S		***Pq***		***E***		***A***		***L***		***BA***
		mean	***S.D.****	***mean***	***S.D.****	***mean***	***S.D.****	***mean***	***S.D.****	***mean***	***S.D.****	***mean***
Wetting Time [sec]	T**	5.2	0.9	22.7	5.4	9.1	1.1	3.4	0.4	6.6	0.8	-
	B**	5.2	0.8	11.6	1.7	9.3	1.0	119.9	0.0	6.8	0.8	-
Absorption Rate [%/sec]	T**	59.7	0.8	26.3	2.3	57.6	5.2	43.9	1.1	60.2	0.9	-
	B**	64.8	1.5	44.6	2.4	64.7	5.3	0.0	0.0	72.9	5.3	-
Max Wetted Radius [mm]	T**	21.7	2.9	13.3	2.8	13.3	2.0	25. 0	0.0	25.0	0.0	-
	B**	21.7	2.9	15.0	0.0	13.3	2.0	0.0	0.0	28.3	2.9	-
Spreading Speed [mm/sec]	T**	3.2	0.7	0.6	0.1	1.3	0.1	4.2	0.2	4.3	0.3	-
	B**	3.3	0.7	0.8	0.1	1.3	0.0	0.0	0.0	4.4	0.3	-
One-Way Transport Capability [%]		55	9	257	22	78	4	-649	26	108	6	-
Overall Moisture Management Capability		0.46	0.05	0.44	0.09	0.32	0.01	0.00	0.00	0.56	0.05	-

** T- top; B – Bottom; * S.D. – S. Deviation

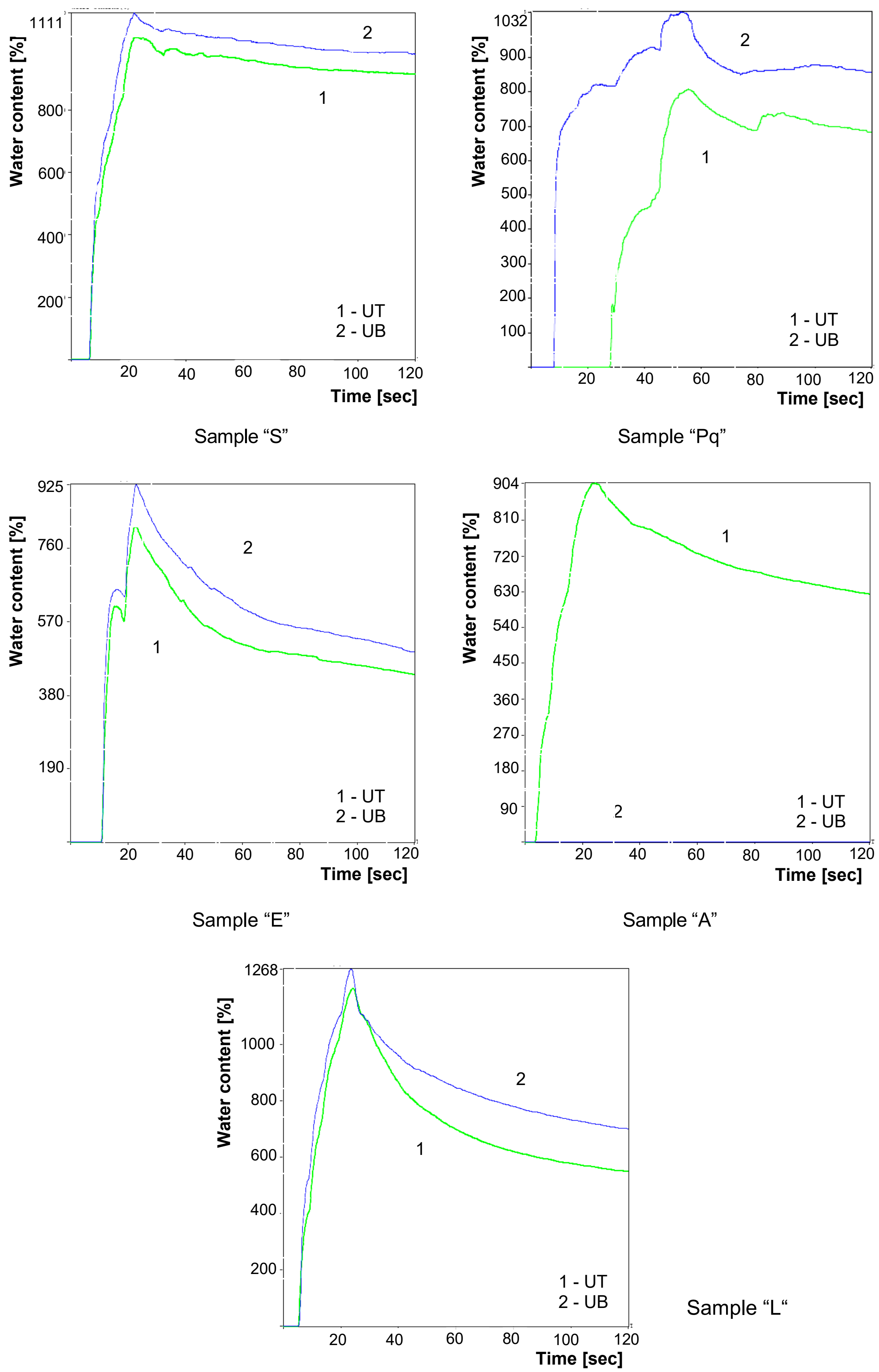

Figure 2 MMT water content curves of the textiles
1 – UT – water content curves of the top surfaces of the textiles
2 – UB – water content curves of the bottom surfaces of the textiles

For sample "S" and sample "L", the water content of the top and bottom surfaces increase very quickly during the pumping time (starting at around 6 seconds). Then the water content on top and bottom surfaces for sample "S" remained almost stable with little change after reaching a maximum, while those of sample "L" decreased gradually until the end of the test. For sample "A", the relative water content on top layer increased abruptly from 0 to more than 900, but on bottom surface remained zero. For sample "E" the trend of the water contents of the top and bottom surfaces was the same.

Figure 3 shows the top surface absorption rate (TAR) and bottom absorption rate (BAR) of each textile. TAR and BAR are the maximum moisture absorption rates of the top and bottom surfaces of the fabric respectively. Samples "S", "E", "L" had the same mean BAR and TAR, indicating that the liquid evenly distributed on the top and bottom surface of these textiles. The sample "A" had the zero BAR and the highest means TAR, indicating that all liquid was distributed only on the fabric top surface.

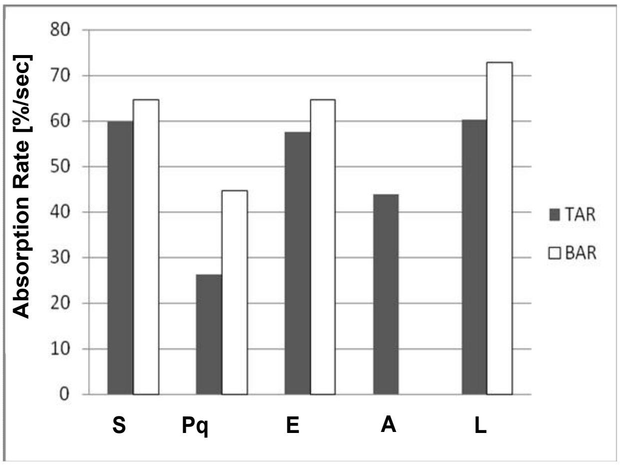

Figure 3 The TAR and BAR of the investigated textiles

Figure 4 shows the top surface maximum wetted radius (TMWR) and bottom surface maximum wetted radius (BMWR) of the textiles. TMWR and BMWR are defined as the maximum wetted ring radius at the top and bottom surfaces respectively. It can be seen that samples "Pq" and "E" had the smallest top and bottom surface wetted radius. For sample "L" and "S" the TMWR and BMWR are nearly the same as are the top and bottom surface water contents. However, for sample "L" the TMWR and BMWR were higher than that of the other samples of textile. In case of the sample "A" the top water content was higher than that of the bottom surface (BMWR = 0 mm). It indicates that liquid was distributed only in the top layer of the textile. Sample "BA" has a water repellent finishing so water did not spread out over the top surface and did not penetrated through the fabric.

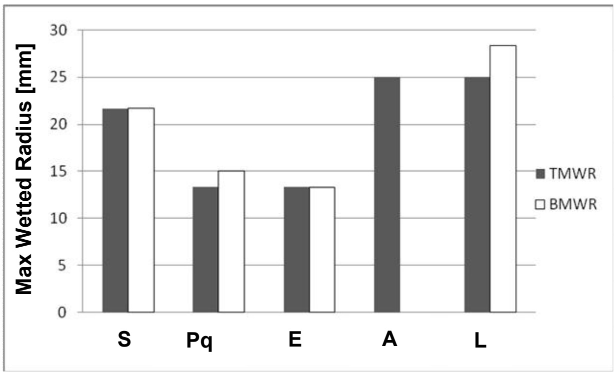

Figure 4 Maximum wetted radius of the top surfaces and maximum wetted radius of bottom surfaces of the fabrics

Figure 5 illustrates the top surface spreading speed (TSS) and the bottom surface spreading speed (BSS). These dates indicate the spreading speeds of the liquid on top and bottom textile surfaces to reach the maximum wetted radius. As one can see from these figures, sample "Pq" had the smallest TSS and BSS among all the textiles. It indicates that the liquid moisture was assembled only on the top surface of the fabric and was not absorbed by the fabric. Sample "A" had only TSS. It indicates faster spread on the top surface of the textile.

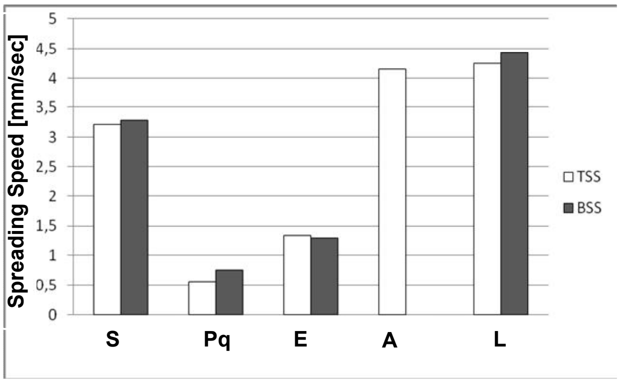

Figure 5 The spreading speed at the top surface (TSS) and the bottom surface (BSS) of the textiles

4 CONCLUSION

As a result of our investigation is creation of data base of moisture management performance of the textiles.

Based on received values of indexes, the investigated textiles are classified into categories:

- water proof fabric – sample "BA";
- slow absorbing and slow drying fabric – sample "A";
- fast absorbing and slow drying fabric – sample "E";
- fast absorbing and quick drying fabric – samples "S", "Pq", "L".

Presented classification gives the opportunity to design multilayer textile composites with predicted and requested liquid moisture transport properties. The requirements to textile composite dictate the order of initial textiles arrangement in multilayer structure. For example, for medical textile with higher liquid absorption and higher liquid resistance performances the order of initial textiles arrangement in multilayer structure is as follows: the first layer have to provide quick absorption and quick transport of water; the next layers must have to provide good liquid distribution ability through layer surface and liquid accumulation and the last one have to serve as good barrier against liquid penetration.

5 REFERENCES

1. Bereznenko N., Kovtun S., Vlasenko V., Bereznenko S.: Composite textile material, Patent 19569 Ukraine, A41D31/00./Ukraine - №200607621; 15.12.06, № 12 – p.4
2. Heinisch T., Těšinová P., Pološčuková L.: Moisture management for different air conditions, Vlakna a Textil (Fibres and Textiles) 24(3), 2017, pp. 64-67, ISSN 1335-0617 (print); 2585-8890 (online version)
3. Achour N.S., Hamdaoui M., Nasrallah S.B.: Sorption ability & wicking on knitted fabrics: Experimental and theoretical studies, Vlakna a Textil (Fibres and Textiles) 24(2), 2017, pp. 25-31, ISSN 1335-0617 (print); 2585-8890 (online version)
4. Hu J., Li Y., Yeung K.W., Wong A.S.W., Xu W.: Moisture management tester: A method to characterize fabric liquid moisture management properties, Textile Research Journal 75(1), 2005, pp. 57-62, doi: 10.1177/004051750507500111
5. Tesinova P., Doncheva S.M., Petrova D.P., Angelova Y., Ryplova P.: Moisture management of the first layer sports material knitted structures, Vlakna a Textil (Fibres and Textiles) 22(1), 2015, pp. 53-56, ISSN 1335-0617 (print); 2585-8890 (online version)
6. Vlasenko V., Kovtun S., Bereznenko N., Suprun N., Murarova A.: Water and heat transfer through multilayer textile composites, Vlakna a Textil (Fibres and Textiles) 13(1-2), 2006, pp. 29-32, ISSN 1335-0617 (print); 2585-8890 (online version)

EVALUATION OF SELECTED DEVELOPMENTAL SAMPLES OF CHELATING AGENTS ON MODEL WASHING

Petra Bayerová, Veronika Hrubešová, Ladislav Burgert, Michal Černý and Radim Hrdina

Faculty of Chemical Technology, University of Pardubice, Czech Republic
petra.bayerova@upce.cz

***Abstract**: This work presents the results of model washing with addition of selected developmental samples of chelating agents. The washing was realized in hard water of 22°dH (given in German degrees of hardness). After 20x repeated washing the content of ash and Ca^{2+} ion were determined. The image of fabric after the model washing was evaluated by means of images from a scanning electron microscope.*

***Key words**: chelating agents, washing of textile materials, model washing.*

1 INTRODUCTION

Water has an irreplaceable role in textile industry. Any textile production is dependent on water and sufficiency of good quality water. Hard water is not useful for various domestic purposes (washing, bathing, drinking) and for many industries such as textile industry and dyeing industry. Dissolved salts like Ca, Mg, Fe and Mn affect many textile processes. Hard water causes the usual problem of deposition of insoluble salts which interfere with the proper dyeing and printing of the fabrics, textile finishing or pre-treatment of textile materials.

Washing is one of the most important activities in the treatment and maintenance of textiles. Detergent is a part of the washing bath. It is a complex mixture containing various systems – surfactants, builders and auxiliary agents. Chelating agents are the most frequent agents used as components of detergents. Chelating agents (sequestering agents, chelating surfactants) are generally compounds creating chelates, which are specific kinds of complex compounds surrounding a cation (such as Ca^{2+}, Mg^{2+}, Fe^{3+}, Cu^{2+}, Mn^{2+}). These substances are used for water softening [1].

Basic indicator of detergent quality is so-called washing efficiency. It can be divided into primary and secondary washing efficiency. Primary efficiency indicates the difference between the amount of soil before and after washing. Secondary efficiency describes how the amount of sediment builds up on washed fabric. Sinking takes place slowly and at least 10 scouring runs are used to determine incrustations [2].

New types of sequestering agents and chelating surfactants were synthetized at the Institute of Chemistry and Technology of Macromolecular Materials of University of Pardubice, Department of Synthetic Polymers, Fibers and Textile Chemistry. These substances were tested in repeated model washing in hard water. Secondary efficacy was determined.

2 EXPERIMENTAL

2.1 Samples of chelating agents

Three types of sequestering agents (sample 1, 2, 3) and two types of chelating surfactants (sample 4, 5) were tested in this study – see Table 1.

Table 1 Structures of chelating agents

Sample	Chemical structure
No. 1	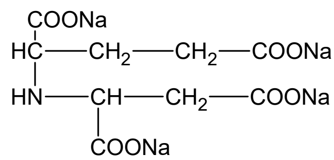 *N*-(1,2-dicarboxyethyl) glutamic acid tetrasodium salt
No. 2	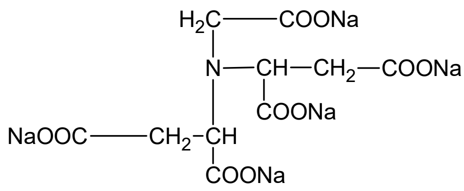 *N*-carboxymethyl-*N*-(1,2-dicarboxyethyl) aspartic acid pentasodium salt
No. 3	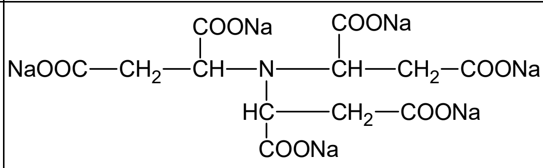 *N,N'*-bis(1,2-dicarboxyethyl) aspartic acid hexasodium salt

No. 4	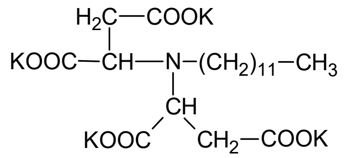 *N*-dodecyl-*N*-(1,2-dicarboxyethyl) aspartic acid tetrapotassium salt
No. 5	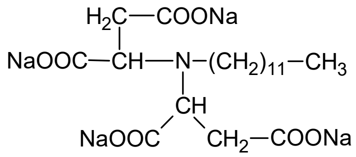 *N*-dodecyl-*N*-(1,2-dicarboxyethyl) aspartic acid tetrasodium salt

2.2 Model washing process

Prepared agents were determined under conditions for model washing. The washed material was a batch of 20 grams of cotton textile at a bath ratio of 1:20. The model detergent chosen consisted of water glass (soln. of sodium metasilicate), carboxy-methylcellulose, sodium carbonate, and sodium sulfate and analyzed chelating agent [3]. Washing bath contents 7 g/l of model detergent.

The washing was repeated 20x in hard water of 22°dH (given in German degrees of hardness) for 30 min at 90°C (Figure1). The hard water was prepared by dissolving $CaCl_2.6\ H_2O$ in distilled water (1°dH = 39.06 mg $CaCl_2.6\ H_2O$).

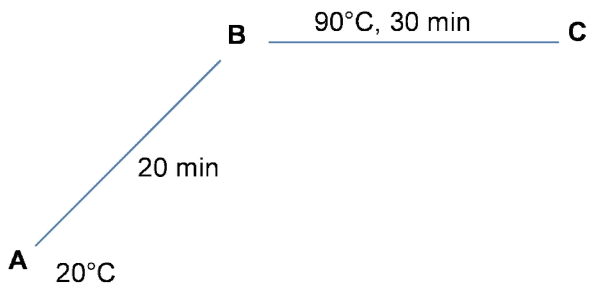

Figure 1 Process of model washing

2.3 The evaluation of content of ash and Ca^{2+} ions

The image of fabric after the model washing was evaluated by means of images from a scanning electron microscope (JEOL JSM – 5500LV).

After 20x repeated washing in hard water of 22°dH for 30 min at 90°C, the content of ash and Ca^{2+} ion were determined. After 20x repeated washing, the textile was incinerated in a platinum crucible and the amount of calcium was evaluated in ash. The content of calcium was determined by optical emission spectrometry with inductively coupled plasma (Integra XL2-GBC Australia).

3 RESULTS AND DISCUSSION

The prepared samples were tested at model washing conditions. The washing with model detergent without sequestering ingredients increased the content of inorganic deposits in cotton textile. The content of ash and calcium in textile was relatively high: 3.18% ash and 15.20 g/kg Ca^{2+}. The addition of prepared samples with chelating effect improved the result as documented by the data in Table 2.

A reduction of the content of ash and calcium mainly by typical sequestering agents (sample no. 1, sample no. 3) was observed. The lowest content of Ca^{2+} was shown in sample no. 3 *N*,*N*'-bis(1,2-dicarboxyethyl) aspartic acid hexasodium salt - see Figure 6. A surprising result is the high content of ash and calcium in textile with using sample no. 2. Sequestration efficiency can be affected by overall chemical structure of molecule.

With the addition of chelating surfactants (samples no. 4 and 5) the content of ash and calcium is lower than without prepared samples, too. The measured values are higher than for sequestering agents, whereas chelating surfactants have a lower value of sequestering capacity.

The image of fabric after the model washing was evaluated by means of images from a scanning electron microscope (Figures 2-8).

Table 2 Content of ash and calcium ion in the cotton textile after twenty times repeated washing in hard water of 22°dH

Sample	Ash content [mass %]	Content of Ca^{2+} [g/kg]
no. 1 + model detergent	0.45	1.97
no. 2 + model detergent	1.99	11.40
no. 3 + model detergent	0.11	0.50
no. 4 + model detergent	2.68	11.10
no. 5 + model detergent	2.18	10.90
Washing without sequestering agents in hard water	3.18	15.20
Washing without sequestering agents in distilled water	0.10	0.36
Original cotton textile	0.10	0.23

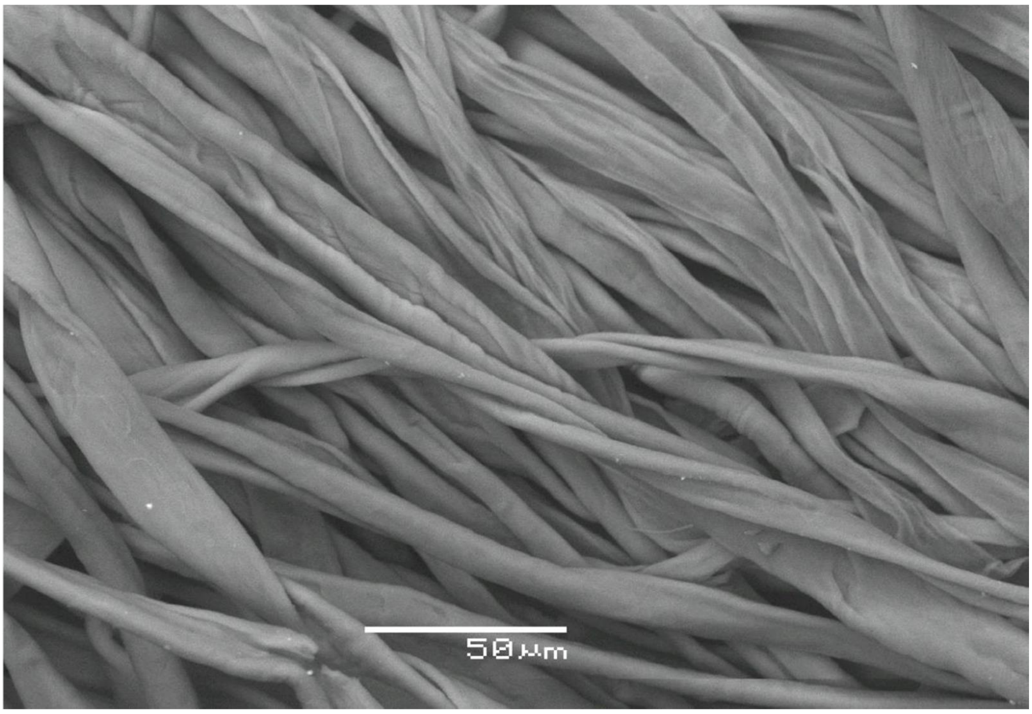

Figure 2 EMS of fiber surface of the original cotton textile

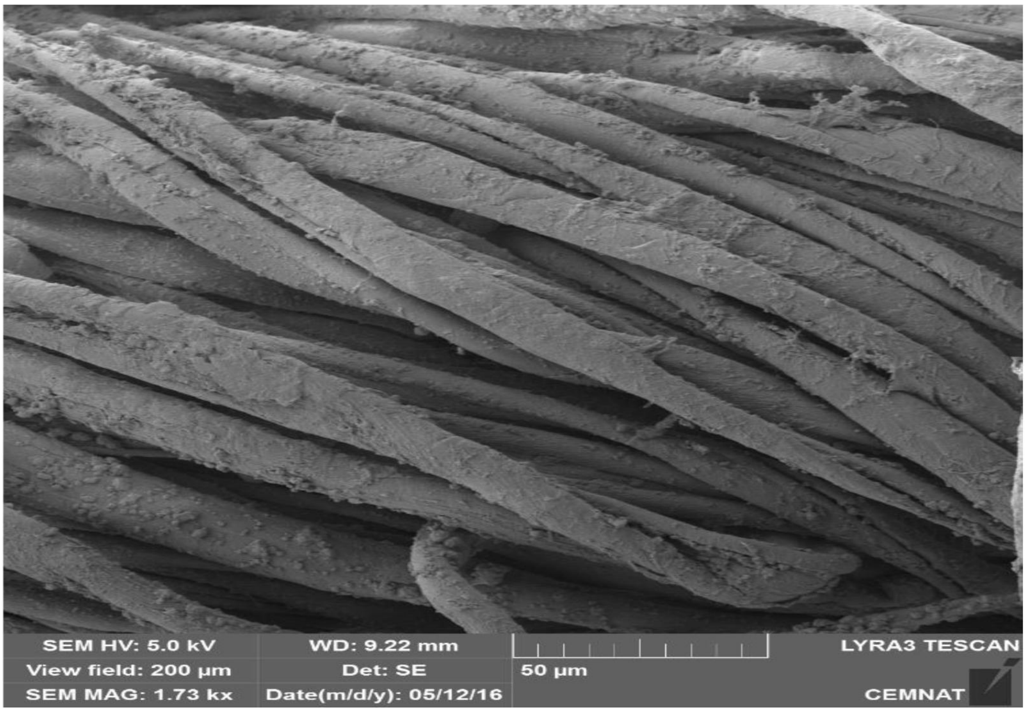

Figure 3 EMS of fiber surface of cotton textile washed without chelating agent with model detergent

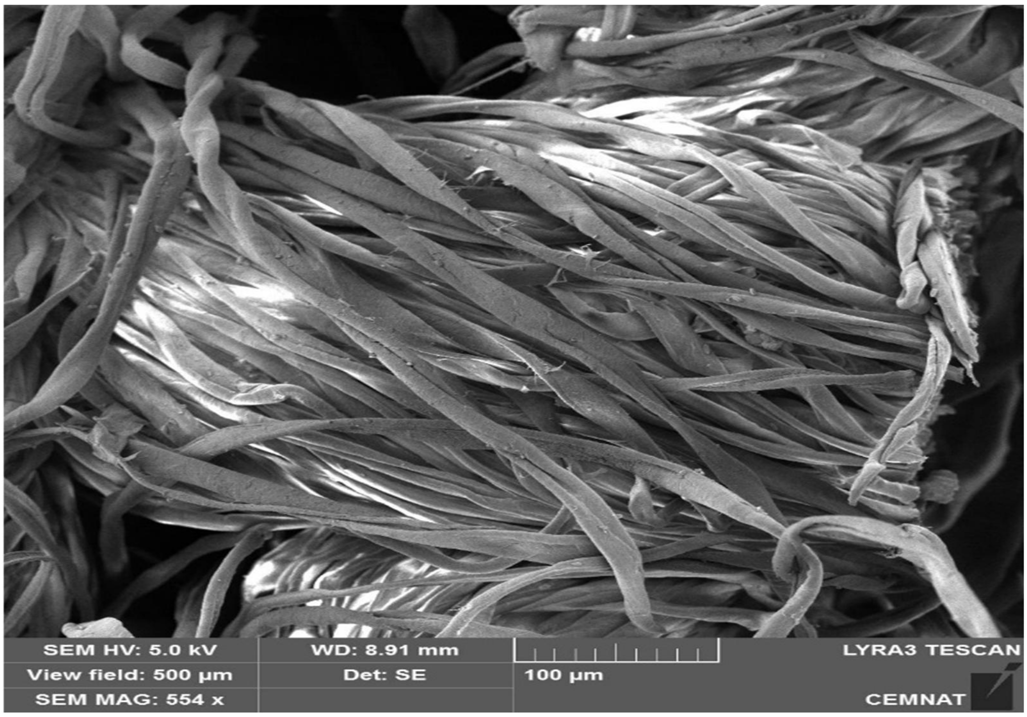

Figure 4 EMS of fiber surface of cotton textile washed with chelating agent no.1

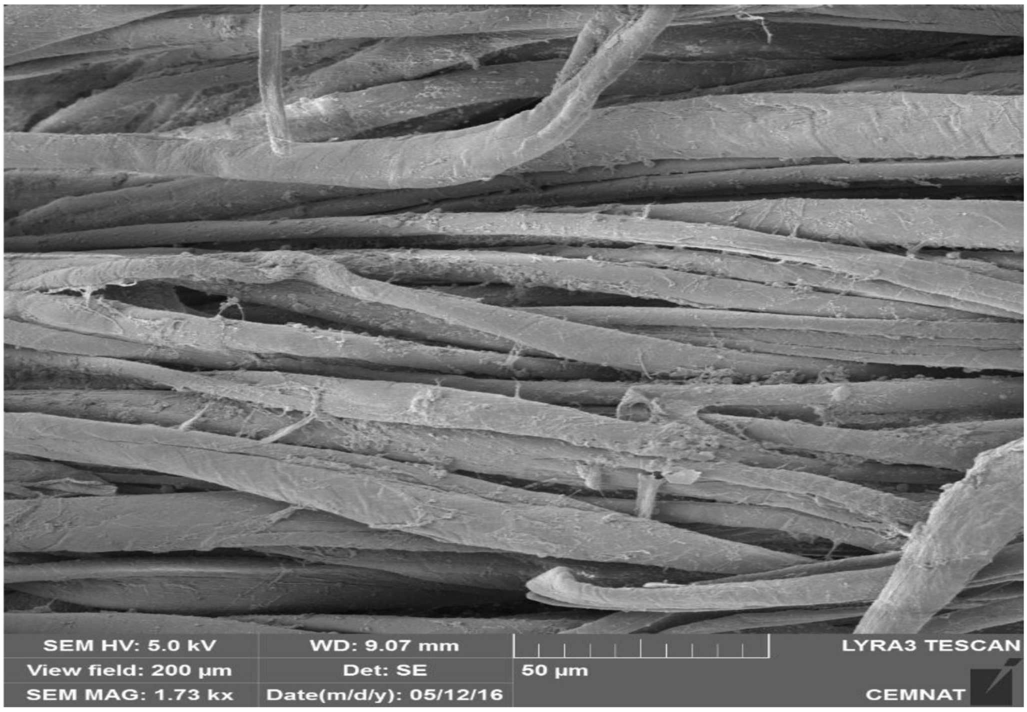

Figure 5 EMS of fiber surface of cotton textile washed with chelating agent no.2

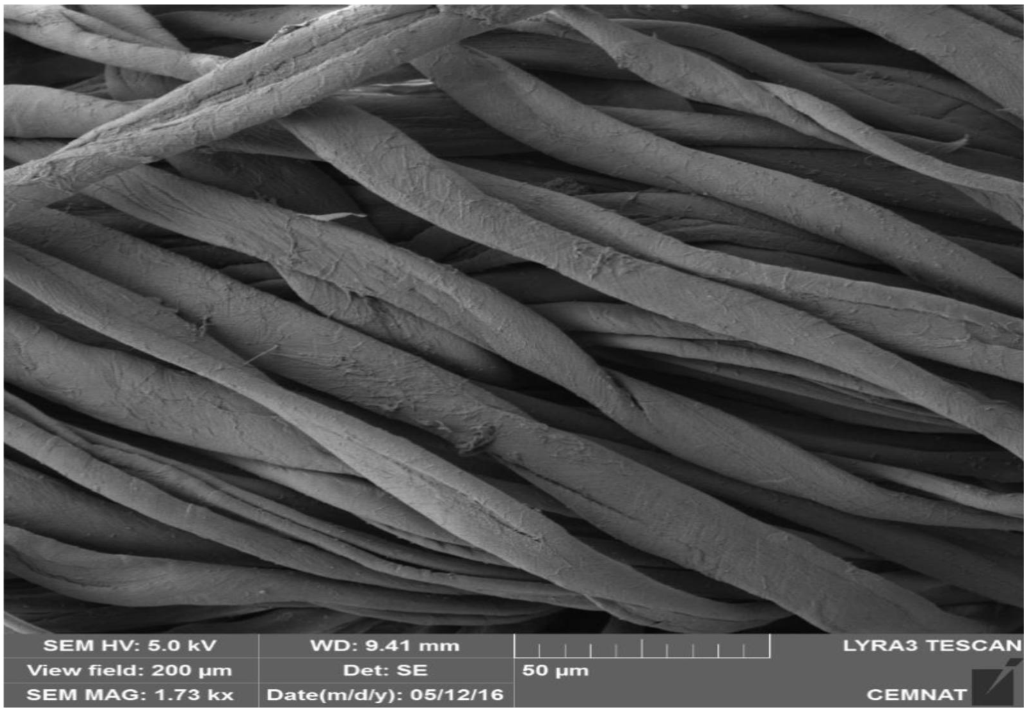

Figure 6 EMS of fiber surface of cotton textile washed with chelating agent no.3

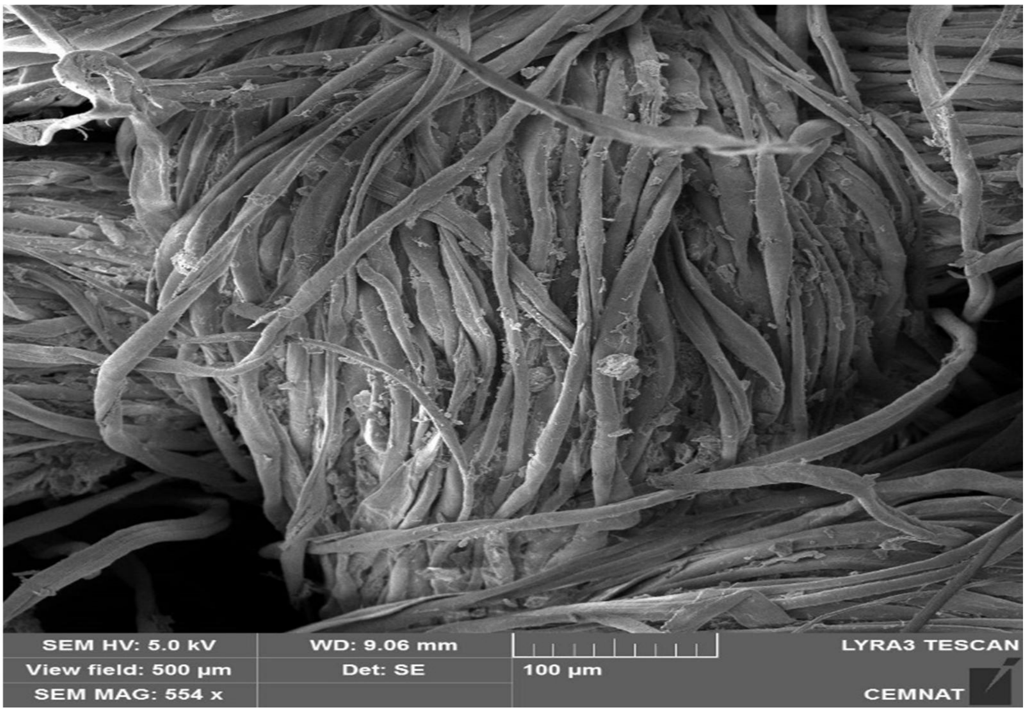

Figure 7 EMS of fiber surface of cotton textile washed with chelating agent no.4

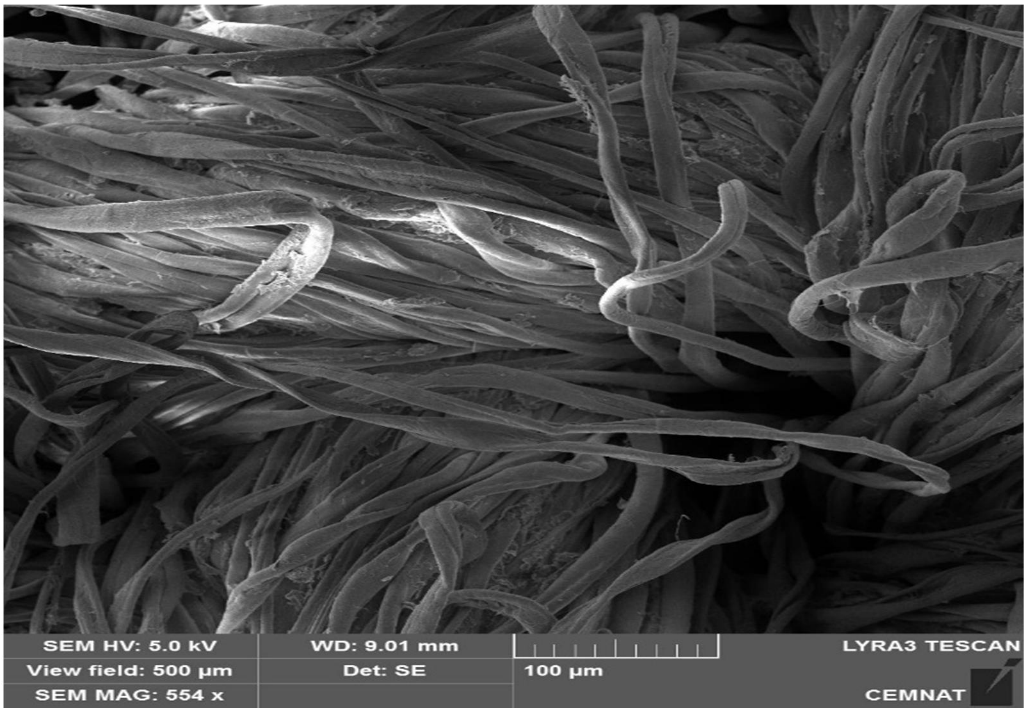

Figure 8 EMS of fiber surface of cotton textile washed with chelating agent no.5

4 CONCLUSIONS

In this work the results of repeated model washing with an addition of selected developmental samples of sequestering agents and chelating surfactants were evaluated. The addition of the prepared chelating samples influences the bath positively. The content of calcium ion is reduced and its negative effect is more limited. The results of the determination of ash values and calcium ion are more favourable in prepared sequestering substances *N*-(1,2-dicarboxyethyl) glutamic acid tetrasodium salt and *N*,*N*'-bis(1,2-dicarboxyethyl) aspartic acid hexasodium salt. Pictures of fiber surface of cotton textile from a scanning electron microscope complement the idea of the sediment for washing material.

It can be concluded that the prepared chelating agents are applicable in many detergent formulas and as textile auxiliary agents for some finishing operations. Sample no. 3 could be recommended as a replacement for existing sequestering agents.

5 REFERENCES

1. Choudhury A.K.R.: Textile Preparation and Dyeing, Enfield NH, USA: Science Publichers, 2006, pp 40-60, ISBN 1-57808-402-4
2. Šmidrkal J., Svobodová J.: Washing efficiency, XLVIII. Seminar on surfactants and detergents, Proceedings of lectures (Prací účinnost, XLVIII. Seminář o tenzidech a detergentech, Sborník přednášek), Velké Bílovice, CZ, 2015, pp. 39-43, (in Czech), ISBN 978-80-7395-942-5
3. Hüls Chemische Werke A.-G. Waschmittelformulierungen mit biologisch abbaubaren Polymeren. Inventors: Beck R., Krause F., Schönkäs U. Int. Cl.: C 11 D 3/37. Ger. Offen. DE 43 19 807, 1994 -11 – 17

SATURATION RATE DETERMINATION DURING ASCENDANT, HORIZONTAL AND DESCENDANT CAPILLARY RISE USING ELECTRICAL RESISTIVITY

Sofien Benltoufa, Ihsene Oueslati, Amal Boughattas and Faten Fayala

Laboratory of Thermal and Energetic Systems Studies (LESTE), National Engineering School of Monastir, University of Monastir, Ibn El Jazzar, 5000 Monastir, Tunisia
sofien.benltoufa@enim.rnu.tn; benltoufa@gmail.com

***Abstract:** In this paper, a saturation rate during the capillary rise of a textile fabric was determined. A mathematical model based on the Archie's law, considering the electrical resistivity, saturation rate and fabric tortuosity was established. In order to determine the saturation exponent a calibration method was introduced. According to this method the spatiotemporal distribution of the saturation rate during the capillary rise is presented. This method was also used to evaluate the saturation rate during the horizontal and downward capillary rise. It was found that the saturation rate remains constant for the case of the horizontal and descending impregnation.*

***Keywords:** capillary rise, electrical resistivity, horizontal-downward capillary, saturation rate.*

1 INTRODUCTION

The comfort afforded by textile fabrics can be improved by understanding the liquid transport mechanism. In capillary flow through textile fabrics, the constitute yarns are responsible for the main portion of the wicking action [1, 2]. Therefore, many researches have been conducted to study the wicking behaviour in textile structure. Among the extensive research in this field, textile yarns were treated either as porous media [3, 4], the liquid transport through which can be described by Darcy's law, or as capillary tubes, the liquid flow through which can be modelled by Lucas–Washburn kinetics. In the first case, however, the characteristic parameters, such as permeability, are difficult to quantify and are always obtained empirically [5]. In the second case, similarly, the effective radius of the capillary tube, the effective contact angle, etc., are also determined by fitting the experimental data [6]. A literature review, previously mentioned [1-8], shows that although broad research has been carried out in this area, a procedure to determine the saturation during capillary flow through textile based is still lacking.

In this work, the saturation rate during the capillary rise is determined using an electrical resistivity method. A theoretical model was developed based on the Archie's law. An experimental validation showed that our model can determine correctly the spatiotemporal distribution of saturation rate in textile structure.

2 FABRIC SATURATION DETERMINATION USING ELECTRICAL RESISTIVITY

There is an analogy between the laws of fluid mechanics and those of electrical conduction. The difference in pressure in a pipe is in fact the analog of a potential difference across a conductor, while the fluid flow is the analog of the electric current. In both cases, the relationship between pressure/flow difference and potential/current difference depends on the geometry (form and length) of the pipe or conductor.

Archie's law [9] has been the standard method for relating the conductivity of a clean reservoir rock to its porosity and the conductivity of the fluid saturating its pores for over 60 years. Initially, it was used as an empirical relationship for a narrow range of rocks and porosities, it has found wide application. It has been verified recently by analytical methods for certain special cases [10, 11] and has been extended for use when the surface conduction is significant, such as at low salinities and in clay-bearing lithofacies [12]. One form of the traditional Archie's law can be expressed as [13]:

$$R_{e-m} = \frac{R_{e-water}}{\tau \varepsilon^{m} S^{n}} . \tag{1}$$

where R_{e-m} [Ω.m] is the bulk effective resistivity of the porous material; $R_{e-Water}$ [Ω.m] is the resistivity of the liquid occupying the pores; ε is the porosity which is assumed to be fully saturated (i.e., identical to the volume fraction of the fluid phase); S is saturation rate, τ is the tortuosity, m is the cementation exponent and n is the saturation exponent (usually close to 2).

The cementation exponent m, also called compacity factor and usually in the range 1.3–2.5, is an index of the pores sizes in the porous media [13]. It has been demonstrated by Keller [14] that the compacity exponent is closely related to the porous compacity level, pores size and distribution.

The use of Archie's law requires the porosity and liquid resistivity determination. Moreover, the exponents m and n are empirical and determined for each sample. Thus, it is necessary to carry out calibration experiments determining these various parameters.

Other researchers evaluated the saturation rate S as a function of the resistivity index I_R, (second Archie's law) defined by:

$$I_R = \frac{R_{e-m}}{R_{e-sat}} = \frac{1}{S^n}. \tag{2}$$

where, $R_{e\text{-}sat}$ [Ω.m] is the resistivity of the saturated material.

By plotting $\ln\left(\frac{R_{e-m}}{R_{e-sat}}\right)$ as a function of saturation rates the constant n is determined. The exponent of "Archie saturation" n is also close to 2 but can reach 10 [15].

3 CALIBRATION METHODOLOGY

A calibration is carried out for each sample in order to evaluate the saturation rates by measurement of electrical resistivity for each saturation rate. Thus, a sample (dimensions 5×5 cm) with dried mass m_d [g] is impregnated in distilled water and then transferred to a support. The mass of the sample is continuously recorded by an electrical balance in order to determine the saturation rate.

The electrical resistivity was measured using the 4339B high-resistance meter from Agilent® (Figure 1).

The non-conductive grid allows the sample to be dried through both sides. Each sample is placed freely on the drying support and not tensioned to avoid deformations that can modify the size of the pores. During drying, wet mass m_w [g] decreases. The saturation rate S is calculated as follows:

$$S = \frac{m_w - m_d}{m_d}. \tag{3}$$

Thus, the calibration procedure consists in measuring the resistivity as a function of the different saturation rates.

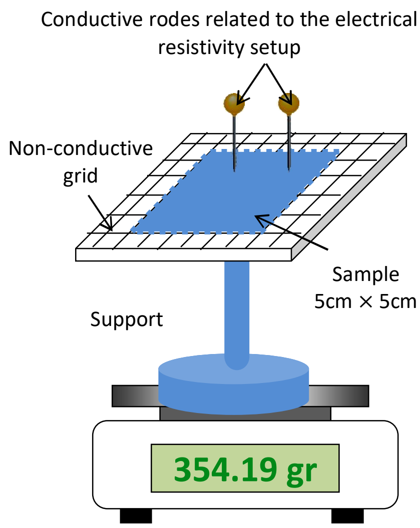

Figure 1 Calibration setup for sample electrical resistivity

Figure 2 illustrates the sample calibration for the saturation exponent n determining. It is noticed that the regression line of the curve is linear with a coefficient of determination R^2 = 0.984 and n = 2.5351.

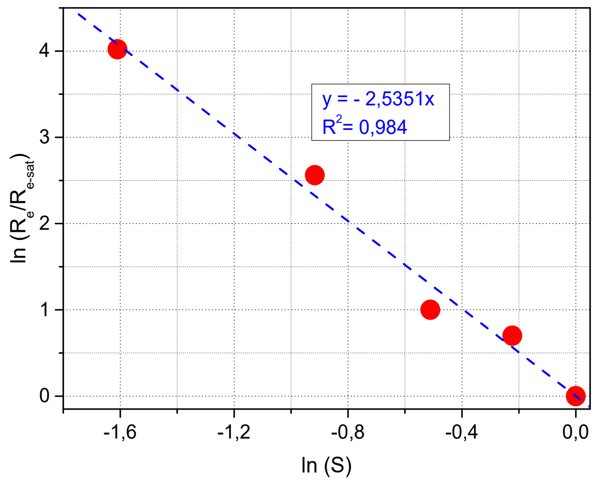

Figure 2 Calibration a sample for determining the saturation exponent n

4 SATURATION RATE DETERMINATION DURING CAPILLARY RISE FROM INFINITE RESERVOIR

A series of experiments on a plain knitted structure was conducted with distilled water as wicking liquid. The experimental apparatus for vertical capillary rise [6]. The experiments were conducted in a standard atmosphere of 20±2°C and 65±2% relative humidity, and the samples were conditioned for 24 hours before testing.

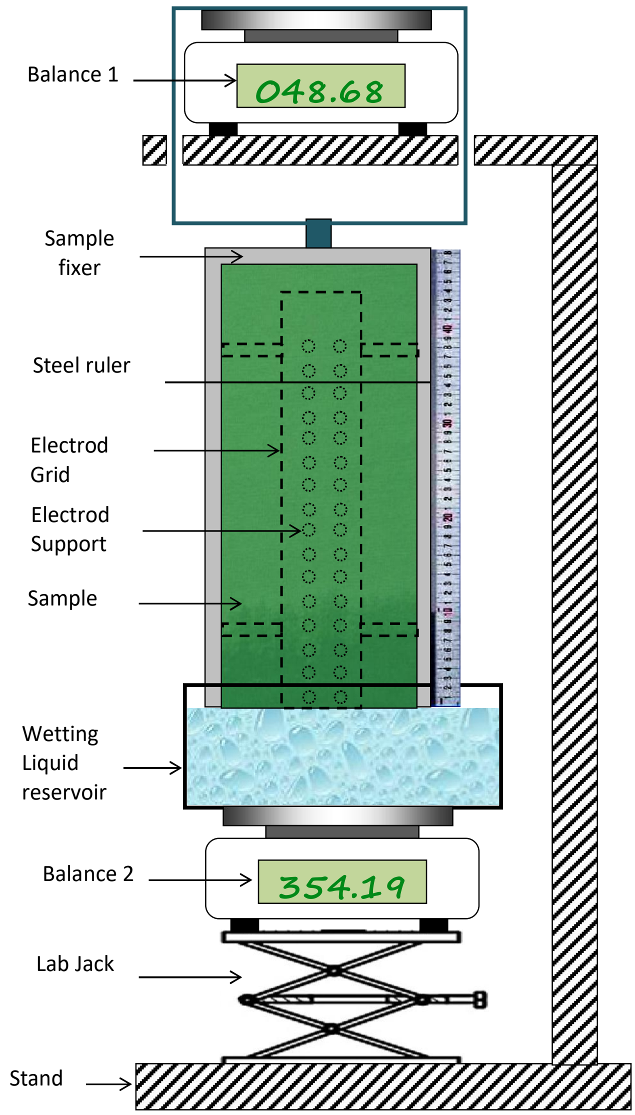

Figure 3 Experimental apparatus for capillary rise considering evaporation [6]

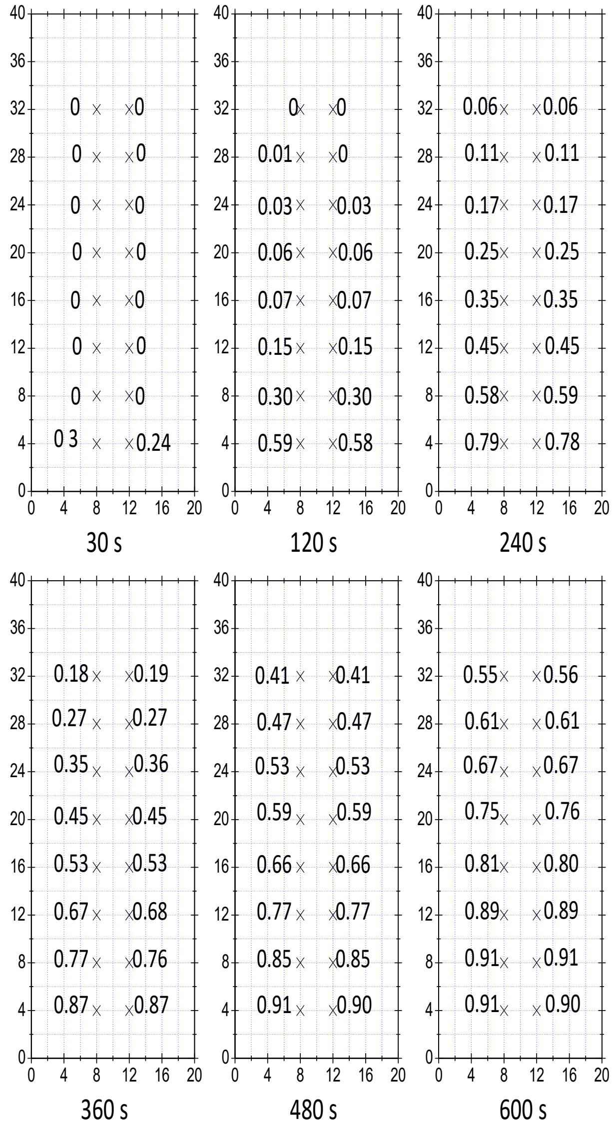

Figure 4 Spatiotemporal distribution of saturation rate in the case of a capillary rise test at 4 cm steps

In the apparatus, the lab jack was used to hoist the liquid reservoir containing the wicking liquid, and the steel ruler to measure the wicking height.

Figure 3 shows the Spatiotemporal distribution of saturation in width and height of a capillary rise test. For the same height, the saturation rate is identical which implies the structure is the same according to the width. According the Figure 3, not surprisingly, the penetration velocity of liquid in early stage is much higher than in subsequent stages. With time passing, the advancement of liquid becomes slower and slower until equilibrium is established. Figure 4 illustrates Spatiotemporal distribution of saturation rate in the case of a capillary rise test at 4 cm steps.

5 SATURATION RATE DETERMINATION DURING HORIZONTAL AND DOWNWARD CAPILLARY FROM INFINITE RESERVOIR

Figure 5 illustrates the variation in saturation rate in the case of horizontal and descending capillary at different vertical positions *ha* at 4 cm and at 8 cm.

In the case of h_a = 4cm, the average saturation rate is about 0.6675 with a standard deviation of 0.0093 and a coefficient of variation of 1.394%. Whereas for h_a = 8 cm, the average saturation rate is about 0.4106 with a standard deviation of the order of 0.0068 and a coefficient of variation of 1.65%. Therefore it can be concluded that the saturation rate remains constant for the case of the horizontal and descending impregnation.

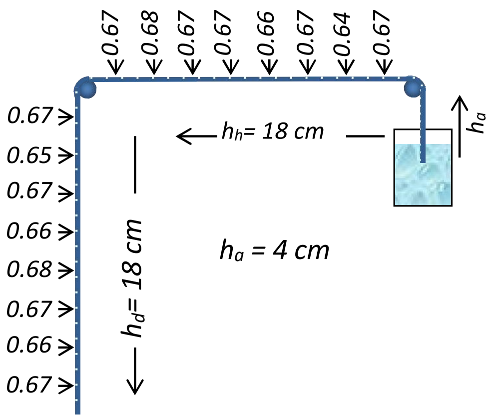

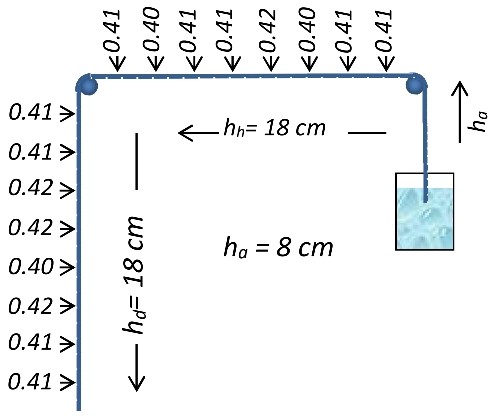

Figure 5 Saturation rate at 2 cm interval: horizontal h_h and downward capillary from infinite reservoir h_d (ascendant capillary h_a = 4 cm and 8 cm)

In addition, the average saturation rate is decreasing by increasing the distance from the reservoir (when h_a increases). Indeed, by increasing h_a, the saturation rate becomes smaller at the level of the horizontal and descending impregnation portion (see Figure 3). This is due to the effect of gravitational forces.

6 CONCLUSION

The saturation rate during capillary rise was investigated. Using modified Archie's law, the saturation was determined based on the electrical resistivity of wetted textile fabric. The calibration method was carried out for each sample to determine the saturation exponent *n* before testing.

The spatiotemporal repartition of the saturation rate during the capillary rise was presented. This method was also used to evaluate the saturation rate during the horizontal and downward capillary rise. It was found that the saturation rate remains constant for the case of the horizontal and descending impregnation. In addition, the average saturation rate is decreasing by increasing the distance from the reservoir when h_a increases. Wicking in textile materials is very complicated and the mechanism has not been fully understood until now.

Nevertheless, this research attempts to gain an insight into this area and to construct a framework for further studies. Modeling the fabric permeability during wicking will form the subject of subsequent researches.

7 REFERENCES

1. Hollies N.R., Kaessinger M.M., Bogaty H.: Water transport mechanisms in textile materials: Part I: The role of yarn roughness in capillary-type penetration, Textile Research Journal 26(11), 1956, pp. 829-835, doi: 10.1177/004051755602601102
2. Hollies N.R., et al.: Water transport mechanisms in textile materials: part II: Capillary-type penetration in yarns and fabrics, Textile Research Journal 27(1), 1957, pp. 8-13, doi: 10.1177/004051755702700102
3. Amico S., Lekakou C.: Axial impregnation of a fiber bundle. Part 1: Capillary experiments, Polymer composites 23(2), 2002, pp. 249-263, doi: 10.1002/pc.10429
4. Amico S., Lekakou C.: Axial impregnation of a fiber bundle. Part 2: Theoretical analysis. Polymer composites 23(2), 2002, pp. 264-273, doi: 10.1002/pc.10430
5. Benltoufa S., et al.: Porosity determination of jersey structure, AUTEX Research Journal 7(1), 2007, pp. 63-69
6. Benltoufa S., Fayala F., Nasrallah S.B.: Determination of yarn and fiber diameters after swelling using a capillary rise method, The Journal of the Textile Institute 103(5), 2012, pp. 517-522, doi: 10.1080/00405000.2011.589573
7. Hussain S. Glombikova V., Havelka A., et al.: Moisture transport phenomena of functional underwears, Vlakna a Textil (Fibres and Textiles) 24(2), 2017, pp. 59-66
8. Heinisch T., Tesinova P., Poloscukova L.: Moisture management for different air conditions, Vlakna a Textil (Fibres and Textiles) 24(3), 2017, pp. 64-69
9. Archie G.E.: The electrical resistivity log as an aid in determining some reservoir characteristics, Transactions of the AIME 146(1), 1942, pp. 54-62, https://doi.org/10.2118/942054-G
10. Mendelson K.S., Cohen M.H.: The effect of grain anisotropy on the electrical properties of sedimentary rocks, Geophysics 47(2), 1982, pp. 257-263, doi: 10.1190/1.1441332
11. Sen P., Scala C., Cohen M.: A self-similar model for sedimentary rocks with application to the dielectric constant of fused glass beads, Geophysics 46(5), 1981, pp. 781-795
12. Salem H.S., Chilingarian G.V.: The cementation factor of Archie's equation for shaly sandstone reservoirs, Journal of Petroleum Science and Engineering 23(2), 1999, pp. 83-93, doi:10.1016/S0920-4105(99)00009-1
13. Glover P.: What is the cementation exponent? A new interpretation, The Leading Edge 28(1), 2009, pp. 82-85, doi: 10.1190/1.3064151

14. Keller G.V.: Rock and mineral properties (Chapter 2), Electromagnetic methods in applied geophysics Vol. 1 Theory, Misac N. Nabighian (Ed.), 1988, pp. 12-51, https://doi.org/10.1190/1.9781560802631.ch2

15. Toumelin E.: Pore-scale petrophysical models for the simulation and combined interpretation of nuclear magnetic resonance and wide-band electromagnetic measurements of saturated rocks, Ph.D. Thesis, University of Texas, Austin, 2006, p. 299

THE USE OF 3D GEOMETRIC MODELS IN SPECIAL PURPOSE KNITWEAR DESIGN AND PREDICTING OF ITS PROPERTIES

Svitlana Bobrova, Tetiana Ielina, Nataliia Beskin, Victoria Bezsmertna and Liudmyla Halavska

Kyiv National University of Technologies and Design, Nemirovich-Danchenko Str. 2, 01011 Kyiv, Ukraine
bobrova.sy@knutd.com.ua, yelina.tv@knutd.com.ua, natalibeskin@gmail.com, vikkytoria2610@gmail.com

Abstract: *The article deals with the issues of predicting special purpose knitted fabrics properties. We suggest solving this problem by designing a 3D geometric model of a knitwear structure. The proposed technique has been used to design a 3D model of a double-layered knitwear structure, which is used for ballistic protective clothing manufacturing.*

Keywords: *3D modeling, weft-knitting, loop length, B-spline, knitted structure, yarn central line geometry, special purpose knitted fabrics, personal protective equipment, armor protection.*

1 INTRODUCTION

The special purpose knitted fabric for personal protective equipment has to meet a number of requirements for physical, mechanical, hygienic and other properties, as it is subjected to various types of force application during wear. It is made of high strength threads and it is used to protect users against the following risks: effects of small arms projectiles, effects of shrapnel from explosives, effects of stabbing and cutting weapons. Clarifying the relationship between threads characteristics and their configurations in a knitted structure on the one hand and protective properties of fabrics on the other hand is a difficult task which demands a special approach and accuracy [1, 2].

Designing of a special purpose knitted fabric is concerned with choosing the optimal physical-mechanical and geometric characteristics.

The invention of the universal computer simulation systems has solved the problem of optimizing the properties of personal protection based on an analysis of raw materials properties. Such systems perform the analysis of physic-mechanical properties under investigation on the basis of their 3D geometric models. Therefore, one of the crucial points for a simulation research of the reliability of individual armor protection products that are made of high tensile strength knitwear is the adequacy of the mathematical description of its structure.

It is known that the structure of knitwear is determined in accordance with the size and configuration of the elements of the fabrics or a knitwear product itself, relative position of the knitting elements and the way these elements interact with each other. The automation of a knit structure design provides an opportunity to use an object model which reflects some properties of the object, particularly significant to the researcher. Thus there is no need to manufacture a sample. The models are called mathematic, when formalized by the means of mathematical tools and language. In other words, the mathematical models show the interrelationships among the parameters of the object and make it possible to estimate the outcome of the project decisions. The important benefit of using the described models is the opportunity to obtain information about the object without conducting the natural experiments. People have created and been improving the model of the knitting loop for approximately a century now. By this time a number of research studies have been done on geometric description of the knitwear structure and defining the interrelationships among its most significant properties. Different ways to define these interrelationships were provided in works by E. Tompkins [3], J. Chamberlain [4], F. T. Peirce [5], G.A.V. Leaf and A. Glaskin [6], D. Munden [7], Vekasi [8], A.S. Dalidovich [9], Korlinski [10], Morroka & Matsumoto [11]. V.R. Krutikova [12], Nutting & Leaf [13], Postle [14], Whitney & Epting [15], Popper [16], Postle & Munden [17], Shanahan & Postle [18], Hepworth & Hepworth & Leaf [19], A.V. Truevtsev [20], and others.

Computer models of the knitwear structure are based on one or several theoretical models (geometric, energetic and/or mechanical). Also a ready-made prototype can be digitized. A theoretical base is required for building special programs which allow to recreate the knitted yarn geometry in the 3D modeling environment. The choice of the base is determined by the purpose of a CAD under construction. Different methods of building 3D models of fabric structure are described in works [21-25] and others. Such models provide good topological yarn alignment in a model and therefore in a sample and also ensure a high level of visual resemblance. The following works [26-29] give a spotlight on fiber length control within elements of the structure for a model and its prototype. It is known that BFS (Backface Signature) depth deformation of knitted fabrics is connected to the redistribution of the yarn in the knitwear structure. Therefore, the model which possesses exactly the same shape and loop length as the prototype is crucial for assessing the reliability of armor protection.

2 LOOP CHARACTERISTIC POINTS POSITIONING

During knitting process, a part of yarn takes a shape of a loop, if pulled through a lower fixative element (in most cases it is the head of the previous loop) and thrown over an overhead fixative element (the feet of the next loop) [26]. In Figure 1 a zone of fixation 1 is shown. It is the overhead one for the loop 2 and the lower one for the loop 3. Each zone of fixation contains two zones of the contact of threads (interlacing zones) 4 and 5 (see Figure 1). In turn, each zone of contact includes two points of contact 6, 7, 8, 9. Yarn interaction forces, as we assume, are applied at these points.

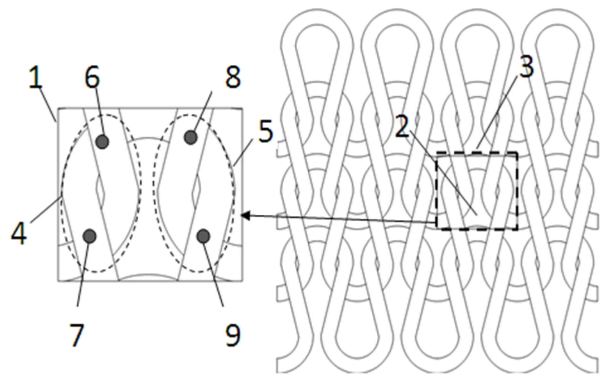

Figure 1 Positioning of contact points in a plain-knitted structure

Regardless which mathematical objects are used for the representation of the yarn configuration in a knitted structure, when modeling in 3D environment they must provide passing its central line through the characteristic points of the loop. Under characteristic points we mean points lying directly on the yarn central line, their location in 3D space has to be defined by using traditional ideas concerning shape of a loop. In Figure 2 such points are:

K – the upper point of the loop head;

B – the point of connection of the needle loop and the loop arm;

T – the central point of the loop arm;

S – as the point of connection of the loop arm and the sinker loop;

W – the lowest point of the sinker loop.

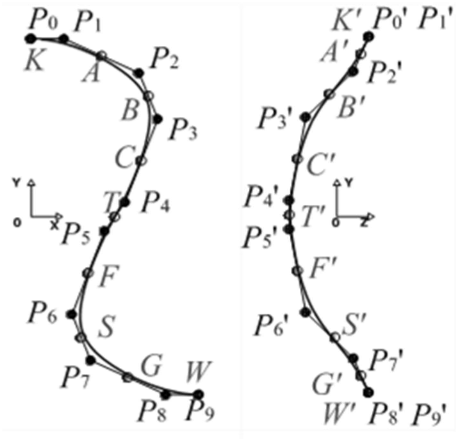

Figure 2 Orthogonal views of the yarn central line of a loop half

Requirements for the curves that can be used for representation of the yarn central line in 3D-modeling systems are given below [29]:

- the spatial curve equation must provide its passing through the characteristic points;
- curvature of line segments between characteristic points must be "changeable";
- length of this spatial curve must correspond to loop length of a real knitted fabric having the corresponding basic structure parameters;
- connections of curves representing the central lines of nearby structure elements of the knitted course in model must be smooth.

It is fundamentally important for a spline to pass through defining points and to make formulas of passing from coordinates of characteristic points to curve equation between them easy to process within our programs. In the paper [29] Catmull-Rom-curves and second-order Bézier curves were considered as possible basis for yarn axial line representation. In our view, quadratic Bézier curves suit the best. But they describe curve between only two neighboring points. Set of these curves could be accepted, however generation of smoothly-joined Bézier curves equation for such number of segments is a very complex task. Since B-spline equation is based on the same functions as Bézier curves, while being more convenient for machine description of continuous, repeatedly bent curve, we chose B-splines.

Consider the task to create the plain-knitted structure 3D model. For an existing sample of a knitted structure, data values of *l*, *w*, *c*, *t*, *d*, where *l* is the loop length [mm], *w* - wale-spacing [mm], *c* - course-spacing [mm], *t* - thickness of the knitted fabric [mm], *d* - yarn diameter [mm], can be defined experimentally or by formulas [9]. In a model, built on recorded data of *w*, *c*, *t*, *d*, the central line of a virtual yarn will pass through the characteristic points. However, through the above mentioned points in space it is possible to conduct a great number of curves with different curvature. The lengths of lines with different values of curvature will differ, respectively. Including a variable, which influences some control vertices position, to the calculation algorithm allows to regulate the length of a virtual loop and line curvature indirectly. Such an independent variable is the angle γ (Figure 3).

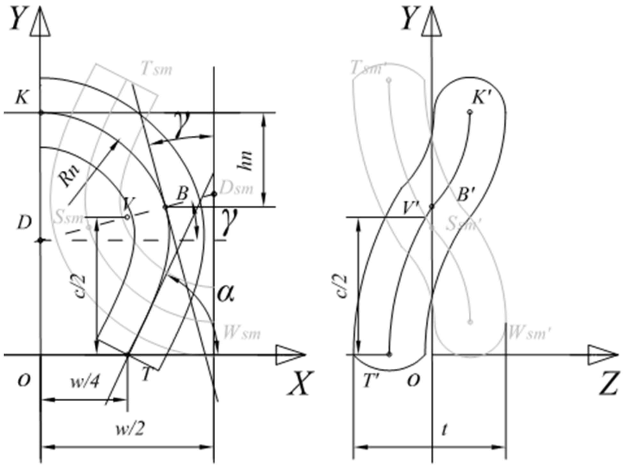

Figure 3 Positioning of characteristic points of a loop in its upper-right part

The fabric plane assumed to contain points *B* and *S* and coincide with plane *OXY* for a coordinate system, in which the axis *OX* is directed along courses and divides a loop into wale direction symmetrically, and *OY* axis is oriented in the wale direction and form the line of symmetry of the loop in the course direction. In the upper-right part of the loop the characteristic points *K, B, T* with coordinates $(X_K; Y_K; Z_K)$, $(X_B; Y_B; Z_B)$, $(X_T; Y_T; Z_T)$ are situated on the yarn central line as shown in Figure 3. As the loop was assumed to be symmetrical relatively to its central axis, the point coordinates of *T* are:

$$X_T = \frac{w}{4}; \quad Y_T = 0; \quad Z_T = -\frac{t-d}{2} \tag{1}$$

In the yarn interlacing zones (4 and 5 in Figure 1) the mutual location of yarns central lines is assumed depending only on the yarn diameter *d*. Also the projection of the needle loop on the *XY* plane is assumed to be a circular arc with the radius R_n (see Figure 3):

$$X_B = \frac{w}{4} + \frac{d}{2} \cdot \cos\gamma; \; Y_B = \frac{c}{2} + \frac{d}{2} \cdot \sin\gamma; \; Z_B = 0 \tag{2}$$

$$R_n = X_B / \cos\gamma \tag{3}$$

$$h_n = R_n \cdot (1 - \sin\gamma) \tag{4}$$

$$X_K = 0; \quad Y_K = \frac{c}{2} + h_n; \quad Z_K = \frac{t-d}{2} \tag{5}$$

The point *D* (Figure 3) is the center of the circular arc, which represents the needle loop, and D_{sm} is the center of the sinker loop of an adjacent loop in projection on the fabric plane. Taking into account the location of the selected coordinates system we can define the coordinates of points *D* and D_{sm} by the following formula:

$$X_D = 0; \qquad Y_D = Y_B - R_n \cdot \sin\gamma \tag{6}$$

$$X_{D\,sm} = \frac{w}{2}; \qquad Y_{Dsm} = Y_D + \frac{w}{2} \cdot tg\gamma \tag{7}$$

Then the angle of the loop arm inclination in the fabric plane *α* will be calculated by the formula:

$$\alpha = arctg\left(\frac{Y_K + Y_{Dsm}}{w/2}\right) \tag{8}$$

3 B-SPLINE CONTROL VERTICES POSITIONING

To record a B-spline equation it is necessary to pass from the coordinates of points belonging directly to the yarn central line (characteristic points), to the coordinates of points that determine directions of tangents built to the curve at its characteristic points. In Figure 4 such points are P_0, P_1, P_2, P_3 and P_4. To define a space location of tangents intersection points, it is easier to begin with operating of their projections on the orthogonal planes [26].

On projection on the planes *XOY* and *XOZ* one fourth part of the yarn axial line is located between straight lines *1*, *2*, and *3* as shown in Figure 4. The line *1* is the tangent to the needle loop at its top point. It passes through the point *K* being parallel to the axis *OX* as well as to the plane *XOY*. Line *2* is the tangent at point *B* therefore it passes through the point *B* and forms an angle γ with a straight line, parallel to the *OY* axis as can be seen in Figure 3. Angle of the line *3* inclination can be found on formula (8). The intersection of lines *1* and *2* is denoted by t_{12} $(X_{t12}; Y_{t12}; Z_{t12})$, and intersection of lines *2* and *3* by t_{23} $(X_{t23}; Y_{t23}; Z_{t23})$. In the *XOY* plane at the point *B* two 2D curves (projections of 3D curve segments) unite. They can be described as two B-splines, or two quadratic Bezier curves. Each of them is defined by three points. For the segment *KB* they are points *K* (X_K, Y_K), t_{12} (X_{t12}, Y_{t12}), and *B* (X_B, Y_B). For segment *BT* they are points *B* (X_B, Y_B), t_{23} (X_{t23}, Y_{t23}), and *T* (X_T, Y_T). Tangents to these curves (curve segments) at the point *B* coincide.

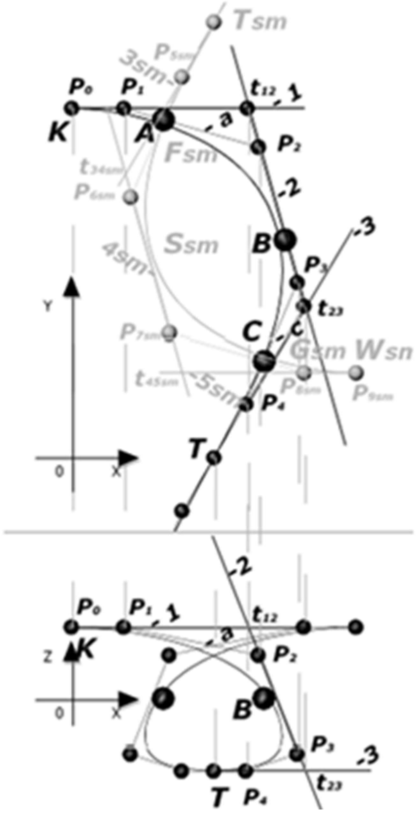

Figure 4 Central line of a yarn segment of an interlacement zone

In a general case the equation of a straight line can be written in as:

$$y = kx + a, \tag{9}$$

where k is the slope of the line, a – ordinate of the point of intersection of the straight line and the axis OY.

The slopes of tangents *1, 2, 3* will be represented by k_1, k_2, and k_3. k_3 respectively and a_1, a_2, a_3 will represent the intersection point with the axis OY. Thus we can apply the following formula:

$$k_1 = 0; \qquad a_1 = Y_K$$
$$k_2 = tg(\frac{\pi}{2} + \gamma); \qquad a_2 = Y_B - k_2 \cdot X_B \tag{10}$$

where X_B, Y_B - are coordinates of point B, defined on formulas (2).

Coordinates of the intersection point of lines *1* and *2* are:

$$X_{t12} = \frac{a_2 - a_1}{k_1 - k_2} \qquad Y_{t12} = Y_K \tag{11}$$

Using the same approach as was employed with the intersection point of straight lines *1* and *2*, we find the intersection point of lines *2* and *3*, taking into account that slope of the line *3* is known from formula (8).

The points of contact between *A* and *C* belong to the curve segments *KB* and *BT* respectively. The easiest way to find their exact location is to use an iterative method in a program environment. Thus, we have coordinates of points *A* (X_A; Y_A) and *C* (X_C; Y_C), and values of parameters of u_a and u_c in these points. Consequently, slopes of tangents to the yarn axial line at points *A* and *C* can be defined by means of differentiation of the B-splines equations.

The point P_1 is located on crossing of tangent to the spline in the point *A* (line *a* in Figure 4) with the line *1*. P_2 is on crossing of the line *a* with the line *2*. P_3 is on crossing of the line *c* with the line *2*, and P_4 - with the line *3*. The coordinates of the point P_0 coincide with the coordinates of *K*, which were found before and coordinates of points P_5 - P_9 can be defined by using the rules of symmetry.

4 THREAD CONFIGURATION IN THE DOUBLE - LAYERED KNITWEAR STRUCTURE

Double-layered knitwear is commonly used for the armor protection manufacturing. The graphs are shown in Figure 5. The center line equations of the thread on different interlacement zones are compiled on the following considerations. In the double-layer knitwear [30] structure four types of threads are formed with different configurations: LC1, LC2, LR1, LR2 (Figure 5).

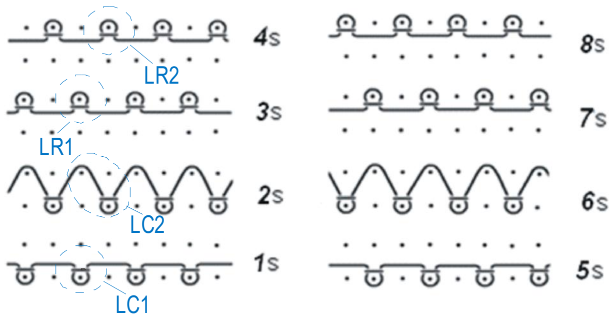

Figure 5 The graphs of double-layered weft knitted structures

For a mathematical description we isolate the repetitive part of the curve in each of these sections, coping of which can be used to recreate the entire section. Sections of the LC1 thread are formed on needles of the cylinder systems 1 and 5 and represent the loops of the single cross miss. Sections of the LC2 thread are also formed on needles of the cylinder systems 2 and 6 as loops with tucks. On needles of the systems 3 and 7 sections of the LR1 thread are formed as loops of the cross miss, on which the loops that are formed in 8 system and tucks of thread LR2 section are dropped. In systems 4 and 8, sections of the LR2 thread are formed as loops of the cross miss, on which loops that are formed in system 7 are dropped.

Table 1 Initial knitting process data for knitted fabrics

Knitting structure		Raw materials in knitting system	Linear density [tex]
double-layer interlock-based	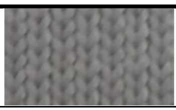	1s, 2s, 5s, 6s – polyamide thread 3s, 4s, 7s, 8s – UHMWPE fiber	29 44

A mathematical description of the LC1 and LR2 section configurations can be constructed by the algorithm for calculating the coordinates of the reference points, which we have developed for the single plain. It was developed in such way that the point P9 was sharpened along the course. For the cross miss loop it will be $x_9=A$ instead of $x_9=A/2$. Consider the configuration of the thread LC2 section (Figure 6).

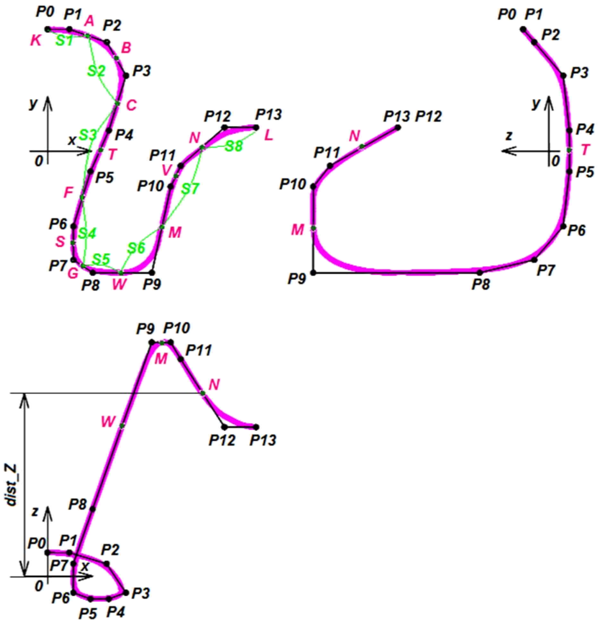

Figure 6 Configuration of the filament axial line, representing half of a loop and half of a tuck (*LC2*)

A thread segment which represents half of a loop and half of a tuck can be divided into 8 separate segments (S_1 – S_8) according to the curvature changes pattern. When considering the projection of half of the thread section in a double-layered weft knitted structures on the *XOY, YOZ* and *XOZ* planes (Figure 6), we observe that the areas S1, S5, S6, S8 don't contain bending points, and the areas S2, S3, S4 contain one, in which the curvature changes sign turns to the opposite In this case the number of reference points, needed to describe a half of a loop and half of a tuck, is *N=14* (*P0 – P13*).

5 YARN CROSS-SECTION SHAPE

One of the crucial points in creating a 3D model in knitted fabric is to set a shape and size of its cross-section in characteristic points of a loop. Independently of the yarn structure detalization, it is possible to formulate the basic features of its cross-section contouring. By definition, the cross-sectional plane of the yarn or thread passing through a given point of its central line is perpendicular to the tangent at this point. Due to the interaction between the mutually interlacing yarn segments, shape of their cross-sections changes, the compression area stay located in the cross-section segment that contains the main normal built to the curve at this point [29]. Then in the models that are using ellipses, circles and ellipses with a flat contact surface as the contour of the cross-section, normal and bi-normal lines can be arranged, as shown in Figure 7.

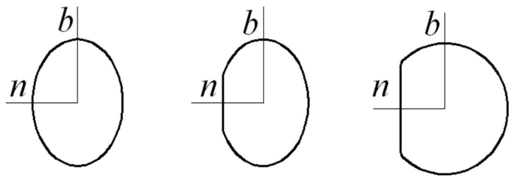

Figure 7 Cross section of yarns, models of which are built without their structural elements displaying

Investigating the link between physic-mechanical properties of a yarn and a cross-section shape is yet another topic which will be studied upon further research.

6 EXPERIMENTAL DATA

During experimental research the plain structure samples made of different raw materials were studied. Basic characteristics of real knitted fabric have been tested under standard conditions and using standard methods of testing. Samples made of 4 yarn types with different loop length (*L* [mm]), flexlife and pilosity were studied. For each sample a 3D model with equal geometric parameters was built up. The values of the variable *γ* ensure a model to be constructed according to the requirements mentioned above (Table 2).

Table 2 Angle γ values for the studied yarn types

Yarn type	№	Loop length of a real fabric [mm]	Values of the angle γ which gives the coincidence of the loop length
Cotton yarn 30x2 tex	1.1	5.1	38
	1.2	5.5	33
	1.3	5.9	32
	1.4	6.3	24
	1.5	6.7	19
Viscose thread 28x2 tex	2.1	5.2	16
	2.2	5.7	12
	2.3	6.2	9
	2.4	6.7	5
	2.5	7.2	2
Wool-mixed yarn 31x2 tex	3.1	5.1	45
	3.2	5.5	40
	3.3	5.9	35
	3.4	6.3	30
	3.5	6.7	25
Wool yarn 31x2 tex	4.1	5.2	37
	4.2	5.7	35
	4.3	6.2	18
	4.4	6.7	16
	4.5	7.2	6
UHMWPE fiber 66 tex	5.1	4.0	36
	5.2	4.4	31
	5.3	4.8	29
	5.4	5.2	20
	5.5	5.6	16

7 RESULTS AND DISCUSSION

The task of predicting of the special purposes knitted fabrics properties might be solved by constructing a 3D geometric model of the knitwear structure. 3D geometric modeling of the knitted fabrics structure requires an exact display of the configuration of the axial line of the yarn in its structural elements [28, 29]. To describe the configuration of the yarn central line in the loop of the weft-knitting the authors have used the mathematic theory of B-spline construction. In the model, the length of the spatial curve varies with the change of the inclination angle of the tangent at the interlacing point as an independent variable. This makes the model flexible and feasible for use in 3D modeling systems where the loop length of the virtual knit pattern must coincide with the loop length of the real prototype. The suggested technique is realized at constructing a 3D model of the structure of double-layer knitwear made of ultra-strong polyethylene threads. We have generated the models of the knitted fabrics structures by using software which was developed by us [27].

It should be noted that 3D models of a double-layered knitted fabrics, constructed by us for the study, were built by using experimental data and selection of construction parameters by analyzing parameters of real structure and observing the structure under a microscope. Results, that we have obtained at this point, help us better understand a framework of model designing and clarify a plan of further research. To develop a theoretical base of passing from such input data as topology and thread properties to building a model, a set of additional experiments is required, as a mechanism of threads mutual impact has not yet been studied.

Figures 8 and 9 show an image of a virtual sample of a plain-knitted structure fragment and a 3D structure of a double-layer knit with tuck connection of layers built by the means of this program [27].

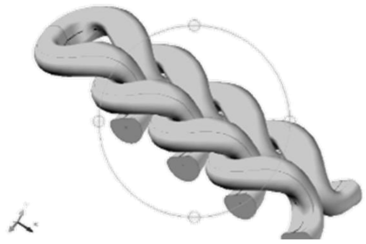

Figure 8 3D geometric model of a plain-knitted structure

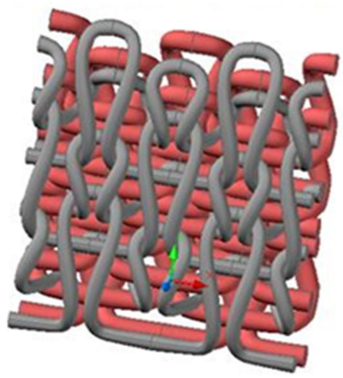

Figure 9 3D geometric model of a weft double-layer knit with tuck connection of layers

There are broad perspectives of using such models for assessing protective properties of the special purpose knitwear. The double-layered knitwear structure with polyethylene threads is used for manufacturing a wide range of protective clothing, including clothing with ballistic protection. Unfortunately, the evaluation of knitted fabric ballistic resistance to impact from different weapon types can hardly be tested under real-life conditions.

When designing special purpose knitwear, for instance for fencing clothing manufacturing, virtual models allow us to predict its pressure bearing capacity against multiple impact points caused by a tip of a fencing weapon. It gives us opportunities to visualize the hits of the blade tip on the loops and predict their deformation and as a result to design an optimal knitwear structure with the specified physic-mechanical properties [31].

During experimental research we produced the weft knit structure samples made of different raw materials and studied their structure parameters. For each sample we designed a 3D model with geometric parameters that coincide with the real prototype parameters. We defined the angle values at tangent point of a fabric for each sample. Changing of an independent angular parameter value used as an independent variable γ, allows getting a spatial curve of a necessary length.

8 CONCLUSIONS

Three-dimensional geometric modeling and simulation of knitted fabric structures requires accurate reflection of the yarn axial line configuration in its structure elements. For configuration description of the yarn central line in a loop of weft-knitted structure, mathematical basis of B-spline can be applied. The developed method of calculation of control vertices for B-spline definition coordinates, using the basic knitted structure parameters is worked out for building a 3D double-layered knitwear structure manufactured with the use of ultra-high-molecular-weight polyethylene fiber (UHMWPE). Changing of an independent angular parameter value used as an independent variable γ, allows getting a spatial curve of a necessary length.

The results of the conducted research have concluded the high level of conformity of the 3D model, namely, by the parameters of the loop length, course spacing and wale spacing the real parameters of its structure.

Further researches will focus on defining the relation between the independent variable γ and yarn physic-mechanical properties which will allow using the developed technique for predicting the stability of knitwear to various dynamic loads without need for making a sample on knitting equipment.

9 REFERENCES

1. Chistyakov E.: Armour materials based on polymeric fibers, Peace and Security 4, 2014, pp.19-25 (in Russian)
2. Bobrova S., Halavska L.: Ballistic knitted fabrics development for body armor production, Bulletin of Kiev National University of Technology and Design 2015, 3(86): A series of "Engineering", pp.114-120 (in Ukranian),http://er.knutd.com.ua/bitstream/123456789/474/1/V86_P133-140.pdf
3. Tompkins E.: The Science of Knitting, London, New York: John Wiley and Sons, 1914, p. 330
4. Chemberlain J.: Hosiery yarn and fabrics,Vol.1, Leicester: City of Leicester Technical College, 1926
5. Pierce F.T.: Geometrical principles applicable to the design of functional fabrics, Textile Research Journal 17(3), 1947, pp. 123-147, doi: 10.1177/004051754701700301
6. Glaskin A., Leaf G.A.V.: An analysis of the stresses in some approximation to a simple knitted loop of monofilament yarn, Journal of the Textile Institute Transactions 44(11), 1953, pp. 534-543, doi: 10.1080/19447025308662615
7. Munden D.L.: The geometry and dimensional properties of plain-knit fabrics, Journal of the Textile Institute Transactions 50(7), 1959, pp. 448-471, doi: 10.1080/19447025908659923
8. Vékássy A.: Examination of the cover-factor and specific weight of weft-knitted or looped basis texture based on the exact value of the loop length, ActaTechnica 31, 1960, pp. 69-102
9. Dalidovich A.: The fundamentals of knitting theory,Moscow, 1970, p. 432 (in Russian)
10. Korlinski W.: Theoretical and empirical generalized model of plain knit goods, Melliand Textilberichte 10, 1985
11. Morooka H., Matsumoto Y.: A geometric analysis of the stitch form of a circular plain knit fabric inserted over a cylinder, Textile Research Journal 68(12), 1998, pp. 930-936, doi: 10.1177/004051759806801208
12. Krutikova V.: Development of the theory of knitwear formation and methods for predicting the technological parameters of the knitting process on flat and circular knitting machines,: Dissertation for a Doctor degree of technical sciences, Kostroma, 2007 (in Russian)
13. Nutting, T.S., Leaf G.: A generalized geometry of weft-knitted fabrics, Journal of the Textile Institute 55(1), 1964, pp. 45-53, doi: 10.1080/19447026408660207
14. Postle R.: The mechanics of the relaxed plain-knitted structure, Ph.D. thesis, Leeds University, 1965
15. Whitney J.M., Epting J.L.: Three-dimensional analysis of a plain knitted fabric subjected to biaxial stresses, Textile Research Journal 36(2), 1966, pp. 143-147, doi: 10.1177/004051756603600207
16. Popper P.: The theoretical behavior of a knitted fabric subjected to biaxial stresses, Textile Research Journal 36(2), 1966, pp. 148-157, doi: 10.1177/004051756603600208

17. Postle R., Munden D.L.: Analysis of the dry-relaxed knitted-loop configuration: Part 1: Two-dimensional analysis, Journal of the Textile Institute 58(8), 1967, pp. 329-351, doi: 10.1080/00405006708629880
18. Shanahan W.J., Postle R.: A Theoretical analysis of the plain-knitted structure, Textile Research Journal 40(7), 1970, pp. 656-665, doi: 10.1177/004051757004000712
19. Hepworth B., Hepworth K., Leaf G.A.V.: The plain knitted structure, Textile Research Journal 40, 1970, p. 863
20. Truevtsev A.: Applied knitting mechanics: the handbook, St. Petersburg, 2001, p. 87 (in Russian)
21. Kurbak A., Ekmen O.: Basic studies for modeling complex weft knitted fabric structures, Part I: a geometrical model for widthwise curlings of plain knitted fabrics, Textile Research Journal 78(3), 2008, pp. 198-208, doi: 10.1177/0040517507082352
22. Demiroz A., Dias T.: A study of the graphical representation of plain-knitted structures, Part I: stitch model for the graphical representation of plain-knitted structures, Journal the Textile Institute 91(4), 2000, pp. 463-480, doi: 10.1080/00405000008659121
23. Kyosev Y., Angelova Y, Kovar R.: 3D modeling of plain weft knitted structures of compressible yarn, Research Journal of Textile and Apparel 9(1), 2005, pp. 88-97, doi: 10.1108/RJTA-09-01-2005-B009
24. Li Yinglin, Yang Lianhe, Chen Suying, Xu Lei: Three dimensional simulation of weft knitted fabric based on surface model, Computer modeling & new technologies 18(3), 2014, pp. 52-57
25. Y.Kyosev: Geometrical and mechanical modelling of textile structures at fiber and yarn level – software and data structures, Vlakna a Textil (Fibres and Textiles) 24(1), 2017, pp. 3-9
26. Ielina T.: Improvement of design of the weft knitted fabric by the three-dimensional geometric modeling of its structure, Dissertation for a candidate degree of technical sciences, Kyiv National University of Technologies and Design, Kyiv, 2013 (in Ukranian)
27. A.S.46469 Ukraine. Computer program «Structura – 3D». Ielina T.V., Galavska L. 46726 from 25.09.2012, published 23.11.2012 (in Ukranian)
28. Ielina T.: Research of compliance of the developed three-dimensional geometric model of a loop of weft-knitted jersey to its real configuration, Bulletin of Kiev National University of Technology and Design 5(67), 2012, pp. 94-99 (in Ukranian), http://er.knutd.com.ua/bitstream/123456789/3299/1/V67_P094-099.pdf
29. Ausheva N., Galavska L., Ielina T.: Geometric representations features of textile yarn in the 3d modeling systems, International Scientific Conference UNITECH-13, 22-23 November 2013, Gabrovo, Bulgaria, vol. III, pp.199-202
30. Halavska L.: Development of scientific bases of integrated knitted fabric manufacture of a functional purpose with the set properties, Dissertation for a Doctor degree of technical sciences, Kyiv National University of Technologies and Design, Kyiv, 2013 (in Ukranian)
31. Beskin N., Halavska L.: Research of knit for fencing suits on resistance against perforation, Book of abstracts of 47th International Federation of Knitting Technologists Congress, 25-26 September 2014. Izmir, Turkey, pp.42-43

THE MOLECULAR MASS EFFECT ON MECHANICAL PROPERTIES OF CHITOSAN FIBERS

Elena Dresvyanina[1,2], Alexandra Yudenko[1,2], Natalia Yevlampieva[3], Ekaterina Maevskaya[1], Vladimir Yudin[1,4], Alexandr Gubarev[3], Maria Slyusarenko[3] and Katja Heppe[5]

[1]Peter the Great St. Petersburg Polytechnic University, Polytechnicheskaya 29, 195251 St. Petersburg, Russia,
[2]Saint-Petersburg State University of Industrial Technologies and Design, B. Morskaya 18, 191186 St. Petersburg, Russia,
[3]Saint-Petersburg State University, 7/9 Universitetskaya emb., 199034 St. Petersburg, Russia,
[4]Institute of Macromolecular Compounds RAS, Bolshoy pr. 31, 199004 St. Petersburg, Russia,
[5]Biolog Heppe GmbH, Gewerbegebiet Queis, Max-Planck-Ring 45, D - 06188 Landsberg, Germany
elenadresvyanina@gmail.com

Abstract: *Chitosan fibers have been prepared from acetic-acid solution (2%) by a coagulation method. It was established that optimal concentration of chitosan solution depends on its molecular mass for fibers preparation. The influence of molecular mass value on mechanical properties of chitosan fibers has been studied. The fibers of the best mechanical properties have been obtained from chitosan of $2.1x10^5$ g/mol molecular mass, these fibers have strength of 188 MPa and Young modulus of 11.5 GPa.*

Keywords: *chitosan, molecular mass, fibers, wet spinning, mechanical properties.*

1 INTRODUCTION

Chitosan, a derivative of the natural polysaccharide chitin, has a biocompatibility, biodegradability, bactericidal activity and high sorption characteristics. Due to such properties chitosan based materials find a lot of applications in pharmacology and medicine. Recently, fibers, films and porous block materials have been applied as matrices for cellular technologies, tissue engineering and transplantology [1-4]. Chitosan-based fibers as mono- and multifilaments are promising materials for biodegradable surgical sutures, one-dimensional matrices for cellular technologies. Application of yarn or threads containing chitosan fibers makes it possible to obtain textile materials with the improved hygienic characteristics and high bactericidal properties [5].

Method of wet (coagulation) spinning of chitosan-based fibers is described in [4, 6-8]. It has been shown that the optimal solvent for chitosan is 2% aqueous solution of acetic acid [4, 8]. An aqueous solution of NaOH or a mixture of alcohol and an aqueous solution of NaOH or an aqueous solution of NaOH and sulfuric acid can be used as a precipitant.

It is known that spinning conditions as well as initial molecular characteristics such as molecular mass and deacetylation degree can have a significant effect on the properties of the wet spun fibers. The influence of spinning conditions, in particular the factor of orientation drawing, on mechanical properties of chitosan-based fibers, has been described at the work [6]. The results of some research of the structure and mechanical properties of chitosan fibers are presented in [6, 7]. The studies of the resorption of chitosan fibers *in vivo* are presented in [9].

But, there is no information practically on the influence of molecular characteristics, primarily chitosan molecular mass, on the process of fibers spinning and their properties. Therefore, the aim of the work was to study the influence of the molecular mass of chitosan on fibers wet spinning as well as on the strength and elastic characteristics of the processed fibers.

2 MATERIALS AND METHODS

Chitosan samples of similar deacetylation degree were used for processing of the fibers. The characteristics of polymers are given in Table 1.

Molecular mass M_{SD} of chitosan samples was determined by an absolute method based on sedimentation and diffusion analysis of their dilute solutions in 0.33 M CH_3COOH + 0.2 M CH_3COONa. Velocity sedimentation was investigated using Beckman XLI analytical ultracentrifuge. Translation diffusion coefficients of chitosan molecules were received by means of the isothermal diffusion study in Tsvetkov diffusometer.

Table 1 The characteristics of chitosan samples

	Raw materials	Deacetylation degree DD [%]	M_{SD} [g/mol]	Manufacturer
1	crab	96	$6.5x10^4$	"Bioprogress" (Russia)
2	crab	92	$1.1x10^5$	"Chitosan Techologies" (Russia)
3	crab	94	$1.5\ x10^5$	"Biolog Heppe" (Germany)
4	shrimp	91.5	$2.1\ x10^5$	"Biolog Heppe" (Germany)

Sedimentation of chitosan has been studied at the solute concentration range 0.1-0.02 g/dl with the rotor speed 42000 rpm at temperature 298 K. The scans were received using Rayleigh interference optical scheme every 60 s within overall experiment time of around 10 hours. The normalized sedimentation coefficient distributions of chitosan samples (Figure 1), corresponding to theirs molecular-mass distributions, have been acquired in velocity sedimentation experiments.

To process fibers the aqueous mixtures (pH = 4-5) of chitosan have been stirred at room temperature for 30 min until the partial dissolution of chitosan and its swelling. The concentration of chitosan in solution was varied from 3.5 to 6.5% and depended on chitosan samples. Then the 2% acetic acid solution in water has been added into the mixtures during a continuous stirring. The mixtures of the solution of chitosan have been stirred in the glass bulb at room temperature during 90 min and then filtered and deaerated for 24 h at the pressure 0.1 atm.

Rheological measurements of polymer solutions were carried out on the rheometer Physica MCR 301 (Anton Paar) at 20°C according to the method of "cylinder in the cylinder" in the regime of shear flow with the shear rates 10^{-4} - 100 sec^{-1}. 5 ml of solution was placed into the rheological cuvette and the dependence of viscosity (η) on the shear rate ($\dot{\gamma}$) was obtained.

The fibers were spun by coagulation method [6-8], at the laboratory equipment developed at the Institute of Macromolecular Compounds RAS. The scheme of this processing is presented in Figure 1. Precipitator was the mixture 10% solution of NaOH and C_2H_5OH in the proportion 1:1. Monofilament processing was flowed through the die hole with the diameter of 0.6 mm, the feed rate of the solution through the die hole was 5.5 mm/sec; the time of precipitation was 150 sec. The factor of orientation drawing λ [%] of the monofilament in the coagulation bath was varied from – 20% (shrinkage) up to +100%. The fibers were washed in the distilled water and then dried at a temperature of 50°C during 10 min.

The studies of the structure were conducted on the microscope Supra-55 VP (Carl Zeiss). The measurements of the mechanical properties of the processed fibers were carried out with Instron 5943 at room temperature and the load speed of 10 mm/min; basic length of the fibers was 100 mm. The cross section S [m^2] of the monofilaments was estimated by the formula $S = T/\rho$, where T is the linear density [tex] of monofilament and specific gravity ρ of chitosan is equal 1400 kg/m^3. Prior to the mechanical testing fibers were placed in special box with relative humidity 66% for 24 hours.

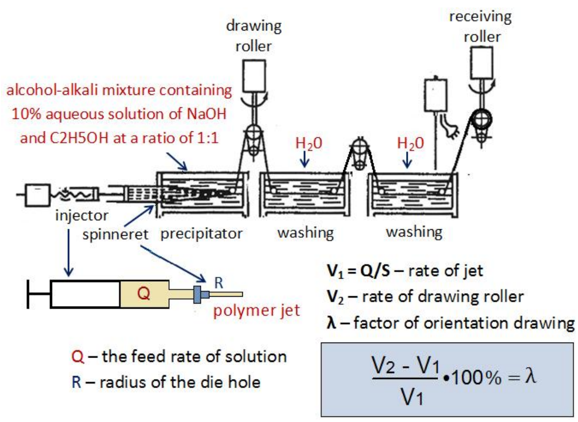

Figure 1 The scheme of chitosan fibers processing

3 RESULTS AND DISCUSSION

All investigated chitosan samples were similar in deacetylation degree but its molecular masses (Table 1) and sedimentation coefficient distributions (Figure 2) were quite different. Sample 2 was characterized by the narrowest distribution among the studied chitosans 2-4, when sample 1 had another type of distribution.

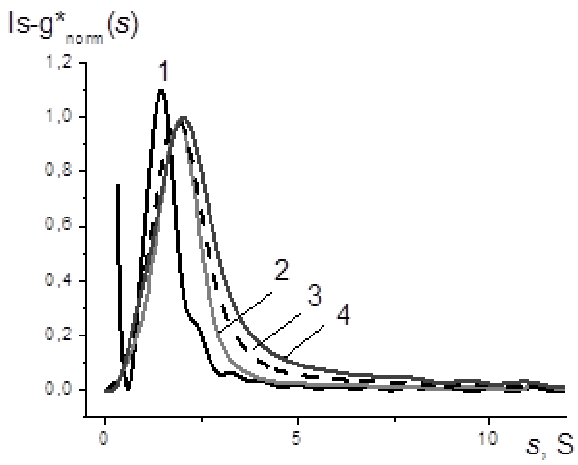

Figure 2 The normalized sedimentation coefficient distributions for samples 1-4 at c = 0.02 g/dl. On x-axis, the values of sedimentation coefficient s are expressed in Svedbergs (S); where one Svedberg unit corresponds to 10^{-13} second

To optimize the process of wet spinning the information about the rheological properties of the chitosan solution is necessary. Figure 3 represents the dependences of the viscosity on the shear rate for the 4% chitosan solutions in 2% acetic-acid solution.

It is obvious that the molecular mass of chitosan has a significant influence on the effective viscosity (η) of solutions and the dependence of the viscosity on the shear rate ($\dot{\gamma}$). The viscosity of solutions increases with increasing molecular mass. The optimum concentration of a solution of chitosan for processing decreases with increasing molecular mass. The dependences of viscosity on shear rate for solutions with similar viscosities and different concentrations of chitosan are shown in Figure 4.

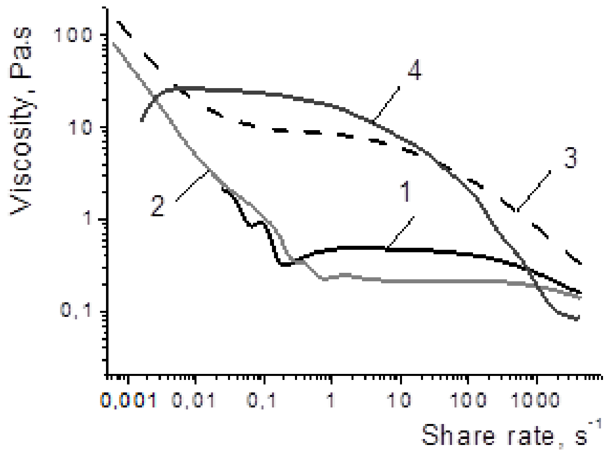

Figure 3 Dependences of viscosity on shear rate for 4% chitosan solutions. The numbers correspond to the sample numbers shown in the Table 1

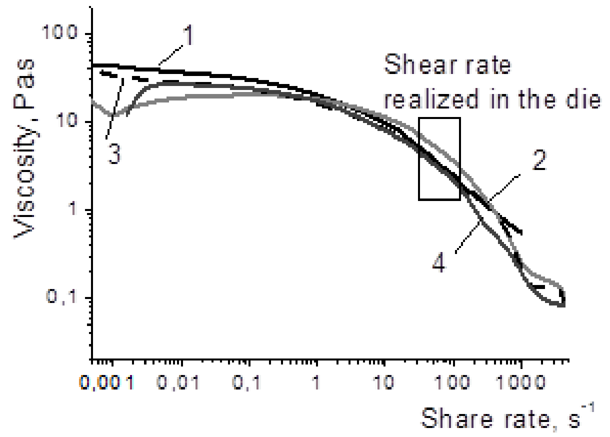

Figure 4 Dependences of viscosity on shear rate for chitosan solutions with different concentrations of chitosan: sample 1 – 6.3%, sample 2 – 5.5%, sample 3 – 5%, sample 4 – 4%

As seen in Figure 4 the dependences of viscosity on shear rate for these solutions are similar and have a nonlinear behavior. The slope of the curves increases substantially with an increase in the shear rate, the significant decrease of viscosity is observed at the shear rate of 10 s^{-1} or more. The decrease in viscosity upon an increase in the shear rate is related to the destruction of the initial structure of the polymer solution and the creation of a new oriented structure that means transition from isotropic state to anisotropic one. The formation of the anisotropic structure of the polymer solution under the action of shear field is typical of the majority of rigid-chain polymers.

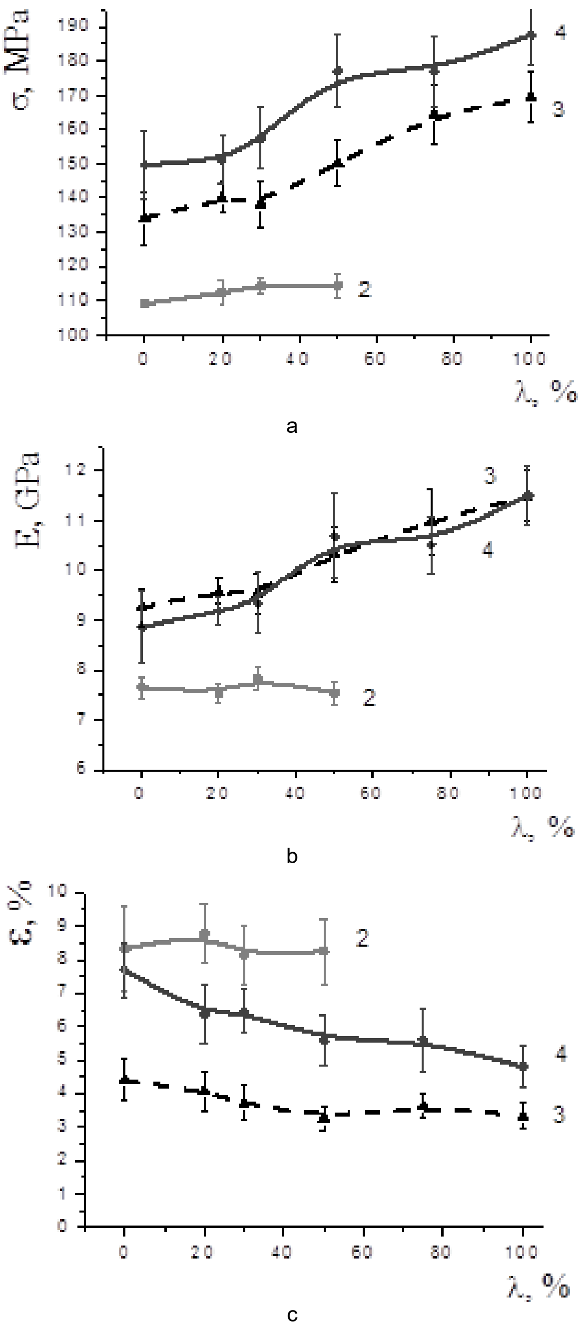

Figure 5 Dependences of the tensile strength (a), Young modulus (b) and elongation at break (c) of the chitosan fibers obtained from 4% solutions on the factor of orientation drawing (λ)

Studies of rheological properties have allowed determining the optimal concentrations of chitosan for processing (Table 2) and the feed rate of solution through die hole. It is shown in [4, 6] that oriented structure of the chitosan fibers is formed during flowing of the solution through the die hole. In turn, the orientation of the macromolecules depends on the shear stress occurring in the die hole. The optimum feed rate Q [mL/min] of the polymer solution through the die hole of the radius R can be calculated according to the proportion $Q = \pi \dot{\gamma} R^3/2$ which is correct for Newtonian liquids [10]. The shear rate $\dot{\gamma}$ should be quite high in order to provide good orientation of the macromolecules but not too high in order to make possible the complete coagulation of the fiber in the alkali/ethanol bath. Thus, the Q has been chosen to ~0.1-0.3 mL/min. This value corresponds approximately to the $\dot{\gamma} \sim 100\ s^{-1}$ as indicated in Figure 4. The solutions have possessed the necessary rheology characteristics preserving the laminarity of the jet in the coagulation bath after the flowing of the solution through the die hole.

It has been found [3, 4, 6] that optimal concentration of chitosan with M_{SD} = 2.1x10^5 g/mol for processing is 4%. In connection with this to study the molecular mass effect on mechanical properties, fibers from 4% chitosan solutions for samples 2-4 have been prepared (Figure 5). The fibers from 4% chitosan solutions for sample 1 could not be spun due to low viscosity of its solution.

It has been shown that molecular mass influences factor of orientation drawing (λ) and the mechanical properties of fibers. Maximum factor of orientation drawing for sample 2 was 50%, the maximum strength of fibers did not exceed 120 MPa. But, the fibers from sample 3 and 4 have been spun with factor of orientation drawing up to 100%, wherein the strength and Young modulus of these fibers grows considerably and elongation at break decreases with an increase in the drawing up to maximum factor of orientation drawing 100%. Fibers spun chitosan with molecular mass 2.1x10^5 g/mol have highest mechanical properties: strength is 188 ± 9.1 MPa, Young modulus is 11.5 ± 0.6 GPa, elongation at break is 4.8 ± 0.6 %.

The mechanical properties of chitosan fiber spun from solution with optimal concentrations of chitosan for each sample are given in the Table 2.

The molecular mass of chitosan doesn't effect on appearance of the fibers. All obtained fibers have a smooth surface and homogeneous internal structure (Figure 6).

Table 2 Properties of chitosan fibers

№ of chitosan sample	Optimal concentration of chitosan in solution [%]	Maximum orientation drawing [%]	Mechanical properties		
			Strength [MPa]	Young modulus [GPa]	Elongation at break [%]
1	6.3	40	110±8.3	7.7±0.6	3.9±0.7
2	5.5	80	156±4.4	10.3±0.4	4.1±0.8
3	4.0-5.0	100	169±7.3	11.5±0.5	4.6±0.8
4	4.0	100	188±9.1	11.5±0.6	4.8±0.6

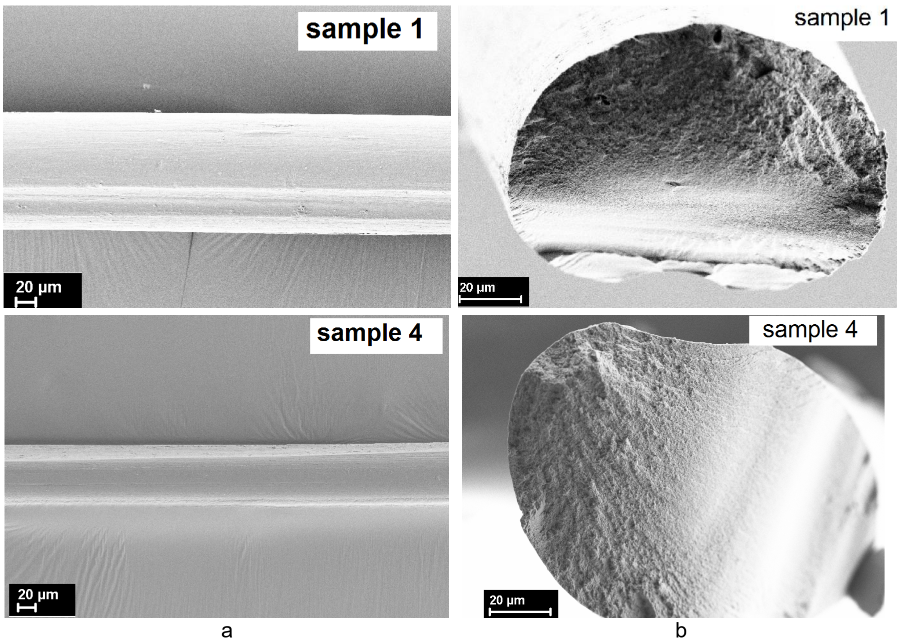

Figure 6 SEM micrographs of chitosan fibers: longitudinal view (a) and cross-section (b)

4 CONCLUSIONS

The molecular mass has a significant influence on the effective viscosity of chitosan solutions. The viscosity of solutions increases with increasing molecular mass, at the same time the optimum concentration of the solution for fibers processing decreases with increasing molecular mass.

The chitosan fibers have been prepared from an aqueous solution of 2% acetic acid by coagulation method. The concentration of polymer was optimal for each chitosan sample:

- 6.3% for chitosan with M_{SD} = 6.5x10^4 g/mol,
- 5.5% for chitosan with M_{SD} = 1.1x10^5 g/mol,
- 4-5% for chitosan with M_{SD} = 1.5x10^5 g/mol
- 4% for chitosan with M_{SD} = 2.1x10^5 g/mol.

The fibers with highest factor of orientation drawing (λ =100%) have been prepared from chitosan with M_{SD} = 2.1x10^5 g/mol, an increase in the strength ceases at $\lambda \sim$ 40% for chitosan sample with M_{SD} = 6.5x10^4 g/mol and $\lambda \sim$ 80% for chitosan sample with M_{SD} = 1.1x10^5 g/mol respectively. Fibers of the best mechanical properties have been spun with M_{SD} = 2.10x10^5 g/mol chitosan sample, whose fibers have a strength 188 ± 9.1 MPa and Young modulus 11.5 ± 0.6 GPa, elongation at break is 4.8 ± 0.6%.

The obtained fibres may be used for preparing the matrices for cell replacement technologies and tissue engineering, biodegradable surgical suture materials or hemostatic material.

Acknowledgement: *The authors are grateful to the Russian Science Foundation Grant # 14-33-00003 for financial support.*

5 REFERENCES

1. Vikhoreva G.A., Gal'braikh L.S.: Chitin and Chitosan. Preparation, Properties and Application [in Russian], Moscow, Nauka, 2002
2. Pillai C.K.S., Paul W., Sharma S.P.: Chitin and chitosan polymers: chemistry, solubility, and fiber formation, Progress in Polymer Science 7(34), 2009, pp. 641-678, doi: 10.1016/j.progpolymsci.2009.04.001
3. Popryadukhin P.V., Dobrovol'skaya I.P., et al.: Composite materials based on chitosan and montmorillonite: prospects for use as a matrix for cultivation of stem and regenerative cells, Cell and tissue biology 1(6), 2012, pp. 82-88, doi: 10.1134/S1990519X12010099
4. Dobrovol'skaya I.P., Popryadukhin P.V., Dresvyanina E.N. et al.: Structure and characteristics of chitosan-based fibers containing chrisotile and halloysite, Polymer Science. Series A 5(53), 2001, pp. 418-423, doi: 10.1134/S0965545X11050038
5. Haji A., Mehrizi M.K., Hashemizad S.: Plasma and chitosan treatments for improvement of natural dyeing and antibacterial properties of cotton and wool, Vlakna a Textil (Fibres and Textiles) 23(3), 2016, pp. 86-89
6. Dresvyanina E.N., Dobrovol'skaya I.P., et al.: Influence of spinning conditions on properties of chitosan fibers, Fibre chemistry 5(4), 2013, pp. 280-283, doi: 10.1007/s10692-013-9446-8
7. Yudin V.E., Dobrovolskaya I.P., et al.: Wet spinning of fibers made of chitosan and chitin nanofibrils, Carbohydrate Polymers 108, 2014, pp. 176-182, doi: 10.1016/j.carbpol.2014.02.090
8. Hiroshi Tamuraa, Yukihiko Tsurutaa, et al.: Preparation of chitosan filament applying new coagulation system, Carbohydrate Polymers 56, 2004, pp. 205-211, doi: 10.1016/j.carbpol.2004.02.003
9. Dobrovolskaya I.P., Yudin V.E., et al.: In vivo Studies of Chitosan Fiber Resorption, J. Appl. Cosmetol. 33, 2015, pp. 81-87
10. Baird D.G.: Viscometry of anisotropic solutions of poly-p-phenyleneterephthalamide in sulfuric acid, Journal of Appl. Polymer Science 22, 1978, pp. 2701-2706

DEVELOPMENT & RESEARCH ON CONSUMER PROPERTIES OF INTEGRATED TWO-LAYER WEFT KNITTED FABRIC FROM ECO-RAW MATERIALS

Liudmyla Halavska and Oleksandra Batrak

Kyiv National University of Technologies and Design, 2 Nemirovich-Danchenko Str., 01011 Kyiv, Ukraine
galavska.ly@knutd.com.ua; sasha01021@gmail.com

Abstract: *Nowadays a lot of people pay attention to various aspects that can preserve and improve their health and standard of living. Therefore, ecological knitwear of a functional purpose made of natural raw materials becomes popular. The authors developed the structure and proposed the set factors for producing the integrated knitted fabric where hemp or nettle yarn will be used to form one of the layers in two-layer knitwear. Such fabric may be used as a functional textile material for manufacturing the linen products of medical treatment and preventive care, in particular for the underwear of wounded servicemen during their treatment and rehabilitation. The new structure is a two-layer fabric with forged connection of layers by main threads. Connecting forged yarn-overs in the fabric are arranged in staggered manner. At places of connecting yarn-overs, blind holes are generated; they provide ventilation and rapid water removal from under the clothes. In the research, it is determined how the type of eco-raw material of one of the layers in integrated two-layer knitwear influences on the linear dimensions of knitwear, the relaxation properties, the level of capillarity and the change in the liquid level in time.*

Keywords: *eco-textiles, environmentally friendly knitwear, hemp yarn, nettle yarn, knitwear, multifunctional knitwear.*

1 INTRODUCTION

The variety of chemical composition and physical-mechanical properties of raw materials makes it possible to obtain knitted materials with predefined properties. A number of experiments are conducted in our laboratories in order to study various physical and mechanical properties of knitted fabric made from natural yarn and to change their properties when this yarn is combined with modern, artificially manufactured components for creating multifunctional knitwear.

Along with such widely known types of natural raw materials as cotton and wool, nowadays items from little-known and still poorly studied types of ecologically pure raw materials become popular. This may be yarn from eucalyptus, banana, coconut, soy, bamboo, maize, hemp and nettle. Along with antibacterial and antiseptic properties, such materials have positive preventive and sometimes also therapeutic effect on a person. From the point of view of tactile sensations, eco-materials do not irritate the skin, and do not become electrified. If eco-raw materials are used to form a functional layer of integrated knitwear, then textile material of medical treatment and preventive care will be formed. In particular, such materials will be helpful for the underwear for wounded servicemen during their treatment and rehabilitation, as well as for use in field operations during warfare.

The purpose of this work is to develop & research consumer properties of integrated two-layer weft knitted fabric from eco-raw materials. In experimental studies, we planned to find out the influence of the type of eco-raw material on the technological shrinkage of integrated knitwear, deformation properties and capillarity.

2 MATERIAL

The advantages of eco-yarn from hemp and nettle over the cotton are obvious. Hypoallergenic properties (very low allergenic capacity) of this yarn are achieved due to the absence of toxic chemicals in the raw materials; these chemicals may be used to control weeds, plant pests and diseases of cultivated plants. The costs of growing hemp and nettle are relatively small while therapeutic and environmental effects are beneficial. Items from hemp yarn are widely used now. Products from this yarn have high consumer and hypoallergenic properties. They create a temperature and energy balance, have antiseptic, wound-healing and anti-allergic functions. Thanks to the porous structure, hemp fibre retains heat and absorbs moisture (it allows the body to breathe during heat). Contact with endocrine glands has rather positive effect on nervous and cardiovascular systems. Hemp fibre reflects ultraviolet radiation. Medical scientists have proved that treatment of small wounds and scars with dressing material from hemp fibre speeds up the healing process by three times. The reason is that hemp fibre retains up to 20% of the oil in its composition; this oil is an effective wound-healing agent [1-3].

But hemp fibre is quite tough and non-uniform in thickness. A large amount of admixtures (a large percentage of inclusions in fibre) complicates the situation. If the yarn is rewound, the influence of these factors is reduced. Thanks to the waxing, the yarn becomes more uniform. To improve the knitting capacity of hemp yarn, moisturizing is necessary.

Little-known raw materials from nettle also have health benefits. It is proved that nettle products help with illness, such as headache and pain in joints. Nettle items improve blood circulation; have a calming effect on the nervous system; favourably affect sleep, overall well-being and even the mood of a person (joy, calmness and confidence); cause pleasant feelings. They help to cope with depression, loss of energy and fatigue. These items have a favourable effect on biologically active points, that is, they harmonize the work of inner parts of human body. They have a warming effect due to which they help to eliminate the inflammatory and stagnant processes in the body. That’s why people use nettle belts and plates as the first aid from pain [4-6].

Nettle raw materials are treated in the same way as flax. The production of nettle yarn is not complicated but it is rather time-consuming [2].

The above mentioned facts enable us to speak of high hygienic properties of knitted fabric made from hemp and nettle yarn. As eco-raw materials from nettle and hemp have advanced medical properties, it is very important to expand the range of their further use, including in underwear for medical treatment and preventive care.

Adequate quality of knitwear is an important problem in the production of special-purpose clothing. Quality parameters of such clothing (sport, underwear, protective), including therapeutic effect, are determined by such consumer properties as changes in linear dimensions after washing, relaxation parameters and capillarity. If the influence of the raw material type in integrated knitwear layers on its consumer properties is determined, then it will ensure the production of knitwear with predefined quality.

A number of scientists tried to the forecast the sorption capacity of knitted fabric with a hydrophobic synthetic polyester thread [1-7]. The authors of the paper draw conclusions about the influence of the knitting density, the special features of structure formation and the type of raw material on the sorption capacity of knitted fabrics. The ability of a knitted fabric to remove vaporous moisture from a human body to the outside of a linen or protective item is an important factor that influences bodily comfort [8, 9]. Therefore, it is necessary to examine the influence of raw materials of integrated knitwear on capillarity and the method of moisture withdrawal.

There is also no information on the influence of these types of eco-raw materials as a hydrophilic layer of integrated knitwear on its functional properties.

3 EXPERIMENTAL

3.1 Material

Despite all the positive features, hemp and nettle fibres are very non-uniform in thickness and quite tough. That’s why these materials are not widely used in knitwear. A lot of admixtures in hemp and nettle make it almost impossible to process these yarns on knitting equipment. Therefore, it is necessary to conduct further research in order to find out parameters that provide normal process of stitch formation [10].

The authors developed technology for production of integrated two-layer knitwear with forged connection of layers by main threads; this technology is produced for the two-bar circular knitting machine. In the fabric, the connecting yarn-overs are arranged in staggered manner. At places of connecting yarn-overs, blind holes are generated; they provide ventilation and rapid water removal from under the clothes.

Graphical record of the weave structure in two-layer knitted fabric is presented in Figure 1.

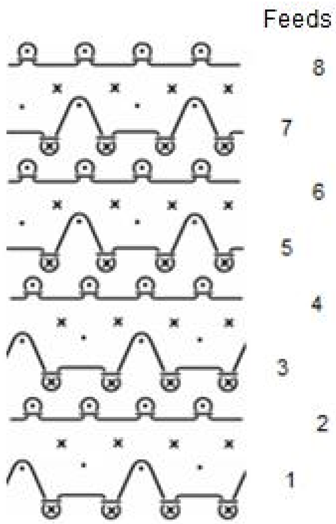

Figure 1 Weave structure (graphical record)

This structure makes it possible to obtain knitted fabric with a clear distinction of functional layers. One layer is of synthetic threads (for withdrawal of vaporous moisture from underwear), the other – of natural one (absorbing and rapidly evaporating moisture). The authors suggest that hemp or nettle yarns should be used as raw materials for hydrophilic layer in two-layer knitwear; these yarns provide therapeutic and preventive properties of knitted fabric.

To form a hydrophobic layer, it was decided to use anti-allergic polyester thread with high capillary capacity. This thread also provides elasticity, shape retention and thermal regulation; it also makes these items attractive to consumers. Moreover, this type of raw material is inert to the development of pathogenic microflora due to its hydrophobic property, it does not absorb extraneous odours and dirty spots may be easily removed during washing.

The set factors for fabric in the developed functional samples are presented in Table 1.

Table 1 Set factors for knitted fabrics

Sample No.	Type of raw materials in knitting system	Linear density [tex]
1	1, 3, 5, 7 Feeds – hemp yarn	25X2
	2, 4, 6, 8 Feeds – polyester thread	16.7
2	1, 3, 5, 7 Feeds – nettle yarn	31X2
	2, 4, 6, 8 Feeds – polyester thread	16.7

The samples were made on a two-bar circular knitting machine of 16th class with a ribbed arrangement of needles. To improve the knitting capacity of hemp and nettle raw materials, the yarn was rewound three times. The rewinding of the yarn made it possible to remove its admixtures and non-uniformity in thickness. In order to reduce the flexural rigidity of the yarn, it was moistened before knitting.

3.2 Shape stability

Shape stability is an important consumer property of sport and linen knitted fabric. These fabrics have to retain their shape in everyday use and after multiple washing cycles. Shrinkage parameters of knitted fabric patterns (removed from machine) after washing and drying are determined according to a standard procedure [11].

In this research, the authors determined in which way the type of eco-raw material influences linear dimensions (technological shrinkage after washing and drying) of the samples of integrated two-layer knitwear after washing and drying. Parameters of developed functional fabrics before and after the first washing are presented in Table 2.

As a result of the first washing, shrinkage of knitted fabric removed from machine took place both along the length and width. The diagrams shown in Figure 2 illustrate the average values of technological shrinkage parameters of knitted fabrics (removed from machine) after the first stage of washing and drying (confidence probability 95%).

The following washing did not cause further change in linear dimensions of samples.

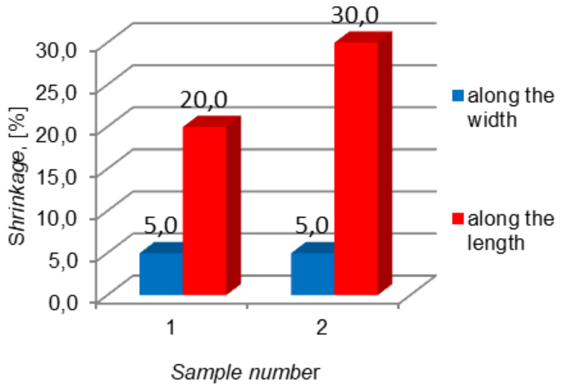

Figure 2 Technological shrinkage of knitted fabric removed from machine after the first stage of washing and drying

In this research it was found that technological shrinkage along width after washing and drying does not depend on the type of eco-raw material of the hydrophilic layer and is equal to 5%. The peculiarities of structure formation in two-layer knitwear, namely the presence of connecting forged yarn-overs, may explain considerable shrinkage along the length, about 20-30%. Significant shrinkage along the length is also caused by moistening of the yarn. When moistened, the connecting yarn-overs (formed from the raw material of considerable rigidity) are aligned due to elastic properties of the thread.

The kind of eco-raw material of the hydrophilic layer in the integrated two-layer knitwear affects the technological shrinkage along the length after washing and drying. If hemp yarn is changed to nettle yarn, then shrinkage along the length of knitwear is increased by 50%. The reason is that nettle yarn has the greater flexural rigidity compared to the hemp yarn.

Significant shrinkage along the length leads to increase in surface density: sample 1 - by 40%, sample 2 - by 70%. The increase in surface density after washing leads to an increase in material consumption of the product. To reduce the shrinkage along the length and, correspondingly, the surface density, it is necessary to reduce the frequency in arrangement of the connecting yarn-overs along direction of knitting.

Table 2 Parameters of knitted fabrics

Sample No.	Before washing			After washing		
	number in 100 mm of knitwear		surface density m_s [g/m^2]	number in 100 mm of knitwear		surface density m_s [g/m^2]
	wales	*courses*		*wales*	*courses*	
1	75	95	255	80	130	355
2	80	90	242	85	130	411

3.3 Deformation characteristics

Shape stability of knitwear may be evaluated based on the known components of the deformation relaxation: fast-moving, slow-rotating and residual. The deformation properties of the samples are determined according to standard procedure [12]. In determining tensile strain of knitwear, the load value was constant and equal to 6 N. The results of the research are presented as graphs (see Figures 3 and 4).

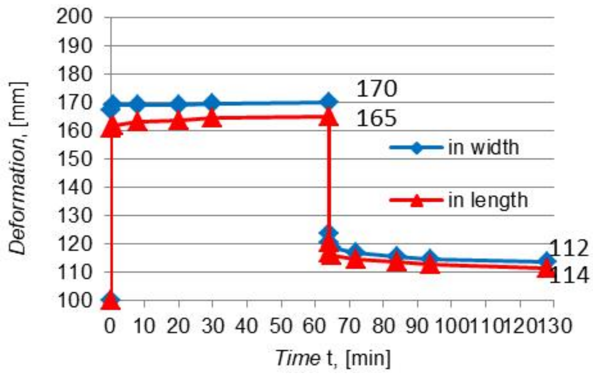

Figure 3 Deformation and relaxation of deformations for the sample 1

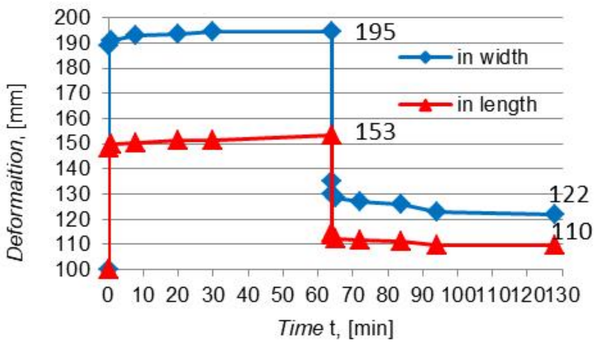

Figure 4 Deformation and relaxation of deformations for the sample 2

As can be seen from the graphs (Figures 3, 4), deformation of samples of knitted fabrics at a load of 6 N is similar. Both for the hemp and nettle yarns, the total deformation in tension along the width (along the wale) is greater than along the length (along the course). However, in sample 2, it varies up to 3%. Compared to sample 1, the total deformation in width is 15% greater, in length - 7% smaller. The residual deformation of the prototypes is within the range 18-23%. This indicates a sufficient elasticity and shape stability of knitted fabrics. Greater part of residual deformation when sample 2 is stretched along the length (by 15%) may be explained by the greater flexural rigidity of the nettle yarn and the greater coefficient of friction for the thread-by-thread, which prevents the reverse process of thread redistribution from the sticks of the hinges to the slip stitch. The diagrams presented in Figures 5 and 6 clearly illustrate the components of the deformation relaxation of the samples. Knitted fabric, where the face layer is produced from nettle yarn, is less shape-stable in length. The obtained results make it possible to predict the behaviour of knitwear under service loads.

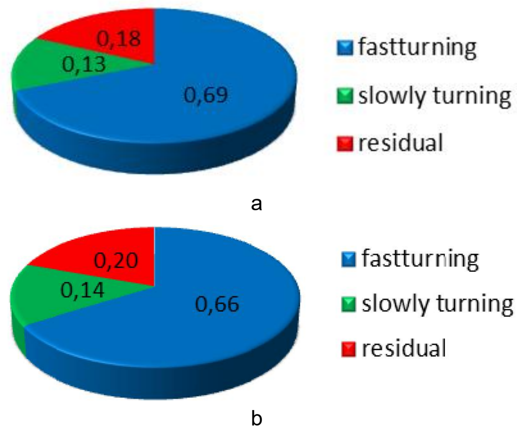

Figure 5 Components of deformation in sample 1 along width (a) and length (b)

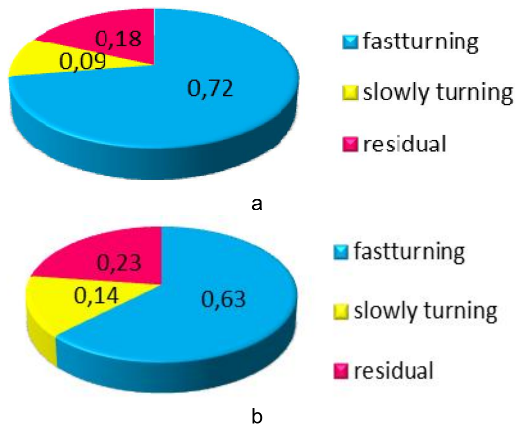

Figure 6 Components of deformation in sample 2 along width (a) and length (b)

3.4 Capillarity

To determine capillarity means to measure the height of the capillary rise of the coloured liquid in 60 minutes' experiment along vertically placed sample of two-layer knitwear. Capillarity of the developed samples of bicomponent two-layer knitwear was examined according to the standard procedure [13]. Capillarity of the developed knitted fabric samples is determined along the wales (along the width of fabric) and the courses (along the height of fabric) both from the hydrophilic side and from the side of the hydrophobic layer. Table 3 shows the average values for the rising in liquid level along the courses and wales in case of hydrophilic layer from hemp yarn (sample 1).

Table 3 Results for raising the liquid level in time, sample 1

Duration of experiment [min]	Raising of liquid level from the side of hemp layer [mm]		Raising of liquid level from the side of polyester layer [mm]	
	along courses	along wales	along courses	along wales
5	5.5	5.6	4.4	2.9
10	7.5	8.4	5.8	4.3
15	9.3	9.3	6.2	5.1
20	10.2	10.1	6.6	5.3
25	10.9	10.8	6.9	6.3
30	11.6	11.5	7.2	6.7
35	12.2	12.1	7.4	7.2
40	12.4	12.5	7.6	7.4
45	12.6	12.9	7.8	7.7
50	12.9	13.1	8.0	8.0
55	13.1	13.4	8.2	8.2
60	**13.3**	**13.6**	**8.3**	**8.4**

To clearly visualize results of research and to determine in which way the height of liquid level depends on the time of experiment, appropriate graphs are generated (see Figures 7 and 8).

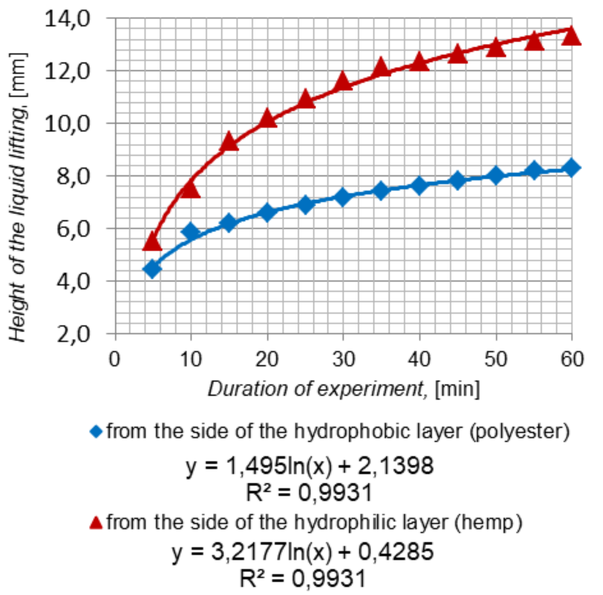

Figure 7 Raising the liquid level along the courses, sample 1

As seen from the graphs, the liquid level from the side of the hydrophilic layer (hemp yarn) is higher than from the hydrophobic side (polyester thread). It is explained by the capillary properties of the raw material.

The difference in liquid levels at the 60th minute of experience, which corresponds to the level of capillarity, along courses is 5.0 mm, along the wales - 5.2 mm. The level of capillarity along the wales is higher because of the high degree of thread orientation in stitches in the direction of wales.

During experiment, the liquid level from the side of the hydrophilic (hemp) layer along the courses is increased by 141.8%, along the wales - by 142%; from the side of the hydrophobic layer (polyester) along the courses - by 88.6%, along the wales – by 189.7%. Thus, the dynamic of liquid level raising from the hemp layer side does not depend on the direction of experiment. But from the side of the hydrophobic layer, the speed of liquid level raising along the wales is more than 2 times higher than along the courses. This may be explained by considerable shrinkage along the length and an increase in fitting density in connecting forced yarn-overs from the side of the hydrophilic layer (hemp yarn).

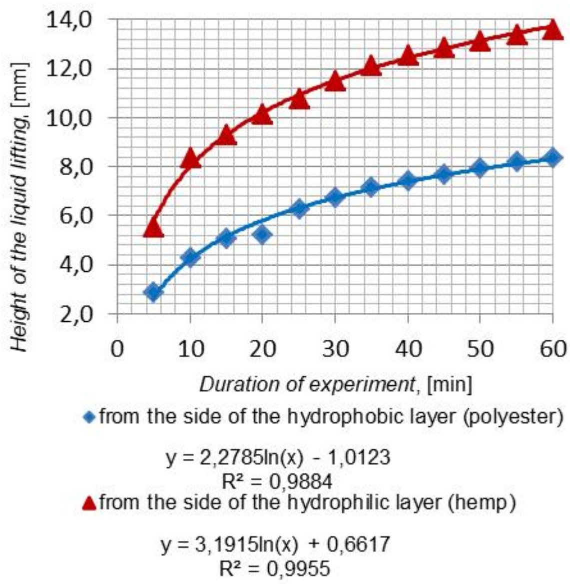

Figure 8 Raising the liquid level along the wales, sample 1

Table 4 shows the average values of liquid level raising along the courses and wales in case of formation of the hydrophilic layer from the nettle yarn (sample 2). Based on the data in Table 4, graphs are generated (see Figures 9 and 10).They clearly illustrate in which way the raising of liquid level depends on the time of experiment.

Table 4 Results for raising the liquid level in time, sample 2

Duration of experiment [min]	The liquid raising from the side of the hemp layer [mm]		The liquid raising from the side of the polyester layer [mm]	
	along the loop rows	along the loop columns	along the loop rows	along the loop columns
5	6.2	5.5	5.8	3.9
10	7.9	7.6	6.9	5.1
15	9.5	8.8	7.9	6.3
20	10.4	9.6	8.4	7.1
25	11.2	10.4	8.8	7.6
30	11.7	11.0	9.1	8.1
35	12.1	11.3	9.5	8.5
40	12.3	11.6	9.8	8.7
45	12.6	11.9	10.2	9.0
50	12.8	12.2	10.4	9.2
55	13.1	12.6	10.7	9.5
60	**13.3**	**12.8**	**10.9**	**9.7**

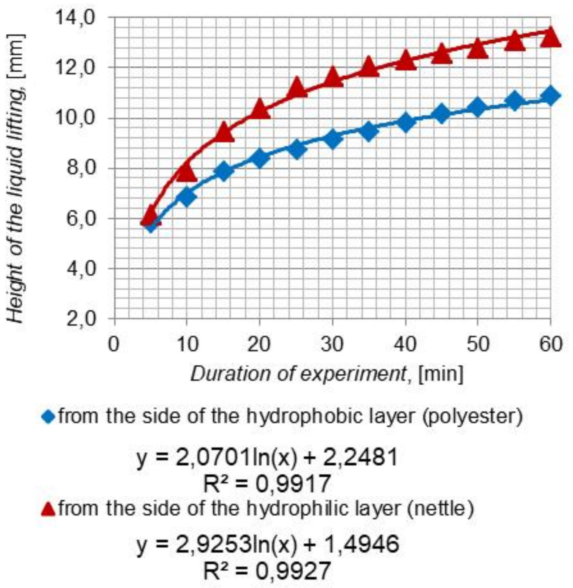

Figure 9 Raising the liquid level along the courses, sample 2

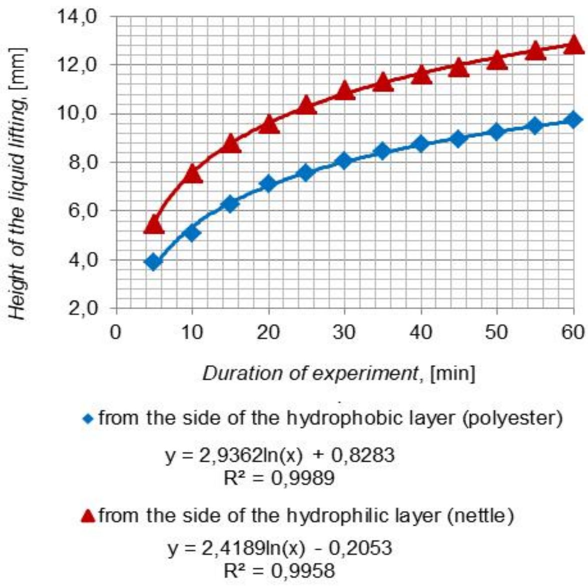

Figure 10 Raising the liquid level along the wales, sample 2

As seen from the graphs, as in sample 1, the liquid level from the side of the hydrophilic layer along the courses and wales is higher than from the side of the hydrophobic layer. The liquid level from the side of the hydrophilic layer along the wales is 15% lower than along the courses.

During experiment, the liquid level from the side of the hydrophilic (nettle) layer along the courses is increased by 114.5%, along the wales - by 132.7%; from the side of the hydrophobic layer (polyester) along the courses - by 87.9%, along the wales – by 148.7%. Thus, the dynamic of liquid level raising along the wales is higher than along the courses. And for a hydrophobic layer, the height of the liquid level raising along the wales is almost 2 times higher than along the courses. This is explained by considerable shrinkage of the knitted fabric along the length (30%).

The indicator of capillarity level of textile material is the height of liquid level at the 60th minute of the experiment. According to the data obtained in Tables 3 and 4, the corresponding capillarity diagrams along the course and wale (Figures 11, 12) are generated; they clearly illustrate the influence of the type of raw material (from which the hydrophilic layer of integrated two-layer knitwear is formed) on the level of capillarity.

As can be seen from the diagrams presented in Figure 11, the capillarity from the hydrophilic layer does not depend on the type of eco-raw material. This may be explained by the same vegetable origin of hemp and nettle eco-raw materials. Moreover, the direction in which capillarity was determined is insignificant. The level of capillarity both along the wales and courses is almost the same.

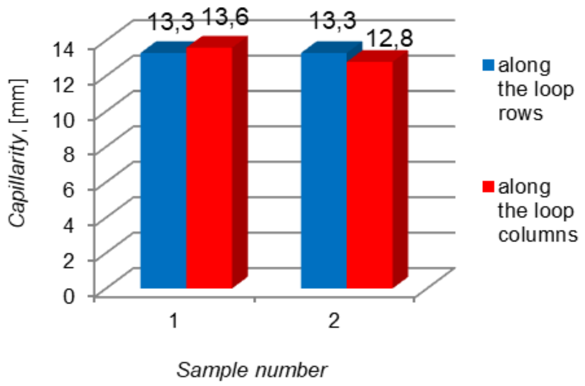

Figure 11 Diagrams of capillarity of the developed samples of two-layer bicomponent knitwear from the side of the hydrophilic (hemp or nettle) layer

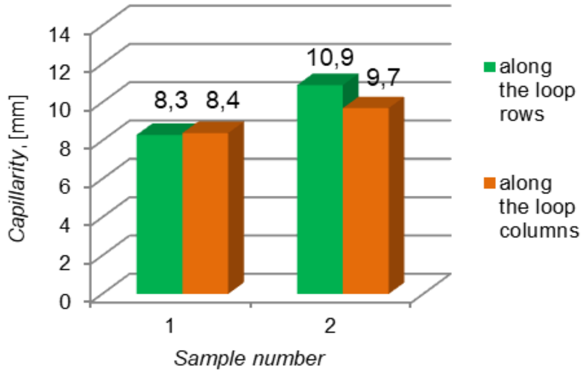

Figure 12 Diagrams of capillarity of the developed samples of two-layer bicomponent knitwear from the side of a hydrophobic (polyester) layer

Connecting elements (from hydrophilic raw materials) that are present in the structure of two-layer knitwear influence the capillarity of hydrophobic layer. However, the type of eco-raw material in the hydrophilic layer (from which connecting yarn-overs are formed) has an influence on the capillarity level from the hydrophobic layer. If the hydrophilic layer is formed from the nettle material, then the capillarity level on the side of hydrophobic layer increases along the courses by 31%, along the wales - by 15.5% (Figure 12).

A greater shrinkage along the length of bicomponent knitwear (where nettle yarn and connecting yarn-overs from it are used as a hydrophilic layer) may be explained by the fact that elastic properties of the yarn appear in horizontal stretches, in particular, by considerable flexible rigidity of the yarn.

4 CONCLUSIONS

When developing bicomponent knitted fabrics in order to form functional properties, special attention should be paid to the type of raw material from which the hydrophilic layer of integrated knitwear is formed. To develop textile material for the items of medical treatment and preventive care, it is advisable to use such eco-raw materials as hemp and nettle.

In experiments on consumer properties of the developed samples of integrated two-layer knitwear, the influence of the type of eco-raw material on linear dimensions was determined. When nettle yarn (from which connecting yarn-overs of the two-layer knitwear are formed) is used for a hydrophilic layer, the shrinkage along the length is increased by 50%. This is due to a significant flexural rigidity of nettle yarn compared to hemp. The deformation properties of knitted fabric are determined. The part of residual deformation (that indicates the shape stability of textile material) is the same along the width of samples and is equal to 0.18. But the part of residual deformation along the length of sample 2, produced from nettle, is more by 15%. The higher coefficient of thread-by-thread friction in the nettle yarn prevents the deformation relaxation. Obtained results enable us to predict the behaviour of knitwear under service loads.

In the study on capillarity, the influence of type of eco-raw material on the capillarity level of samples is determined. The change in liquid level is determined in time over the functional layers of the integrated two-layer knitwear using the eco-raw material as the hydrophilic layer. The results of studies on the water-absorbing properties of bicomponent two-layer knitwear testify that type of raw material of the hydrophilic layer has an influence on the capillarity level from the hydrophobic side. It was found that the capillarity in sample 2 from the side of the hydrophobic layer is higher than that of sample 1: along the courses - by 31%, along the wales - by 15.5%. More significant influence in the direction of the courses is explained by the transverse direction of the formation of stitches from one yarn in the course of knitwear.

5 REFERENCES

1. Halavska L., Batrak O.: The properties of weft knitted fabric medical and preventive treatment action using eco-raw materials, IOP Conference Series: Materials Science and Engineering 141(1), 2015, pp. 012013, doi: 10.1088/1757-899X/141/1/012013
2. Rastorgueva M.Y., Zakora O.V.: Problems of using bast fibers in the textile industry, In: Proceedings of the Third International Scientific and Practical Conference "Science in the Information Space", October 29-30, 2007
3. Hemp [Electronic resouce]. – Access mode: http://buklib.net/books/30385/
4. Galik I.S., Semak B.D.: Ecological safety of textiles: problems and solutions, Journal of KHNU: Technical sciences 6(219), 2014, pp. 88-90
5. Suprun N.P., Vlasenko V.I., Arabuli S.I.: Textiles and multifunctional textile composite materials in products for the disabled and seriously ill, KNUTD, 2011, 182 p.

6. Suprun N.P., Shchutskaya G.V.: Modern problems of safe-to-use and environmentally friendly textiles production, Kafedra, 2013, 112 p.
7. Achour N.S., Hamdaoui M., Ben Nasrallah S.: Sorption ability & wicking on knitted fabrics: experimental and theoretical studies, Vlakna a Textil (Fibres and Textiles) 24(2), 2017, pp. 25-31
8. CSE. Study on pollution of Bandi river by textile industries in pali town, Centre for Science and Environment, 2006
9. Stämpfli R., Brühwiler P.A., Rechsteiner I., Meyer V.R., et al.: X-ray tomographic investigation of water distribution in textiles under compression – Possibilities for data presentation, Measurement: Journal of the International Measurement Confederation 46(3), 2013, pp. 1212-1219, doi: 10.1016/j.measurement.2012.11.009
10. Halavska L.: Research of double-layer bicomponent knit content of hemp yarn on the capillarity, VISNYK KNUTD 5(90), 2015, pp. 183-191
11. DSTU ISO 5077-2001. Textile materials. The method of the linear dimensions changes after washing and drying
12. GOST 8847-85. Knitted fabrics. Methods for determining discontinuous characteristics and extensibility under loads less than discontinuous
13. DSTU GOST 3816:2009 (ISO 811-81). Cloths textile. Methods for determination of hygroscopic and water-repellent properties

PERMEABILITY PROPERTIES AND ABRASION RESISTANCE OF COATED POLYPROPYLENE FABRICS

Sukran Kara, Sevil Yeşilpinar and Aysun Akşit

Dokuz Eylul University, Engineering Faculty, Textile Engineering Department, Turkey
sukran.kara@deu.edu.tr

Abstract: *Protective garments constitute an important class of technical textiles and they serve for various application areas such as active sports, military, medicine and fire-fighting. One of the most shared properties of protective garments is providing a barrier against water or liquid penetration. Also these garments should exhibit water vapour permeability and protect from wind in order to maintain wearer comfort. These expectations for the protective garments may be provided by waterproof-water vapour permeable coatings.*

In this study, polypropylene fabric was coated in order to examine its usability in protective sportswear. Effects of coating polymer type and curing temperature on the specimen permeability properties and abrasion resistances were investigated in order reveal their usability. According to test results, waterproofness of samples did not increase to the desired levels but windproof samples were obtained from coated polypropylene samples. Polyether type polyurethane coated samples gave more preferable and consistent results when compared to polyether type polyurethane coated equivalents after washing. Coating improved the abrasion resistance of all coated samples.

Keywords: *coating, polyurethane type, curing temperature, polypropylene fabrics, protective garments, permeability properties, abrasion resistance, scanning electron microscopy.*

1 INTRODUCTION

Protective garments possess various functional properties such as resistance to chemicals, fire retardancy, ballistic protection etc. according to their end-uses. In addition, most of the protective garments are expected to show waterproofness at least to a certain level. For this purpose, coating or lamination is applied to protective fabrics [1, 2]. Some functional properties such as fire retardancy, liquid and dust impermeability and hand changes can also be provided by coating.

Coated fabrics can be defined as engineered flexible composite materials that are coated with a polymer layer from one or both sides. Woven, knitted or non-woven fabrics can be used as the base fabrics for coating. Coating polymers are applied to base fabric surfaces as viscous solutions or dispersions. After the application of the polymer layers, the liquid phase is removed by heat and the polymer forms a continuous layer on the fabric surface. Coating can be applied by using hot melt polymers, too [3-5].

Main polymers for textile coating are natural and synthetic rubber, polyurethane (PU), polyacrylic, polyvinyl acetate and polyvinyl chloride [6]. In addition to these main types, their variants, copolymers and terpolymers are also synthesized for coating. PU is a multipurpose coating polymer which can be used for the coating of protective garments, upholstery, artificial leather, inflatable boats and etc. PU is not a single polymer but it consists of a polymer group with similar chemical structure. The repeating unit of PU is given in Figure 1. By changing the R, R' groups, various PU types can be obtained and desired properties can be engineered. Mostly known types of PU polymers are polyether and polyester types for textile coatings. Polyester and polyether type PUs can give different modulus, tensile strength, hardness, thermal oxidative stability or hydrolytic stability to the end product [6, 7].

PU coating polymers may be solvent-based or water-based. PU coatings are frequently done by using organic solvents. This increases problems such as flammability, toxicity, disposal and recycling. Also solvent systems are usually more expensive. Water-based PU types are more attractive as they are eco-friendly and less harmful for human health during production. Using water based coating polymers may be a good alternative for textile applications [6, 8].

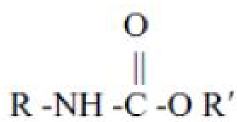

Figure 1 Urethane [5]

Polypropylene fiber (PP) consumption is increasing day by day according to its advantageous properties such as low cost, lightweight, wicking property and fast drying. However, it is not preferred for protective garments as it has some technical problems like low melting point [9].

In the literature, research works exist in which common fabrics were coated and their properties such as water resistance, water vapour permeability, mechanical properties and etc. were tested to be used in different areas. In these researches mostly cotton [10, 11], polyamide [12-17], polyester [18] and blended fabrics [15, 19, 20] were coated. Polypropylene was coated very rarely [21]. Mostly used coating polymers at these studies were PU, PU copolymers or PU blends as PU is a versatile polymer.

In this study, polypropylene fabrics were coated in order to create an alternative for protective garments. This is expected to expand the usage of polypropylene fibers.

Two PU coating polymer types and two curing temperatures were selected as the experimental variables for this study. As mentioned before, PU polymer can be engineered by using different kinds of monomers. Therefore, in this study, coatings were made by using both polyether and polyester based PU coating polymers in order to make comparisons for permeability properties [6]. Water-based PU types were selected as the coating polymers of this study due to their advantageous properties.

2 MATERIALS AND METHODS

2.1 Materials

Polypropylene base fabric, aliphatic polyether (R) based PU, polyester (W) based PU, cross-linking agent and thickener were the materials of this study. Properties of polypropylene base fabric are given in Table 1.

2 types of water-based PU dispersion were used for coatings in this study. Properties of coating polymers are given in Table 2.

An anionic, blocked isocyanate type cross-linking agent was used as the auxiliary material. Density of the cross-linker is 1.1 g/cm^3 at 25°C and the pH is 7-10.

As the thickener, anionic acrylic polymer dispersion was used. Density of the thickener is 1.1 g/cm^3 at 20°C and the pH is 6.

Table 1 Properties of PP base fabric

Yarn type	Weave	Warp density [warp/cm]	Weft density [weft/cm]	Unit mass [g/m^2]
100% PP multifilament	2/2 twill	56	40	76

Table 2 Properties of coating polymers

Polymer type	Polyether type PU (R)	Polyester type PU (W)
Chemical structure	Aliphatic polyether polyurethane dispersion	Polyester polyol and aliphatic isocyanate polyurethane dispersion
Appearance	White dispersion	White emulsion
Ionic structure	Anionic	Anionic
pH	7.5-8.0	7.0-9.0
Density (at 25°C)	1.0 g/cm^3	1.06 g/cm^3
Viscosity (at 25°C)	50-400 cps [centipoise]	50-400 cps

2.2 Methods

Methods of the study consist of coating of samples and analyses of the obtained samples.

2.2.1 Coating

Recipes of coating pastes are given in Table 3.

Viscosities of the coating pastes were measured by using Brookfield viscometer. Polypropylene base fabrics were coated with the above mentioned coating pastes by using laboratory type blade coating machine, as two layers of coating. Coated samples were cured at 120 and 140°C for 2 minutes.

As a result, 4 types of coated samples were obtained by changing the polymer type and curing temperature. Samples were coded as in Table 4.

Table 3 Polyether and polyester type PU coating pastes

Content	Polyether type PU paste	Polyester type PU paste
PU [parts]	100	100
Cross-linking agent [parts]	10	10
Thickener [parts]	0.3	0.7
Viscosity [cps]	9000	27800

Table 4 Codes of samples

Polymer type	Curing temperature	Sample code
Polyether type PU (R)	120°C	R120
	140°C	R140
Polyester type PU (W)	120°C	W120
	140°C	W140

2.2.2 Fabric tests

Coated samples were tested in order to reveal their usability for protective garments. As permeability properties; air permeability, water vapour permeability and waterproofness of samples were determined before washing and after 5 washing cycles. Also sample abrasion resistances were tested. Sample thicknesses and unit mass values were determined in order to detect the physical changes of samples after coating. In addition, fabric surfaces were evaluated by using scanning electron microscope (SEM).

All the tests were performed under standard atmosphere conditions (20±2°C temperature and 65±2% relative humidity).

Determination of sample thickness and unit mass

Unit mass changes of samples are related to added polymer by coating. To determine the add-on value, sample unit mass values were determined before and after coating process according to TS 251 standard [22]. Add-on [%] values were calculated according to:

$$\text{add-on}\,[\%] = \frac{w_s - w_i}{w_i} \times 100 \qquad (1)$$

where: ws - unit mass after coating, wi - unit mass before coating.

Thickness values of samples were determined according to TS 7128 EN ISO 5084 standard [23] by using James Heal RxB Cloth Thickness Tester under 5 g/cm^2 pressure. Thickness and unit mass measurements were repeated 5 times for each sample type.

Determination of air permeability

Air permeability of samples was measured according to TS 391 EN ISO 9237 standard [24] by using Textest FX3300 air permeability tester. Air pressure was kept as 200 Pa during test. Measurements were performed on 20 cm^2 sample area and test was repeated for 15 times for each sample type.

Determination of water vapour permeability

Water vapour permeability is related to breathability of samples. Water vapour permeability of samples was determined by using SDL Atlas International M261 model water vapour permeability tester, according to BS 3424-34: 1992-Method 37 [25]. The amount of water vapour passed through the samples was determined after 24 h and permeability values were calculated. Test was repeated 3 times for each sample type.

Determination of waterproofness

Waterproofness values of samples were determined according to TSE 257 EN 20811 standard [26] by using Textest FX 3000 Hydrostatic Head Tester III. Pure water was used as the test liquid. Water pressure gradient was kept 60 cm/min during tests. Test area was 100 cm^2. Water pressures, when the third water drops appeared on the sample surfaces, were recorded as the waterproofness values. Test was repeated 3 times for each sample type.

Determination of abrasion resistance

Coated surfaces of samples were abraded according to TS EN ISO 12947-3 standard [27] by using Nu-Martindale Abrasion and Peeling tester (James H. Heal Co. Ltd.). Test was repeated 3 times for each sample type. Samples were abraded 80000 abrasion cycles and weighed after each 2500 cycles. Test was performed by using 9 kPa pressure.

Determination of washing resistance

Samples were subjected to domestic washing cycles according to TS 5720 EN ISO 6330-2002 6A standard [28]. “A” type laundry machine was used. Main washing temperature was selected as 40°C and washing time was 24 min. 4 g/l non-phosphate ECE reference detergent without optical brightener was used. Samples were dried via straight hanging. Samples were objected to 5 washing cycles.

SEM analysis

Sample surfaces were observed by using scanning electron microscope (Jeol 6060, Tokyo, Japan). Both coated and uncoated surfaces of samples were evaluated microscopically.

3 RESULTS

3.1 Thickness, unit mass and mass change values of samples

Thickness, unit mass, add-on [%] and mass changes after washing are given in Table 5 and visualized in Figures 2-3 (with 95% confidence intervals).

As seen from Table 5, average fabric thickness is 0.223 mm for polypropylene base fabric where thickness is between 0.213-0.237 mm for coated samples. From Figure 2, it is understood that fabric thickness was increased only for R140 sample in the level of 6%. In contrary, sample thickness values decreased between 0.5% and 4.5% for R120, W120 and W140 samples. Similar thickness decrements after coating were experienced in the literature for polyester/rayon fabrics [19].

Table 5 Thickness, unit mass, add-on % and mass changes of samples (*PPZ represents PP base fabric)

Sample code	Thickness [mm] (Standard dev.)	Unit mass [g/m^2] (St. dev.)	Add-on [%]	Mass change after 5 washing [%]
PPZ	0.223 (0.0054)	76 (0.7)	0	4.36
R120	0.213 (0.0089)	92 (1.8)	21	-1.45
R140	0.237 (0.0531)	107 (8.8)	40	0.85
W120	0.215 (0.0114)	99 (2.6)	30	-1.68
W140	0.222 (0.0054)	111 (7.7)	46	-1.34

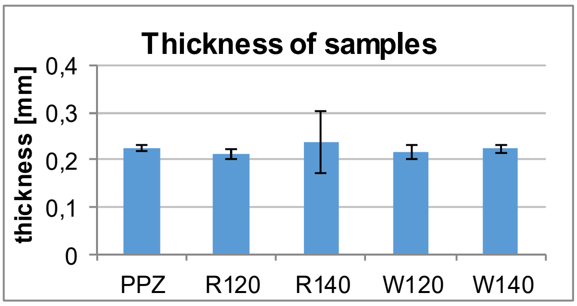

Figure 2 Thickness of coated samples

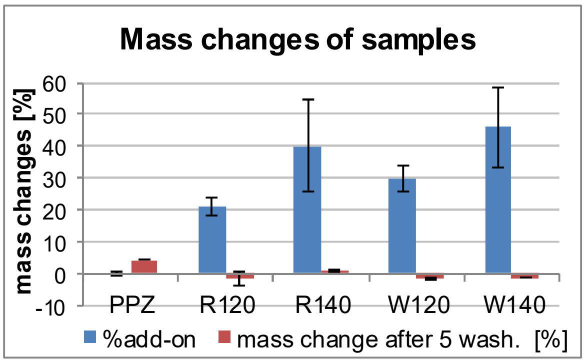

Figure 3 Add-on % and mass changes of coated samples

Add-on values and mass changes after washing are showed in Figure 3 (with 95% confidence intervals).

Coated samples showed unit mass increments between 21-46%. Add-on was higher for W coated samples which had a higher paste viscosity before coating. Also, R140 and W140 gave higher unit mass values. It was thought to be related to shrinkages of PP fabric under higher curing temperatures. After 5 washing cycles, mass changes were detected up to 2%.

In spite of unit mass increments up to 40%, sample thicknesses reduced after coating. It may be related to penetration of coating polymer to the inner parts of base fabric and stretching of samples during heat application. For further evaluation, samples were exposed to air permeability and waterproofness tests and examined microscopically by using SEM.

3.2 Waterproofness of samples

Waterproofness results of samples are given in Table 6. When the results were evaluated generally, it was concluded that both base fabric and coated samples showed very low waterproofness even before washing. Highest waterproofness was obtained from R120 sample before washing (164.3 mm water column) but it was also lower than the lowest limit of waterproofness for many application areas. According to Sen and Damewood (2005) [6], a waterproof-breathable fabric should not permit water passage until 1300 mm water column hydrostatic pressure. Similar low waterproofness results were obtained for water-based PU coated cotton fabrics in the literature [7].

Table 6 Waterproofness of samples

Sample code	Waterproofness [mm water column] (Standard Deviation)	
	Before washing	After washing
PPZ	71.5 (23.5)	35.3 (4.2)
R120	164.3 (19.2)	37 (15.4)
R140	150.7 (28.9)	24.0 (8.2)
W120	33.0 (6.1)	0.0 (0.0)
W140	61.0 (29.5)	0.0 (0.0)

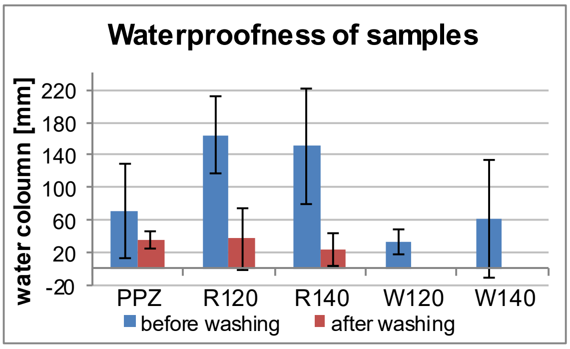

Figure 4 Waterproofness results with 95% confidence intervals

Samples coated with R (polyether) type polymer gave higher waterproofness when compared to base fabric (Figure 4). When the observations during waterproofness tests were considered, it was noticed that W (polyester) type polymer coated samples got wet before the starting time of test and many water drops appeared on the surface after starting the test. According to preliminary thermogravimetric analysis/differential thermal analysis (TGA/DTA) on the polyether and polyester type PU (with 10% cross-linking agent), it was concluded that polyester type PU might not have completed its cross-linking at 120 and 140°C during curing. TGA/DTA analysis results are given in Supplementary work. The TGA/DTA curves indicated that polyether type PU had a cross-linking temperature around 120-130°C (around exothermic peak interference) and polyester type PU had a cross-linking temperature around 120-140°C. Because of polypropylene melting and softening temperature limitations, 120 and 140°C were selected as the curing temperature. Polyester type PU had higher cross-linking temperature than polyether type PU. An insufficiency of curing procedure may have resulted with lower waterproofness of polyester type PU.

Waterproofness of all coated samples decreased after 5 times of washing. Polyester type PU coated samples did not give any water column after washing. As a result of visual inspection, it was understood that coating polymer partly removed from the sample surfaces after washing.

This was due to lower hydrolytic resistance of polyester type PU when compared to polyether type PU [6]. Also it might be related to poor adhesion between coating polymer and polypropylene or insufficient cross-linking.

3.3 Water vapour permeability of samples

Water vapour permeability of samples are tabulated in Table 7 and visualized in Figure 5 (with 95% confidence intervals).

Table 7 Water vapour permeability of samples

Sample code	Water vapour permeability [g/m^2/24 h] (St. dev.)	
	Before washing	After washing
PPZ	838.0 (11.8)	800.5 (15.2)
R120	300.0 (25.9)	434.8 (26.6)
R140	445.0 (91.5)	418.7 (105.1)
W120	458.0 (5.2)	683.4 (8.5)
W140	64.0 (31.4)	646.2 (13.4)

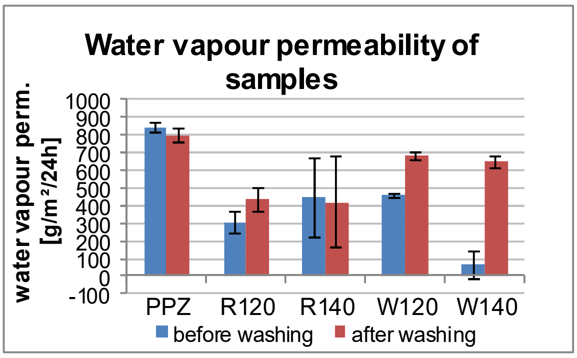

Figure 5 Water vapour permeability of samples

Highest water vapour permeability was obtained from PP base fabric with 838 g/m^2/24 h permeability value before washing. Water vapour permeability of unwashed coated samples reduced to approximately 50% of base fabric. This was due to additional PU coating layer which contributed mass transfer limitation through the fabric. Even the most breathable coating polymer was applied to the samples; it would add a resistance to the vapour flow by closing the pores and creating an additional layer [29].

When the results before washing were considered generally, any relation between the curing temperature, polyurethane type and water vapour permeability was not found. But the sample with higher add-on, namely W140, showed the lowest water vapour permeability.

After washing, water vapour permeability of coated samples increased especially for polyester type PU coated samples. It was due to removed polymer from the sample surfaces which resulted with a more open sample structure.

3.4 Air permeability of samples

Air permeability values of samples are given in Table 8 and Figure 6 (with 95% confidence intervals).

Before washing, PP base fabric had higher air permeability when compared to coated samples as it had open pores (Table 8, Figure 6). In contrary, unwashed coated samples showed air permeability lower than 8.5 L/m^2/s independent of curing temperature and coating polymer type. This is due to filling of the gaps between the fibers and yarns by coating polymer. Sample W140 with lowest water vapour permeability, also showed the lowest air permeability among all the samples, before washing.

According to Sen and Damewood (2005) [6], air permeability of fabrics should be lower than 1.5 ml/cm^2/s at 1 mbar in order to provide windproofness. This corresponds to 15 L/m^2/s at 100 Pa pressure. According to test results, before washing, coated samples belonged to windproof fabric class despite being measured at 200 Pa.

After washing, air permeability values of polyester type PU coated samples increased in big amounts as for water vapour permeability results. It was again due to the removed coating polymer from the sample surfaces. Air permeability of polyether type polyurethane coated samples remained almost the same after coating and they remained to be windproof after washing.

Table 8 Air permeability of samples

Sample code	Air permeability [L/m^2/s = mm/s] (St. dev.)	
	Before washing	After washing
PPZ	205.7 (6.7)	190.6 (10.6)
R120	8.4 (6.9)	7.3 (7.0)
R140	7.8 (4.2)	10.5 (8.7)
W120	7.1 (7.0)	142.5 (7.8)
W140	0.0 (0.0)	99.7 (24.7)

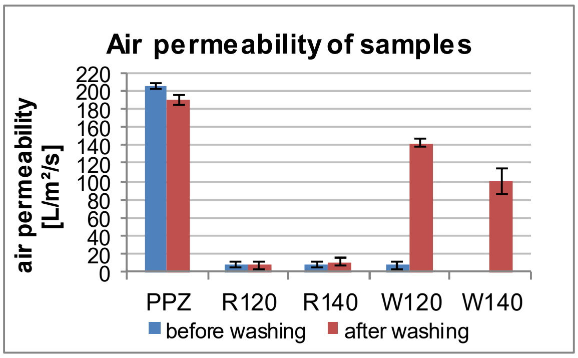

Figure 6 Air permeability of samples

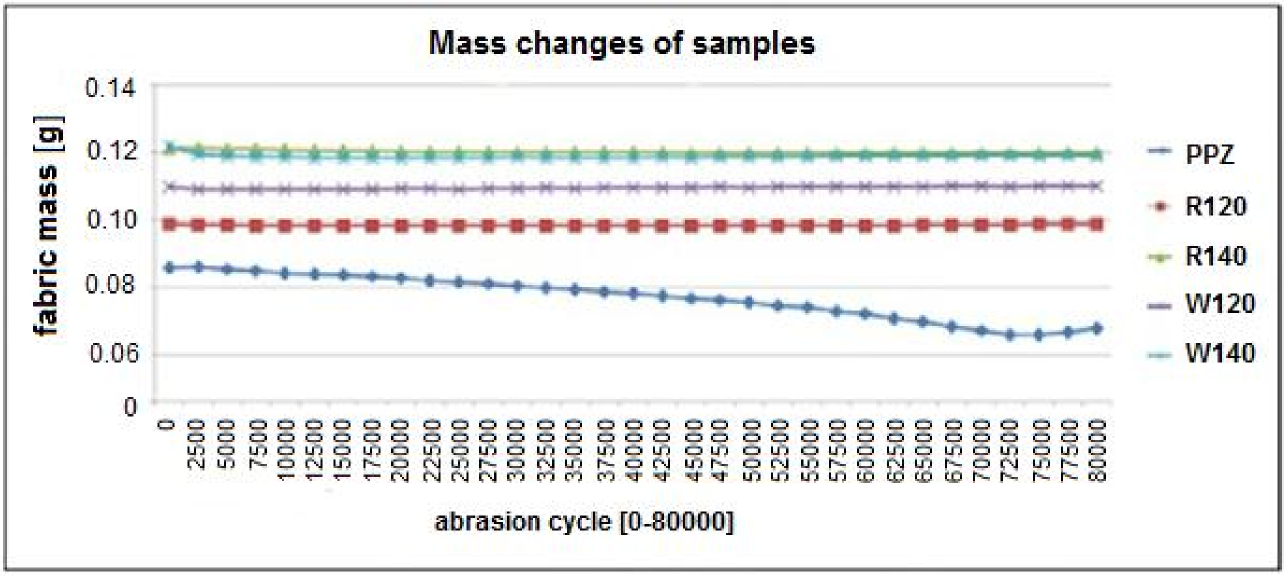

Figure 7 Mass changes of samples after abrasion cycles

3.5 Abrasion resistance results of samples

Average weight losses of samples were calculated after every 2500 abrasion cycles up to 80000 cycles. Weight losses are given in Table 9. Also results are visualized in Figure 7.

Table 9 Weight losses of samples after abrasion cycles

No. of abrasion cycles	PPZ	R120	R140	W120	W140
2500	0.2	-0.2	0.0	-0.7	-1.9
5000	-0.5	-0.2	-0.2	-0.7	-2.3
7500	-1.1	-0.3	-0.4	-0.8	-2.5
10000	-1.9	-0.4	-0.5	-0.79	-2.7
12500	-2.1	-0.4	-0.7	-0.7	-2.8
15000	-2.5	-0.4	-0.7	-0.8	-2.9
17500	-3.2	-0.5	-0.7	-0.7	-2.9
20000	-3.7	-0.5	-0.9	-0.6	-2.9
22500	-4.3	-0.4	-0.9	-0.6	-2.8
25000	-4.9	-0.4	-1.0	-0.6	-2.8
27500	-5.5	-0.5	-1.0	-0.5	-2.7
30000	-6.4	-0.5	-1.0	-0.5	-2.7
32500	-6.9	-0.5	-1.0	-0.3	-2.7
35000	-7.8	-0.5	-1.1	-0.5	-2.7
37500	-8.4	-0.5	-1.2	-0.4	-2.7
40000	-8.9	-0.5	-1.1	-0.3	-2.8
42500	-9.8	-0.5	-1.1	-0.2	-2.6
45000	-10.5	-0.4	-1.2	-0.2	-2.7
47500	-11.2	-0.4	-1.2	-0.2	-2.6
50000	-12.0	-0.4	-1.3	-0.2	-2.6
52500	-13.0	-0.4	-1.3	-0.1	-2.6
55000	-13.7	-0.4	-1.2	-0.1	-2.6
57500	-14.9	-0.3	-1.3	-0.1	-2.4
60000	-15.9	-0.4	-1.3	-0.1	-2.4
62500	-17.4	-0.4	-1.3	-0.2	-2.4
65000	-18.8	-0.3	-1.2	0.0	-2.3
67500	-20.2	-0.2	-1.3	0.1	-2.3
70000	-21.7	-0.1	-1.4	0.2	-2.2
72500	-22.9	-0.1	-1.3	0.0	-2.2
75000	-24.4	0.0	-1.4	0.2	-2.3
77500	-22.2	0.1	-1.3	0.1	-2.2
80000	-20.9	0.1	-1.4	0.1	-2.3

According to test results, abrasion did not cause important weight losses for coated samples. On the other hand, PP base fabric lost approximately 21% of its weight after 80000 abrasion cycles. Holes were formed on the base fabric after abrasion.

Highest weight loss was observed for W140 specimen after 20000 abrasion cycles, around 2.87%. Weight losses of coated samples fluctuated in a narrow range. This is related to sticking of fibers of abrasion fabric to the coated samples. Weight loss was lower than 1% for R120 and W120 samples after 80000 abrasion cycles and 1.35 % for R140 sample. Surface gloss of coated fabrics increased visibly after abrasion.

3.6 SEM evaluation of samples

SEM images of coated samples are given in Figure 8. SEM images were taken from both coated and uncoated sides of samples. As seen from the Figure 8, in the coated sides, coating polymer covered the gaps between the fibers on the surface of samples. In contrary, any polymer residue was not observed on the uncoated sides of the samples. As the coating pastes were viscous enough, coating polymers did not penetrate to the other side of the polypropylene fabrics. On the other hand, although coating the samples as two layers, all the coated surfaces of the samples were not covered by a polymer film. Coating polymer mainly filled the gaps between fibers but some gaps between the yarns can be observed especially in W120 and W140 samples. It is thought to be the reason of very low waterproofness as every unfilled point attributed to water passage at high pressures. A continuous polymer film is needed on the surface of base fabric for a very good waterproofness level.

Despite not producing a continuous coating polymer film on the surface, polymer which was deposited between the fibers reduced the air permeability effectively.

The surface images were not enough to determine the level of penetration of coating polymer. But, as a distinct polymer film was not detected on the surface, it is understood that some amount of applied polymer penetrated to a deepness of the fabric cross-section. But it did not leak to the other side (uncoated sides) of samples as seen from Figure 8. This supports the phenomena that coated fabrics did not thicken after coating.

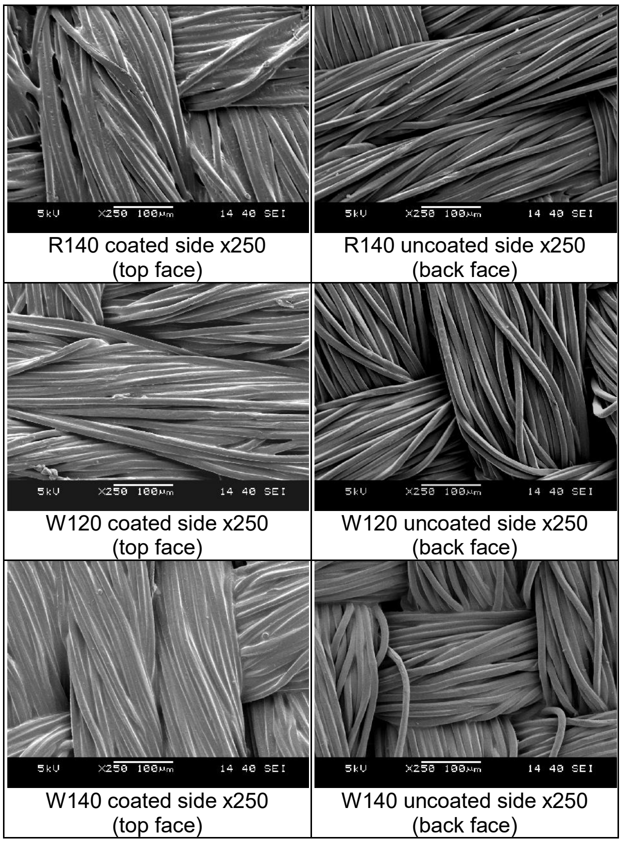

Figure 8 SEM images of coated samples

4 DISCUSSION

In this study, polypropylene fabric was coated systematically to be used in protective sportswear. Permeability properties and abrasion resistance of samples were determined in order to reveal the usability of these samples. Also physical properties such as thickness and unit mass were measured in order to observe physical changes after coating. Sample surfaces were observed by SEM in order to support test results.

When the results before washing were considered generally, add-on [%] was found higher for samples cured at 140°C and it was thought to be related to thermal shrinkages at higher temperatures. Air permeability of coated samples was found very low independent of coating polymer type and curing temperature. It was found advantageous as the samples showed windproofness. In contrary, water vapour permeability values of samples decreased in lower amounts. This showed that coating polymer penetrated to pores of fabric but the water vapour was permitted at some amount through the coating layer. Partly coverage of pores by coating polymer was supported by SEM evaluation. Coating procedure did not increase the waterproofness of samples to the desired levels. Polyether type PU gave relatively higher waterproofness for coated samples. Coated samples showed very high abrasion resistance when compared to base fabric.

After washing cycles, it was observed that coating polymer partly removed away from polyester type polyurethane coated samples. It affected the waterproofness, water vapour permeability and air permeability results. Waterproofness of polyester type polymer coated samples decreased to zero, while air permeability and water vapour permeability increased. The increments in the water vapour permeability and air permeability were interpreted as negative related to the absence of waterproofness. Some inferiority at permeability properties was obtained for polyether type polymer coated samples too, but the degree of the inferiority was lower. It was due to higher hydrolytic stability of polyether type polyurethane when compared to polyester type polyurethane [6].

Coated samples of this study are proposed to be used as windbreaker for sportswear. To be used in intensely water contacting sports such as sailing and mountaineering, waterproofness of polypropylene fabrics should be enhanced by using different coating parameters and coating polymer types. Also, compatibility between polypropylene base fabric and coating polymer should be enhanced in order increase waterproofness. In the literature polypropylene fibers were modified by using additives, making polymer blends or graft polymerization. By these modifications, water sorption and dyeability of polypropylene fibers were enhanced [30-32]. Similarly, polypropylene fibers hydrophilicity and polarity may be altered by fiber modifications and their compatibility to coating layer may be improved in the further studies.

ACKNOWLEDGEMENT: *Samples of this study were coated in Rultrans Transmisyon A.S. (Izmir, Turkey). Also, coating polymers and auxiliary materials were supported by Rudolf Duraner (Bursa, Turkey) and Organik Kimya San. ve Tic. A.S. (Istanbul, Turkey), kindly. Authors thank the companies for their supports.*

5 REFERENCES

1. Fung W.: Coated and laminated textiles, Boca Raton: CRC Press, 2002
2. Zhou W., Reddy N., Yang Y.: Textiles for protection, R.A. Scott. (Ed.), Cambridge, Woodhead Publishing, 2005
3. Shishoo R.: Textiles for sports, Cambridge, Woodhead Publishing, 2005
4. Aydemir H.: Seminar notes - Tekstil bitim islemlerinde kaplama ve uygulamalari, ITA coating applications and special effects in textile finishing, Training, Istanbul, 2011
5. Dembický J., Jain S., Charaya V.: Characteristics of coating process, Vlakna a Textil (Fibres and Textiles) 15(1), 2008, pp. 19-27
6. Sen A.K., Damewood J.: Coated textiles: Principles and applications, Boca Raton, CRC Press, 2005
7. Jassal M., Khungar A., Bajaj P., et al.: Waterproof breathable polymeric coatings based on polyurethanes, Journal of Industrial Textiles 33(4), 2004, pp. 269-280, doi:10.1177/1528083704045179
8. Szycher M. (Ed.): Szycher's handbook of polyurethanes, Boca Raton, CRC press, 1999
9. McIntyre J.E.: Synthetic fibers: Nylon, polyester, acrylic, polyolefin, Cambridge, Woodhead Publishing, 2005
10. Bulut Y., Sular V.: Effects of process parameters on mechanical properties of coated fabrics, International Journal of Clothing Science and Technology 23(4), 2011, pp. 205-221, doi: 10.1108/09556221111136476
11. Mondal S., Hu J.L.: Water vapor permeability of cotton fabrics coated with shape memory polyurethane, Carbohydrate Polymers 67(3), 2007, pp. 282-287, doi: 10.1016/j.carbpol.2006.05.030
12. Matkovic V.M.P., Skenderi Z.: Mechanical properties of polyurethane coated knitted fabrics, Fibres & Textiles in Eastern Europe 100(4), 2013, pp. 86-91
13. Vilder I.D., Vanneste M., Peltonen C., et al.: Safe@Sea: Protective clothing for improved safety and performance in the fisheries. Development of comfortable wear resistant and stain repellent coated materials, Abstract book of 5th European Conference on Protective Clothing and NOKOBETEF 10, "Future of Protective Clothing: Intelligent or not", 2012, p. 30
14. Padleckiene I., Petrulis D., Rubeziene V., et al.: Breathability and resistance to water penetration of breathable-coated textiles after cyclic mechanical treatments, Materials Science (MEDŽIAGOTYRA), 15(1), 2009, pp. 69-74, ISSN 1392–1320
15. Padleckiene I., Petrulis D.: Effect of abrasion on the air permeability and mass loss of breathable-coated fabrics, Fibres & Textiles in Eastern Europe 73(2), 2009, pp. 50-54
16. Kwak Y.S., Kim E.Y., Kim H.D., et al.: Comparison of the properties of waterborne polyurethane-ureas containing different triblock glycols for water vapor permeable coatings, Colloid Polymer Science 283(8), 2005, pp. 880-886, doi: 10.1007/s00396-004-1230-0
17. Jeong W.Y., An S.K.: The transport properties of polymer membrane-fabric composites, Journal of Materials Science 36(19), 2001, pp. 4797-4803, doi: 10.1023/A:1017995509102
18. Rochery M., Vroman I., Campagne C.: Coating of polyester with poly(dimethylsiloxane)- and poly(tetramethylene oxide)-based polyurethane, Journal of Industrial Textiles 35(3), 2006, pp. 227-238, doi: 10.1177/1528083706055755
19. Lee K., Cho G.: The optimum coating condition by response surface methodology for maximizing vapour-permeable water resistance and minimizing frictional sound of combat uniform fabric, Textile Research Journal 84(7), 2014, pp. 684-693, doi: 10.1177/0040517513509870
20. Padleckiene I., Petrulis D.: The change of air permeability and structure of breathable-coated textile materials after cyclic stretching, Materials Science (MEDŽIAGOTYRA) 14(2), 2008, pp. 162-165
21. Mondal S., Gupta B., Singh H.: Coating of polypropylene nonwovens with acrylic copolymers, Journal of Industrial Textiles 33(1), 2003, pp. 33-41, doi: 10.1177/1528083703035098
22. TS 251: Determination of Mass Per Unit Length and Mass Per Unit Area of Woven Fabrics, 1991
23. TS 7128 EN ISO 5084: Textiles-Determination of thickness of textiles and textile products, 1998
24. TS 391 EN ISO 9237: Textiles-Determination of permeability of fabrics to air, 1999
25. BS 3424-34: Testing coated fabrics. Method 37. Method for determination of water vapour permeability index (WVPI), 1992
26. TSE 257 EN 20811: Textiles-Fabrics-Determination of Resistance to Water Penetration-Hydrostatic Pressure Test, 1996
27. TS EN ISO 12947-3: Textiles - Determination of the abrasion resistance of fabrics by the Martindale method - Part 3: Determination of mass loss, 2001
28. TS 5720 EN ISO 6330- 6A: Textiles- Domestic washing and drying procedures for textile testing, 2002
29. Song G. (Ed.): Improving comfort in clothing, Cambridge, Elsevier, 2011
30. Vencelová P., Ujhelyiová A., Ryba J.: Thermomechanical and sorptive properties of metallocene polypropylene fibres modified polyvinyl alcohol and cloisite, Vlakna a Textil (Fibres and Textiles) 17(4), 2010, pp. 3-6
31. Deanko P., Čižmárová D., Šest J.: Surface dyeing of polypropylene fibres, Vlakna a Textil (Fibres and Textiles) 17(4), 2010, pp. 7-12
32. Kristofic M., Naciniakova Z., Legen J., Ryba J.: Polypropylene fibres modified by copolyamides Part I. Preparation of modified fibres and their properties, Vlakna a textil (Fibres and Textiles) 12(3), 2005, pp. 104-110

CHARACTERISATION OF ELECTROSPUN FIBERS MADE OF PVA OR PVAc AND COLLAGEN DERIVATIVE

Maksym Koliada, Olena Ishchenko, Viktoriia Plavan and Volodymyr Bessarabov

Kyiv National University of Technologies & Design, Nemirovich-Danchenko str. 2, 01011 Kyiv, Ukraine
maksym.koliada@gmail.com

Abstract: *One of the greatest potential in electrospun fiber is the area of bioengineering. For many biomedical applications, the materials used have to be biocompatible, thus natural polymers have a distinct advantage over synthetic materials. In this study, electrospinning of collagen derivative (CD) of porcine skin with polyvinyl alcohol (PVA) and polyvinyl acetate (PVAc) were carried out. We investigated morphology of the prepared fibers. The optimal distance between syringe needle and collector was 9-12 cm. Obtained nonwoven materials from PVAc and PVA with the addition of Gelatin and Collagen derivative have a diameter of fibers in the range of 0.502-0.894 µm and 0.443-0.895 µm for PVAc:CD and PVA:CD composition respectively.*

Keywords: *collagen, PVA, PVAc, electrospinning.*

1 INTRODUCTION

Leading global trend in the fibers production technology is to reduce the diameter of threads filament to micro- and nanoscale size. Nanofibers became an important group of one-dimensional nanostructures because of their unique properties such as high surface area, high porosity, and their high safety in comparison with other nanomaterials [1, 2]. These abilities improve the quality of products and allow creation of innovative materials. Today there are many methods of ultrafine fibers forming: melt-spinning, aerodynamic spraying molten fibers in the form of a jet of compressed air (melt-blowing), forming a molten mixture of polymers and nanofibers by electrospinning.

Electrospinning has several advantages over other production methods such as the relative ease of use and being cost-effective, production of fibers in a diameter range of lower than 100 nm, easy incorporation of active materials such as drugs, vitamins, antioxidants, metallic nanoparticles, etc. This technology allows obtaining new nanofibers with controlled porous structure. Moreover, organic and inorganic materials, which are temperature sensitive, are resistant to electrospinning process due to the absence of heat [1, 3]. There has been a wide array of polymers used with electrospinning to create structures composed of sub-micron diameter fibers. These include the common synthetic polymers poly(lactic acid) (PLA), poly(glycolic acid) (PGA), polycaprolactone (PCL), polydioxanone (PDO), polyvinylalcohol (PVA) [4], polyvinylpyrrolidone (PVP) and polystyrene (PS). Z.M. Huang et al [5] have given a comprehensive summary of polymers that have been successfully electrospun.

Due to diversity of applications in electrospinning, considerable amount of work is focused on extending the applications and end-uses. Electrospun nanofibers can be used to collect pollutants as filtration materials through chemical adsorption as they have high specific surface area [6, 7]. A wide range of natural polymers including gelatin, collagen, elastin, silk and fibrinogen have also been used, as well as blends of natural and synthetic polymers can be electrospun [8-10]. This method is very suitable to process natural polymers and synthetic biocompatible or bioabsorbable polymers for biomedical applications [11].

Gelatin is widely employed in food industries, cosmetics, pharmaceutical and medical applications due to its biodegradability and natural abundance. In addition, gelatin has shown a great interest in fiber formation via electrospinning technology according to its unique chemo-physical properties such as surface tension along with its viscosity and conductivity [12]. Collagen is the major structural protein of connective tissue such as skin, bone, cartilage, tendons and ligaments. Because of its biological properties and availabilities, it is widely used as a biomaterial with multiple physical forms such as sponges, films membranes, wire and fabrics [13]. Untanned or limed leather can be a source of collagen, gelatin and collagen hydrolysate [14]. Collagen hydrolysate is a polypeptide composite made by further hydrolysis of denatured collagen.

In the present work, we investigated the possibility of application of collagen derivative (CD) in electrospinnable solutions by using the mixture of CD with polyvinyl alcohol (PVA) and polyvinyl acetate (PVAc) in suitable ratios.

2 MATERIALS AND METHODS

2.1 Reagents

Polyvinyl alcohol PVA (grade 16/1, Mass portion of acetate groups not more than 0.9-1.7%) was purchased from Himlaborreactiv (Kyiv, Ukraine). Polyvinyl acetate PVAc (dry matter 15%) was supplied from a local market in a form of glue. Food grade, beef-hide gelatin (200 bloom) was supplied from a local market.

2.2 Electrospinning

The electrospinning set-up (Figure1) consisted of a syringe pump to deliver electrospinning solution to the spinneret – stainless steel blunt needle (0.5 mm inner diameter) at a flow rate approx. 0.5 ml/min. Electrospinning of the various solutions was performed using an applied voltage of 30 kV and a spinneret-to-collector distance 9-12 cm. Electrospun samples were collected using a stainless steel plate covered with polytetrafluoroethylene (PTFE) film substrate in the form of nonwoven matrices. The temperature within the setup was maintained at 25±1°C. The spinning geometry was upwards, this allows obtaining of nonwoven materials without drops of electrospinning solution on the sample. Obtained matrices after sufficient drying were peeled off from the collector with the aid of a surgical knife and transferred on the clean slide glass until subjected to characterization.

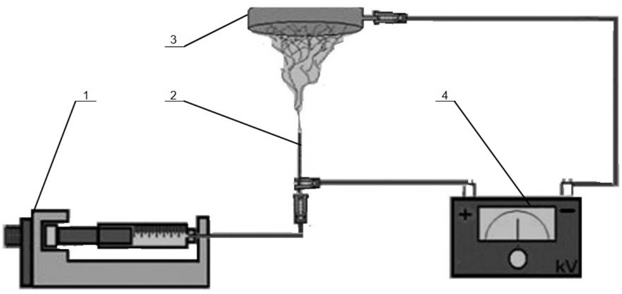

Figure 1 Capillary type electrospinning setup (1-syringe pump, 2-needle, 3-collector, 4-hight voltage power supply)

2.3 Obtaining of collagen derivative

Preserved pig skin was purchased from local slaughterhouse in Kyiv, Ukraine. After it was fleshed, unhaired, neutralized and washed as by conventional technology of leather production beamhouse processes, the dermis of the skin was cut into small pieces (1x1 cm). Collagen derivative (CD) was then extracted from the pieces by acid hydrolysis using 0.1 M acetic acid. Ratio skin:acid 1:3, duration 6 hrs., at 70-75±1°C. The obtained collagen solution was then neutralized with a 25% solution of Na_2CO_3, (pH=4.0±0.5, dry matter 9.75%, ash 1.46%).

2.4 Preparation of electrospun solutions

PVA (10% solution) and PVAc (10% solution) was prepared by stirring for 40 minutes on a water bath. Afterwards, PVA or PVAc was incorporated into the CD or gelatin (Gel) solution; the dispersion was maintained at 25-30°C for 30 min under stirring until complete dissolution. Table 1 displays the test combinations chosen for this study (PVA:CD; PVAc:CD and PVA:Gel; PVAc:Gel).

Table 1 Composition ratio details on PVA, PVAc, collagen derivative and gelatin used for electrospinning

Sample	PVA, PVAc	Collagen Derivative, Gelatin
1	9	1
2	8	2
3	7	3
4	6	4
5	5	5

2.5 Morphological characterization

The morphology and diameters of the produced fibers were examined by using a light microscope Biolam-C11. Fiber diameter analysis was carried out by randomly counting 100 fibers per experiment using software (ImageJ, 1.51 P). The diameter values of the obtained fibers were statistically analyzed by using the Minitab-18 program (Minitab Inc., USA).

3 RESULTS AND DISCUSSION

Experimental ratios for both PVA and PVAc composition are 9:1, 8:2 and 7:3. Table 2 shows the experimental results of the performed runs for PVAc combinations. The optimal distance between syringe needle and collector was 9-12 cm. While increasing the CD content takes place drop formation, which leads to impossible electrospinning formation. This requires further studies of rheology characteristics of compositions, the inner diameter of needle and distance between syringe needle and collector.

Table 2 Parameters of PVAc electrospinning

Sample	PVAc	Collagen Derivative, Gelatin*	Distance between electrodes [cm]	Formation stability
1	9	1	9-10	+
2	8	2	10-12	+
3	7	3	10	+
4	6	4	9	±
5	5	5	9-10	-
1*	9	1	10-12	+
2*	8	2	12	+
3*	7	3	12	+

* PVAc:Gelatin compositions

Ratios 6:1 and 5:5 performed insufficient electrospinning, the fibers were short and teared on small pieces even after reducing the distance between electrodes (ex. >9 cm). Compositions containing gelatin were unstable by mean of rheology (gelation occurs), temperature 25-30°C is too low to maintain them sufficient and runny. Higher viscosity causes beads.

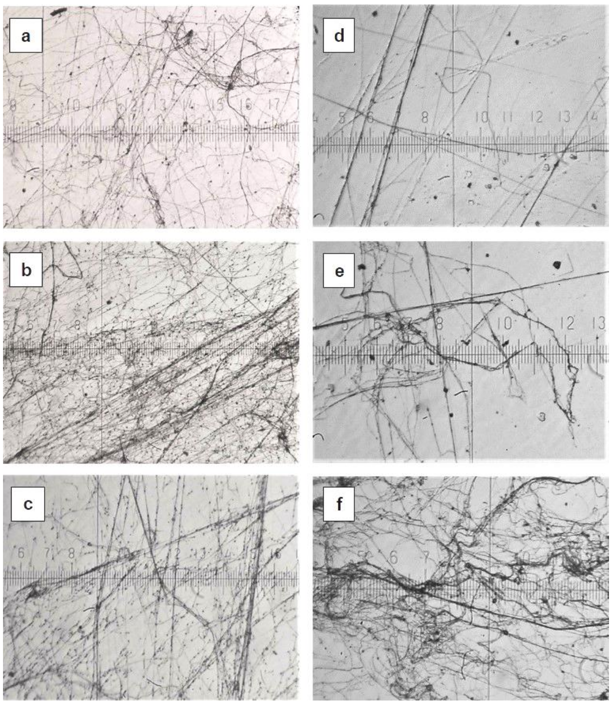

Figure 2 Representative microphotographs of the electrospun solutions a,b,c – PVAc:CD; d,e,f – PVAc:Gel of the ratios 9:1, 8:2, and 7:3 respectively

It has been well know that the concentration of polymer solution, applied voltage and conductivity affects bead formation, bead density, morphology of the electrospun fibers, and average diameter of the fibers [2, 15]. A comparison of CD and Gelatin with respect to ability to spin fibers and electrospinning process conditions showed that CD could spin fibers and gave practically defect-free (drops, thickenings) nanofibers. Mixed compositions containing Gelatin were rather difficult to process by this method because of the poorly disperse solutions and unstable in time viscosity that plugged the capillary orifices.

The morphology of electrospun PVAc containing CD or Gelatin shows in Figure 2. It is clear from the figure that no phase separation has been observed in the same time the homogeneity of the obtained fiber can be easily observed. According to the obtained data (Figure 3) PVAc:CD composite shows the increasing of the beads diameter size. A network of fibers could be observed along with beads. The fiber density increased as well as the fiber networking.

High-density fibers for both addition of Gelatin or CD along with beads were observed at ratio PVAc:CD/Gel and PVA:CD/Gel as 7:3. Therefore, for more accurate evaluation of the fibrous material morphology, additional studies were performed on light microscope Biolam-C11. Figure 3 shows diameter ranged between 0.496-1.443 µm and 0.502-0.894 µm for PVAc:Gel and PVAc:CD respectively.

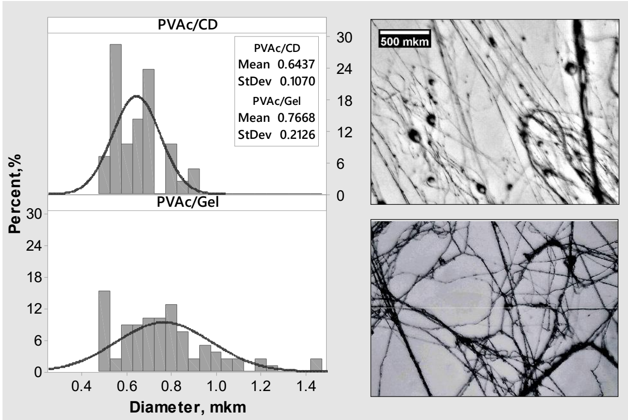

Figure 3 Images and bar graphs of diameter ranges of electrospun PVAc/CD and PVAc/Gel fibers – 7:3 ratio

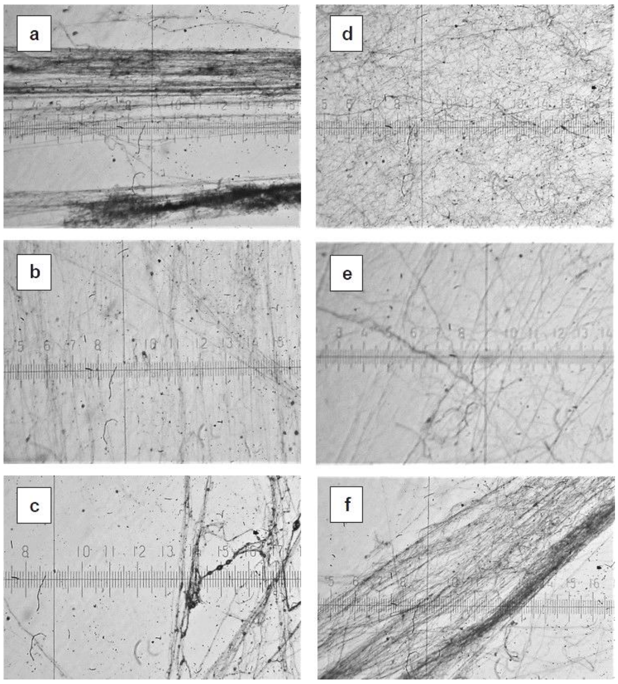

Figure 4 Representative microphotographs of the electrospun solutions a,b,c – PVA:CD; d,e,f – PVA:Gel of the ratios 9:1, 8:2, and 7:3 respectively

Table 3 shows the experimental results of the performed runs for PVA combinations with Gelatin and CD. The resulting fibers also showed that the incorporation of the CD into the composition not only decrease the average diameter but also reduced the diameter distribution of the electrospun fibers from 0.766 µm and 0.773 µm for PVAc:Gel, PVA:Gel, to 0.643 µm and 0.606 µm for PVAc:CD PVA:CD respectively, as shown in Figures 3 and 5.

Table 3 Parameters of PVA electrospinning

Sample	PVA	Collagen Derivative, Gelatin*	Distance between electrodes [cm]	Formation stability
1	9	1	9-10	+
2	8	2	10	+
3	7	3	10	+
1*	9	1	10	+
2*	8	2	12	+
3*	7	3	12	+

* PVA:Gelatin compositions

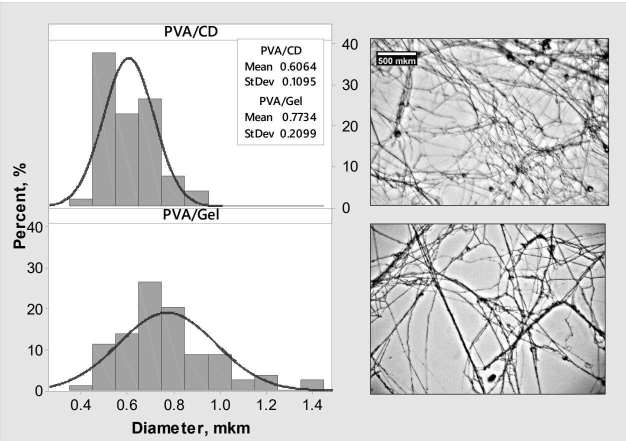

Figure 5 Images and bar graphs of diameter ranges of electrospun PVA:CD and PVA:Gel fibers – 7:3 ratio

4 CONCLUSION

Described the features of the structure (diameter – up to 1 µm) and properties of nonwoven polymeric materials obtained by electrospinning method. Obtained nonwoven materials from PVAc and PVA with the addition of Gelatin and Collagen derivative have a diameter of fibers in the range of 0.502-0.894 µm and 0.443-0.895 µm for PVAc:CD and PVA:CD composition respectively. The optimal distance between the electrodes ranges between 9-12 cm for established voltage of 30 kV for both compositions. We studied the influence of Gelatin and Collagen derivative on the morphological characteristics of fibers. It had been shown that adding of CD in compositions with PVA and PVAc leads to obtaining fibers with diameter >0.500 µm of 38% and 26% (of whole volume) respectively. Application of collagen derivative allows expanding the applications of final nonwoven polymer materials due to the wide range of reactive groups of collagen and their incorporation with other modifiers such as drugs, vitamins, antioxidants etc.

5 REFERENCES

1. Noruzi M.: Electrospun nanofibres in agriculture and the food industry: a review, J. Sci. Food Agr. 96(14), 2016, pp. 4663-4678, doi: 10.1002/jsfa.7737
2. Ramakrishna S., Fujihara K., Teo W.E., et al.: An introduction to electro- spinning and nanofibers, New Yersey, World Scientific, 2005
3. Haghi AK.: Electrospinning of Nanofibers in Textiles, Oakville, CRC Press, 2011
4. Ishchenko O.V., Plavan V.P., Kovalchuk O.V., et al.: The preparation of biocompatible polymeric fibers by electrospinning method, Technology Audit and Production Reserves 4(4(30)), 2016, pp. 22-26, doi: 10.15587/2312-8372.2016.76522
5. Huang Z.M., Zhang Y.Z., Kotaki M., et al.: A review on polymer nanofibers by electrospinning and their applications in nanocomposites, Composites science and technology 63(15), 2003, pp. 2223-2253, doi: 10.1016/S0266-3538(03)00178-7
6. Emo B., Eberlin C.T., Hixon K.R., et al.: A study on the potential of doped electrospun polystyrene fibers in arsenic filtration, Journal of Environmental Chemical Engineering 5(1), 2017, pp. 232-239, doi: 10.1016/j.jece.2016.11.039
7. Zhao R., Li X., Sun B., et al.: Branched polyethylenimine grafted electrospun polyacrylonitrile fiber membrane: a novel and effective adsorbent for Cr (VI) remediation in wastewater, J. Mater. Chem. A 5(3), 2017, pp. 1133-1144, doi: 10.1039/C6TA09784G
8. Engel E., Michiardi A., Navarro M., et al.: Nanotechnology in regenerative medicine: the materials side, Trends in biotechnology 26(1), 2008, pp. 39-47, doi: 10.1016/j.tibtech.2007.10.005
9. Kwak H.W., Shin M., Lee J.Y., et al.: Fabrication of an ultrafine fish gelatin nanofibrous web from an aqueous solution by electrospinning, International Journal of Biological Macromolecules 102, 2017, pp. 1092-1103, doi: 10.1016/j.ijbiomac.2017.04.087
10. Mendes A.C., Stephansen K., Chronakis I.S.: Electrospinning of food proteins and polysaccharides, Food Hydrocolloids 68, 2017, pp. 53-68, doi: 10.1016/j.foodhyd.2016.10.022
11. Babitha S., Rachita L., Karthikeyan K., et al.: Electrospun protein nanofibers in healthcare: A review, International journal of pharmaceutics 523(1), 2017, pp. 52-90, doi: 10.1016/j.ijpharm.2017.03.013
12. Oraby M.A., Waley A.I., El-Dewany A.I., et al.: Electrospun gelatin nanofibers: effect of gelatin concentration on morphology and fiber diameters, J. Appl. Sci. Res. 9(1), 2013, pp. 534-540
13. Sionkowska A., Skrzyński S., Śmiechowski K., et al.: The review of versatile application of collagen, Polymer. Adv. Tech. 28(1), 2017, pp. 4-9, doi: 10.1002/pat.3842
14. John Sundar V., Gnanamani A., Muralidharan C., et al.: A. Recovery and utilization of proteinous wastes of leather making: a review, Rev. Environ. Sci. Biotechnol. 10(2), 2011, pp. 151-163, doi: 10.1007/s11157-010-9223-6
15. Park J.Y., Shim W.G., Lee I.H.: Modeling and optimization of electrospun polyvinylacetate (PVAc) nanofibers by response surface methodology (RSM), J. Nanosci. Nanotechnol 11(2), 2011, pp. 1359-1363, doi: 10.1166/jnn.2011.3420

THE TESTS OF LOW CYCLIC LOADING OF COMPOSITES WITH TEXTILE STRUCTURE ON TEST MACHINE WITH VIDEO-EXTENSOMETER

Jan Krmela and Vladimira Krmelova

Alexander Dubček University of Trenčín, Faculty of Industrial Technologies, I. Krasku 491/30, 020 01 Púchov, Slovakia
jan.krmela@fpt.tnuni.sk, jan2.krmela@post.cz

Abstract: *In this contribution, the composites with textile reinforcement and rubber matrix are studied experimentally. The reinforcement is in the form of fibre and material is PA66. These composite with textile structure are applied in tire casings for passenger cars and conveyor belts. The aim of research work of authors is propose and evaluate the experimental procedures for tests cyclic loading of selected composites, which consist of textile reinforcement with a different cord angle. The image analysis is applied for obtaining of information about geometry parameters of cords for specimen design for tests. The test machine Autograph AG-X plus 5kN – Schimadzu with a video-extensometer is used for the tests of low cyclic loading in tensile with cycle loops. The results of tests and geometry parameters are needed for creation of computational models of composites such as parts of tire casing.*

Keywords: *composite, textile fibre, PA66, tire, low cyclic loading, video-extensometer, cycle loop.*

1 INTRODUCTION

For computational modeling of parts of tire casings and tires, the material parameters of matrixes and reinforcements are necessary as input data for the computational model and the experimental data of composite structures can be used as the verification criteria for the comparison of computational outputs with test results [1]. The static tests are not able to provide the information about the operational behavior. For computational modeling of a tire casing, the results from experimental data from cycle tests are needed.

It is necessary to deal with cyclic tensile tests of long-fiber composites with textile and steel reinforcement together as tire casings or conveyor belts. Therefore, the aim is also to propose and evaluate the experimental procedures for cyclic loading tests of selected composites, which consist of textile reinforcement with a different cord angle. The optimization of an angle of textile reinforcement in composites is possible on the basis of the results from the test of cyclic loading. A standard automobile radial tire casing consists of elastomer parts and parts with textile-cords (Table 1) and steel-cords in a tire tread as reinforcements.

The structure parts applied into passenger car radial tire casings are: textile carcass plies, a textile cap ply (called an overlap belt) and steel-cord belts [2, 3].

These structures of tire have got different cord material, angle and numbers of layers. The behavior of such materials as tire belts under mechanical loading is in many ways different from the behavior of commonly used technical materials [4, 5].

Table 1 Materials of textile-cords for tires [3]

Material	Labeling of construction [tex]	Application
Polyester	PES 144x1x2 PES 167x1x3	Carcass plies
Polyamide 6	PA6 94x1x2 PA6 94x1	Cap ply
Polyamide 66	PA66 140x1x2	Cap ply
Rayon (viscose)	VS 184x1x2 VS 244x1x2	Carcass plies
Aramid	Aramid 110x1x2	Carcass plies for sport tire casings

The PA66 and PES textile fibers are used for passenger tires, especially for common purposes. The aramid fibers, especially Kevlar, are used for tires of sport and high-speed cars. Kevlar has a high strength (up to 2750 MPa), a low modulus of elasticity, low elongation and dimensional stability [3].

The sidewall also shows the material of cords and number of plies in the sidewall and under the tread of tire casing. The sidewall of a tire for passenger cars consists of one polyester carcass ply with a cord angle of 90° and in the tread, there are four plies: one polyester ply, two steel plies with a cord angle approx. 21–27° in ply and one polyamide cap ply with a cord angle approx. 0°, see Figure 1.

A tire with the symbol Extra load (XL) may have two polyester- or two polyamide plies. The textile carcass density (it is a number of ends per one meter of width, marked as EPM) is from 700 to 1150 m^{-1}. The EPM of a textile cap ply is 1100–1200 m^{-1}.

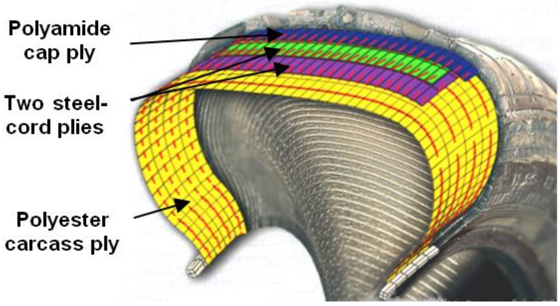

Figure 1 The structure of tire casing – cord angles

Tests of specific long-fiber composite materials with an elastomer are not standardized. The paper [5] describes the geometric parameters of single-layer specimens of tire casings with different cord-angles (0°, 25°, 45°, 60° and 90°) for tensile tests. Some standards describe the testing procedure and conditions of testing, the shape and geometric parameters of the test specimens for static tensile tests [12, 13]. E.g., the standard ASTM D-3039-76 [14] describes the width of test specimens of fiber-resin composites in the form of strips 25 mm wide, 2-4 mm thick with the working length of 150 mm. Therefore, for tests of cyclic loading the shape of single-layer specimens with textile cords and an elastomer must be designed.

The dynamic-mechanical properties of such composites can also be described by an elastic, viscous modulus and a loss factor [6]. For computational modeling, the modulus of elasticity and Poisson ratio are used as material input parameters of textile reinforcements. The LASE modulus from the producer of a textile cord is used [7]. LASE is a modulus of elasticity for elongation 5% (LASE is an acronym of Load At Specific Elongation 5%). Another option is the determination of modulus as stress necessary for elongation by 100% obtained by extrapolation for elongation by 2%. After the vulcanization process and during the industrial process of a tire casing, the modulus can be changed (the influence of heat during vulcanization). The conditions of tire's vulcanization process are the temperature of 193°C, the pressure of 1534 kPa and time 10 min.

The static tensile modulus of elasticity of PA66 is from 900 to 3450 MPa or from 9 to 50 cN/dtex [3, 8, 9]. It is a broad range. In case of rayon, the modulus is from 600 MPa to 11 GPa or 8–120 cN/dtex. Typically values of modulus of elasticity are in Table 2. Usually the test conditions are a temperature of 20±2°C, humidity of 65±5% and an initial length between clamps of a test machine (gauge length) 500 mm [10]. The Poisson ration of PA66 is approx. 0.4.

Table 2 Modulus of elasticity of textile cords [11]

Material	Labeling of construction [tex]	Modulus of elasticity [GPa]
Polyester	PES 110x1x2	4
Polyamide 66	PA66 94x1x2	3.4
Rayon (viscose)	VS 184x1x3	11
Aramid	Aramid 167x1x2	25

The low-cyclic loading of composites is still actual and has been discussed increasingly, because the obtained experimental can be really good information in relation to the composite behavior and they can be used as input parameters for computational modeling. Therefore the aim of research work of authors is propose and evaluate the experimental procedures for tests cyclic loading of selected composites.

2 EXPERIMENTAL METHODS

2.1 Image analysis of cross-section of tire casing

The geometric configuration of reinforcements is the main factor for the specification of material parameters, which would be used for the description of the whole area of casing under the tread. The photo camera Canon EOS 600 D and a standard light microscope were used to obtain the images. The software IMPOR 5.0 with plug-in Object Measuring is used for the image analysis.

The cord structure of the selected tire casing Continental 245/40 R18 97Y XL is represented in Figures 2 and 3. The tire has polyamide cords in cap ply, the detail of polyamide cord is in Figure 3 bellow. The cord structure for different tire casing Dunlop 215/40 R17 87V XL is in paper [15].

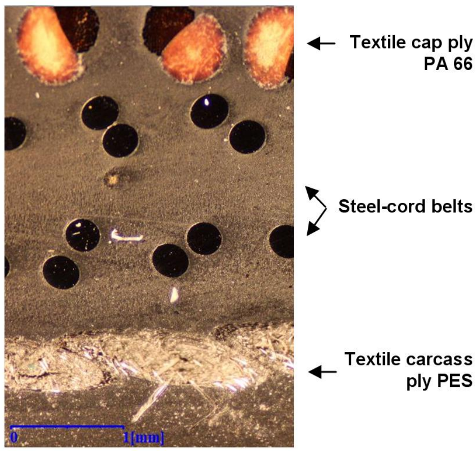

Figure 2 The structure of tire casing 245/40 R18 by photo camera

The image analysis is applied for obtaining the information about geometric parameters of cords such as distances between cords and ply thickness for specimen design for tests of low cyclic loading.

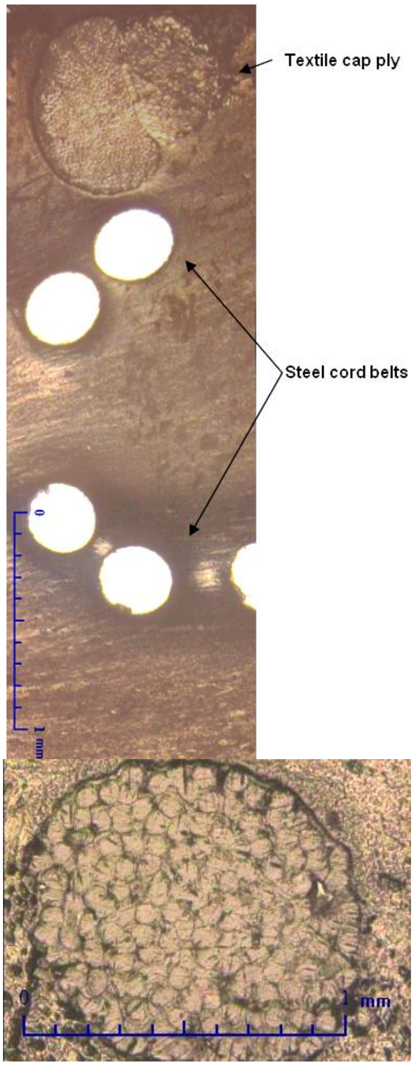

Figure 3 The detail of structure by light microscope with polyamide cord in cap ply of tire casing 245/40 R18 by light microscope

2.2 Specimen design

Before carrying out the mechanical tests, the geometric parameters of test specimens had been proposed and test conditions with respect to the test apparatus had been determined. The composite specimens with an angle of the textile reinforcement 0° (textile reinforcement is perpendicular to the direction of loading), 45° and 60° are used for the cyclic tests. The composite specimens are consisted of one layer. The PA66 is used as textile reinforcement and elastomer for production of radial tire carcass is used as matrix.

The geometric parameters of rectangle shape specimens are a length of 195 mm, a width of 35 mm, initial length between clamps of a test machine 100 mm and a thickness of the specimen of 1.05 mm. The cord diameter is 0.5 mm. The EPM is 870 m^{-1}. The specimens were produced by the authors. The initial length between the points for a video-extensometer is 50 mm, see Figure 4.

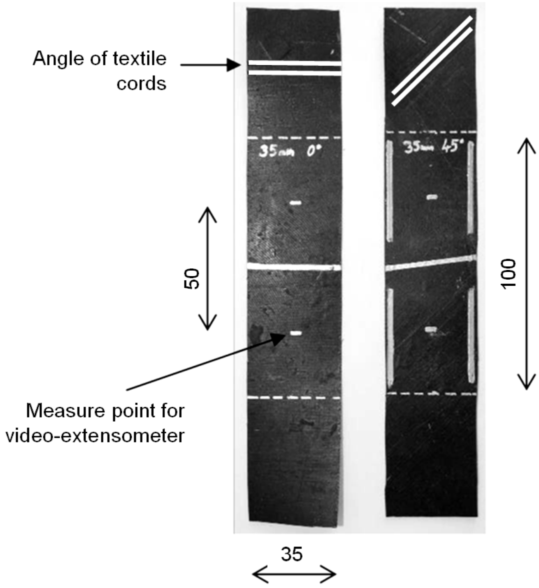

Figure 4 Specimens with geometric parameters (in mm)

2.3 Methods of cyclic loading

The tests of cyclic loading of these composites are requested for the verification analyses between tests and computational modeling of tires. Standards and a methodology of optimal testing of composites with the textile structure have not been determined yet but the determination can be based on the behavior of elastomers under the cyclic loading [16]. For elastomers under the first cycle, there is the occurrence of Mullins effect. This effect is characterized by a big hysteresis. In the second cycle, there is a typical stress drop, which decreases in each following cycle. In case of the cyclic deformation with constant amplitude, the stress-elongation characteristics are stabilized over several cycles (usually up to 10 cycles). For textile materials, the DIN 53835-13 standard is defined [17] and according to the mentioned standard, the conditions are taken into consideration during the first 5 cycles.

The design of method for cycle loading tests of composites with a textile fiber and an elastomer matrix on a test machine with a video-extensometer has these conditions: the loading speed 250 mm/min for cycles and 50 mm/min for a pre-test by force value 2 N [17]. Five cycle loops are applied. Every cycle loop consists of five cycles. Every cycle is defined as loading to a certain percentage of elongation between clamps of a test machine and unloading to a certain percentage of elongation between clamps of a test machine.

For angles 0° and 45°, the first cycle loop consists of cycles with loading to 30% and unloading to 3% of elongation (not 0% because the negative force is not possible during tensile testing for certain composite specimens with the textile reinforcement). The second loop consists of cycles with elongation higher by 10%: loading to 40% and unloading to 10%

of elongation. The third loop consists of five cycles that have loading to 50% and unloading to 20% of elongation, the fourth loop with cycles has loading to 60% and unloading to 30% of elongation. The fifth loop has cycles with different elongations, the loading to 60% is the same as fourth loop and unloading is 5% of elongation. The final step is loading to 100% of elongation. The specimens with a cord angle of more than 45° have a higher rigidity, so the method is different for an angle of 60°: all values of elongations are multiple 0.4 of values of elongations for angles of 0°, 30° and 45°.

2.4 *Experimental apparatus*

The test machine Autograph AG-X plus 5kN – Schimadzu with a video-extensometer for large strain as tensile tests of composite materials with elastomer and viscoelastic materials with the test mode Control of software Trapenzium X version 1.4.5 is used for the tests of cyclic loading in tensile with cycle loops. Before the tests, calibration of the video-extensometer is required.

The software Matlab was used for separation of data for every cycle for obtain graphic curves.

3 RESULTS AND DISCUSSION

3.1 *Geometrical parameters of cords*

The geometric parameters of the reinforcements of tire casing 245/40 R18 in place end of steel-cord belts are showed on the Figure 5 and schematic structure in the center of the tread is on the Figure 6.

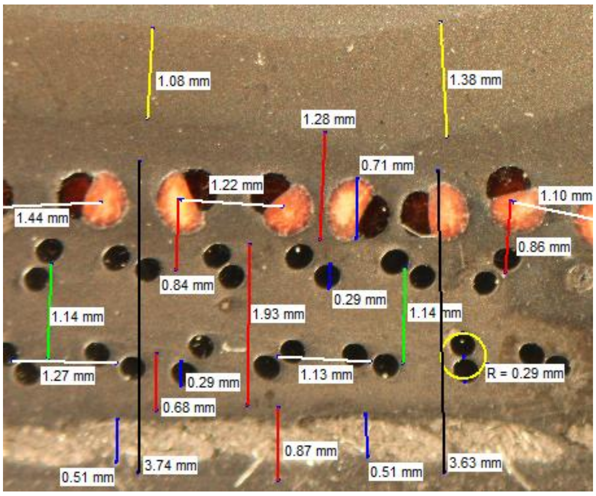

Figure 5 The image analysis of part of tire casing 245/40 R18

The EPM of the textile cap ply is approx. 850 m^{-1}. The diameter of cords is 0.69 mm and the thickness of the cap ply is approx. 1.2 mm. The textile carcass has 0.5 mm diameter of cords and the thickness is 0.92 mm. The steel cord belts consist of two plies with a density of 920–960 m^{-1} and the cord construction is 2x0.30 mm. The thickness of the steel cord belt (two plies altogether) is 1.94 mm. The thickness of layers of elastomer under tread is visible on the Figure 6.

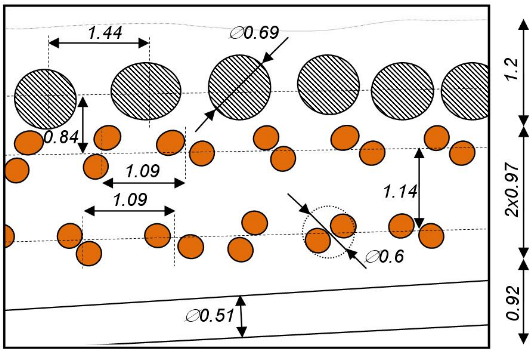

Figure 6 Geometrical parameters of cords in cross-section

The geometric parameters (Figure 6), which were obtained by an image analysis of the cross-section (the accuracy of the parameters is 95%), will be used as necessary geometric input data in order to create a computational model with a real configuration of cords.

The obtained information about the geometric arrangement of reinforcements can be used also for an optimization of arrangement of cords in a tire casing in order to gain better stiffness parameters in individual directions.

3.2 *Composite after tests of cycle loading*

Deformations of specimens are shown in Figure 7. The geometrical change of the specimen shape is not symmetrical for an angle of 45°, a part of the specimen was pulled from jaws of the testing machine during the test. White lines on a side of the surface of the sample are signs of better representation of deformation during the test.

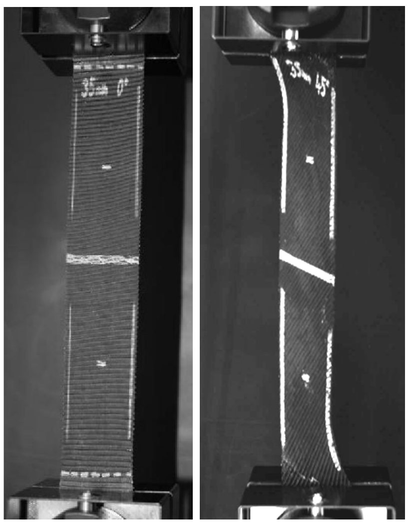

Figure 7 Photos of specimens by a video-extensimeter for the deformation 100 mm (photos obtained by a video-extensimeter)

Raw data from Trapezium X have over 46 000 rows for every angle. The further data processing is difficult because of a large number of data fields in Microsoft Excel. Therefore the software Matlab was used for searching of cycle maximum and minimum from raw data.

Dependences of true stress on elongation between points for a video-extensometer (marking as elongation ex.) are:

- the Figures 8 and 9 (in Figure 8 dependences of engineering stress on elongation between clamps of the test machine are only for comparison with true stress - elongation ex.) for a cord angle of 45°;
- the Figure 10 for a cord angle of 0°;
- and the Figure 11 for a cord angle of 60° (a different method).

The behavior of specimens during the tests is very different.

The fifth cycle in every cycle loop can be considered as a stable cycle because difference between fourth and fifth cycle is about to 5%. Therefore the dependences of fifth cycle of every cycle loop are important for the comparison between the cord angles. The comparisons of the fifth cycles are given in Figure 12 as dependences of true stress on elongation ex.

The approximate the dependences for a cord angle of 0° (Figure 12) can be used as input material parameters of an elastomer matrix.

The envelope curve for a cord angle of 45° is in Figure 13. This curve can be used as input material data, which describes a textile cap ply as a whole, for computational modeling of a specific tire carcass e.g. a sport bike tire [18].

The computation modeling and calculations of long-fiber composites are very difficult because the accurate materials characteristics of matrixes [19] and reinforcement are needed but these accurate materials characteristics have to be obtained from the tests of cycle loading.

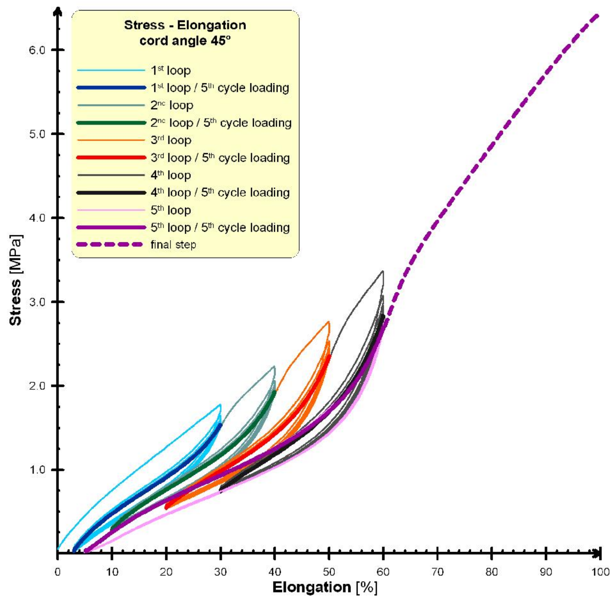

Figure 8 Dependences of engineering stress on elongation between clamps for a cord angle of 45°

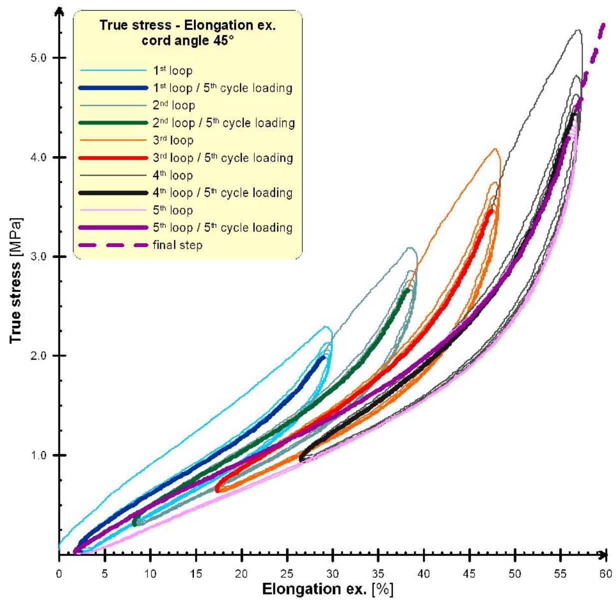

Figure 9 Dependences of true stress on elongation between points for a video-extensometer for a cord angle of 45°

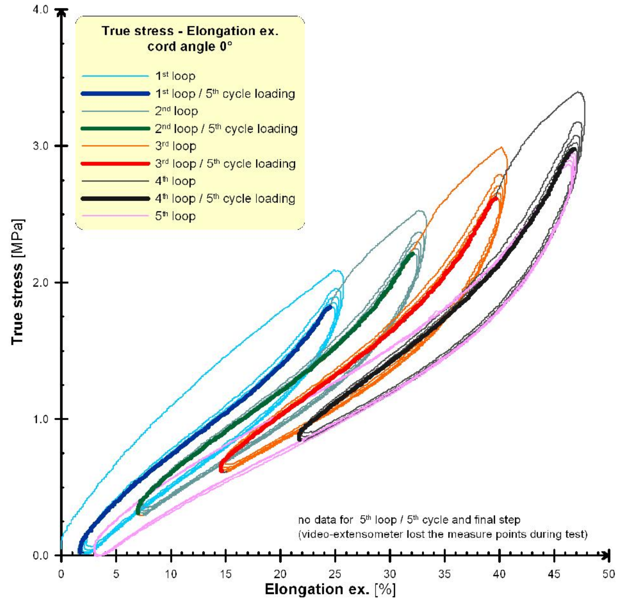

Figure 10 Dependences of true stress on elongation between points for a video-extensometer for a cord angle of 0°

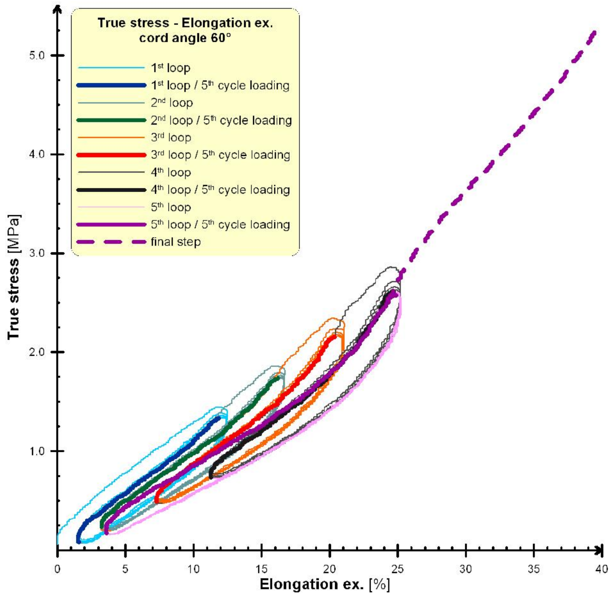

Figure 11 Dependences of true stress on elongation between points for a video-extensometer for a cord angle of 60°

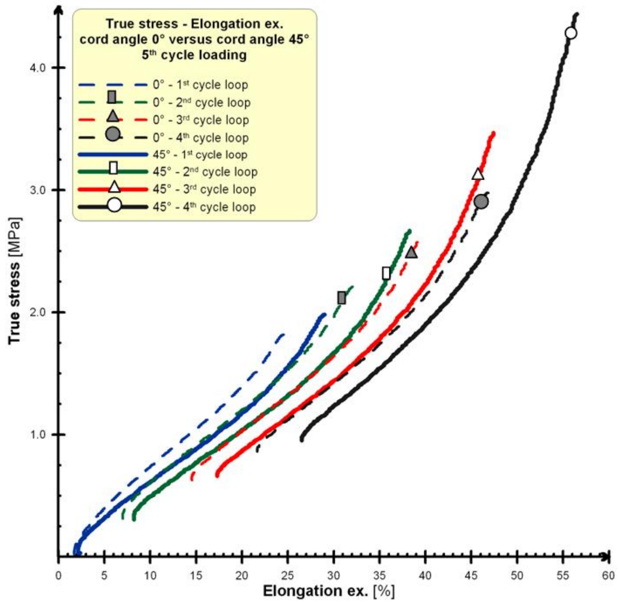

Figure 12 Comparison of the fifth cycle of cord angles 0° and 45°

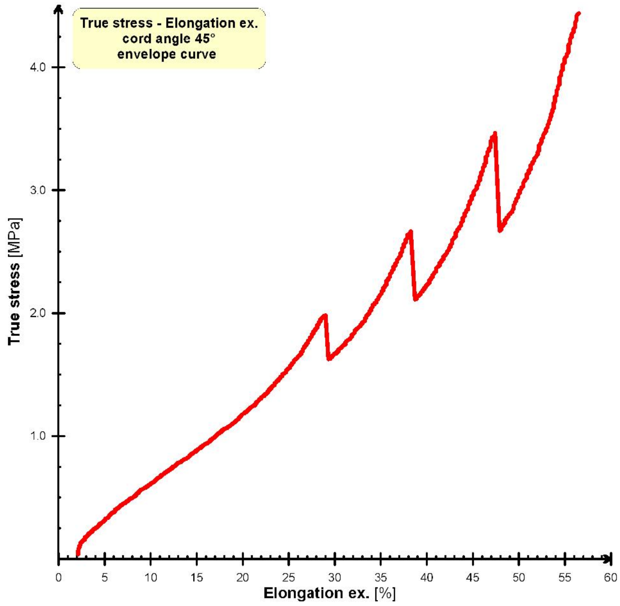

Figure 13 The final envelope curve for a cord angle of 45°

4 CONCLUSSIONS

The geometric parameters, which were obtained by the image analysis of cross-section, will be used as necessary geometric input data in order to create the computational model with real configuration of cords. The geometric parameters, which were obtained by an image analysis of the cross-section (the accuracy of the parameters is 95%), will be used as necessary geometric input data in order to create a computational model with a real configuration of cords. The results can be used for an optimization of the deposition angle of textile reinforcement in composites.

In this study, methods for testing of textile composites with five cycle loops for different elongation with five cycles in every cycle loop have been designed with following finding:

- The fifth cycle in every cycle loop can be considered as a stable cycle, because difference between fourth and fifth cycle is small.

- The values of true stress for a cord angle of 45° are approximately 20–25% higher than values for a cord angle of 0° (reinforcement has right angle to loading force).
- Suggestion for the second option of the method: unloading for the next cycle loop only to the maximum elongation from the previous cycle loop.

A mathematical description of the envelope curve from the fifth cycles (Figure 13) is search. The curve can be replaced by polynomial of 9th degree.

The results from tests of low cyclic loading can be used for the optimization of the deposition angle of textile reinforcement in composites.

For the specimens with steel-cord, different (lower) elongations for definition of cycle loops must be used because the specimens of steel-cord belt have higher stiffness than the specimens of composite with textile reinforcement such as a tire carcass.

The test machine Autograph AG-X plus 5 kN – Schimadzu has a hybrid temperature-humidity chamber allowing the tests from -70 to 180°C and from 20 to 80°C, it is possible to change the humidity from 30 to 95%. Future research is needed for the tests of cyclic loading of composites, which will be realized at different temperatures.

***Acknowledgement**: The contribution was supported by the Cultural and Educational Grant Agency of the Slovak Republic (KEGA), grant No. KEGA 005TnUAD-4/2016 and the project „Centrum pre testovanie kvality a diagnostiku materiálov" ITMS code 26210120046 of the Operational Program Research and Development funded from European Fund of Regional Development.*

5 REFERENCES

1. Barbero E.J.: Introduction to composite materials design, Taylor and Francis, 2010, ISBN 978-1-4200-7915-9
2. Koštial P., Krmela J., Frydrýšek K., Ružiak I.: The Chosen Aspects of Materials and Construction Influence on the Tire Safety, Composites and Their Properties, Chapter 13, InTech, Rijeka, 2012, pp. 265-298, ISBN: 978-953-51-0711-8. doi: 10.5772/48181
3. Composite authors: Rubber Technology, GC Tech Peter Gerši, Trenčín, 2006, ISBN 80-969189-5-8
4. Nideröst K.J., Walters M.H.: Cord reinforced elastomers, In: Comprehensive Composite Materials, New York, Elsevier, 2000, pp. 77-105. ISBN: 978-0-08-042993-9
5. Shiguo R. et al.: Mechanical Properties and Failure Behaviour of Cord/Rubber Composites, Applied Composite Materials 11(6), 2004, pp. 353-357, doi: 10.1023/B:ACMA.0000045312.61921.1f
6. Ferry J.D.: Viscoelastic properties of Polymers, New York, John Wiley & Sons, 1980, 117, ISBN: 978-0471048947
7. Jambrich M.: Štruktúra a vlastnosti výstužných technických vlákien (Structure and properties of reinforcing technical fibers), Proceedings of SRC (Slovak Rubber Conference), Púchov, 2001, (in Slovak)
8. Tanner J.A.: Computational methods for frictional contact with applications to the space shuttle orbiter nose-gear tire, Hampton, Virginia, NASA Langley Research Center, 1996, 58 p., NASA-TP-3573
9. The Pneumatic Tire, Gent A.N., Walter J.D. (Eds.), NHTSA, 2006, 705 p., US DOT HS 810 561
10. ISO 2062:2009, Textiles – Yarns from packages – Determination of single-end breaking force and elongation at break using constant rate of extension (CRE) tester
11. Marcín J., Zítek P. :Gumárenské výroby I – Pneumatiky (Rubber Manufacturing I – Tires), SNTL, Prague, 1985, 490 p., ISBN 04-626-85 (in Czech)
12. Krmela J., Dvořák Z., Pešlová F.: Long-Fibre Composite Experimental Modelling, Scientific Bulletin – 7th International Multidisciplinary Conference, Baia Mare, North University of Baia Mare 21, 2007, pp. 369-374, ISSN 1224-3264, Access mode: http://www.nordtech.ubm.ro/issues/2007/2007.01.57.pdf
13. Eric Greene Associates: Marine Composites, 1999, Access mode: http://www.ericgreeneassociates.com/images/MARINE_COMPOSITES.pdf
14. ASTM D-3039-76:1985, Standard Test Method for Tensile Properties of Fiber-Resin Composites
15. Krmela J., Krmelová V.: Tire casing and their material characteristics for computational modeling of tires, Proceedings of 16th International Scientific Conference Engineering for Rural Development, Jelgava, 2011, pp. 206-211, doi: 10.22616/ERDev2017.16.N043, ISSN 1691-5976
16. Le Cam J.B., Toussaint E.: Cyclic volume changes in rubber, Mechanics of Materials 41(7), 2009, pp. 898-901, doi: 10.1016/j.mechmat.2009.02.004
17. DIN 53835-13:1983, Testing of textiles; determination of the elastic behaviour of textile fabrics by a single application of tensile load between constant extension limits
18. Krmela J., Vančo M.: Bike tire with textile reinforcement - experiment and computational modelling, Vlakna a Textil (Fibres and Textiles) 21(3), 2014, pp. 31-34
19. Krmela J.: Tire Casings and Their Material Characteristics for Computational Modeling, Scientific monograph. Czestochowa, Poland: Oficyna Wydawnicza Stowarzyszenia Menadżerów Jakości i Produkcji (Printing House The Managers of Quality and Production Association), 2017, 109 p., ISBN 978-83-63978-62-4

EVALUATION OF SURFACE WATER ABSORBENCY OF TERRY FABRICS

Jela Legerska

Alexander Dubček University of Trenčín, Faculty of Industrial Technologies, I. Krasku 491/30, 020 01 Púchov, Slovakia
jela.legerska@fpt.tnuni.sk

Abstract: *The main aim of this paper was to evaluate the surface absorbency of loop terry fabrics using a new method. Evaluated loop terry fabrics with the different material composition and structural parameters were intended for the manufacturing of terry towels. After the detailed analysis of the thread as well as fabrics themselves, the new measurement method was used for determination of the surface water absorbency and subsequently, the drying time of terry fabrics was also specified. The results of measurements indicate that the surface water absorbency is not related to the material composition, but the drying time is closely connected with the given composition. Based on the observation and investigation, the surface water absorbency is related to the structural parameters of fabric and threads. The new testing method could be included into the new evaluation methods of surface water absorbency or it could be even used instead of current methods which are applied for assessment of the terry fabrics absorbency.*

Keywords: *surface water absorbency, drying time, height and number of terry loops, loop terry fabric, material composition and structure of fabric.*

1 INTRODUCTION

Bath body cleansing is the most natural and the most common activity which leads to the refreshment of human skin and regeneration of all human body. After hygienic body cleansing the towel is used in order to wipe the skin and this is the moment when the towel in the close contact with human body skin. Generally, the towels, which are used in our bathrooms, have to meet the following requirements: a high absorption capacity, moisture wicking, tactile softness and fineness [1].

Other requirements that should be characterized in relation to terry towels are: non-allergy, antibacterial effects, antimycotic effects, odour resistance, fast drying up and easy maintenance [2]. Some of these properties are described in this. Moreover, a very important component of the towel comfort is the wet thermal feeling, which was not studied in the submitted manuscript [3].

In relation to the towels assortment, the process or course of the water transfer does not exhibit the same features in comparison with the clothing fabrics where the water is transferred from the skin through clothes and then it gets quickly to the ambient environment. In the case of the towels, the transfer of water is divided into two specific phases [4]. In the first phase, the water is quickly transferred from the skin to the towel. Taking into account the specific time interval after the first phase, the second phase occurs. In relation to this second phase, the moisture evaporates from terry towel to the environment and long-term desiccating process occurs. Based on the predetermined investigation procedures and steps, the following evaluation is introduced in this paper:

- evaluation of the first phase of surface water absorbency in relation to the terry towel,
- evaluation of the second phase, which stands for the time interval of the terry towel desiccating process, which is based on the water evaporation to the environment [4].

The main objective of the paper was to specify the influence of the material composition and the influence of the basic parameters of terry fabrics on their surface water absorbency as well as the time of desiccating process. The measurements were repeated after every washing (max. number of washing procedures = 5 times). The new method was designed and tested in relation to measurement of surface water absorbency, while the given method was based on the simulation of the practical application of the terry fabrics in order to determine their surface water absorbency during the hygienic body cleansing. Fabrics, which were used for investigation as samples, were made of cotton, regenerated cellulose, lyocell fibres, and their mixtures. Besides the thread and fabrics evaluation, the specification of number and measurement of loops height had been performed before the measurement of the surface water absorbency properties were investigated. The research program involved the measurement of the absorbency and wicking of the terry fabrics.

2 METHODS AND USED MATERIAL

2.1 Materials

Terry towels belong to the special type of fabrics. A terry towel is described as a textile product which has a loop piles on one or both sides, generally covering the entire surface or forming stripes, some areas or any patterns (with end hems or fringes and side hems or selvages) [5], (Figure 1). It is formed directly in the process of weaving through the warp thread system. Besides one type of weft threads, two systems of warp threads are required – basic warp and loop warp in relation to the production of these textiles. The loops are formed of terry warp, using the weaving in a special way. The stability of the woven system is based on lacing of basic warp threads with the weft threads. During the finishing treatment, the loops can be shortened by cutting.

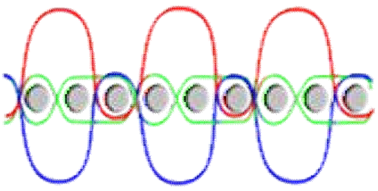

Figure 1 Cross-section of double-sided terry fabrics [5]

The selection and evaluation was closely connected with the terry woven fabrics, the weaving system of which was based on a trivalent or tetravalent cross rips according to [5]. The warp wise was formed by threads of basic warp along with the threads of loop warp in the ratio of two warp threads to the two loop threads (2:2). This interlacing was repeated in the case of all woven samples except the sample designated as n.5, where the ratio was determined for one warp thread and the one loop thread (1:1). Assortment of terry fabrics was used for preparation of individual samples for which a detailed structural analysis of the following characteristics was made: dimensional changes according to [6], area density of fabric and fineness of thread according to [7], the thickness of the fabric according to [8], number of threads in the fabric according to [9], (Table 1). The height and number of loops of terry fabrics was also assessed. The measurement of the loops was done using a metal measuring instrument which was placed between the individual lines of loops (Figure 2). The measurement was repeated ten times for each sample after every washing process. After the loops had been straightened, the height of these loops was measured in various sites of terry towel. Based on the microscopic observation, the images with the minimum and maximum height of loops were selected. From Figre 2, it can be seen that the shorter loops on the fabric were formed into a U-shape and the longer loops twisted themselves along their length. Table 2 shows that the average height of loop terry fabric was different. The height of loops, measured after each washing process, was changed minimally. The number of loops over the area of 100×100 mm was also measured. The given number was counted in the warp and weft direction after each washing process. Table 2 shows the average value of the number of loops. The number of loops was also changed minimally after each washing process.

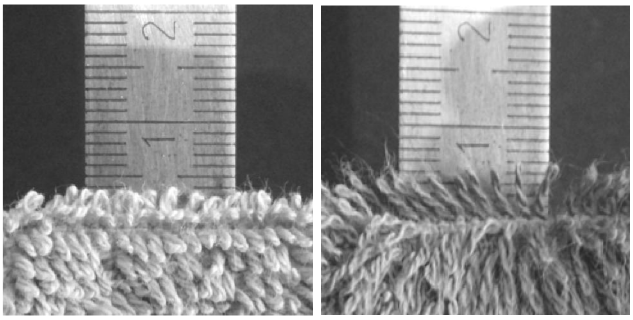

Figure 2 Measurement of height of the loops – sample n.4 (left) and sample n.9 (right)

Table 1 Properties of terry fabrics and threads

n.	Materials	Thickness [mm]	Unit weight [gm^{-2}]	Fineness [tex] weft/2 warps
1	100% cotton	400	2.22	35/56/35
2	100% cotton	450	2.23	38/61/35
3	100% cotton	500	2.39	38/60/34
4	100% cotton	600	3.21	38/57/55
5	100% microcotton	400	2.63	48/60/44
6	70% cotton 30% tencel	450	2.05	40/60/37
7	60% cotton 40% regenerated cellulose	450	2.05	40/57/37
8	55% cotton 45%regenerated cellulose	450	2.16	41/63/37
9	50% cotton 50%regenerated cellulose	450	2.56	37/57/38

Table 2 Average height and number of loop terry fabric

n.	Properties	
	Height *l* [mm]	Number *n* [100x100mm]
1	3.7	3840
2	3.1	4216
3	4.0	4480
4	2.3	4096
5	3.3	4080
6	2.8	4464
7	3.3	3840
8	4.0	4096
9	5.4	4224

2.2 Measured surface water absorbency

The main objective of this work was to measure the surface water absorbency of the terry fabrics. After the each measurement of the mentioned properties, the washing process of towels was carried out. Washing conditions were determined according to [10] as follows: temperature of the wash bath was 60°C, the ratio of solution to the sample was 50:1, the number of rinses in cold water was 2 and washing time was 60 min. ECE detergent [3] was used as a testing washing agent for preservation of colour fastness. A new type of device was designed and constructed for simulation of the surface water absorbency. Figure 3 shows the components needed to construct the given device.

Relating to surface absorbency ability of terry towels, the tests were performed under the strict conditions determined for tested samples. Two measurement points or areas were designated for the each one sample. At first, the tested sample was fixed in the holder and then, 50 ml of distilled water was poured into the funnel, from which the given water flowed down onto the surface of the terry fabric. To preserve the same conditions for all tested samples relating to water speed, the speed of the water flow was determined to be constant and it was 8 s. The testing procedure was connected with determination or detection of the overflowed distilled water which was not absorbed by terry fabric [11].

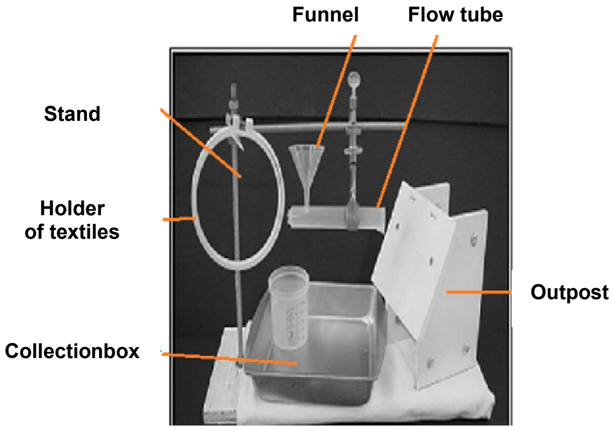

Figure 3 Parts of device necessary to measure the surface water absorbency of terry fabric

The overflowing water was collected in the collection box and then poured into a measuring cylinder. Subsequently, the value of overflowed water was subtracted from the original amount of distilled water (volume) and this calculation led to the result of the testing procedure and it was the determination of average value of surface water absorbency of the terry fabric in the predetermined area. After the each measurement of the mentioned properties, the washing process of towels was carried out. Terry fabric samples were washed for 5 times at all.

3 RESULTS AND DISCUSSION

The new method is based on descriptions in literature resources referring to surface water absorbency [3] and it is similar to the method for evaluation of the resistance of fabrics to surface wetting according to [12]. From Figure 4, it is clear that repeated washing process led to increase of the surface water absorbency.

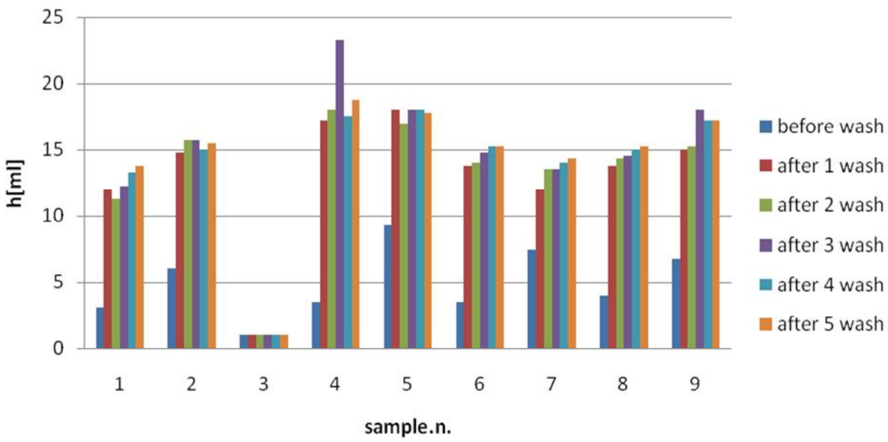

Figure 4 The average values of the surface water absorbency *n* (ml) of terry towels – reference samples (before washing - 0) and after 1, 2, 3, 4, 5 washing

The measurement was performed on one sample at two areas. The highest increase of surface water absorbency was observed for all the samples after the first washing process in comparison with these samples before the first washing process. The highest value of surface water absorbency was observed in the case of the samples designated as n.4 and n.5. The sample no.3 was an exception, because the value of the surface water absorbency was the lowest in comparison with all tested samples and moreover, the given value was not changed during the whole testing process. Table 3 shows the increase in surface water absorbency and thickness after the first and last washing process.

Table 3 Increase of surface and thickness

	Increase of surface water absorbency *n* [%]	Increase of thickness *h* [%]
1	15	8
2	5	18
3	0	19
4	9	7
5	1	9
6	11	25
7	19	24
8	11	24
9	15	21

The correlation dependences were used for the evaluation of the impact of structural parameters, such as thickness (Table 1, 2), on surface water absorbency. From the correlation dependence, it can be seen that the thickness of the towel has the main impact on surface water absorbency (Figure 5).

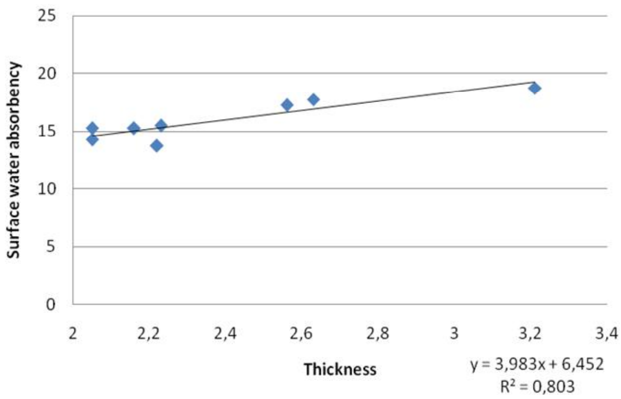

Figure 5 Dependence of surface water absorbency on the thickness

Increase in the thickness of the towel leads to the increase in the surface water absorbency. This dependence was evaluated and verified after the each repeated washing process. The obtained results after each one washing process are in the accordance with values, which can be seen in Figure 5, where the correlation dependence after the last wash is shown. The sample designated as n.3 was excluded from the correlation dependence due to different results of surface absorption (see Figure 4).

In the second phase of testing procedure of loop terry fabrics, the evaluation was focused on the ability to desorb and transport the moisture into the ambient environment. The tested samples were washed in detergent under according to the predetermined conditions and they were left to desiccate in air at relative humidity of 60±1% and ambient temperature of 21±1°C. The washing conditions and the composition of the wash bath are given and explained in part 2.2**.** In relation to the defined time intervals, samples were weighed on the analytical balance. The weighting of the samples was repeated until the value of the weight of the dried sample was the same as it was before the test. Table 4 shows the total desiccating time of individual terry fabric samples. After mutual comparison, drying speed and trend in humidity decrease are different because they are influenced by the various material compositions.

Table 4 Time of terry fabrics desiccating

Sample	1	2	3	4	5	6	7	8	9
Time of desiccating [h]	42	48	48	42	54	54	54	54	60

4 CONCLUSION

The work was focused on evaluation of loop terry towel (fabric). The surface water absorbency of predetermined areas or sites of terry fabrics was observed and evaluated in relation to material and structural composition. The main objective was to simulate real conditions of surface water absorbency of terry towels. The constructed device for measurement of surface absorbency of towels was designed and constructed. The given constructed device could be used for more precise measurement of the absorbency of the towels because it represents the reliable simulation of the surface absorbency of towel during its contact with the wet human skin. Compared to other methods, which have been used for determination and evaluation of water absorbency and of water absorption according to [13], wicking process according to [14], the evaluation of surface water absorbency is more impartial (objective) and more accurate for the given towel assortment. The results of the measurements show that samples designated as n.4 and n.5 have the best surface water absorbency. In the case of these samples, there is very good transport of moisture from the skin and therefore, they are a good representatives of wet sorption while this sorption is based on the structure of terry fabric. The impact of material composition and structural parameters of terry towel fabrics on surface water absorbency was also evaluated. Based on the obtained results, it is important to point out that material composition did not have any significant impact on changes of observed properties. Relating to findings, it can be concluded that the addition of tencel and regenerated cellulose to the cotton mixture does not have any impact on the increase of the surface water absorbency. In comparison with the cotton, the mentioned components exhibit better antimycotic and antibacterial properties as well as better odour resistance [2]. Repeated washing process and subsequent measurement of surface water absorbency of towels led to increase of the surface water absorbency after each one washing process. Moreover, the measured values are stabilized after the fifth washing. Interesting results were obtained in relation to sample designated as n.3, because there were not any changes observed after the repeated washing process (the given sample exhibited the same values of surface water absorbency after each washing and measurement) and it can be attributed to high surface tension, which is caused by significant deterioration of surface water absorbency leading to malfunctioning of terry towel fabrics. Terry towel fabric made of 100% cotton (samples designated as n.1, 2, 4) exhibited increase in surface water absorbency along with the increase in area density and thickness. The evaluation of the structure of terry towels, based on the number and the height of the loops lead to the interesting results because the increase in the number and height of loops led to the opposite effect in comparison with the expectations. Especially, the terry fabrics with lower number of loops and smaller height exhibited the higher surface water absorbency. In relation to the second phase standing for the evaluation of the desiccating process of towel samples, the given terry fabric samples, which contain cotton combined with other more absorptive component, exhibit much longer time interval of desiccating. The reason was mainly based on the different values for the humidity additions of regenerated cellulose and tencel in comparison with cotton.

Although the results of the introduced method are not so clear, the investigated measurement process of surface absorbency is more objective (in comparison with the older universal methods). Our task is to continue in the verification of the method, using the different types of towels. Moreover, models with satisfactory prediction for other structures of towels are going to be found. In addition, the wet thermal contact feeling could be included into the investigation processes as well as models.

5 REFERENCES

1. Sun G, Xu X.: Durable and regenerable antibacterial finishing of fabrics: biocidal properties, Textile Chemist and Colorist 30(6), 1998, pp. 26-30
2. Gupta D., Bhaumik S.: Antimicrobial treatments for textiles, Indian Journal of Fibre and Textile Research 32(2), 2007, pp. 254-263
3. Substrata D.: Performance of Home Textiles, Part: Evaluation of Home Textiles, Woodhead Publishing India, 2010, pp. 161-197
4. Horcickova L.: Influence of the material composition on the hydromechanical properties of loop fabrics, FPT Púchov 2016, Thesis VP 19240
5. Legerska J.: Weave fabrics, FPT Púchov TuAD Trenčín, 2015, pp. 119-120, ISBN 978-80-8075-683-3
6. STN EN ISO 3759: Textiles. Preparation, indication and measurement of sample surface textiles and garments in tests determination of dimensional changes, SUTN Bratislava, 2011
7. STN EN ISO 2060: Fineness of yarns, taken off from fabric according to STN ISO 7211-5, chemical fibers and cables according, SUTN Bratislava, 1998
8. STN EN ISO 5084: Textiles. Detecting the thickness of textiles and textile products. SUTN Bratislava, 1999
9. BS EN 1049-2: Textiles. Woven fabrics. Methods of analysis. Determination of number of threads per unit length, 1994
10. STN EN ISO 6330 (80 08 21): Textiles. Procedure of home washing and drying textiles, UNMS Bratislava, 2012
11. Heinisch T, Tesinova P, Poloscukova P.: Moisture management for different air conditions, Vlakna a Textil (Fibres and Textiles) 24(3), 2017, pp. 64-67
12. STN EN 24920 (800827): Textiles. Determination of the resistance to surface wetting (spray test) of fabrics, UNMS Bratislava, 1997
13. STN 80 0831: Absorbency of surface fabrics, UNMS Bratislava, 1970
14. STN 80 0828: Determination of water absorption, wicking process, UNMS Bratislava, 1992

THE EMPOWERMENT OF DESIGN AND MANAGEMENT FOR NON-MACHINARY *LURIK* WEAVING INDUSTRY IN CENTRAL JAVA INDONESIA

Mulyanto[1], Nadia Sigi Prameswari[1] and Rakotoarisoa Maminirina Fenitra[2]

[1]*Lecturers of Arts Education Department, Faculty of Teacher Training and Education, Sebelas Maret University, Jl.Ir.Sutami 36A Surakarta, 57216, INDONESIA*
[2]*Magister Management, Faculty of Economic and Business, Sebelas Maret University, Jl.Ir.Sutami 36A Surakarta, 57216, INDONESIA:*
mulyanto@staff.uns.ac.id; nadiasigi87@gmail.com; fenitra.rakotoarisoa@gmail.com

Abstract: *The objective of this research is to formulate a model for the establishment of Non-Machinery Weaving Tool (called ATBM) lurik textile industry in Klaten Regency, Indonesia. This research was an action research involving ten persons. The data were gathered through in-depth interview, participatory observation, and focus group discussion. The establishment model was applied through three phases, that is, 1) conducting need analysis, 2) arranging action plan, and 3) implementing a model of small bussiness management plan. The establishment program was developed through several actions, namely: developing an innovative lurik design, manipulating the non-machinery weaving tools, diversifying the lurik weaving patterns and techniques, growing the capacity of sekir sketcher, granting the capital support, managing the work agreement and contract, motivating the entrepreneurs and workers, and developing the promotional media.*

Keywords: *non-machinery weaving, industry, lurik, textile, design*

1 INTRODUCTION

Lurik textile is one of the oldest and classic weaving fabrics that still exist on many traditional weaving textiles industries in Java Island in Indonesia. Its solid texture and specific design with paralel hard-lines have been the preference clothing for most average people from villages in Central Java. Its traditional function is weakening due to the modernisation in the industrial production of textiles. This partly comes from the way the *lurik* are produced that only relied on the non-machinary weaving tool called *Alat Tenun Bukan Mesin* (from here on called ATBM). The competition of modern textiles indutries to provide a qualified textile with more advance design makes the *lurik* textiles more vulnerable. Although wearing the *lurik* textiles is considered less modesty, this material is still produced by small bussiness unit. The *lurik* (which literary means parallel lines) textile industry, however, is now considered as an important national asset that must be renewed to keep them alive as part of Indonesian traditional pride. This paper aims to share a model to empowerment of the small weaving industry and to preserve the *lurik* textiles to become a better design and production.

According to the Law of the Republic of Indonesia, Number: 20 of 2008, micro business is a business unit which owns the net asset of fifty million Indonesian Rupiahs (hereafter the Indonesian rupiah is written as Rp) at the most excluding the land and building for the business site, or a business unit which annual sale result ranges estimated Rp300 million to Rp2.5 billion [1]. This kind of small industry is weaving craft production. Weaving is a fabric made through a simple way by weaving the warp yarns and P*akan* yarns by crisscrossing them at 900 [2-4]. The ATBM weaving is a weaving craft whose production process is done manually by using the non-machinery weaving tools (ATBM).

One of the weaving craft center resides in Klaten, Central Java. Their production house is mostly located in the villages, such as in Burikan, Tulas, Karangmlese, Juwiran, and Jobotan. The generic problems they encountered are varied but a multifaceted difficulty. Viewing from their business scale point of view, most of the ATBM weaving industries is considered in the micro-scale industries. Viewing from their motifs, nearly all of the weaving fabrics produced have tradition *lurik* motifs. Viewed from their product use, the *lurik* weaving fabrics produced are used as carrying the shawl with the dimension of 70x250 cm, serviette with the dimension of 60x60 cm, sarong with the dimension of 2x60x220 cm, as garment per piece with the dimension of 110x20 cm or 70x300 cm, and other household accessories.

Moreover, the problem is caused by human resources and skills. The weaving businessmen or entrepreneurs generally only hold a low education background, that is, primary school, and are aged more than 40 years old. They by and large inherit the business from their parents. Most of their employees (90%) are females. They are aged more than 40 years old and hold a primary school education only, and even some of them are illiterate. Despite their limitations and the low values of the products that they produce, they can still run their production activities up to the present time. This national asset really needs many empowerment programs to keep survive in this highly economic and business competition.

On the other hand, the youths around the ATBM weaving craft centers of Klaten are generally less interested in managing such a business. The female youths tend to choose between working at the medium and large-scale industries in the city although the wages that they earn are lower than the wages if they work as weaving craftsmen. They think that working at the medium and large scale industries is more respectable than working at the ATBM weaving micro-scale business units at home. In addition, the male youths tend to choose work out of their villages, working in other cities or even recently in other countries.

The conditions of social and cultural environment of the community around the weaving craft centers of Klaten are mutual, collaborative, and agrarian and traditional in natures. Based on the internal conditions of the micro-weaving business units, the social and cultural conditions of the local community, the environmental conditions, this research is aimed on formulating an empowerment model of the *lurik* ATBM weaving micro-scale business units through design development.

The empowerment of micro-scale weaving business units or weaving craftsmen is defined as an effort to improve life quality, the prosperities of the businessmen and their employees such as the improvement their economy,social prosperity, education, health, freedom, and security sustainably [5]. It is an educational activity to convey the truths that have been believed. The empowerment must grow as an independence or autonomy, but must not create dependence. The empowerment through design development means that the *lurik* ATBM weaving to design is planned, which includes the aspects of raw materials, processes, products, aesthetics, and functions. At the planning of product design such as weaving product, Prasetyawibowo [6] and Rizali [7] claim that it must consider functional, technical, ergonomic, economic, environmental, social, cultural, and artistic aspects.

2 METHODOLOGY

This research was conducted at the ATBM weaving micro-business unit called YS in the Burikan village, Cawas sub-district, Klaten Regency, Central Java, Indonesia. This business unit is regarded being able to reflect the conditions of such ATBM weaving micro-business units in Klaten regency, which have many weaknesses, but which can survive until now. The location of the business unit is in a remote village.

This research used the qualitative study and action researched. The researcher was involved directly in the process of the ATBM weaving design development and production process. In addition, the researcher also was involved as a facilitator or an agent of change [8] who is responsible to influence the decision-making process done by benefit recipients (businessmen and employees) in adopting innovation. The researcher as a facilitator must have four qualifications, namely: communication ability, attitude, knowledge ability, and social and cultural characteristics [9, 10].

The subjects and samples of the research were determined by purposive and time sampling techniques. The data onto the research were obtained from 10 persons, namely: the entrepreneurs (whole family members), a sekir artisan, 2 yarns dying workers, and 4 weavers. Furthermore, the data were also obtained from the production process sites and activities [11]. The data were gathered through in-depth interview, [12], actively participatory observation [13] and focus discussion group [14].They were validated by using source triangulation, technique triangulation, peer debriefing, and review for key informants. The data were then analyzed by using the interactive model of analysis [15].

3 ANALYSIS

3.1 Conditions of the ATBM weaving micro-business unit prior to action

Since the beginning of 2010, the ATBM weaving micro-business unit has occupied two buildings with the total area of 150m^2. The first building is the residence for the family; it is also used for the production process (sekir process, yarn rolling process) and for storing the raw materials and products. The second building with dirt floor and woven bamboo wall is used for weaving process.This room accommodates 10 looms. The ATBM owned by the entrepreneurs includes 1 yarn rolling process tool, 3 palettes, 3 plastic pails and one drum for boiling the yarns.

The micro-business unit of “YS” is owned and managed by Siti Lestari who was born in 1974 in the same village. She has only primary school education. Her husband is a Junior Secondary School teacher. The business unit has 13 employees, 3 males and 10 females. The former is employed as yarn dyeing, product packaging, and product marketing workers. Of the latter, one works as a sekir artisan, 2 yarn rolling workers who are aged 70 years old and 7 weavers. Most of them only hold primary school education, even some are illiterate. Viewed from the innovation adoption levels as claimed by Rogers [16], which include 5 levels, namely: innovators (risk takers), early adopters (hedgers), early majority (waiters), late majority (skeptics), and late adopters (slowpokes); most of the workers can be classified as late adopters (slowpokes) except the sekir artisan whose innovation adoption can be categorized into a higher one that is early adopters.

The raw materials to make *lurik* woven fabrics are yarns, and dyeing substances. The materials used for warp yarns and pakan yarns are mercerized yarns with the size of 40/2 so that the woven fabrics produced are quite thick. The dyeing substance used is remazol substance.The *lurik* design motifs produced are the ATBM woven fabrics with traditional *lurik* motifs, dominantly using black, brown, red, green, and blue colors. The monthly production level of the micro-business unit of the YS is 12 warp beams and 1 beam consists approximately of 80 meters. The sale value of woven fabrics with the width of 105-110 cm is Rp24.000 per meter or is equal to US $2. Therefore, the average income of the entrepreneur is approximately Rp23.034.000 per month or Rp276.480.000 per year. Based on its average revenue per year, the business unit of the YS is classified as a micro-scale business unit [1].

The ATBM weaving micro-business industries are mostly situated in remote villages. Its surrounding environments are mostly rice fields and mountainous areas. The communications with cellular phones are obstructed due to the bad signals. The social-cultural environment conditions of the local people where it operates are traditional agrarian society [17]. When the rice season comes, (rice planting, harvest season, post-harvest seasons), the weavers leave their jobs. In addition, they also leave their jobs when there are social mutual assistance activities, particularly wedding parties [18]. According to Mulder [19], the personality of Javanese is social in nature. One is good when the society regards so. For example, when the sekir artisan (Semi) is absent from work, she is substituting her husband to join mutual assistance activities to build a village office.

3.2 A model for empowerment of the ATBM weaving micro-business unit

Based on the data analysis, the result of the research shows that the model for empowerment of the ATBM weaving micro-business unit through the design development consists of the following phases:

- the first phase is conducting the need analysis;
- the second phase is arranging the program plan
- the third phase is implementing the program.

3.3 The need analysis

The need analysis phase by the entrepreneur is to identify the existing problems and real needs. The former are discovered through direct observation and focus group discussion (FGD) between the researcher, entrepreneur and the employees. There are four problems identified with the research, namely: the production process is less efficient, the motifs and patterns of the produced woven fabrics are still monotonous, the entrepreneur's working capital is inadequate and the entrepreneur is confident that the weaving business unit cannot support their family life. The less efficient production process is caused by the less efficient tools, types of yarn materials, number of yarn materials and production facilities. The produced woven fabrics have monotonous motifs and patterns because *lurik* fabrics have only combinations of vertical lines. The entrepreneur is less courageous of conducting experiments to create new motifs and patterns which go out of the traditions.

The third problem is that the entrepreneur is less confident about her business growth and development. She is worried that her business will be unable to compete with other business units which produce weave fabrics with Machinery Weaving Tool (ATM). The fourth problem is related to the working capital. The entrepreneur does not have working capital. The capital required to purchase the raw materials and to pay for production cost of each beam of yarns (fabric with the size of 110x8.000 cm) is approximately Rp1.760.000 (one million seven hundred and sixty thousand rupiahs). The real needs of the entrepreneur to run her business are as follows: Firstly, the entrepreneur needs knowledge of ATBM weaving processes such as variety of developments of ATBM weaving motifs, selection of weaving yarn types, selection of dyes and their applications in dyeing process, sekir process (yarn rolling process) and weaving process. Secondly, the entrepreneur needs working capital. Third, the entrepreneur and the employees needs work motivation.

3.4 The arrangement of problem-solving plan

The first three before mentioned problems, namely: the less efficient production process, the still monotonous motifs and patterns of produced woven fabrics and the lack of confidence of the entrepreneurs that the weaving business unit can support their family life, are solved by conducting a comparative study with other successful ATBM weaving industry units in other place in Troso village, Jepara regency.

The objective of the research is to learn the weaving design development comprehensively, which includes production planning, fabric motif planning, yarn dyeing process, weaving process, weaving tools, products of weaving motifs and patterns, wage and marketing system. Based on the results of the comparative study the weaving tool manipulation and design development training are planned, to be the production process more efficient. In addition, the problem of the less confidence of the entrepreneur and employees is solved by giving motivation through FGD. The limitation of working capital is planned to be solved by conducting working capital assistance. This can be done through order and consignment system, revenue sharing system and concessional interest loan system. These three systems are applied according to the need and development of the financial capability of the business unit.

3.5 The implementation of problem-solving action of the business unit

The problem-solving phase of the business unit at the action level includes the following actions:

1) developing the *lurik* motif designs in accordance with the demand of the consumers by using pakan yarns whose size is larger than that of lusi yarns;
2) manipulating the weaving tools;
3) diversifying the motifs and weaving techniques by establishing cooperation with partners;
4) growing a creative process of the sekir artisan;
5) providing working capital aids;
6) developing a promotional media;
7) managing the work contract system between the entrepreneur and the weavers,
8) improving the motivation of the entrepreneur and employees.

3.5.1 Activity 1

The improvement on the motivation of the entrepreneur and employees is done through the comparative study and FGD. The site for the comparative study was the advanced ATBM weaving business unit, that is, Lestari business unit in Troso village, Jepara Regency. The participants of the comparative study were the entrepreneur, her husband as the weaving tool technician, the sekir artisan, one of the marketing staffs and the facilitator or the researcher. The comparative study was done for two days at the aforementioned ATBM weaving business unit. The results of the comparative study are as follows:

1) The participants understand variety of weaving yarns and their application. The size of pakan yarns is larger than that of the *lusi* yarns. This difference aims at accelerating the weaving process and reducing the production cost.
2) The dye mixture is added with kitchen salt, as to cut the production cost, but the result of the dyeing easily fades.
3) The participants, particularly the entrepreneur, are surprised the fact that the weavers at the business unit in Troso are dominantly young males. It is very different from the one in the business unit of the entrepreneur which is entirely done by females.
4) The motifs of the produced woven fabrics by the weaving business unit in Troso village are varied. One of the motifs, which draw the interest of the participants of the comparative study, was the technology to produce the presence of tuwis motifs among the *lurik* motifs. The impact on the comparative study is that the participants are very much motivated to develop them.

3.5.2 Activity 2

The *lurik* motif design development is adjusted to the taste consumers by using the pakan yarns, which are thicker than lusi yarns. The process of design development is actually the empowerment of human resources, the entrepreneurs and employees. According to Maxell [20], the empowerment of human resources has three aspects, namely: providing good information, improving skills into a better state, and delegating authority to the employees non-managerially. In addition, the empowerment must satisfy the employees. The development of the creative process in the ATBM weaving designs can be done through four Ps, namely: person, process, product and press [21]. In the development of the ATBM weaving designs the personal uniqueness of theindividuals (the entrepreneur and the employees) needs to be appreciated. The entrepreneur and the sekir artisan need to have discussions to determine the weaving design concepts to be developed and the production cost for each beam of yarn. Based on the discussed concepts, which are predicted to fulfill the taste of markets [22] and which comply with the culture of the community [6, 23], the researcher, as facilitator, designes *lurik* weaving motifs on A4 paper.

The development of the ATBM weaving motifs was done by the aid of computer media. It was to accelerate the design process so as to improve the business [24]. The entrepreneur and the sekir artisan were encouraged to be creative and were given independence [25] to choose one or two *lurik* design motifs from the motifs offered by the facilitators and which were supposed to be able to realized by the sekir artisan and to be accepted by the markets.

Based on the comparative study to accelerate the weaving process, the size of the pakan yarns is larger than that of the lusi yarns. Therefore, in the yarn dyeing process the comparison between the number of the lusi yarns and that of the pakan yarns in each beam of yarns to be dyed according to the proportion of colors in motif designs. The yarns were after dyeing rolled on spools. Then the sekir artisan composed them on the sekir tools according to the selected motif designs. This sekir process was the main phase of the development of the ATBM *lurik* weaving motif designs. When the sekir process was accomplished the yarns were moved to the warp beams. Next, the beams were fitted to the weaving tools or looms (tutstel) and the lusi yarns were entered into yarn combs. Then the palette yarns were attached to the cocoon for weaving process.

3.5.3 *Activity 3*

The third activity was to grow the creative process of the sekir artisan and weavers. The development of the ATBM weaving product designs lied on the sekir process conducted by the sekir artisan. The sekir process is a technique to arrange the lusi yarns, what is the extended material, based on the color compositions. The larger number of the colors and the more complicated the color composition are in the weaving motif plan, the more complicated is the arrangement of the yarns or the sekir process. To grow and improve the creativity level of the sekir artisan, the training on composing colors was conducted. In addition, the sekir artisan was also trained to understand the correlation between the ATBM weaving motifs and the backgrounds of their consumers or users. The trainee was given psychological independence and security [25] (Rogers in Minandar, 2009) meaning that the sekir artisan was granted autonomy to develop the motifs according to their creativities and the results of the creativity should not be criticized, which could decline their efforts and motivation.

3.5.4 Activity 4

The fourth activity was the provision of working capital. In the development of the ATBM *lurik* weaving motif designs, each motif design or one beam of yarns required the capital of approximately Rp1.800.000 (one million and eight hundred thousand Indonesian rupiahs). Due to such a big amount of initial capital, the entrepreneur didn't dare to take risk. The owner was worried that the new motif's weaving products would not be sold as expected. It was understandable because they usually produced only the *lurik* motifs which were already acceptable to consumers or markets. To develop such different *lurik* motif designs the entrepreneur required working capital assistance with the revenue sharing system. In relation to the development of the new weaving motif designs in this system, all of the production costs (at approximate of Rp1.800.000 or around US $150.) was borne by the facilitator. When the new design products were not sold out, the entrepreneur would not bear any loss. Conversely, when the new weaving motif products were sold out, the profits were shared by the entrepreneur and the facilitator. Each earned 50%. Furthermore, the initial capital and profits were used to produce the next new *lurik* weaving motif products or the one ordered by consumers. This model of working capital assistance was done for one year based on the need of the entrepreneur.

After the entrepreneur felt that the new weaving motif designs were accepted by the consumers, the entrepreneur decided to use her own capital in order to earn larger profits. Based on such conditions, the entrepreneur decided to have working capital with "soft loan" model. In this model, the entrepreneur was given loan with the fixed interest of 1% per month. The principal loan and its interest of 1% per month was paid in monthly installments for ten months. The first installment was given the grace period of 2 months. It was enough to give entrepreneur opportunity the conduct the production process and marketing. This soft loan used a collateral system.

The application of the interest and collateral system was merely to educate the entrepreneur to have sense of responsibility, meaning that the entrepreneur was empowered and confident to stand independently and able to deal her capital limitations as well as able to fulfill the consumers' demand on the weaving motifs.

3.5.5 Activity 5

Manipulating the looms. The small looms sized 80 cm was able to produce only waeves fabrics with wide of 70 cm. The package of one piece of woven fabric required for clothing was 70 cm in width and 300 cm in length, or 110 cm in width and 200 cm in length. Both sizes had the same selling value that is Rp50.000 (fifty thousand rupiahs). However, two sizes required different length of time to produce of each. The first required longer time than the second. Thus the looms used to produce fabrics, projected for clothing, were less efficient. They were effective and suitable to produce fabrics for shawls, serviettes, and others that use such a dimension of fabrics. Viewed from economic aspects the aforesaid products had a very low economic value. Their weaving motifs were monotonous, and their consumers were relative. The consumers were traditional herbalists (Jamu) or villagers with low economic class. Therefore, some of the small looms were modified to be the larger ones with the size of 120 cm, producing fabrics up to the wide of 110 cm. This modification aimed at creating efficiency in the weaving process which in turn improved the income of the weavers. Furthermore, the modified loom can still produce the fabrics with the width of 70 cm in addition to those with the width of 110 cm. Thus, the manipulation of the looms is closely related to innovation, ability of workers, needs of consumers and capital [26].

3.5.6 Activity 6

Diversification of weaving motifs and techniques was done through cooperation with partners. The luring weaving motif designs, developed by the entrepreneurs, were tumpal motifs in which one of the fabric edges has a different motif. In addition, the entrepreneur also developed "drizzle" motifs, "hordes of ants out of their nest" motifs and other motifs. The entrepreneur with her artistic experiences could determine her creative process and during the creation she was controlled by her aesthetic experiences [27]. The efforts of developing the *lurik* weaving motifs were developed not only to the *lurik* weaving motifs but also to those integrated with other motifs through other techniques.

The development of designs conducted by the entrepreneur included the following:

1. The lurik weaving motifs were integrated with the batik motifs. It was done through stamping technique. The integration of the two different motifs was done collaboratively with partners - the batik entrepreneurs in other regency, namely the Sragen Regency which is located about 60 km from the weaving site. It was mediated by the facilitator.
2. The *lurik* weaving motifs and design were integrated with the flower motifs. This integration was done through painting technique.
3. The *lurik* weaving motifs with the flower design were integrated into embroidery technique.

The new motifs and array design of the *lurik* are developed in various colours and lines composition. As seen in the Figure 1, the original *lurik* motif was mostly with solid parallel lines on purple, blue or black.

Figure 1 The original *lurik* motif with solid parallel lines on purple, blue or black.

After several trials and actions the ATBM *lurik* weaving industry provided a more dynamic patterns and varied designs. Here are some examples of the innovation in the design and motifs (Figs. 5-7).

Figure 2 *Lurik* pattern with varied composition and colors

Figure 3 *Lurik* pattern with additional decoration of *tumpal* in one end

Figure 4 *Lurik* pattern with randomly mixture woven to create a rainy accent

Figure 5 *Lurik* pattern with cross and match configuration to produce rectangle motif

a

b

c

Figure 6 *Lurik* materials with combination the *batik* and stamped technique

Figure 7 *Lurik* material designed as traditional clothing with drawing flowers applied

3.5.7 Activity 7

The seventh activity was the development of promotional media. Due to the limited access of the weaving enterprise – the location of the enterprise is difficult achievable by consumers, promotional media are very necessaary. The development included the business cards of the entrepreneur and enterprise, product catalogues and product packaging. The three promotional media was designed with the same concept that accentuating the *lurik* motifs dominated with red colors.

3.5.8 Activity 8

The eighth activity was the application of work contract. In the second year, following the expanding market regions and the increasing product demands, the entrepreneur had to recruit more weavers. To motivate the prospective weavers to have self-confidence that the weaving job could operate well and could increase their income sustainably, they were asked to have discussions on the finding of their real needs and problems that they encountered. There were two aspects that the prospective weavers had to understand, namely:

1) the product's inefficiency due to the small looms they used and ways to deal it;
2) two contract systems as to improving their incomes, that is, contract work and "plasma" business contract.

In the first work contract system, the prospective weavers played role as contract labor workers whose income was determined by the length of the woven fabrics that they produced. For each meter of the ATBM woven fabrics that they produced, they were paid Rp3.000 (three thousand rupiahs). When a prospective weaver produced eight meters of woven fabrics in a day, she earned Rp24.000 (twenty four thousand rupiahs). The weavers did not bear any risks in this contract system. They were not responsible for the sale of the products and they still received their wages whether or not the fabrics that they produced were sold out. The current incomes were better than the former one when they only produced serviettes (60x60 cm) or carrying shawls (60x250 cm) with the small looms on which they earned only less than one dollar a day (Rp 8.000 – Rp10.000 per day.).

In the second arrangement, the prospective weavers played role as "new entrepreneur or plasma", meaning that the weavers had looms with the size of 110 cm (manipulated looms) but they did not have initial capital. The capital (yarns) was provided by the plasma core, that is, the entrepreneurs or the micro business unit of YS. The initial capital included 1 boom of lusi yarns whose motifs have been processed (sekir) on the base oo the color compositions by the entrepreneurs and several palettes of pakan yarns. The required yarns were 3 hanks of yarns with the amount of Rp1.520.000 (one million five hundred and twenty thousand rupiahs). When the yarns were woven into a fabric, the fabric was then sent to the entrepreneurs or the micro business unit of the YS to be marketed. When the fabric was sold out, the revenue was used to pay for the initial capital (Rp1.520.000) and Rp160.000 (Rp2.000 x 80 meters of fabric) for the entrepreneurs. The rest was given to the weaver as "her profit". One beam of yarns requires 3 hanks of yarns. After processing, it was produced the fabric approximately 80 m in length with the width of 110 cm. The price for each meter of the fabric was Rp25.000 and the price of 1 fabric's beam was Rp2.000.000. Thus, the plasma weaver worked approximately 8 hours a day for 10 days, he got the income of Rp320.000 or Rp32.000 per day. It was found that the benefit, that the weaver obtained with this system, was bigger compared to the one obtained with the contract work system. The weaknesses of this system were that the plasma weavers received their benefits only when the fabrics, that they produced, were sold out and the profit the entrepreneur obtained depended on the price of fabrics in the market during the buying and selling transaction.

The profit of the entrepreneur (core plasma) would be bigger if she was autonomous, meaning that the yarn processing and weaving process were done independently. In this way, she could earn the profit of Rp240.000 (18%) for each warp beam. However, she would have to bear risks if she got a larger volume of order and she could not fulfill the demand. In this way she had to be helped by the weavers. If the entrepreneur positions herself as the plasma core, she only did yarn processing. Meanwhile, the weaving process was conducted by plasma weavers. In this way, she would only receive the profit of Rp160.000 for each warp beam and the profit of weavers would be more or less Rp320.000 (16%) for each warp beam.

In the following Table 1 are presented the initial capital for yarn processing, the benefit of the plasma core (entrepreneur) and the plasma weavers.

3.6 Condition of the ATBM weaving micro-business unit following the treatment

Following the empowerment through study and treatment for two years, there have been several changes in the ATBM weaving micro-business unit. The changes are as follows:

1) The annual income of the business unit increased from Rp276 million to Rp750 million, meaning that the status of the business unit improved from micro business unit to small-scale business unit. In addition, the wages that the workers earn also improved significantly. For example, the wages of the weavers increased from Rp10.000 to Rp24.000 per day.
2) The entrepreneur was able to identify her own problems and real needs and possessed bargaining power against yarn suppliers and to determine the price.

Table 1 The processing cost for 1 beam of yarns

No	Types of material	Entrepreneur [Rp]	Plasma Weaver [Rp]
1	Price of 3 press of yarns@Rp300.000	900.000	900.000
2	Price of dyeing substances 400g @90.000	360.000	360.000
3	Dyeing cost of 3 press of yarns @Rp30.000	90.000	90.000
4	Yarn spooling cost of 15kg@Rp4.000	60.000	60.000
5	Palette cost of 15kg @4.000	60.000	60.000
6	yarn rolling process cost of 15 kg	50.000	50.000
7	Weaving cost: 80 m x Rp3.000	240.000	0
8	Total yarn processing cost (1-6)	-	1.520.000
9	Total production cost (1-7)	1.760.000	-
10	Revenue of product sale (80 m x Rp25.000	2.000.000	2.000.000
11	Profit of core entrepreneur: 80 m x Rp2.000	160.000	160.000
12	Profit of autonomous entrepreneur (10 subtracted by 9)	240.000	-
13	Profit of new entrepreneur (10 subtracted by 8 and 11)	-	320.000

3) The entrepreneur was able to calculate the production cost and time for production each beam of the *lurik* fabric so that she was more daring to speculate to receive order.
4) The entrepreneur was more courageous to develop designs of the weaving motifs and to conduct motif and technique diversification.
5) The number of fabric products produced increased from 12 beams to 40 beams. Furthermore, the number of motif designs and quality also improved significantly.
6) The number of workers increased from 13 to 40, particularly those working as weavers. Moreover, the workers were more skillful in their own fields, and the sekir artisan even dared and was able to do innovations in the new *lurik* motif designs by utilizing the remaining yarns.
7) The cooperation network with partners also increased. The network has been established with batik industries, convection business units, bigger yarn suppliers, dyeing substance suppliers, marketing divisions and governmental institutions.

4 CONCLUSION

Based on theaforementioned discussion, a conclusion can be drawn that the empowerment of the non-machinery tools of ATBM *lurik* weaving micro-business unit need to be taken seriously. This research for two years achieved enhancement in many parts, that is, the improvement of annual sales from Rp276 million to Rp750 million, the improvement of wages of workers (weavers) from Rp10.000 to Rp24.000 per day, the courage of the entrepreneur to take decisions in developing the weaving motif designs, the increase of the number of workers, the improvement of production, and the improvement of business network.

The relevant model of empowerment of the *lurik* ATBM weaving micro-business unit includes the following:

1. conducting need analysis; the entrepreneur is motivated to identify her own problems and real needs
2. planning programs to deal with the problems and needs;
3. executing actions based on the stipulated plan through the following:
    - improving the work motivation of the entrepreneur and workers;
    - developing the *lurik* motif designs that meet the taste and demand of consumers by using the pakan yarns whose size is bigger than that of the *lusi* yarns;
    - growing the creativity process of sekir artisan;
    - providing working capital with the models of “revenue-sharing” or “soft loan” in compliance with the entrepreneur’s needs;
    - manipulating the small looms to be bigger ones according to the needs;
    - integrating between the *lurik* weaving motifs, design and techniques and the other motifs and techniques through cooperation with other different business units;
    - developing the promotional media;
    - applying the work contracts between the entrepreneur and the weavers through a contract work system called a plasma system based on the weavers’ needs.

ACKNOWLEDEMENT: *A big thanks to IPTEKDA LIPI and FKIP UNS Surakarta for the financial help that has been provided for the smooth running of this research and also to all of the participants who are involved in this research.*

5 REFERENCES

1. Republik Indonesia, 2008, Undang-undang Republik Indonesia Nomor 20 Tahun 2008 tentang Usaha Mikro Kecil Menengah. (The Republic of Indonesia Law no 20/2008 about Micro Bussiness of Small and Middle), Lembaran Negara Tahun 2008 Nomor 93
2. Gillow J., Sentance B.: World textiles: A visual guide to traditional techniques, London: Thames&Hudson, 1999, ISBN 10: 0500019509; ISBN 13: 9780500019504
3. Gunadi: Textile design, Jakarta: UPN Veteran, 1985
4. Jumaeri: Textile design, Bandung: Institute of Textile Technology, 1984
5. Mardikanto T.: The Concepts of Society Empowerment. Surakarta: FP and UNS Press, 2010, ISBN 978-498-543-0
6. Prasetyowibowo B.: The Design of Industrial Product, Bandung: Eight Ten Foundation, 1998
7. Rizali N.: The Review of Textile Design. Surakarta: LPP UNS, 2006
8. Rogers E.M.: Diffusion of Innovations, Third edition, New Yok: Free Press, 1983, ISBN 0029266505 9780029266502
9. Berlo D.K.: The process of communication; an introduction to theory and practice, New York: Holt, Rinehart and Watson, 1960, ISBN 0030074908 9780030074905
10. Abiddin N.Z., Ismail A.: Building excellent workforce through effective coaching for coaches’ development, International Journal of Education 4(1), 2012, pp. 101-109, DOI: https://doi.org/10.5296/ije.v4i1.1503
11. Sutopo H.B.: Qualitative Research Methodology: Theoretical Basis and Its Application in The Research, Surakarta: March Eleventh University Press, 2002
12. Bogdan R.C., Biklen S.K.: Qualitative Research for Education: An Introduction to Theory and Methods. USA: Allyn and Bacon, 1982, ISBN 0205076955, 9780205076956

13. Spradley J.P.: Participant Observation, New York: Holt, Rinehart and Winston, 1980, ISBN 10: 0030445019, ISBN 13: 9780030445019
14. Greenbaum T.L.: The Practical Handbook and Guide to Focus Group Research, USA: Lexington Books, 1988, ISBN 10: 0669147753; ISBN 13: 9780669147759
15. Miles M.B. Huberman A.M.: Qualitative data analysis: A Sourcebook of New Methods, London: Sage Publications, 1984, ISBN-10: 0803922744; ISBN-13: 978-0803922747
16. Rogers E.M., dan Shoemaker F.F.: Communication of Innovations: A Cross-Cultural Approach. 2nd Edition, New Yok: Free Press, 1971
17. Sztompka P.: The Sociology of Social Change, Jakarta: Prenada Media, 2004
18. Koentjaraningrat: Metality Culture and Development, Jakarta: Gramedia, 1984
19. Mulder N.: Java Personality and National Development, Yogyakarta: Gajah Mada University Press, 1973
20. Maxwell J.R.: Management of employee empowerment, Journal of Organizational Culture, Communications and Conflict 9(1), 2005, pp. 61-68, Print ISSN: 1544-0508; Online ISSN: 1939-4691
21. Kaufman J.C., dan Sternberg R.J.: Creativity, Change: The Magazine of Higher Learning 39(4), 2007, pp. 55-60, DOI: 10.3200/CHNG.39.4.55-C4
22. Friences: Be An Entrepreneur, Yogyakarta: Science Hall, 2011
23. Bahari N.: Aesthetic Characteristic Endurance and Java Symbolism at Silver Craft at Gede City Industrial Center in The Context of Socio-cultural Environmental Change, Dissertation, FSRD ITB Bandung, 2004
24. Li J., Merenda M., Venkatachalam A.R.: Business process digitalization and new product development: An empirical study of small and medium-sized manufacturers, International Journal of E-Business Research 5(1), 2009, pp. 49-64, DOI: 10.4018/jebr.2009010103
25. Munandar U.: Developing The Creativity of Talented Child, Jakarta: Rineka Cipta, 2009
26. Chang J., Levy M., Powell P.: Process re-engineering success in small and medium sized enterprises, International Journal of Enterprise Information Systems 5(3), 2009, pp. 14-27, DOI: 10.4018/jeis.2009070102
27. Sumardjo, J. 2000. The Art Phylosophy. Bandung: ITB

STUDY OF CZECH MALE BODY DIMENSION AND EVALUATION OF MEN´S TROUSERS PATTERNMAKING METHODS

Blazena Musilova and Renata Nemcokova

Technical University of Liberec, Faculty of Textile Engineering, Department of clothing, Czech Republic
blazena.musilova@tul.cz, renata.nemcokova@tul.cz

Abstract: *This study deals with the effect of different male somatotypes and different pattern making methods on the men´s trousers pattern design. First, the research is focused on the analysis of the 200 Czech men anthropometric data in order to define Czech somatotypes. The definition of the Czech somatotypes is according to the rules of the standard "EN 13402–3: Measurements and Intervals". Six men´s trousers pattern drafting methods including two Czech, German, English, Italian and Swedish were analysed. The result indicates that the trousers patterns are mostly drawn by using a constant numerical value for generating the design dimensions instead of using a regression equation for value calculation. These pattern making methods are totally inadequate for pattern drafting in order to fit a wide range of men's bodies (male morphology). To solve this problem, this paper examines a proposal for a pattern making method for men´s trousers that uses the result of regression formula of Czech pattern making method called NVS to match the pattern design parameters. This method will increase the efficiency of construction parameters and thus to automate the pattern grading process of the trousers pattern in a wide range of sizing.*

Keywords: *Czech male somatotype, male trousers pattern making method, size designation.*

1 INTRODUCTION

Research activities in frame of the garment mass-production are generally associated with the idea that the quality of fitting of the garment depends on a relatively high degree of our knowledge of the body dimensions of the target wearers [1].

This case reveals the need for study the population body silhouette and body proportions as well as selects the size changes possible to implement in clothing construction modifications.

This also reveals that the problem of improper fitting may be due to not only the body sizes but also the inappropriate pattern drafting methods [2].

For this reason, it is meaningful to deal with an effect of the anatomical changes in the human body on the clothing pattern design and to study the body proportions as well as to analyse their properties by means of statistical methods [3].

Using results from the regression analysis of anthropometric data of target population in the clothing design methodologies seems to be very effective. Resulting regression equations can be simply used for determination of clothing pattern design parameters using value of corresponding part of body measurement. Thus a dependent value of one clothing pattern dimension is calculated as a percentage of an independent value of a body measurement or of other pattern dimension.

In order to size mass-produced clothes, the body size of the intended wearer has to be defined and identified with the nearest size on a table of standard sizes. The tables of measures as described in the document EN 13402 "Size designation of clothes" [4] constitute the grouping of body sizes appropriate to the European population. The somatotype is defined by the appropriate primary and, where necessary, secondary dimensions. The nearest whole number in the tables for that dimension is used for purposes of size designation. As the results of the sizing surveys of the different countries vary, the tables in this document provide the required flexibility.

In order to accommodate variations in body measurements by country/company, a system with defined intervals is standardized, which means that a country/company may select any number from the tables with a range that may be extended to the left and right of Tables [4].

The aim of this research is:

- to obtain the accurate definition of the Czech male somatotypes;
- to define the body sizes of the Czech somatotype by the appropriate primary and secondary dimensions;
- to set accurate tables of the grouping of body sizes according to the rules of the standard

"EN 13402–3: Measurements and Intervals" appropriate to the target Czech wearers;

- to find out the appropriate pattern design method of an effective construction algorithm suitable for mass-produced men´s trousers for the Czech male customers.

2 EXPERIMENTAL METHOD AND OBJECTIVES

2.1 Subjects and observed anthropometrical data

The basis for this study is the anthropometric data of 200 Czech men aged 18-60, which were measured in the survey conducted by TUL Department of Clothing in 2006. The measured population was divided into three age categories and percentage of the measured subjects was determined according to the Czech population structure in that period: 51 subjects aged 18-29; 77 subjects aged 30-44; 72 subjects aged 45-60 [5].

The observed data set was reduced. It contains 130 male subjects. It is determined according to criteria of the most sold sizes of the BUSHMAN brand trousers for the Czech male customers: 48, 50, 52 and 54. These somatotypes are defined by the standardized primary body dimension of the waist girth (Waist) and by secondary dimension of the Height [6].

2.2 Analysis of the men´s trousers pattern drafting methods

In this study six Men´s trousers pattern making methods are evaluated. Two Czech methods: NVS [7] and UNIKON plus [8], Italian method: Fernando Burgo [9], German method: M.Müller & Sohn [10], English method: Winifred Aldrich [11], Swedish method: Inger Öberg [12].

3 RESULTS AND DISCUSION

3.1 Analysis of the Czech male body measurement data

The European standard EN 13402-2 defines for trousers one primary dimension (PD). This is the Waist according to which the product must be labelled. For some types of trousers, a single measure may not be sufficient to select the right product. In these cases, one or two secondary dimensions (SD) can be added to the label. In case of trousers, it is Height or Inside Leg Length [4].

With the goal to study the relationship between those characteristic body dimensions the considerable research of the Czech male body measurement data was carried out [5].

Figure 1 represents the mean value of Height and Waist in each age category 18-29; 30-44; 45-60 and 18-60 (entire range), respectively. We can see the increasing trend of the girth dimension Waist (PD), in connection of increasing age, unlike of decreasing trend in case of Height (SD).

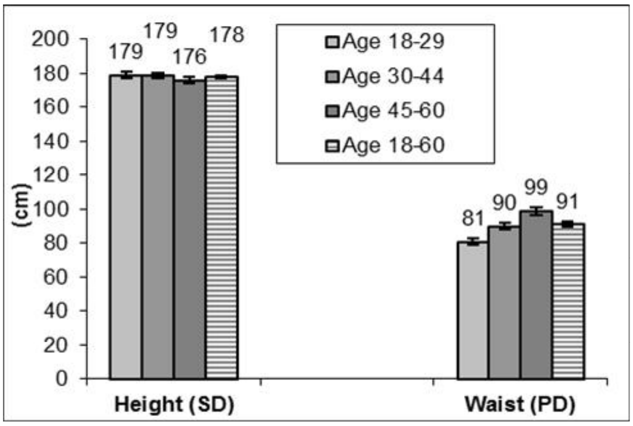

Figure 1 Comparison of body dimensions: height and waist

These results are beneficial to study the proportional relationships between the width and length of the trousers. They reveal the need to study body proportions of a target customers inside each age category as well as. Then body size changes can be to implement into a trousers construction.

3.2 Statistical analysis of the Czech anthropometrical data

These findings are an interesting output of statistical analysis of Czech male anthropometrical data: The large differences between the waist girth (measurement was taken in the lowered waist level by 4 cm from origin waist) and the hip girth. The difference amounted to more than 10 cm in 41% of the observed subjects. However, the results of examining the differences in the given dimensions suggest that even in the male population there is a more marked difference between the dimensions mentioned, as is in the case of the female body shape [6]. Due to the fact that the design parameter of the hip girth (Hip) determines the resulting shape of the trousers, it is important to test these body disproportions.

The Hip is not a typical male standardized dimension, and also is not listed in the label states of characteristic dimensions within the EN 13402-2 [4]. There is one more idea, to add the Hip in the size marking pictogram as the important secondary dimension and thus to perfectly inform the customer about a dimension in hip area.

3.3 Evaluation of the men´s trousers pattern drafting methods

The analysis of the Men's trousers pattern drafting method was focused to find out a suitable pattern making methodology for mass-production for target national customers. It is supposed that the design line segments are mostly expressed using a regression equation of the type (1).

$$\overline{ABi} = K_{D1(ABi)} * D_1 + K_{D2(ABi)} * D_2 + A_{ABi} + e_i \qquad (1)$$

where: $\overline{ABi}$ is a dependent variable - computed *i*-design dimension, $K_{D1(ABi)}$, $K_{D2(ABi)}$ egression coefficients, D_1, D_2 is an independent variable –body measurements, A_{Abi} absolute value, e_i ease allowances

That is a good way how to use a relationship between a dependent variable (a main body dimension) and one or more independent variables (subordinate pattern design parameters). This method allows an application of anthropometric changes of body proportion of any population to the shape of a trousers construction within the whole sizing range. Unlike the way of design line segments are expressed by setting a numerical value for all sizes, regardless of different shape of a body.

For experimental evaluation there are the same selected design line segments and pattern drafting formulas in the set of those observed men´s trousers pattern making methods: 13 segments for front trousers block and 11 segments for back trousers block.

Quantitative analysis of these observed methods shows: The largest number of the design line segments is expressed using regression formula within the Czech method NVS. More details we can see on Figure 2.

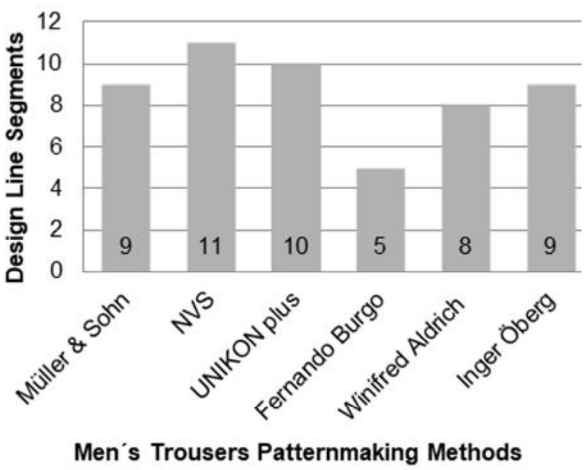

Figure 2 The number of the design line segments which are expressed using regression equation

3.4 Evaluation of the trousers design block procedure

There is an analogy between the above mentioned trousers patternmaking methodologies. Similarities are evident as in the design of construction net as well as in tracing lines of the shapes of the cutting edges.

In the Figure 3 there is the trousers block. The part of trousers block that covers the pelvic part of a body is described. The distances between the individual design points that correspond with the anatomical surface points delimit the design line segments.

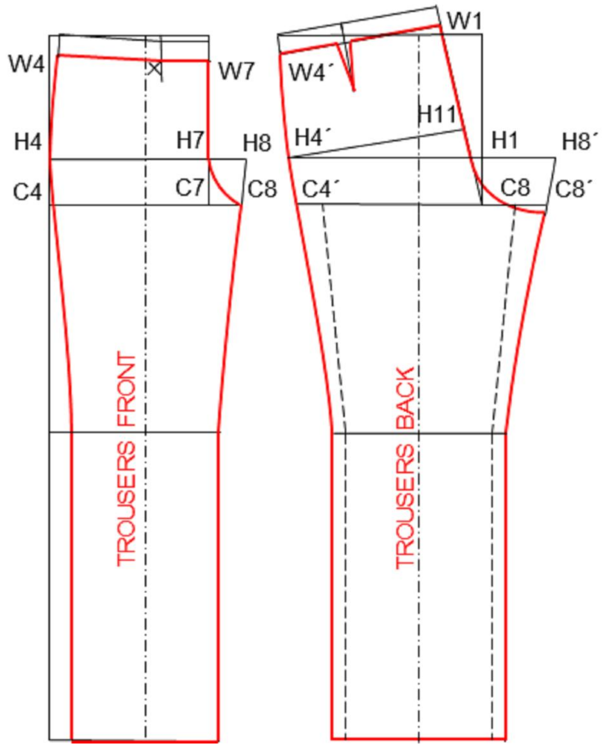

Figure 3 The male trousers block

On Trousers Front there are: C4 – H4 (Hip Height); H4 – H7 (Hip Width); H7 – H8 (Part of Hip Width); C7 – C8 (Part of Crotch Width); W4 – W7 (Waist Width).

On Trousers Back there are: H4´ – H11 ((Hip Width); H1 – H8´ (Part of Hip Width); C8 – C8´ (Part of Crotch Width); W1 – W4´ (Waist Width).

The resulting cut shape for this area is affected by the mutual proportions between the waist and the hip circumferences and what way is used to implement proportions into the design process.

The comparison of the values of the selected design line segments of Male Trousers Block are listed in Table1.

To determinate these values the male subject is selected for the body measurements: Waist = 88 cm and Hip = 104 cm. He is a represent ant of the most numerous group of observed subjects in middle age category in the Czech male body measurement data: Age 30-44.

Although the input design parameters of the basic trousers block are of the same body measurements of same male subject, the values of the line segments are different, as we can see in Table 1.

Table 1 The values of the selected design line segments of male trousers

Line	Dimensions [cm] within pattern drafting methods					
	Müller & Sohn	*NVS*	*UNIKON plus*	*Fernando Burgo*	*Winifred Aldrich*	*Inger Öberg*
Design line segments of trousers front						
C4 – H4	8.2	7.2	-	-	6.5	7.5
H4 – H7	26	25	23.7	27	28	27.3
H7 – H8	6.2	-	6.9	-	-	-
C7 – C8	-	5.1	-	5.2	7	4.7
W4 – W7	22	22.5	21	21	24.5	26.5
Design line segments of trousers back						
H4 – H11	29.5	28	26.8	28	29	27.5
H1 – H8´	13.9	-	13	-	-	-
C8 – C8´	-	4.6	-	-	3.8	-
W1 – W4´	24	25	24	24	26.5	24.5

3.5 Fitting test of the tailored trousers

The fit of trousers which was made according to the shape of the cut created using the experimental tested pattern making method NVS was checked. The master patterns of the male trousers were drawn using the algorithm, which include linear distances and curves from this method, using individual male body dimensions. The subject of the size 52 was selected. He is the customer in middle age and wearer of the BUSHMAN brand products. He represents one of the most numerous group of tested subjects and his body dimensions are: Height = 182 cm, Waist = 94cm, Hip = 108 cm. Under the standard EN 13402 [5] this subject is the somatotype "J" which is defined with the help of Drop = waist girth − hip girth = - 14 cm.

Consequently, the men trousers were tailored and test-fitted to five individual customers whose body dimensions correspond to the Czech somatotype of the size 52. All trousers were made of the same 100% cotton woven fabric without any elastic textile material. The fitting test results confirmed that the patterns drafted using the NVS patternmaking method provide adequate fit. Figure 4a) and 4b) shows a fit testing procedure.

a

b

Figure 4 a) Front view [6] and 4b) side view [6]

3.6 The definition of the Czech male sizes according to the rules of the standard "EN 13402–3: Measurements and intervals"

The tables - scales with intervals in at least of the primary dimension for each garment type are listed in standard EN 13402–3 [4]. Size intervals define the differences between two adjoining body measurements (primary and secondary dimension).

There must be a proportional relationship between these dimensions that corresponds to certain somatotypes. Where a somatotype i.e. body shape is characterised by a number of girth dimensions and height. The nearest whole number inside of interval in the tables for these dimensions is used for purposes of size designation.

This research constitutes an attempt at the definition of somatotype appropriate to the Czech male population. It consists of the steps:

- to study the sizing tables of measures as described in the EN 13 402-3 [4] constitute the grouping of body sizes appropriate to the European population. The intervals listed in the tables in case of Waist and Hip girth measurements for men – garments for lower body.
- to define the range of intervals of the Waist measurements for Czech male customers.

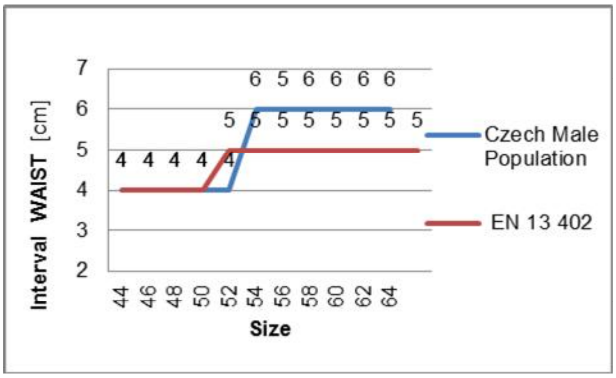

Figure 5 The range of intervals of the waist in EN13 402-3 and the range of the intervals of the Czech male customers of the BUSHMAN brand products

For this study, the somatotypes of the EU size of the range from size 44 to size 64 were selected. The male subject of EU size 52 was a reference - basic size of the open system with inbuilt flexibility of standard EN 13402-3. Interval ranges for smaller sizes and larger sizes were evaluated. The interval of the 4 cm is applied to size range of somatotypes till the appropriate EU size 50 of the mean value of Waist = 90 cm (range 88 - 93 cm) including. The interval of the 5 cm starts from appropriate EU size 52 of the mean value of Waist = 95 cm (range 93-98cm), see Figure 5.

This was proven by tests of the fitting of already made trousers by cutting method NVS and in frame of these sizes hanging on the EU interval of the Waist, see Figure 5. The results showed the disproportion on the cut of the trousers in area which corresponding to upper hip part of body. This caused discomfort to wearers. Therefore, the size interval of the Waist has been changed.

Based on results of a study of the body proportion of the Czech male population the interval of the 4 cm was applied to size range till the appropriate size 52 of the mean value of Waist = 95 cm (range 93-98 cm) including.

The interval of the 6 cm starts from size 54 of the mean value of Waist = 100 cm (range 98-103 cm), see Figure 5.

Recommended interval of the 5 cm due to the standard EN 13402-3 was not suitable for Czech somatotypes in size range 54-64.

4 CONCLUSION

Being successful in frame of garment mass-production is generally associated with the goal to produce product in high quality. This means using both the high-quality of textile materials and attends to the needs of the comfortable fit of garment for the target wearers.

To clearly label a clothing according to valid standards so that the size symbol of the given clothing should be corresponding with the body proportions of the target wearer.

This study can provide solutions for garment production companies to precisely carry out the men´s trousers pattern construction for target Czech male population.

We can describe these partial conclusions and recommendations:

- to provide the systematic research of anthropometric data which allows to update information of the body proportions of target population as well as to define the body size changes possible to systematically implement into clothing pattern design procedure. For this purpose, to take body dimensions separately in each country due to significant ethnic differences in body silhouettes that prevents the transfer of European data to specific countries.
- to use pattern construction algorithms of the design line segments to be at the most of them calculated using regression formulas. This method will increase the efficiency of construction parameters and thus to automate the pattern grading process of the trousers pattern in a wide range of sizing.

***Acknowledgement**: The authors would like to thank the Faculty of Textile Engineering, Technical University of Liberec for the support and also to the student Ján Masaryk for his assistance in the experiment.*

5 REFERENCES

1. Musilova B., Komarkova P., Kus Z.: Project on assessment methods of constructional allowances for looseness of clothing, Vlakna a Textil(Fibres and Textiles) 10(2), 2003, pp. 18-22.
2. Musilova B., Nemcokova R.: Study of Czech male body proportions and evaluation of men´s shirt pattern making methods, Tekstil ve Konfeksiyon 24(4), 2014, pp. 399-404
3. Komarkova P., Glombikova V.: The effect of anatomical changes in the female body during pregnancy on pattern designs for maternity, Tekstil ve Konfeksiyon 23(4), 2013, pp. 409-415
4. ČSN EN 13402-3. Označování velikostí oblečení, Český normalizační institut (Clothing Size Labeling, Czech Standards Institute), Praha, 2013 (in Czech)
5. Glacova D.: Statistické zpracování údajů somatometrického šetření souboru dospělých mužů zaměřený na tvorbu konstrukčních rozměrů v relaci s normou EN 13402, (Statistical processing of the data of the somatometric survey of the adult male population aimed at the creation of structural dimensions in relation to the standard), Diploma thesis TUL, 2006 (in Czech)
6. Masaryk J.: Vývoj konstrukční metodiky střihu pánských kalhot (Development of the structural design of the men's trousers), Bachelor thesis TUL, 2015 (in Czech)
7. VÚO Prostějov: Střihové konstrukce pro dolní část těla muže v NVS, (Cutting structures for the lower part of the male body), Prostějov 1991, (in Czech)
8. SW PDSTailorXQ: Method Unikon plus, Available from http://www.classicad.cz/cz/garment_cz.htm, Accessed: 2017-06-10
9. Burgo F.: Il Modellismo, Instituto di Moda Burgo, Milano, 2008, pp. 256-257, ISBN 88900101-5-0
10. Műller M. & Sohn: HAKA Schnittkonstruktionen nach Műller & Sohn. Rundschau, Műnchen, 1997, pp. 35, ISBN:3-929305-10-0
11. Aldrich W.: Metric Pattern Cutting for Menswear, Blackwell Publishing, Fourth edition, 2006, pp. 78-79
12. Öberg I: Mönster och konstruktioner för herrkläde, Stockholm, 1989, CM Garment AB, ISBN 91-36-02722-7

COMPARATIVE STUDY OF RADIANT HEAT FLUX DENSITY TRANSMISSION THROUGH FIREFIGHTER PROTECTIVE CLOTHING

Jawad Naeem, Adnan Mazari, Zdenek Kus and Pavel Kejzlar

Faculty of Textile Engineering, Technical University of Liberec, Studentská 2, 461 17 Liberec 1, Czech Republic
jawadnaeem.qau@gmail.com; adnanmazari86@gmail.com; zdenek.kus@tul.cz; pavel.Kejzlar@tul.cz

Abstract: *The main purpose of this research is to find out possibility of improvement in thermal protective performance (TPP) of fire fighter protective clothing (FFPC) when subjected to radiant heat flux density of 10 kW/m^2. Enlargement of TPP is related to the increase of time period when subjected to radiant heat flux density may provide surplus time for fire fighter to carry out duties without enduring harmful injuries. Each FFPC specimen constitutes outer shell, moisture barrier and thermal barrier. However, aerogel blanket was also utilized as substitute to thermal barrier because of its excellent thermal insulation property and inflammable nature. Preliminary testing was related to evaluating thermal resistance and thermal conductivity. Later experimentation involves exposure of multilayer FFPC specimen to radiant heat flux density of 10 kW/m^2. It was witnessed that those combinations in which aerogel blanket was utilized deliver higher thermal resistance i.e.0.1748 m^{2}K/W and improved TPP behavior in terms of transmitted heat flux density Q_c (0.70 kW/m^2) and percentage transmission factor (6.70%).*

Keywords: *Fire retardant fabrics, aerogel blanket, thermal insulation, thermal protective performance.*

1 INTRODUCTION

Protection of human body against exterior climate is the most pertinent aspect of clothing, which serves as heat exchange medium between human body and nearby climate [1]. Clothing is responsible for breeding a microclimate between human body skin and surrounding atmosphere to maintain thermal equilibrium of human body [2-5]. Exchange of heat in clothing implicate radiation from one textile substrate layer to other substrate layer, convection of air gap and conduction of air gap and textile substrate layer [6].

In case of absenteeism of stream of air, radiation is the solitary mode of heat exchange between the body and nearby climate [7]. Emission of thermal radiation takes place from all the bodies and expulsion of heat through thermal radiation takes place in the form of infrared rays.

Fire fighter protective clothing (FFPC) is a multilayer fabric layer arrangement providing safeguard to firefighter from hazards of external radiant heat flux, spilling of chemical, flame and delivers thermal equilibrium of human body [8]. Fire fighter protective clothing encompasses outer layer, moisture barrier and thermal barrier [8]. The exterior shell comprises of those substrates which are engineered to have interaction with flame and heat without degenerating or burning i.e. they avoid ignition when have direct connection with flame and must have property of water repellence and water vapor permeability. Mostly fibers like meta aramids (Nomex), combination of meta aramid and par-amid (Nomex III A), polybenzimidazole (PBI), Zylon and some fibers with flame resistant finishes like Proban and Pyrovatex for improving TPP performance. The moisture barrier is located between exterior layer and thermal barrier. This layer is impermeable to water but permeable to water vapors. Its primary objective is to shield the body of fire fighters from blood pathogens and liquefied chemicals. Moisture barrier is hydrophilic membrane obtainable in the market as Goretex, Proline, Cross tech, Action, Neo Guard. The thermal barrier protects human body by blocking the environmental heat and utilizes flame retardant fibers and their blends. It can be laminated woven, nonwoven, quilted batting, lining fabric and knitted fabric and spun laced [8, 9].

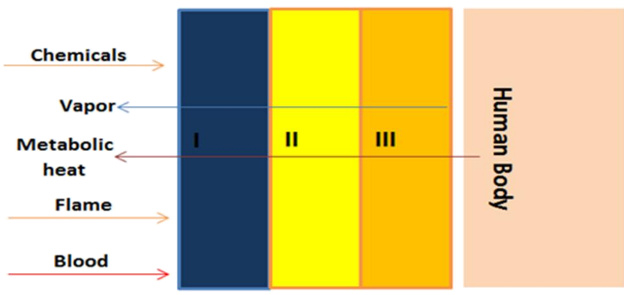

Figure 1 Arrangement of multilayer protective clothing [8, 9]

Time is the pivotal factor in terms of Thermal protective performance (TPP) of FFPC specimen.

Improvement in thermal protective property of firefighter protective clothing may increases the time period for firefighter to accomplish their activities without acquiring major injuries. As a consequence, firefighters can devote more time in hazardous environment saving precious lives and damages caused by fire without injuring themselves [10]. Evaluation of TPP might be conducted by several tests like thermal manikin (full scale methodology) and Heat guard plate and TPP tester (bench scale test) [11] or full scale test methodology like thermal manikin [12].

For last three decades, scientists are conducting lot of research for enhancement of TPP of FFPC. One approach is to employ silica based aerogel or aerogel blankets in FFPC assemblies. It is produced from gel by exchanging liquid phase with gaseous phase and has very low mass and porous structure [13]. There are several types of aerogels. Among various type of aerogels, silica based aerogels have very remarkable properties because of inflammable nature and lesser thermal conductivity than static air in same environmental conditions. Silica based aerogel is hydrophobic in nature with specific surface area around 1000 m^2/g having porosity greater than 90%. The thermal conductivity (λ) of silica based aerogel is approximately 0.015 W/(m.K) [14]. All these attributes allow silica aerogels a promising contender for utilization in firefighter protective clothing (FFPC) as thermal barrier. The main objective of this research is to escalate TPP of FFPC specimen. Several multilayer FFPC combinations were made. Each combination consists of outer shell, moisture barrier and thermal barrier. These specimens were characterized by Alambeta, and then finally evaluated by X637 B machine (ISO 6942-2005 standard) for determining transmission of heat through multilayer protective clothing assemblies at 10 kW/m^2 to figure out TPP of these multilayer clothing assemblies.

2 MATERIALS AND METHODOLOGY

All FFPC specimens were supplied by Kivanc group turkey and Vochoc company Czech republic. Pyrogel 2250 blanket was supplied by Aspen Aerogel Company. This layer was used as substitute layer to thermal barrier. Two different outer shells, one moisture barrier and one thermal liner were employed. Four different arrangements of FFPC assemblies were made. These combinations were made by superimposing outer shell, moisture barrier and thermal liner of the fabric without any stitching and lamination.

3 EXPERIMENTAL WORK

The evaluation of thermal resistance, thermal conductivity and thickness of monolayers and multilayers clothing arrangement was done with the help of Alambeta. It is a patent of prof. Lubos Hes and I. Dolezal which was manufactured by Sensora Company [15]. Radiant heat flux density transmission through FFPC arrangement was carried out by X637 B machine as per ISO 6942 standard.

3.1 Alambeta

Alambeta is computer-controlled device utilized to determine thermal characteristics of textile substrates. It is non-destructive equipment [16] comprises upper hot plate affixed to thin heat power sensor which falls down and have contact with surface of FFPC substrate positioned on lower cold plate. The computer records flow of heat due to temperature gradient between upper heated plate and specimen on cold plate. Temperature of upper plate is kept at 32°C and lower plate is kept at ambient temperature i.e. around 20°C. All measurements in same fabrics are recorded and serve for automatic calculation of mean value and variation coefficient.

Table 1 Specifications of multilayer clothing arrangement

Layer	Fabric Code	Component	Weave type	Fabric weight [g/m^2]	Thickness [mm]
Exterior shell 1	E1	70/28/2% Meta-aramid/Para-aramid/Antistatic	Rip stop	200	0.74
Exterior shell 2	E2	100% cotton	Twill	280	0.88
Moisture barrier	MB	PU membrane laminated to nonwoven	Nonwoven	120	0.94
Thermal barrier	TB	40/30/30% Aramid/Viscose/FR icastar	Needle punching nonwoven	380	3.424
Aerogel blanket	P	Silica based aerogel with reinforced polymers (OPAN)	Nonwoven	380	2.85

Table 2 Combinations of clothing assemblies

Sr #	Fabric arrangement in multilayer clothing assembly	Fabric Code	GSM [g/m^2]	Thickness [mm]
1	Exterior shell(E1) + Moisture barrier (MB) + Thermal barrier (TB)	Specimen 1	700	5.100
2	Exterior shell (E2) + Moisture barrier (MB) + Thermal barrier(TB)	Specimen 2	780	5.262
3	Exterior shell (E1) + Moisture Barrier (MB) + Aerogel blanket (P)	Specimen 3	700	4.538
4	Exterior shell (E2) + Moisture Barrier (MB) + Aerogel blanket (P)	Specimen 4	780	4.676

3.2 Relative water vapor permeability (RWVP) percentage

PERMETEST was employed to determine relative water vapor permeability. It is patent of prof. Lubos Hes (non-destructive method) and was developed by Sensora company under steady state conditions as per ISO 11092 standard and this method is also non-destructive method [17]. The higher the value of relative water vapor permeability, the lesser will be the water vapor resistance and there will be better thermal comfort [18]. Five measurements were taken for each specimen.

3.3 Radiant heat transmission machine

The radiant heat testing equipment X637 B is employed to investigate radiant heat flux density through material or material assembly according to ISO 6942 standard [16]. The apparatus consists of six carbide rods serving as radiation heat source, a small curved copper plate calorimeter, a moveable test frame having cooling device and specimen holders. The size of the sample was 230×80 mm which is placed on the face side of calorimeter and subjected to a specific level of radiant heat and time for temperature acceleration of 12°C and 24°C in the calorimeter was determined and conclusions are mentioned in the form of radiant heat transmission index (*RHTI 12* and *RHTI 24*) and the percentage heat transmission factor (*% TF* Q_o) [19]. Before experimentation, all specimens were pre-conditioned for 24 hours at temperature of 20°C and have relative humidity of 65% [19]. Five specimens are required for testing at each level of heat flux density. At first the calibration of the instrument is done and incident heat flux density is evaluated from the following equation.

$$Q_o = \frac{C_p R M}{a.A} \tag{1}$$

where: A = area of the copper plate [m^2], a = the absorption coefficient of the painted surface of calorimeter, M = mass of copper plate [kg], C_p = specific heat of copper 0.385 kJ/Kg°C), R = rate of rise of the calorimeter temperature in the linear region in °C/s.

Afterwards, the specimen is mounted on face of calorimeter by applying mass of 200 g. The time t_{12} for accomplishing temperature rise of 12°C and time t_{24} for acquiring 24°C are recorded in calorimeter in seconds and expressed as *RHTI 12* and *RHTI 24* [19]. The transmitted flux density, Q_c [kW/m^2] is evaluated by the following equation:

$$Q_c = \frac{M C_p 12}{A.(t_{24} - t_{12})} \tag{2}$$

where: $\frac{12}{(t_{24}-t_{12})}$ = mean rate of escalation of the calorimeter temperature [°C/s] in the region between 12 and 24°C rise where t_{12} designates time to attain increase of 120±0.1°C rise in temperature` t_{24} means time to attain increment of 24±0.2°C

Percentage age heat transmission factor, [*% TF* Q_o] for incident heat flux density level is explained by equation 3:

$$\% \, TF \; Q_o = 100.\frac{Q_c}{Q_o} \tag{3}$$

4 RESULTS AND DISCUSSION

4.1 Evaluation of thermal resistance and thermal conductivity

Thermal conductivity, thermal resistance and thickness were evaluated by Alambeta for monolayer and multilayer protective fabric assemblies and the outcomes are shown in Figure 2 and Figure 3 respectively.

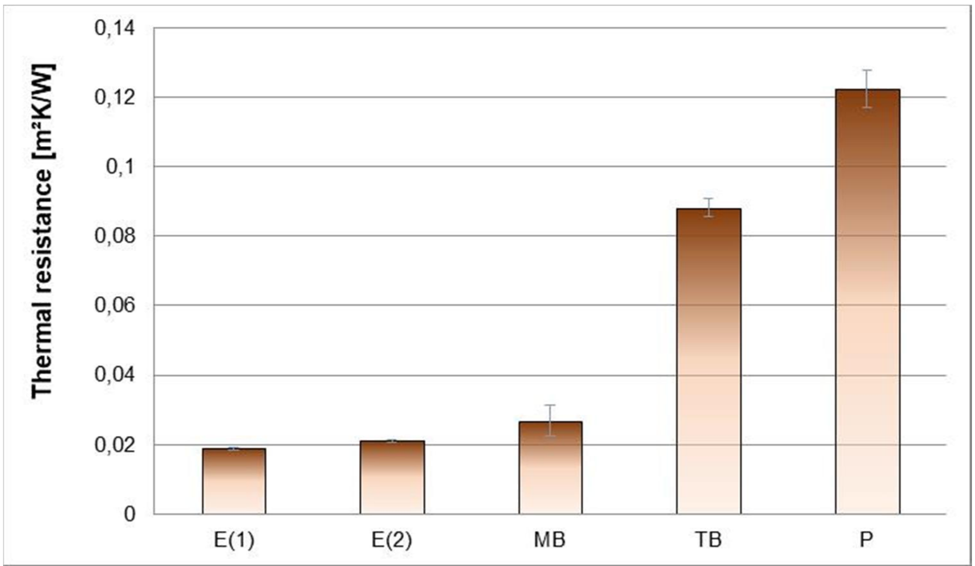

Figure 1 Thermal resistance of single layer fabrics

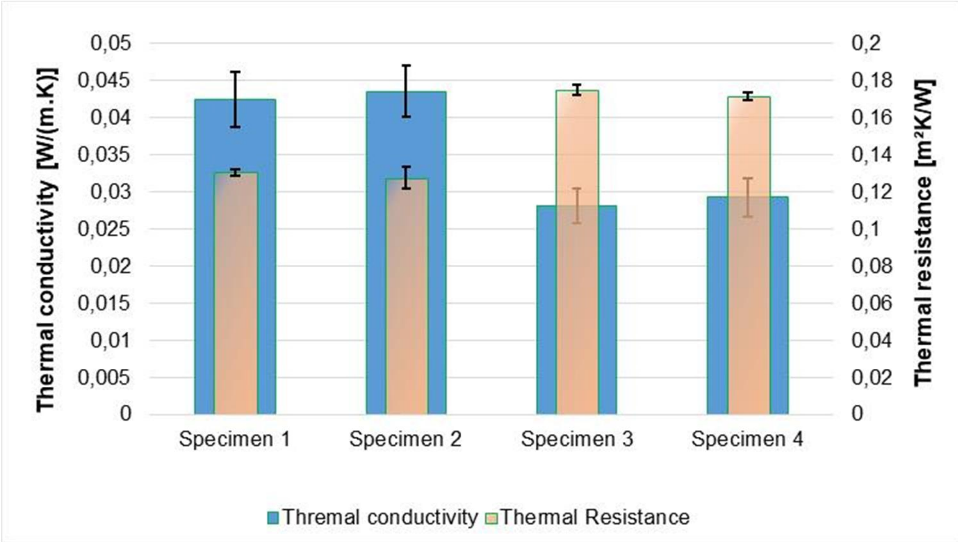

Figure 2 Thermal characteristics of multilayer FFPC specimens

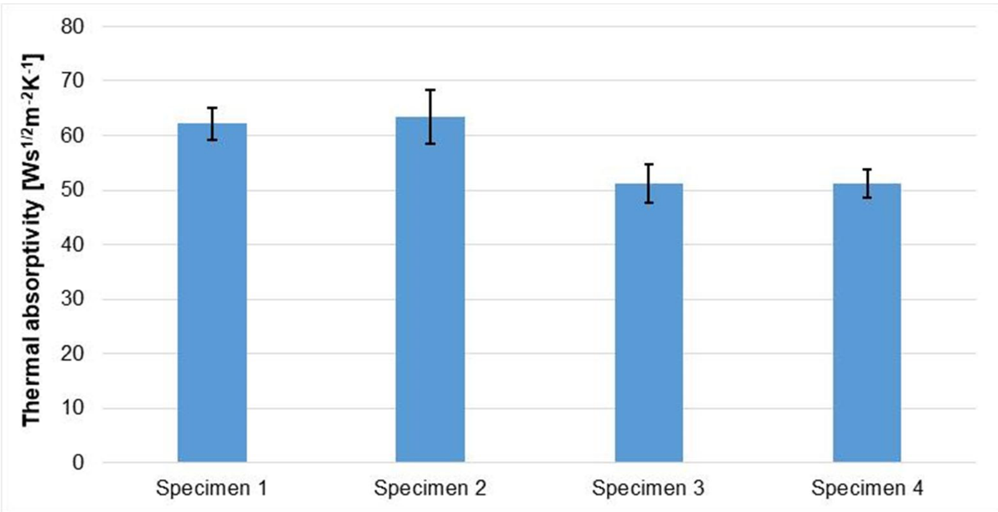

Figure 3 Thermal absorptivity of multilayer FFPC specimens

The relationship between thermal resistance and thermal conductivity is illustrated by following equation:

$$R_{th} = \frac{h}{\lambda} \tag{4}$$

where R_{th} is thermal resistance [m^{2}K/W], h is thickness of specimen and λ is thermal conductivity.

This thermal resistance is inversely proportional to thermal conductivity. Thermal resistance directly proportional to thickness [m] and inversely proportional to thermal conductivity [W/(m.K)]. However, thermal resistance is not only reliant on thickness of specimen but also on physical and chemical characteristics of specimen. Furthermore, the porosity and density of the textile medium have pivotal part in thermal characteristics of textile substrate. Those textile substrates which have closed and small pores are able to enclose static air inside them have high value of thermal resistance as air has very less value of thermal conductivity [20-22].

From Figures 2 and 3, it can be witnessed that a greater value of thermal resistance was witnessed in aerogel layer as compared to single layer and arrangement of FFPC specimen having aerogel layer as a substitute to thermal liner i.e. specimen 3 and specimen 4. This might be due to reason that silica based aerogel which has very low thermal conductivity even lesser than still air due to nanometer pore size making silica based aerogels are extremely high insulating materials [14]. Gaseous structure might avert conductive heat exchange [22]. Furthermore, aerogel does not permit circulation of air [22]. Thus, specimen C and D utilizing aerogel layer delivers higher thermal resistance and lower thermal conductivity as compared to specimen A and B.

Thermal absorptivity is the property of textile substrate highlights warm/cool feeling of textile substrate at the moment of connection with human skin. Thermal absorptivity is explained by following equation [23]:

$$b = \sqrt{\lambda \rho C} \tag{5}$$

where λ is thermal conductivity, ρ is density and C is the specific heat of textile substrate.

If thermal absorptivity is high, fabric will deliver cooler feeling. A perusal of Figure 4 revealed, that specimen 3 and specimen 4 having aerogel blanket as a substitute to thermal barrier delivers lesser thermal absorptivity values in comparison with specimen 1 and specimen 2.

4.2 Determination of Relative water vapor permeability

It was explained by Barker et al. [24] that the impact of moisture on thermal protective performance of Firefighter clothing (FFC) is contingent on conditions of exposure, properties of insulation and permeability of FFC and quantity of moisture in the turnout system. A perusal of Figure 5 acknowledged that specimen 3 and specimen 4 having aerogel blanket have low water vapor permeability. This might be due to fact that aerogel blanket has hydrophobic nature and presence of closed pores inside the configuration of aerogel blanket. On the other hand, some permeation of water vapor in specimen 3 and 4 which might be due to the high absorbing capabilities of aerogel, enabling the aerogel blanket enabling it to absorb moisture due to wetting and transport it to environment [25-30].

4.3 Transmission of radiant heat flux through multilayer protective clothing

The temperature of surrounding environment was maintained between 15 to 35°C. The rise of temperature was evaluated at back of specimen's by calorimeter which resulted in two threshold times i.e. *RHTI 12* and *RHTI 24*, Q_c and percentage heat transmission factor *(% TF Q_o)*.

Table 3 Incident temperature on surface of specimen when exposed to incident heat flux density of 10 kW/m^2

Heat flux density	10 kW/m^2
Incident temperature on surface of specimen	205°C
Distance of specimen from carbide rods	37.1 cm

A careful examination of Table 4 discloses that transmitted heat flux density Q_c and percentage transmission factor *(% TF Q_o)* that least values of transmitted flux density Q_c (kW/m^2) were observed for the samples having aerogel blanket as thermal liner.

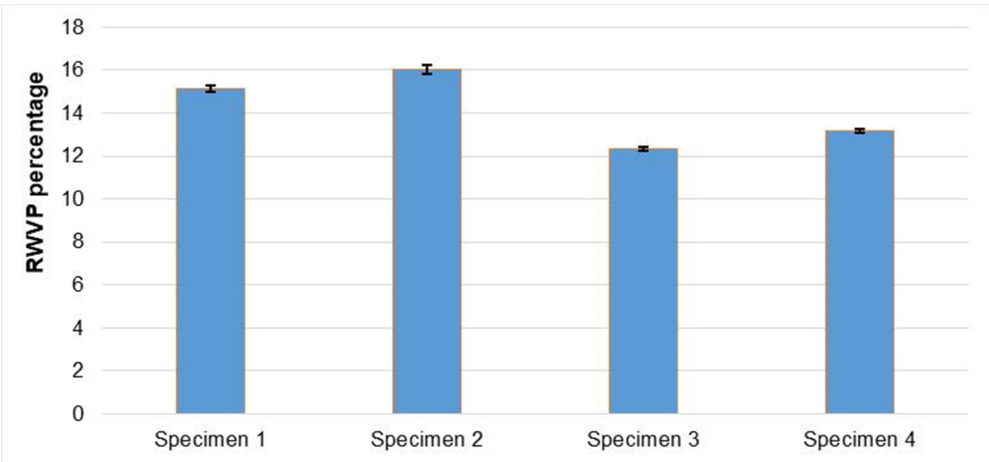

Figure 5 Water vapor permeability of multilayer FFPC specimen

Table 4 Time for rise of 12 and 24°C (*RHTI 12, RHTI 24*), transmitted flux density Q_c and percentage transmission factor (*% TF Q_o*) through FFPC combinations

Sr #	Name of material	Distance [cm]	RHTI 12 [sec]	RHTI 24 [sec]	Q_o [kW/m^2]	Q_c [kW/m^2]	% TF Q_o
1	P	37	54.6±2.828	102.6±2.969	10	1.4±0.005	13.6
2	Specimen 1	37	58.2 ±0.424	101.0±0.015	10	1.6±0.010	15.5
3	Specimen 2	37	74.1±0.707	128.7±0.997	10	1.3±0.050	12.1
4	Specimen 3	37	84.6 ±0.777	163.4±0.897	10	0.9±0.030	8.3
5	Specimen 4	37	97.4±0.898	195±0.672	10	0.7±0.150	6.7

An analogous pattern was observed in percentage *TF* Q_o values for the specimen having aerogel sheet i.e. specimen 3 and specimen 4 respectively. This might be due to reason that aerogel blanket contains almost 96 percentage of air and air is a good insulator delaying the amount of heat that will be exchanged through the specimen [31-33]. Furthermore, these aerogel samples consist of oxidized polyacrylonitrile (OPAN) polymer which has very respectable thermal stability and can endure greater amount of incident radiant heat flux [33]. The lesser the value of transmitted heat flux density, the minor will be quantity of radiant heat transmitted through fabric assemblies giving more amount of time to wearer (firefighter) to conduct their duties efficiently and effectively before acquiring any burn injuries. Table 4 also depicts that greater difference between *RHTI 12* and *RHTI 24*, lesser will be the value of transmitted flux density Q_c [kW/m^2] which indicates that specimen can withstand respected heat flux for longer time period allowing firefighters to perform their duties for longer duration before getting burn injuries.

A careful examination of Figure 6 reveals that the curves of specimen 3 and specimen 4 are more flat than that of the curves of specimen B, specimen A and aerogel layer (P) respectively at 10 kW/m^2. The flat curve indicates that rate of rise of temperature takes place at slower rate with respect to time. This might be due to reason that infrared radiation that performs a pertinent part in transference of heat may also be absorbed by aerogel [26-29] due to which aerogel blanket delivers improved thermal stability and insulation as compared to other specimens. The steep curve highlights, that rate of rise of temperature occurs at higher rate with respect to time, indicating swift exchange of radiant heat towards calorimeter. In consequence, the flatter curve will result in the slower transmission of heat exchange. Figure 6 also reveals that as curve becomes steeper curve, it shows certain increment of thermal conductivity and sudden decline in thermal resistance with the increase of time period [sec] which might be due to deterioration in the structure of FFPC specimen. The less steep the curve, the slower will be rate of increase in temperature, which will give more time of exposure to specimen when subjected to radiant heat flux. The flatter curve also indicates less damage to the corresponding fabric layers of the specimen. This might be due to fact that Infrared radiation that plays a substantial role in transference of heat can also be absorbed by aerogel [26-29] due to which aerogel blanket offers better thermal stability and insulation as compared to other specimens.

The images of specimen before and after exposure of 10 kW/m^2 are shown in Figure 7.

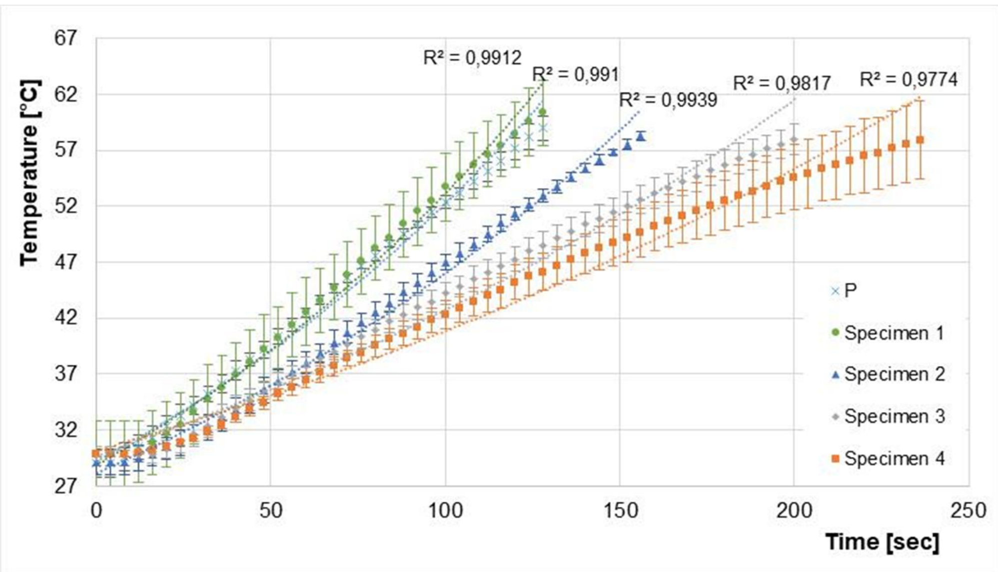

Figure 4 Heat transmission at 10 kW/m²

Specimen E1 before exposure

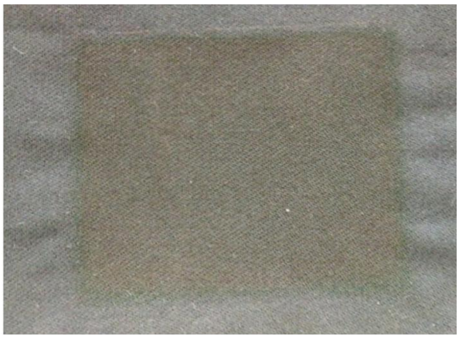

Specimen E1 after exposure to 10 kW/m^2

Specimen E2 before exposure

Specimen E2 after exposure to 10 kW/m^2

Figure 7 Comparison of images of outer shell before and after exposure to10 kW/m^2

From Figure 7, it is evident that after exposure to 10 kW/m^2 the color of the fabric became more black which indicated certain damage or deterioration of outer shell after being exposed to radiant heat flux density of 10 kW/m^2.

5 CONCLUSION

It might be deducted that safety of firefighters is contingent on the protective performance of firefighter protective clothing. If this protective performance can upsurge time of exposure of fire fighters against radiant heat flux, it may result in saving precious lives and useful stuff. When FFPC samples were subjected to radiant heat flux density of 10kW/m^2, it was observed that that aerogel layer was employed as an alternate to thermal barrier yield higher thermal resistance and improved thermal protective performance as it delayed the amount of heat transmitted through specimen. The gaseous structure, high percentage of static air, non-flammable nature of silica based aerogel is responsible for its better thermal protective behavior which offers better thermal stability against radiant heat flux density.

***ACKNOWLEDGMENT**: This study is supported under student grant scheme of SGS-21246 from Technical University of Liberec Czech Republic.*

6 REFERENCES

1. Holmer I.: How is performance in the heat affected by clothing? Textile Bioengineering and Informatics Symposium Proceedings 1, 2008, pp. 700-705
2. Das A., Alagirusamy R.: Science in comfort", 2nd ed., Wood Head Publishing, New Delhi, 2011, pp. 4-5
3. Li, Y.: Science in clothing comfort, Layton J.M. (Ed.), Manchester: Textile Institute International, Textile Progress 31(1/2), 2001, pp. 1-138, https://doi.org/10.1080/00405160108688951
4. Thermal comfort (2005a), Environmental Engineering Science 1, 21.07.2005, http://www.esru.strath.ac.uk/Courseware/Class-16293/6-Comfort.pdf
5. Stoecker W.F., Jones J.W.: Refrigeration and air conditioning, 2nd ed., McGraw-Hill, Singapore, 1982
6. Havenith G., Holmer I., Parsons K.: Personal factors in thermal comfort assessment: clothing properties and metabolic heat production, Energy and Buildings 34(6), 2002, pp. 581-591, id:81c53010-c49d-44ae-afe0-0bdaa1c34611
7. Holmer I.: Protective clothing in hot environments, Industrial Health 44(3), 2006, pp. 404-413
8. Lawson J.R.: Fire fighters protective clothing and thermal environments of structural fire- fighting, ASTM Spec. Tech. Publ. 1273, 1997, pp. 334-335
9. Lu J., Kyounga H., Keejong Y.: Effect of aerogel on thermal protective performance of firefighter clothing, Journal of Fiber Bioengineering and Informatics 6(3), 2013, pp. 315-324, DOI: 10.3993/jfbi09201309

10. Holcombe B.V.: The heat related properties of fire fighters protective clothing fabrics, Fire Safety Journal 6(2), 1983, pp. 129-141, https://doi.org/10.1016/0379-7112(83)90058-9
11. Salmon D.: Thermal conductivity of insulations using guarded hot plates, including recent developments and sources of reference materials, Measurement Science and Technology 12(2), 2001, pp. 1-89, DOI: 10.1088/0957-0233/12/12/201
12. Celcar D., Meinander H., Gersak J.: Heat and moisture transmission properties of clothing systems evaluated by using a sweating thermal manikin under different environmental conditions, International Journal of Clothing Science and Technology 20(4), 2008, pp. 240-252, https://doi.org/10.1108/09556220810878865
13. Pierre A.C., Rigacci A.: SiO_2 aerogels (chapter 2), Aerogels handbook, Advances in Sol-Gel Derived Material and Technology, Aegerter M.A., Leventis N., Koebel M.M. (Eds), New York: Springer Science+Business Media, 2011, pp. 21-45, ISBN 978-1-4419-7589-8
14. Pierre A.C., Pajonk G.M.: Chemistry of aerogels and their applications. Chem Rev 102(11), 2002, pp. 4243-4266, DOI: 10.1021/cr0101306
15. Hes L., Dolezal I.: New method and equipment for measuring thermal properties of textiles, Journal of the Textile Machinery Society of Japan. 42(8), 1989, pp. 24-28, DOI:10.4188/transjtmsj.42.8_T124
16. Matusiak M.: Investigation of the Thermal Insulation Properties of Multilayer Textiles, Fibres&Textiles in Eastern Europe 59(5), 2006, pp. 98-112
17. Hes L. Araujo M.: Effect of mutual bonding of textile layers on thermal insulation and thermal contact properties of fabric assemblies, Textile Research Journal 66(4), 1996, pp. 245-250, DOI:10.1177/004051759606600410
18. Matusiak M., Kowalczyk S.: Thermal-insulation properties of multilayer textile packages, AUTEX Research Journal 14(4), 2014, pp. 299-307, DOI:10.2478/aut-2014-0030
19. Meb G.W., P. GmbH P.: Combustion behavior test equipment, Keplerstraße Berlin, 2002
20. Bogusławska-Bączek M., Hes L.: Effective water vapour permeability of wet wool fabric and blended fabrics, Fibres&Textiles in Eastern Europe 97(1), 2013, pp. 67-71
21. Oğlakcioğlu N., Marmarali A.: Thermal comfort properties of some knitted structures, Fibres Textiles in Eastern Europe 64-64(5-6), 2007, pp. 94-96
22. Hes L., Loghin C.: Heat, moisture and air transfer properties of selected woven fabrics in wet state, Journal of Fiber Bioengineering and Informatics 2(3), 2009, pp. 141-149, DOI:10.3993/jfbi12200901
23. Schneider A.M., Holcombe B.V.: Properties influencing coolness to the touch of fabrics, Textile Research Journal 61(8), 1991, pp. 488-494, https://doi.org/10.1177/004051759106100810
24. Barker R.L., Heniford R.C.: Factors affecting the thermal insulation and abrasion resistance of heat resistant hydro-entangled nonwoven batting materials for use in firefighter turnout suit thermal liner systems, Journal of engineered fibers and fabrics 6(1), 2011, pp. 1-10
25. Baetens R., Jelle B.P., Gustavsen A.: Aerogel insulation for building applications: A state-of-the-art review, Energy and Buildings 43(4), 2011, pp. 761-769, https://doi.org/10.1016/j.enbuild.2010.12.012
26. Shahid A., Furgusson M., Wang L.: Thermophysiological comfort analysis of aerogel nanoparticle incorporated fabric for fire fighter's protective clothing, Chemical and Materials Engineering 2(2), 2014, pp. 37-43, DOI: 10.13189/cme.2014.020203
27. Fricke J.: The pore structure determination of aerogels, Springer-Verlag, 4, 1998, pp. 187-195
28. Lee D., Stevens P.C., Zeng S.Q., Hunt A.J.: Thermal characterization of carbon-opacified silica aerogels, Journal of Non-Crystalline Solids 186, 1995, pp. 285-290, https://doi.org/10.1016/0022-3093(95)00055-0
29. Fricke J.: Thermal properties of silica aerogels, Le Journal de Physique Colloques 50, 1989, pp. 4-4
30. Onofrei E., Dupont D., Petrusic S., Soulat D., Bedek S., Codau T.C.: Modeling of heat transfer through multilayer firefighter protective clothing, Industrial Textila 65(5), 2014, pp. 277-282
31. Xu B., Cai J.Y., Finn N., Cai Z.: An improved method for preparing monolithic aerogels based on methyltrimethoxysilane at ambient pressure Part I: Process development and macrostructures of the aerogels, Microporous and Mesoporous Materials 148(1), 2012, pp. 145-151, https://doi.org/10.1016/j.micromeso.2011.08.012
32. Venkataraman M., Mishra R., Kotresh T.M., Sakoi T., Militky J.: Effect of compressibility on heat transport phenomena in aerogel-treated nonwoven fabrics, The Journal of Textile Institute 107(9), 2015, pp. 1150-1158, https://doi.org/10.1080/00405000.2015.1097084
33. Anon. Aspen aerogels. Safety data sheet, pyrogel 2250, 2008

TWO-DIMENSIONAL STUDIES OF THERMOMECHANICAL PROPERTIES OF TEXTILE MATERIALS FOR 3D FORMATION

Mykola Riabchykov, Sergiy Vilkov, Svitlana Nechipor and Tetyana Popova

Ukrainian Engineering Pedagogic Academy, Universitetskaya st. 16, 61003 Kharkov, Ukraine
nikolryab@uipa.edu.ua

***Abstract:** The article defines the parameters of forming and form resistance of textile materials taking into account the properties of anisotropy on the basis of constructing a model of thermomechanical deformation of textile material, experimental research on three-dimensional deformation. The model of two-dimensional thermomechanical deformation is presented. Correlation dependencies between parameters of thermomechanical deformation and structural characteristics of a material are determined.*

***Keywords:** uniformity, form formation, thermomechanical characteristics, structural parameters, two-dimensional tests, three-dimensional deformation.*

1 INTRODUCTION

The ability of textile materials to form is a very important property that determines the choice of an optimal method for obtaining the silhouette of garments and affects their quality. The required form for product parts is provided by means of wet-heat treatment, which is a very important part of the technological process of making clothes. Formation of new materials in wet-heat treatment is not sufficiently studied, which makes it difficult to manufacture products from them. As the assortment of new materials is constantly updated, there is a problem of constant experimental research of their formation in the wet-heat treatment. In connection with this study of the formation of textile materials is an urgent task.

The real form of a textile product has a pronounced three-dimensional character. At the same time, the process of wet-heat treatment involves changing the shape and size of textile materials having different thermomechanical properties in different directions. It should be noted that modern processes of wet-heat treatment of textile materials are insufficiently provided with scientifically grounded regimes. In studies conducted on the determination of the properties of textile materials, as a rule, their anisotropy is not taken into account.

Problems of the formation of textile materials for light industry, in particular by means of thermomechanical transformations, are considered in a number of papers [1-2]. The application of theories of deforming textile materials under the action of heat and load was carried out in [3], in particular, the heat transfer theories for the design of processes was taken into account, although real regimes were not considered.

Attempts for mathematical modeling of deformation processes of textile materials are periodically carried out, although their practical application is difficult to implement. For example, in [4], a method for solving this problem by employing finite element (FE) techniques in two scales was presented, using the results of analysis at the meso scale (the scale of the repeating unit) to provide an equivalent non-linear spring behavior for each textile link at the macro-scale. It should be determined that finite-element is a very powerful method but not always adapted to reality. In addition, it requires the definition of real mechanical and thermal characteristics.

Attempts to simulate the thermomechanical characteristics for the purpose of designing deformation processes were also made in [5]. The main thermomechanical effects arising in textile materials are discussed in [6], the effects of the influence of force and temperature - in [7], especially the materials for the production of clothing - in [8].

Experimental studies that determine the properties of textile materials in two directions were carried out in works [9-10], although the model of double-sided deformation was not built. Multifunctional modeling of the processes of the thermoelastic behavior was carried out in [11], although the results are difficult to distribute to real textile materials.

The purpose of this work is to determine the parameters of shaping and shape resistance of textile materials taking into account the properties of anisotropy on the basis of constructing a model of thermomechanical deformation of textile material, experimental studies on three-dimensional deformation.

2 EXPERIMENTAL PART

As already mentioned, the real modes of deformation of materials are at least two-dimensional in nature. It is also necessary to take into account the real properties of polymers, which also include textile materials. The most characteristic feature is anisotropy - different properties of materials in different directions. These properties must be taken into account when designing the technological processes of changing the shape.

Unfortunately, data on two-dimensional deformation of materials is practically absent. We have developed the experimental device, then worked out technique and obtained the results in a two-dimensional test of polymer materials (Figure 1). During realization of this experiment, the sample is loaded in two perpendicular directions. At the same time it was heated. Changes in size were fixed in two directions.

The group of dependences of the longitudinal and transverse deformation of the material were constructed by changing the ratio of longitudinal and transverse forces.

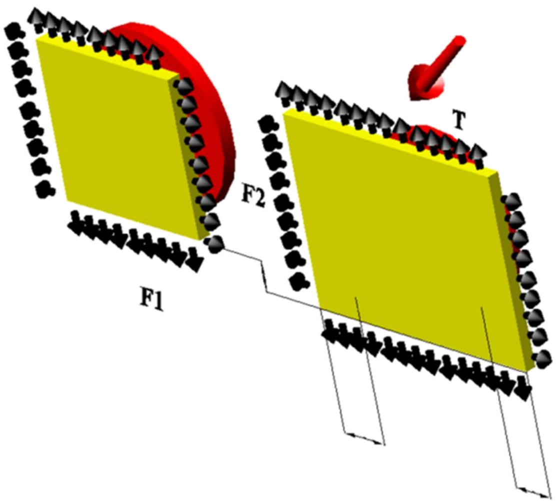

Figure 1 Definition of two-dimensional thermomechanical characteristics

As a result of the obtained studies a complex of dependencies is suggested, which for a particular material can be written as a system:

$$\begin{cases} \varepsilon_1 = f_{11}(t)\cdot\sigma_1 - f_{12}(t)\cdot\sigma_2 \\ \varepsilon_2 = -f_{21}(t)\cdot\sigma_1 + f_{22}(t)\cdot\sigma_2 \end{cases} \quad (1)$$

where ε_1, ε_2 - relative deformations in two directions, σ_1, σ_2 - mechanical stresses in these directions, f_{ij} - thermomechanical characteristics of stiffness, found from the experiments.

Let's write down the voltage through the deformation. We'll get it.

$$\begin{cases} \sigma_2\left(f_{22} - \dfrac{f_{12}\cdot f_{21}}{f_{11}}\right) = \varepsilon_2 + \dfrac{f_{21}}{f_{11}}\cdot\varepsilon_1 \\ \sigma_1\left(f_{11} - \dfrac{f_{12}\cdot f_{21}}{f_{22}}\right) = \varepsilon_1 + \dfrac{f_{12}}{f_{22}}\cdot\varepsilon_2 \end{cases} \quad (2)$$

In the case of known values of deformations from the system, we can obtain the values of stresses that determine the external loads on the material, as well as the necessary temperature distribution on the material surface to provide the given deformations (Figure 2).

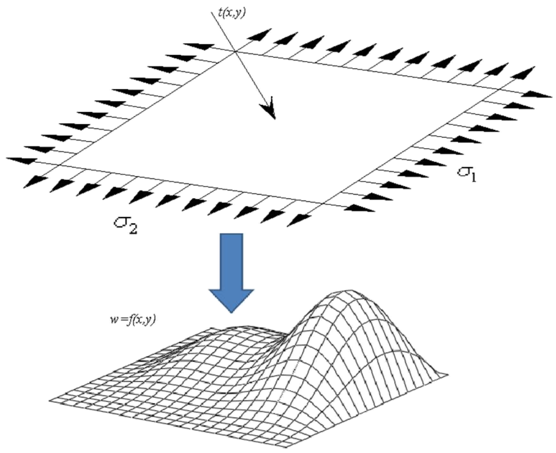

Figure 2 Thermomechanical deformation of textile material

Thus it is possible to solve the problem of creating a convex form of the surface of a textile material by its stretching with simultaneous heating. In the future, we will call the shaping the value of the convexity. The convexity of the material that occurs when heated with the simultaneous loading of the textile material determines its shaping.

The study of the formation of textile materials was carried out on an experimental device, which is depicted in Figure 3.

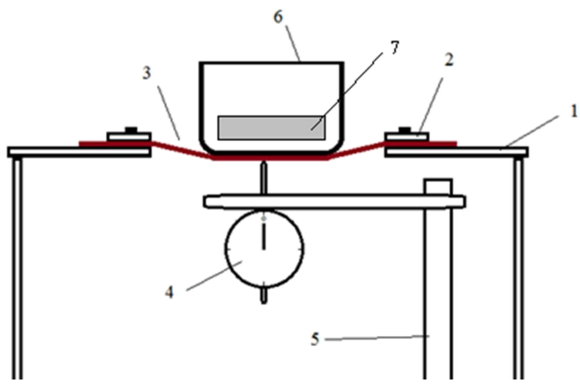

Figure 3 The scheme of measurement of formation during heating; 1 - the platform, 2 - clamp of the fabric, 3 - sample of the investigated fabric, 4 - indicator of movement, 5 - tripod of indicator, 6 - capacity with electric heater

The device is imagines, from from your point of view, as a platform with a round hole and a special clamp to hold the fabric. On a stretched fabric was a container with a convex surface, inside which was an electric heater. The temperature of the fabric was measured at regular intervals using the infrared thermometer MS6530.

Ten samples of tissues have been selected and studied for research. These fabrics are characterized by surface density, a kind of weaving and fibrous composition. For the experiment, blended fabrics containing wool with polyester fibers were selected in different ratios.

3 RESULTS AND DISSCUSSION

Figures 4-6 show the results for fabrics with different content of polyester fibers. For the experiments, fabrics with a content of polyester fibers of 18, 22, 34, 48, 56, 67, 74, 87 percent were chosen, designated respectively T9, T8, T7, T6, T5, T4, T3, T2, T1.

Dependence of temperature *T* [ºC] on the time *t* [s×10²] for the investigated fabrics is presented in Figure 4. The temperature range of the measurement were changed from 20 to 210°C.

The graph shows that the heating rate of the samples was approximately the same, which indicates the same conditions for conducting experiments. The temperature of the fabrics for all samples initially rose intensively, then the rate of lifting slowed down and then practically did not change.

The dependence of shaping *F* [%] of time *t* [s×10²] for the investigated tissues is presented in Figure 5.

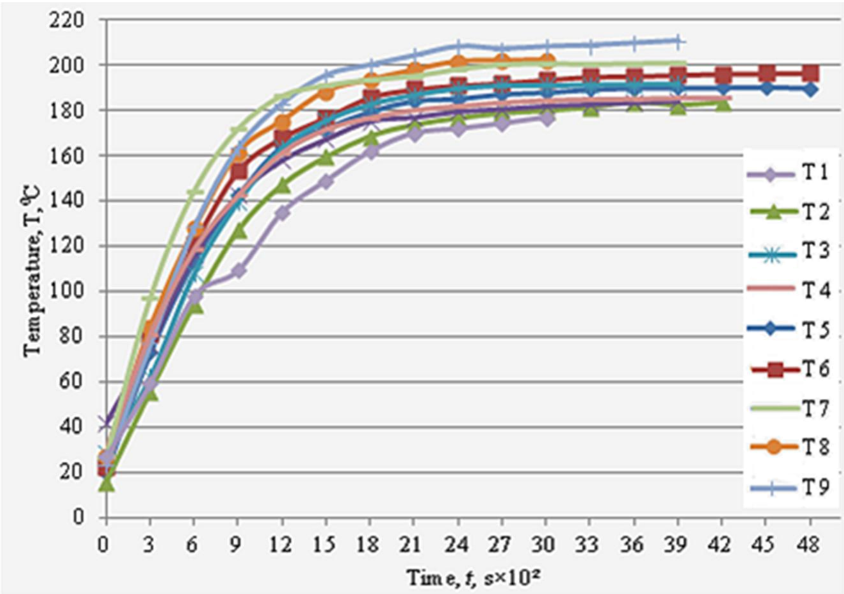

Figure 4 Dependence of temperature on time for investigated fabrics

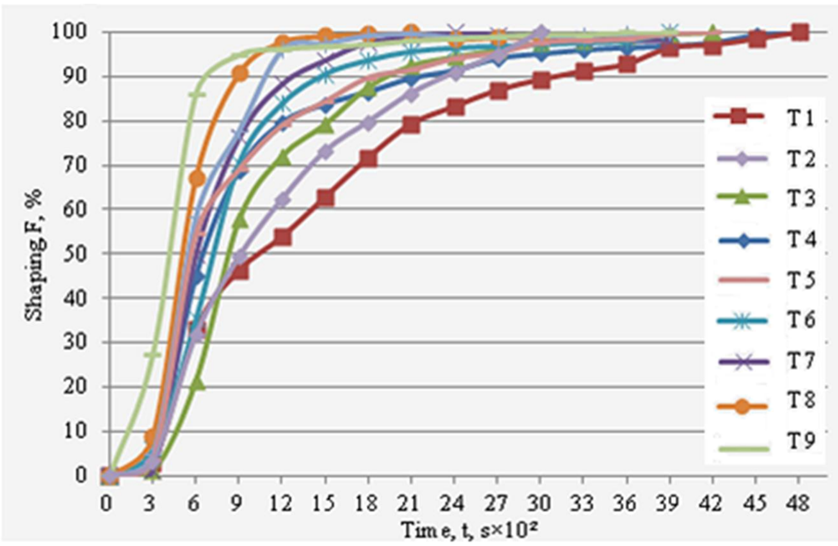

Figure 5 The dependence of shaping on time for investigated fabrics

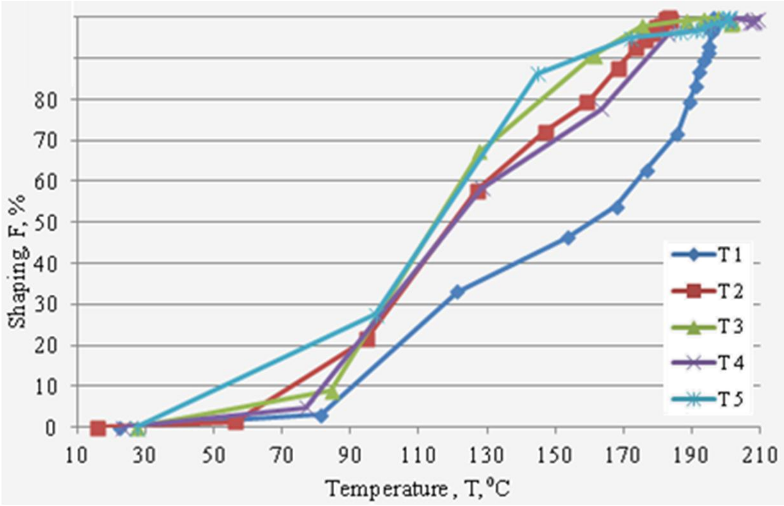

Figure 6 Dependence of shaping on temperature for selected fabrics

As it follows from the graph for all samples before 300 second, the formulation increased very rapidly, and then slowed down. In the sample number 9, the formation became the fastest, and for the sample number 2, the slowest.

Dependence of shaping *F* [%] on temperature *T* [°C] for the group of samples is presented in Figure 6.

In all samples the formation began to increase strongly at a temperature of 55-95°C, the fastest formation took place at temperatures 170-190°C.A sufficiently high correlation is observed for the correlation coefficients between shaping and linear filling (Figure 7).

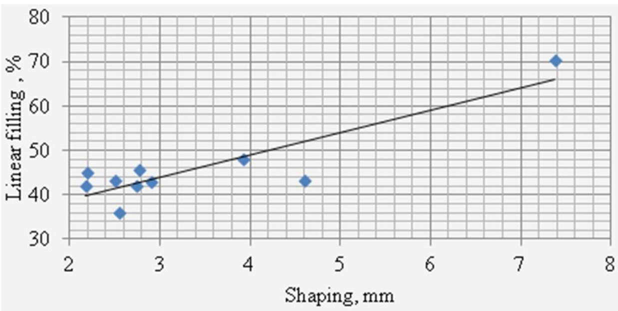

Figure 7 Correlation between shaping and linear filling

Also, the correlation of the rather high level is observed between the formation and the coefficient of connectivity. The correlation coefficient reaches R = 0.71, the correlation is high.

Thus, the magnitude of linear filling by weft unambiguously increases the possibility of shaping a textile material, with the magnitude of the maximum deformation approximately proportional to the magnitude of linear filling. The magnitude of the coupling coefficient unambiguously reduces the ability to shaping, while the reduction of the size of the formation is roughly proportional to the value of the coupling coefficient.

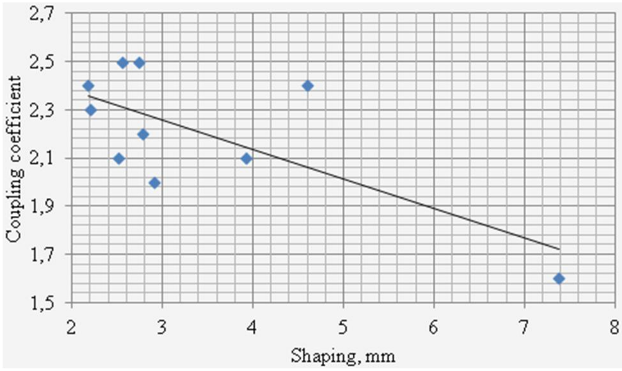

Figure 8 Correlation between shaping and coupling coefficient

After cooling the samples, measure the depth of formation. The measuring device is aligned so that the zero was at the level of the clamper fabric on the table of the installation.

Form resistance will be called the final deformation that remains in the textile material after cooling.

It was determined the influence of various factors on the form of resistance and correlation between them, in particular:

- deformation of the sample after cooling and deformation of the sample after ironing; uniformity and surface density; shape resistance and tendency to crunching, shape resistance and tendency to trickle down the duct; uniformity and draping properties; discontinuous efforts to form and break away after forming; relative elongation to formation and relative elongation after formation.

At the same time, the maximum influence on the value of the shape resistance gives the values of linear density and thickness of the threads (Figures 10 and 11). It was also determined the correlation between the discontinuous effort and the formation of the bursting forces after the formation, which is presented in Figure 9.

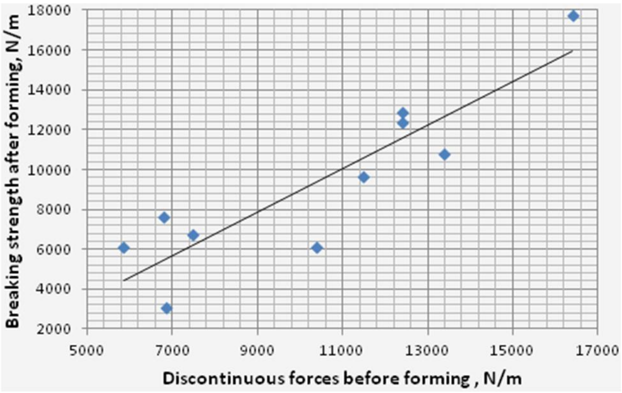

Figure 9 Correlation between discontinuous forces before forming and breaking strength after forming a weft

A high correlation is observed between the discontinuous forces before forming and the bursting forces after the formation of a weft, because R = 0.88. One can conclude that the effect of forming on the bursting force on the thread of weft is greater than the base thread.

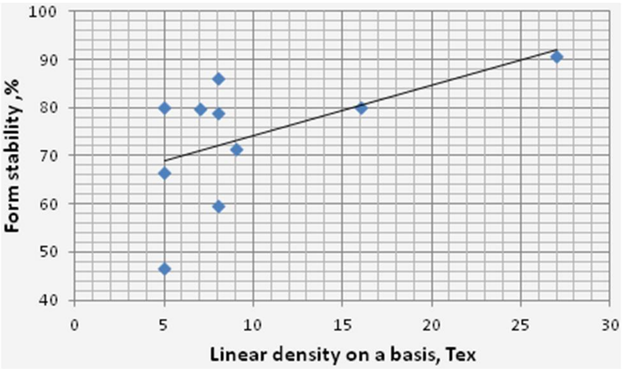

Figure 10 Correlation between form stability and linear density

There is the average correlation between the uniformity of form and the linear density, because R = 0.8. One can conclude that the greater the linear density on the basis, the better the shape resistance.

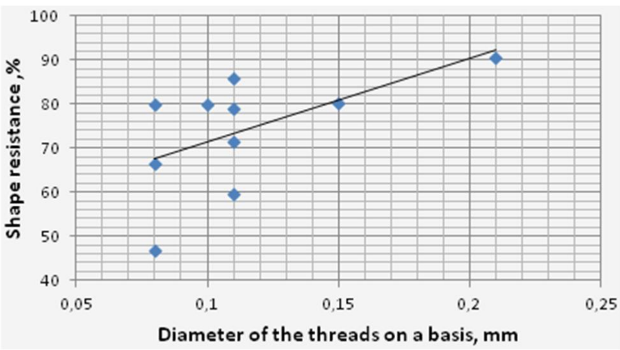

Figure 11 Correlation between the shape resistance and the diameter of the threads

There is the average correlation between the uniformity of the form and the diameter of the threads on based, because R = 0.78, which means that the larger the diameter of the threads on the basis, the better the shape resistance.

4 CONCLUSION

The conducted studies have proved the validity of two-dimensional thermomechanical characteristics of textile materials for the design of wet heat treatment processes.

The main indicators of the process of wet heat treatment of textile materials, shaping and shape resistance are functions of structural characteristics of materials.

The linear filling of the textile material uniquely increases the possibility of shaping the textile material, with the magnitude of the maximum deformation roughly proportional to the linear filling value. The value of the coupling coefficient unambiguously reduces the ability for shaping, while the reduction of the size of the formation is approximately proportional to the value of the coefficient of connectivity

Structural characteristics of materials also affect the shape resistance of textile materials. According to the research carried out, the structural integrity of the materials under investigation is mainly influenced by the linear density, the diameter of the filaments and the linear filling.

5 REFERENCES

1. Product developments and innovations in textiles and apparel Textile Outlook International 2013(164), 2013, pp. 54-95
2. Gibson P.W.: Effect of wool components in pile fabrics on water vapor sorption, heat release and humidity buffering, Journal of Engineered Fibers and Fabrics 6(1), 2011, pp. 11-18
3. Ip R.W.L., Iok Cheong W.: New use heat transfer theories for the design of heat setting machines for precise post-treatment of dyed fabrics, Defect and Diffusion Forum 312-315, 2011, pp. 748-751, DOI: 10.4028/www.scientific.net/DDF.312-315.748
4. Crookston J.J., Long, A.C., Bingham G.A., Hague R.J.M.: Finite-element modelling of mechanical behaviour of rapid manufactured textiles, Proceedings of the Institution of Mechanical Engineers, Part L: Journal of Materials: Design and Applications 222(1), 2008, pp. 29-36, DOI: 10.1243/14644207JMDA161
5. Marrey R.V., Sankar B.V.: Thermo-mechanical properties of and residual stresses in textile structural composites, Proceedings of the American Society for Composites, 1994, pp. 499-508
6. Bodur M.S., Bakkal M., Sonmez H.E.; The effects of different chemical treatment methods on the mechanical and thermal properties of textile fiber reinforced polymer composites, Journal of Composite Materials 50(27), 2016, pp. 3817-3830, DOI: 10.1177/0021998315626256

7. Heinrich C., Aldridge M., Wineman A.S.,Waas A.M., Shahwan, K.W.: The role of curing stresses in subsequent response, damage and failure of textile polymer composites, Journal of the Mechanics and Physics of Solids 61(5), 2013, pp. 1241-1264, DOI: 10.1016/j.jmps.2012.12.005
8. Khoun L., Challagulla K., Hubert P.: Thermo-mechanical properties of 5-harness satin fabric composites, Journal of Composite Materials 46(25), 2012, pp. 3121-3136, DOI: 10.1177/0021998312436990
9. Kelly, P.A., Bickerton, S., Cheng, J.: Transverse compression properties of textile materials Advanced Materials Research 332-334, 2011, pp. 697-701, DOI: 10.4028/www.scientific.net/AMR.332-334.697
10. Vencelová P., Ujhelyiová A., Ryba J.: Thermomechanical and sorptive properties of metallocene polypropylene fibres modified polyvinyl alcohol and cloisite, Vlakna a Textil (Fibres and Textiles) 17(4), 2010, pp. 3-6
11. Alzina A., Toussaint E., Béakou A.: Multiscale modeling of the thermoelastic behavior of braided fabric composites for cryogenic structures, International Journal of Solids and Structures 44(21), 2007, pp. 6842-6859, DOI: 10.1016/j.ijsolstr.2007.03.013

IMPACT OF ASPIRATION AIR PRESSURE IN THE SPINNING SHAFT ON THE FORMATION OF HOLLOW POLYAMIDE 6 FIBRES

Tatjana Rijavec[1], Anela Kljajić[1] and Sabina Jakomin[2]

[1]*University of Ljubljana, Faculty of Natural Sciences and Engineering, Aškerčeva 12, 1000 Ljubljana, Slovenia*
[2]*AquafilSLO, Letališka cesta 15, 1000 Ljubljana, Slovenia*
tatjana.rijavec@ntf.uni-lj.si, sabina.jakomin@aquafil.com

Abstract: *An influence of aspiration air pressure under spinnerets on properties of hollow polyamide 6 fully drawn multifilament yarns is presented in the article. Experiment was made on an industrial spinning machine. Aspiration air pressure in the spinning shaft of 50 Pa and 100 Pa influenced on decreasing of spinnerets temperature, on a quantity of monomer in yarns and breaking force, which both increased, but breaking elongation of yarns decreased. The changes of mechanical properties are related with changes in supramolecular structure and ability of yarns for dyeing.*

Keywords: *hollow fibre, polyamide 6, fully drawn yarn.*

1 INTRODUCTION

Polyamide 6 (PA 6) is a fibre forming polymer formed from a monomer ε-caprolactam in a ring-opening polycondensation reaction [1, 2]. At the end of the polymerization reaction, 2–10% of unreacted monomer and acyclic/cyclic oligomers (i.e. low molecular weight fraction) are always present in the polymer melt [3]. Before spinning of PA 6 fibres, low molecular weight fraction is partially extracted from PA 6. Low molecular weight fraction influences on rheological properties of polymer melt and also on fibres properties, particularly on their tensile properties [3].

At spinning of PA 6 yarns, low molecular weight fraction, particularly monomer, evaporates from jets under the spinnerets at a length of a first 5-15 cm [3]. Monomer deposits on spinnerets and on spinning shaft walls, where a few millimeters thick layers in few days can be formed. Monomer can be removed by mechanical cleaning in regular time intervals. To prevent monomer deposition, an aspiration of cooling air under the spinnerets is used. Aspiration is carried out with the help of:

(i) A water pump, which creates a vacuum to aspirate cooling air under the spinneret, and monomer condensates and dissolve in a water jet.

(ii) A vacuum suction of cooling air through gaps, mounted under the spinnerets, which is the most often used method. Gaps are usually mounted on each spinning position, near the extruded filaments. Lower air pressure in gaps than in a spinning shaft causes an aspiration of the cooling air. Effective monomer suction is only if the gaps are transient.

Aspiration of monomer under the spinnerets can influence on solidifying process of polymer jets. In the case of spinning hollow filaments, irregularities of openings or clogging of hollow filaments may occur. Similar to solid filaments, hollow filaments are also prone to breaking filaments in spinning line [4]. In this study an influence of aspiration air pressure on morphology, structure and properties of hollow fully drawn PA 6 filament yarns was studied in real, industrial conditions.

2 EXPERIMENTAL

2.1 Materials

Yarns for the experiment were produced on an industrial fully drawn yarn (FDY) spinning machine Teijin Seiki (Japan). All the yarns were made from the same semi dull polymer polyamide 6. Solidification of the extruded jets was accelerated by using cross air flow. Temperature of blown cooling air was around 19°C. Due to heat emitted by spinnerets and polymer jets cooling air was heated up under the spinnerets up to 100°C. The cooling air under the spinnerets carried monomer and oligomers. The velocity of aspirated cooling air through the gaps was higher than the velocity of the blown cooling air and was adopted to prevent deposition of monomer and oligomers on the gaps and filling them up. In our experiment the velocity of the aspiration air (Table 1) was between 0.0 (no aspiration) and 4.0 m/s (aspiration air pressure 100 Pa). Samples were collected from twelve bobbins made on two spinning positions (six bobbins per position). Before winding the yarns, filaments were interlaced. Winding velocity was a little over 4000 m/min. Spinneret temperature in the spinning line was measured with a laser thermometer Raytek Rayngver MX. Yarn stress was measured with tensiometers on-line in five positions (Figure 1).

Table 1 Designation and spinning conditions of samples

Sample	Aspiration air pressure [Pa]	Aspiration air velocity [m/s]	Average spinneret temperature [°C]	Average yarn stress, measured in spinning line positions 1 to 5 (Fig. 1) [cN/yarn]				
				1	*2*	*3*	*4*	*5*
AP0	0	0.0	243	3.5	6	8.3	3	4
AP50	50	0.2–0.3	240	3.7	6	8.5	3.5	4.2
AP100	100	2.5–4.0	237	3.9	6.2	9.3	3.8	4.9

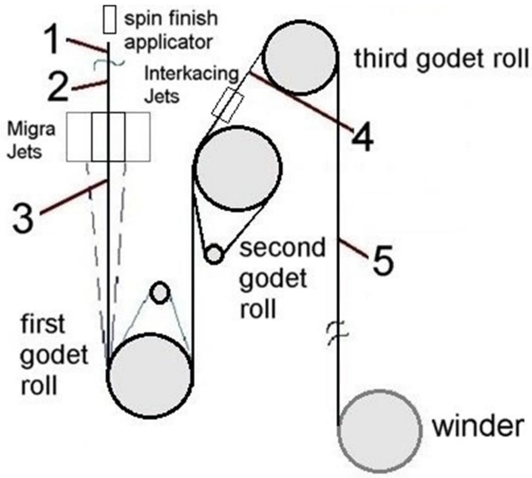

Figure 1 Schema of spinning line between application of spin finish and winding of yarns, with positions of on-line tensiometers (numbers 1–5)

2.2 Methods

Linear density was measured gravimetrically in accordance with a standard EN ISO 1973:1999. Breaking force and elongation were measured on a dynamometer Statimat M (Textechno, Germany) according to standard EN ISO 2062:2010. Dynamic thermal tensile test was made on a Dynafil C apparatus (Textechno, Germany) at temperature 150°C, pretension 30 cN, yarn speed 200 m/min and extension of 30%. Quantity of monomer and low molecular weight fraction were determined from extracts, which were prepared by treatment of samples in methanol at 95°C for four hours. With a HPLC method quantity of monomer and oligomers was determined. Samples were firstly dissolved in HCOOH for HPLC analysis. Average molecular weight was determined from viscosity measurements of samples solution of 0.1% sulfuric acid. Longitudinal view and filaments cross section were made on a scanning electron microscope Jeol JSM-6060, where filaments diameter was also measured.

3 RESULTS AND DISCUSSION

Measured spinneret temperature was 243°C without using aspiration of cooling air (Table 1). Aspiration of cooling air caused decreasing of spinneret temperature for 6°C when the aspiration air pressure was 100 Pa. Decreasing spinneret temperatures influenced on increasing yarns stress in all measured positions 1–5 (Figure 1) with increasing aspiration air pressure.

3.1 Linear density and filament cross section

Aspiration of cooling air had no significant influence on linear density, but caused some imperfections of filament cross-section:

- Average linear density of yarns samples was 37.4 dtex (Table 2). Considering the expected linear density of 44 dtex for solid filament yarn made at the same spinning conditions, the hollow filament yarns had for about 15% lower linear density than solid filament yarns would have. Filament thickness was in the range 20.8-22.8 μm. Aspiration air pressure had no significant influence on samples linear density.
- Cross-section of filaments (Figure 2) was circular with triangular openings in the middle. Decreasing of spinneret temperature accelerated solidifying of polymer jets. Average cross-section area was calculated on the basis of SEM micrographs (Figure 2). It was 406.5 μm^2 for samples AP0 and AP100, but for the sample AP50 it was a little lower, 384.2 μm^2 (Table 3). On the Figure 2 are seen two incomplete formed cross-sections on the sample AP100 (marked with arrows), which was the consequence of the too fast solidifying spinning jets, before two ends merged together and formed hollow filaments. Average hollowness, calculated from the average cross-section of filaments and average cross section of the middle hollow part of filaments, was between 10.60 and 11.64%.

Table 2 Yarn linear density and filament thickness

Sample	Yarn linear density [dtex]			Filament thickness [μm][a)]	
	Average	*SD*[b)]	*Range*	*Average*	*SD*
AP0	37.3	0.135	37.3–37.1	20.83	1.00
AP50	37.4	0.15	37.7–37.2	22.75	1.05
AP100	37.35	0.11	37.5–37.3	21.43	0.97

[a)] Number of measurements = 10; [b)] Standard deviation

Table 3 Filaments cross-section area and hollowness

Sample	Cross-section area [μm^2]		Hollowness [%]	
	Average	*SD*	*Average*	*SD*
AP0	406.54	40.61	10.60	1.98
AP50	384.16	32.56	11.64	2.61
AP100	406.55	41.60	10.60	4.61

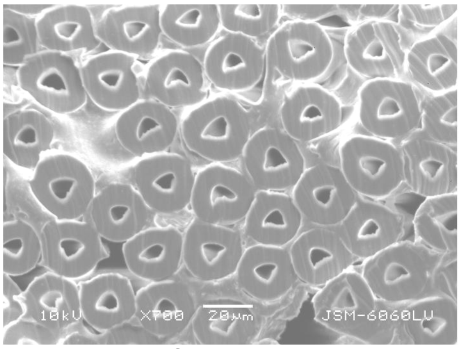

Sample AP0

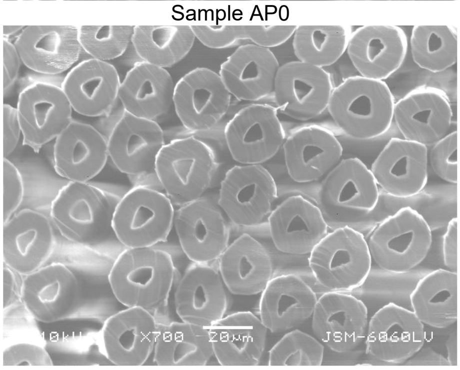

Sample AP50

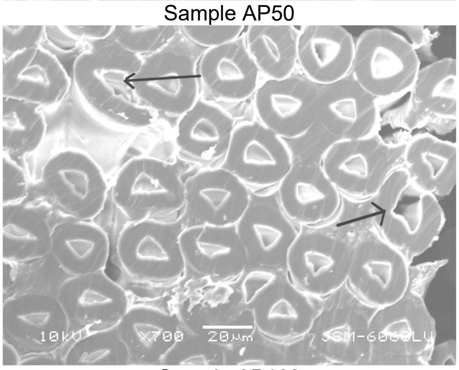

Sample AP100

Figure 2 Influence of aspiration air pressure on a cross-section of fully drawn polyamide 6 yarns (SEM, magnification 700x)

3.2 Tensile properties

From the tensile properties of samples is seen that aspiration of cooling air influenced on filament supramolecular structure, because:

- Samples made at aspiration air pressure of 50 Pa and 100 Pa showed higher average breaking force and lower average breaking elongation as sample AP0, made at aspiration air pressure zero (Figure 3).
- Influence of aspiration air pressure is evident on the curves of specific stress/elongation (Figure 4). Samples AP50 and AP100 show a little higher specific stress in the whole deformation range. Modulus of elasticity was in the range of 4.19-4.53 GPa.
- Dynamic thermal analyses showed for about 10% higher tensile force of samples, made with aspiration cooling air in comparison to sample AP0, made without it (Table 4).

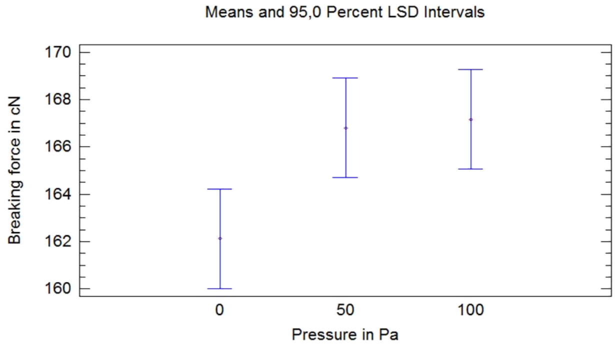

a)

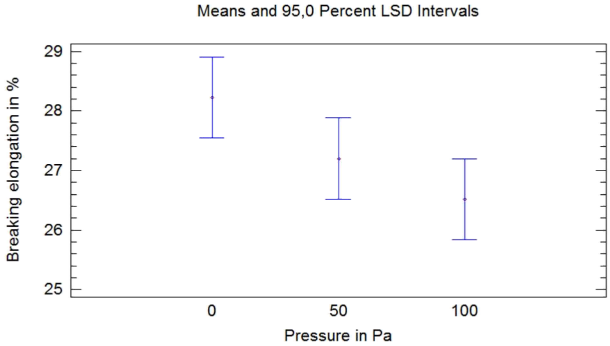

b)

Figure 3 Influence of aspiration air pressure on breaking force (a) and breaking elongation (b) of hollow PA 6 fully drawn yarns

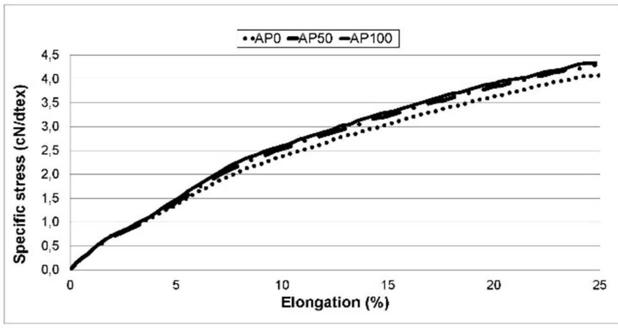

Figure 4 Specific stress-elongation curves of samples

Table 4 Dynamic thermal analyses

Sample	F [cN]	SD [cN]	F_{max} [cN]	F_{min} [cN]
AP0	67.635	0.54	68.22	66.845
AP50	74.435	1.225	76.135	73.295
AP100	74.945	1.13	76.085	73.32

3.3 Quantity of monomer and oligomers

Measured average viscosity molecular weight was the same for all samples, 15185.89 g/mol. With an extraction of samples in methanol, 2.05% of extract from the sample AP100 was obtained, 1.95% from the sample AP50 and 1.92% from the sample AP0. Lower spinneret temperatures at higher aspiration air pressure influenced on slower evaporation of monomer and oligomers from the spinning jets therefore higher quantities were kept in the filaments. Analysis of the extracts (Figure 5) has shown an increasing of quantities of monomer, trimers and hexamers in yarns made with aspiration of cooling air. On the other hand the quantities of dimers, tetramers, pentamers and hexamers have decreased with aspiration of cooling air. The most pronounced change was at monomer, which increased from 7.5% (AP0) to 13.55% (AP100).

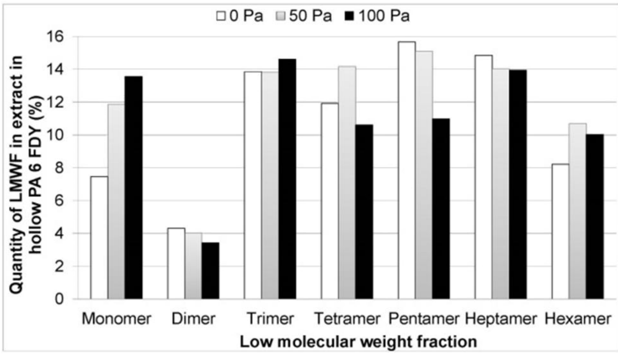

Figure 5 Influence of aspiration air pressure on a quantity of low molecular weight fraction (LMWF) of hollow PA 6 FDY

4 CONCLUSION

In the study was found out that aspiration of cooling air under the spinnerets which effectively prevents the monomer deposition on the spinnerets and on the spinning shaft walls, influenced also on the lower monomer evaporation from spinning jets. On the other hand aspiration of cooling air has a definite negative influence on the morphology of hollow filaments (incomplete forming hollows of filaments) and mechanical properties (increasing of breaking force, decreasing of breaking elongation, increasing of tensile force in dynamic thermal analysis). Changes of mechanical properties were small, but statistically proven. All these changes of yarn's properties originated from the changes in yarns supramolecular structure, because of decreasing of spinneret temperature.

5 REFERENCES

1. Reimschuessel H.: Polyamide fibers. In Handbook of fiber science and technology, Volume IV. Fiber chemistry, Edited by Menachem Lewin, Eli M. Pearce, New York, Basel, Marcel Dekker, 1985, pp. 74-81, Maxwell J. C.: A Treatise on Electricity and Magnetism, Oxford: Clarendon, 1892
2. Sbrolli W.: Nylon 6. In Man-made fibers. Science and technology, Volume 2, Edited by H.F. Mark, S.M. Atlas, E. Cernia, New York, London, Sydney, Interscience Publishers, 1968, pp. 232-239
3. McIntyre J.E.: Synthetic fibres: nylon, polyester, acrylic, polyolefin, Cambridge, Woodhead Publishing, 2005
4. Periyasamy, A.: Chapter 4. Production of manufactured fibers [online], Slide share [cited 6.7.2017], Available on: https://www.slideshare.net/abiramprince/production-of-manufactured-fibers

WARP YARN TENSION DURING FABRIC FORMATION

Volodymyr Shcherban', Gennadiy Melnyk, Marijna Sholudko and Valerij Kalashnyk

Kyiv National University of Technologies and Design, 2 Nemirovicha-Danchenko Str. Kyiv, 01011, Ukraine
melnik2000@ukr.net

Abstract: *Tension of warp yarn, before it enters the weaving area, is the value which determines intensity of the weaving process and cloth structure. Increased value of warp yarn tension, before entering the fabric formation area, causes a spiralling number of breaks, and decreased value does not allow to ensure shed cleanliness. Tension of warp yarns, before they enter the fabric formation area, includes input tension and additional tension, arising by virtue of frictional forces between warp yarns and surfaces of guiding and working components of cylinder form or one close to it.*

This work represents experimental research in interaction between different in itself natural warp yarns and cylindrical surfaces imitating separating rod of yarn break detector as well as heddle eye for automatic shuttleless pneumatic rapier looms. As a result of the experiment regression dependences were obtained between warp yarns and value of the cylinder radius, as well as between contact angle and warp yarn tension just before the guide. Consistent application of the data of regression dependences allows to determine warp yarns tension before they enter the fabric formation area for different kinds of natural raw material of warp yarns for wide range of looms.

Keywords: *tension, warp yarns, weaving area, contact angle, curvature radius.*

1 INTRODUCTION

Tension of warp yarn, before it enters fabric weaving area, is a value determining intensity of the weaving process and cloth structure [1, 3-4, 7-8]. Tension of warp yarns, before they enter fabric weaving area, comprises both input tension and additional tension, which arises by virtue of frictional forces between warp yarns and surfaces of guiding and working components having cylinder form or one close to it [2, 4, 8]. Figures 1a and 1b represent guiding and working components of the loom the warp yarn interacts with when entering the weaving area.

a b

Figure 1 Guides and working components of the loom: a - tension rail; b - heddle eyes

Curvature radius of the provided surfaces, which have cylinder form or one close to it, both significantly longer as compared to radius of the cross-section a warp yarn and commensurate with it [2, 4]. Such type of interaction also occurs in implementation of similar technological processes [5, 6]. Simulation of the warp yarn processing using a loom involves study of interaction between warp yarns and cylindrical surfaces. These surfaces are dummies for surface of separating rods, which are components of the yarn break detector, as well as heddle eyes for automatic shuttleless pneumatic rapier looms [1-3, 7]. When drafting the plan of the experiment, the direction connected to slip of rubbing surfaces [9], speed of yarn or guiding surface [10, 14] and radius of the curvature of cylindrical surface [11, 13] should be taken into account. Keeping in mind that spun yarn and multi-filaments are used as warp yarns, flexural rigidity can be ignored [3-4, 7-8, 12].

Figure 2 shows warp yarn threading system for a loom. It is divided into three areas for our purpose: I area – between warp beam and separating warp stop motion; II area – between tension rail and heddle frames; III area – between separating warp stop motion and fell of the cloth. Increase in intensity of warp yarn tension divided into areas represented by green, blue and red color. These colors have been used during modelling of response surfaces and plotting of warp yarn tension. Indexes for designation warp yarn tension, contact angles, curvature radius of the cylindrical surfaces shall correspond to areas' numbers.

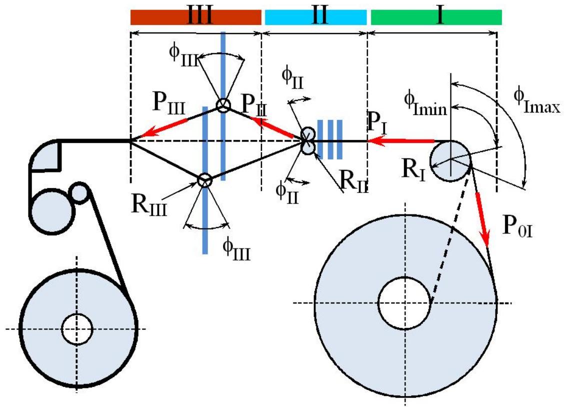

Figure 2 Warp yarn threading system for a loom

2 EXPERIMENT

Three types of yarn have been chosen for experiment.

Series A: carded cotton yarn 18.5 x 2 tex. It is used as warp yarns for spring-autumn fabric of tartan twill weave.

Series B: bleached flax of wet spun 41 tex, obtained from dressed flax. It is used as warp yarns to manufacture sindon.

Series C: wool 31.2 x 2 tex. It is used as warp yarns to manufacture pure-wool suit cloth of boston twill.

For each series A, B, and C to define joint impact of input tension of warp yarn P_0, radius of cylinder guide R and computed value of contact angle φ_P on output tension of the warp yarn P, the secondary orthogonal design was prepared and implemented for three factors [3, 7-8]. Standard form of regression equation shall be as follows

$$P = b_0 + b_1x_1 + b_2x_2 + b_3x_3 + b_{12}x_1x_2 + b_{13}x_1x_3 + b_{23}x_2x_3 + \\ + b_{11}x_1^2 + b_{22}x_2^2 + b_{33}x_3^2 \qquad (1)$$

The range of factors variability in equation (1) is determined by real conditions of yarns processing on looms. Threading line for warp yarn is divided into three areas: **I** is the area from warp yarn run-off point from beam to stop motion; **II** is the area from warp yarn entrance into stop motion to heddle frame; **III** is the area from warp yarn exit from stop motion to the fell of the cloth (Figure 2). Within the I area warp yarn interacts with tension rail. Within the II area warp yarn contacts separating stop motion rod. Within the III area warp yarn contacts heddle eye.

Factor x_1 is the value of the threading tension within I area before tension rail for shuttle looms, shuttleless looms, and pneumatic rapier looms:

A - for carded cotton yarn P_{0I} = 20 cN;
B - for bleached flax of wet spun made P_{0I} = 25 cN;
C - for wool P_{0I} = 35 cN.

Factor x_2 - cylinder (tension rail) radius within I area for: shuttle looms R_I = 56 mm; shuttleless looms R_I = 63 mm; pneumatic rapier looms R_I = 32 mm.

Factor x_2 - cylinder (left separating rod in stop motion) radius within II area for: pneumatic rapier looms shuttle looms R_{II} = 9 mm; shuttleless looms R_{II} = 4 mm; pneumatic rapier looms R_{II} = 3 mm.

Factor x_2 - cylinder (heddle eye) radius within III area for: shuttle looms R_{III} = 1.1 mm; shuttleless looms R_{III} = 0.6 mm; pneumatic rapier looms R_{III} = 0.5 mm.

Factor x_3 - calculated value of the contact angle with cylinder (tension rail) within I area for: shuttle looms φ_{IP} = 60° with maximum beam diameter 600 mm and φ_{IP} = 110° with minimum beam diameter 146 mm; shuttleless looms φ_{IP} = 70° with maximum beam diameter 600 mm and φ_{IP} = 100° with minimum beam diameter 220 mm; pneumatic rapier looms φ_{IP} = 90° with maximum beam diameter 600 mm and φ_{IP} = 115° with minimum beam diameter 100 mm.

Factor x_3 - calculated value of the contact angle with cylinder (left separating rod in the stop motion) within II area for: shuttle looms φ_{IIP} = 75° with maximum shed opening and 0° with closed shed; shuttleless looms φ_{IIP} = 75° with maximum shed opening and 0° with closed shed; pneumatic rapier looms φ_{IIP} = 76° with maximum shed opening and 0° with closed shed.

Factor x_3 - calculated value of the contact angle with cylinder (heddle eye) within III area for: shuttle looms φ_{IIIP} = 29° with open shed and φ_{IIIP} = 0° with closed shed; shuttleless looms φ_{IIIP} = 22° with open shed and φ_{IIIP} = 0° with closed shed; pneumatic rapier looms φ_{IIIP} = 41° with open shed and φ_{IIIP} = 0° with closed shed.

At the first stage the tension within the I area after the tension rail is determined. Table 1 shows orthogonal matrix of the second order for three series A, B and C.

Table 1 Orthogonal matrix of the second order for three series A, B and C for zone I

No.	Factors							
	Input tension				Curvature radius		Contact angle	
	x_1	P_{0I} [cN]			x_2	R_I [mm]	x_3	φ_{IP} [°]
		A	B	C				
1	+1	25	35	45	+1	65	+1	120
2	-1	15	15	25	+1	65	+1	120
3	+1	25	35	45	-1	35	+1	120
4	-1	15	15	25	-1	35	+1	120
5	+1	25	35	45	+1	65	-1	100
6	-1	15	15	25	+1	65	-1	100
7	+1	25	35	45	-1	35	-1	100
8	-1	15	15	25	-1	35	-1	100
9	-1.215	14	14	23	0	50	0	110
10	+1.215	26	26	47	0	50	0	110
11	0	20	25	35	-1.215	32	0	110
12	0	20	25	35	+1.215	68	0	110
13	0	20	25	35	0	50	-1.215	98
14	0	20	25	35	0	50	+1.215	122
15	0	20	25	35	0	50	0	110

Connection between natural and encoded values for I area shall be as follows:

series A

$$x1 = \frac{P_{0I} - 20}{5}, \quad x2 = \frac{R_I - 50}{15}, \quad x3 = \frac{\varphi_{I\,P} - 110}{10}, \qquad (2)$$

series B

$$x1 = \frac{P_{0I} - 25}{10}, \quad x2 = \frac{R_I - 50}{15}, \quad x3 = \frac{\varphi_{I\,P} - 110}{10}, \qquad (3)$$

series C

$$x1 = \frac{P_{0I} - 35}{10}, \quad x2 = \frac{R_I - 50}{15}, \quad x3 = \frac{\varphi_{I\,P} - 110}{10}. \qquad (4)$$

At the second stage the tension within the I area after the left separating rod in stop motion is determined. As an input tension P_{0II} we shall take the output tension of the warp yarns after I area P_I. Table 2 shows orthogonal matrix of the second order for three series A, B and C.

Table 2 Orthogonal matrix of the second order for three series A, B and C for zone II

No.	Factors							
	Input tension				Curvature radius		Contact angle	
	x_1	P_{0II} [cN]			x_2	R_{II} [mm]	x_3	$\varphi_{II\,P}$ [°]
		A	B	C				
1	+1	36	48	60	+1	8	+1	80
2	-1	20	18	30	+1	8	+1	80
3	+1	36	48	60	-1	2	+1	80
4	-1	20	18	30	-1	2	+1	80
5	+1	36	48	60	+1	8	-1	10
6	-1	20	18	30	+1	8	-1	10
7	+1	36	48	60	-1	2	-1	10
8	-1	20	18	30	-1	2	-1	10
9	-1.215	18	15	27	0	5	0	45
10	+1.215	38	51	63	0	5	0	45
11	0	28	33	45	-1.215	1	0	45
12	0	28	33	45	+1.215	9	0	45
13	0	28	33	45	0	5	-1.215	3
14	0	28	33	45	0	5	+1.215	88
15	0	28	33	45	0	5	0	45

Connection between natural and encoded values for II area shall be as follows:

series A

$$x1 = \frac{P_{0II} - 28}{8}, \quad x2 = \frac{R_{II} - 5}{3}, \quad x3 = \frac{\varphi_{II\,P} - 45}{35}, \qquad (5)$$

series B

$$x1 = \frac{P_{0II} - 33}{15}, \quad x2 = \frac{R_{II} - 5}{3}, \quad x3 = \frac{\varphi_{II\,P} - 45}{35}, \qquad (6)$$

series C

$$x1 = \frac{P_{0II} - 45}{15}, \quad x2 = \frac{R_{II} - 5}{3}, \quad x3 = \frac{\varphi_{II\,P} - 45}{35}. \qquad (7)$$

At the third stage the tension within the III area after the heddle eye. As an input tension P_{0III} we shall take the output tension of the warp yarns after II area P_{II}.

Table 3 shows orthogonal matrix of the second order for three series A, B and C.

Table 3 Orthogonal matrix of the second order for three series A, B and C for zone III

No.	Factors							
	Input tension				Curvature radius		Contact angle	
	x_1	P_{0III} [cN]			x_2	R_{III} [mm]	x_3	$\varphi_{III\,P}$ [°]
		A	B	C				
1	+1	50	58	70	+1	1.4	+1	40
2	-1	20	18	30	+1	1.4	+1	40
3	+1	50	58	70	-1	0.6	+1	40
4	-1	20	18	30	-1	0.6	+1	40
5	+1	50	58	70	+1	1.4	-1	4
6	-1	20	18	30	+1	1.4	-1	4
7	+1	50	58	70	-1	0.6	-1	4
8	-1	20	18	30	-1	0.6	-1	4
9	-1.215	17	14	26	0	1	0	22
10	+1.215	53	62	74	0	1	0	22
11	0	35	38	50	-1.215	0.5	0	22
12	0	35	38	50	+1.215	1.5	0	22
13	0	35	38	50	0	1	-1.215	0
14	0	35	38	50	0	1	+1.215	44
15	0	35	38	50	0	1	0	22

Connection between natural and encoded values for II area shall be as follows:

series A

$$x1 = \frac{P_{0III} - 35}{15}, \quad x2 = \frac{R_{III} - 1}{0.4}, \quad x3 = \frac{\varphi_{III\,P} - 22}{18}, \qquad (8)$$

series B

$$x1 = \frac{P_{0III} - 38}{20}, \quad x2 = \frac{R_{III} - 1}{0.4}, \quad x3 = \frac{\varphi_{III\,P} - 22}{18}, \qquad (9)$$

series C

$$x1 = \frac{P_{0III} - 50}{20}, \quad x2 = \frac{R_{III} - 1}{0.4}, \quad x3 = \frac{\varphi_{III\,P} - 22}{18}. \qquad (10)$$

Figure 3 shows experimental setup, which includes 9 units. The first unit 1 is a device for threading and tension of warp yarn. In order to avoid ballooning, warp yarns 9 were wound on a cylindrical take-up which fed it into the measurement zone. Slack-side tension was created using cymbal tension device.

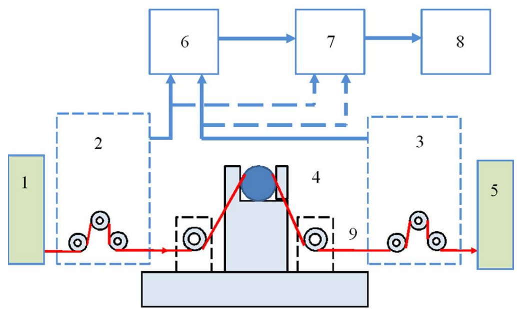

Figure 3 Scheme of the experimental setup:
1 - warp yarn threading unit; 2 - metering unit for warp yarn input tension; 3 - metering unit for warp yarn output tension; 4 - environment modelling unit; 5 - warp yarn take up unit; 6 - amplifier; 7 - analog to digital converter ADC; 8 - personal computer; 9 - warp yarn

The second 2 and third 3 units (Figure 3) are intended to measure input and output tension of the warp yarn 9. Based on the value of the input tension of the warp yarn 9 two types of measuring assembly were used in the work.

For tension range 50 cN to 500 cN the fixed tension meter for moving monofilament MT 320M by METROTEKS company with movable outer rollers was used (Figure 4): range of the motion speed for warp yarn 9: 1-6000 m/min, metering accuracy 2%, velocity 0.1 sec, analog output 0-1 B. For tension range 20 cN to 50 cN the second type of the measuring assembly was used. The one that includes two rollers mounted in bearing parts on the fixed axles. The third roller mounted on the cantilever fitted beam in such a way that inner bearing ring was fixed on the beam itself, and outer bearing ring stiffened to roller that interacts with yarn. Friction forces in bearings can be ignored. A warp yarn was supplied to the pulleys in such a manner that slack-side and tight-side appeared to be on the sides of an isosceles triangle. The middle bar flexed under the warp yarn tension, and that led to changing resistance of the tension meter. This has been registered at the corresponding channel of the amplifier 8АНЧ-7М [1, 2].

Crosswise and lengthwise dimensions of the beam have been chosen to make its natural oscillation frequency equal to 1400 Hz. This frequency is many times higher than the frequency of the highest component of tension.

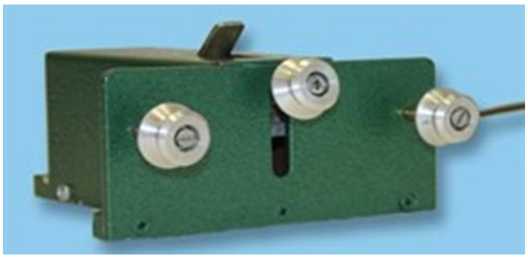

Figure 4 Input and output warp yarn tension metering unit MT 320M

Figure 5 shows the fourth main unit 4 of the experimental setup. It is intended for simulation of interaction conditions between warp yarn 9 and cylinder guides [1, 2]. Two slider pairs, on which aluminium rollers are fixed in rotation bearings, are installed on the foundation in the horizontal grooves. The position of the slider pairs with respect to the central fixed bracket is changed by turning the two levers on the left and on the right. The central, fixed vertical bracket serves to secure the cylinder guides of different diameters, needles of knitting machine, heddles. The fastening is carried out by two screw pairs and clamping bars.

The warp yarn 9 speed was varied due to a fixed-ratio round belt transmission (the fifth unit in Figure 3). Driving pulley of the transmission is rotated by AC motor that was firmly fixed to the foundation of the main measurement system.

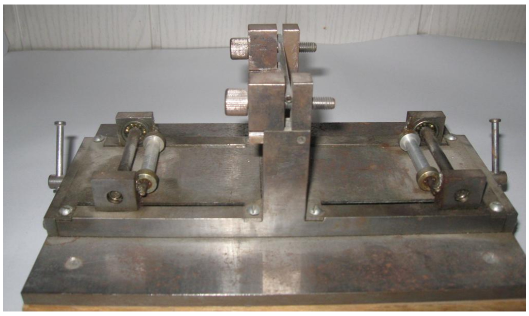

Figure 5 Unit for simulation of interaction conditions

Analog signals from the 3rd and 4th units measuring warp yarn tension (for the first type of the measurement assembly) or from the amplifier 6 (for the second type of the measurement assembly) is being received by analogue-to-digital converter ADC 7 (Figure 6), enabled as a multifunction board L-780M with signalling processor ADC 14 bit/400 kHz having 16 differential input analog and output digital channels, which is connected to the PCI-connector 8. It is possible to generate interrupts after filling a part of FIFO-buffers of ADC and DAC.

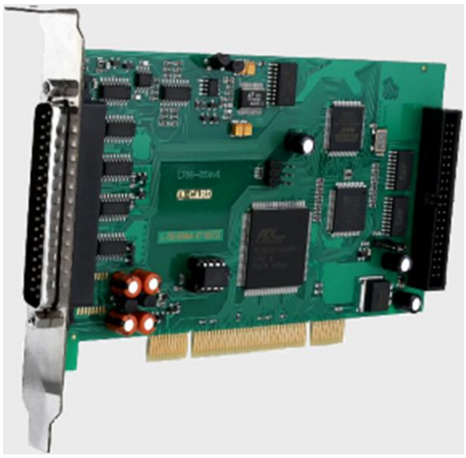

Figure 6 Analogue-to-digital converter ADC

3 RESULTS AND DISCUSSION

As a result of implementation of experimental designs (Tables 1-3) for each series A, B, and C, as well as for each area I, II, and III, 10 concurrent metering were conducted. Table 4 shows their average values.

Applying well-known methods to determine coefficient in the regression equation (1) for orthogonal design of the second order [1-2], taking into account dependences (2-10), the following regression dependences are obtained:

For area I:

series A

$$P_I = 0.02 + 0.91P_{0I} + 0.01R_I + 0.01P_{0I}\varphi_{IP}, \qquad (11)$$

series B

$$P_I = 211.44 + 1.91P_{0I} - 0.72R_I - 3.71\varphi_{IP} + \\ + 0.003P_{0I}\varphi_{IP} - 0.02P_{0I}^2 + 0.01R_I^2, \qquad (12)$$

series C

$$P_I = 0.37 + 0.92P_{0I} + 0.02R_I + 0.01\varphi_{IP} + 0.001P_{0I}R_I + \\ + 0.003P_{0I}\varphi_{IP} - 0.0002R_I^2, \qquad (13)$$

For area II:

series A

$$P_{II} = 1.28 + 0.99P_{0II} - 0.32R_{II} - 0.001\varphi_{IIP} + 0.003P_{0II}\varphi_{IIP} + \\ + 0.001R_{II}\varphi_{IIP} + 0.02R_{II}^2, \qquad (14)$$

series B

$$P_{II} = 1.68 + 0.98P_{0II} - 0.29R_{II} - 0.002\varphi_{IIP} + 0.002P_{0II}\varphi_{IIP} + \\ + 0.0012R_{II}\varphi_{IIP} + 0.018R_{II}^2, \qquad (15)$$

series C

$$P_{II} = 2.45 + 0.99P_{0II} - 0.44R_{II} - 0.002\varphi_{IIP} + 0.002P_{0II}\varphi_{IIP} + \\ + 0.002R_{II}\varphi_{IIP} + 0.03R_{II}^2, \qquad (16)$$

For area III:

series A

$$P_{III} = 2.86 + 1.08P_{0III} - 4.21R_{III} + 0.004\varphi_{IIIP} + 0.002P_{0III}\varphi_{IIIP} - \\ - 0.05P_{0III}R_{III} + 2.02R_{III}^2, \qquad (17)$$

series B

$$P_{III} = 2.66 + 1.06P_{0III} - 3.67R_{III} + 0.004\varphi_{IIIP} + 0.002P_{0III}\varphi_{IIIP} - \\ - 0.04P_{0III}R_{III} + 1.77R_{III}^2, \qquad (18)$$

series C

$$P_{III} = 3.96 + 1.07P_{0III} - 5.54R_{III} + 0.007\varphi_{IIIP} + 0.002P_{0III}\varphi_{IIIP} - \\ - 0.04P_{0III}R_{III} + 2.62R_{III}^2. \qquad (19)$$

Figure 7 shows response surfaces warp yarn tension dependence on tension and radius of the cylinder were obtained subject to fixed value of the calculated contact angle of the cylinder. This value corresponded to the centre of the experiment (Tables 1-3).

Adequacy of the obtained regression dependences was verified using SPSS software application for statistical processing of experimental findings [2]. Analysis of significance of the coefficient of the regression equations (11-19) allowed to discard insignificant ones [3, 7-8].

Obtained graphical dependences between warp yarn tension and cylinder radius are of interest, taking into account fixed value of the input tension and calculated contact angle of the cylinder. These values corresponded to the center of the experiment (Tables 1-3).

The analyse of graphical dependences provided existing bending points. These points have the minimum warp yarns tension within I, II, and III areas. This allows to raise a question of geometric sizing of guiding and working components of a loom.

Using regression dependences (11-19) we have found values of the warp yarn tension in the III area before fell of the cloth for different moments of the cloth components formation at the shuttleless looms. Values of the deflection of warp yarns, during shedding, battening and removal of cloth, was taken into account as a value of the input tension in I area.

Table 4 Average values of tension by zones I, II and III

Experiment No.	Output tension of warp yarn *Pi* [cN]								
	Cotton yarn 18.5 x 2 tex			Flax 41 tex			Wool 31 x 2 tex		
	i=I	*i*=II	*i*=III	*i*=I	*i*=II	*i*=III	*i*=I	*i*=II	*i*=III
1	36.12	44.77	56.71	48.06	57.72	64.45	60.08	70.48	77.03
2	21.92	25.06	22.84	20.99	21.92	20.18	33.91	35.61	33.27
3	35.67	44.79	58.75	47.47	57.60	66.32	59.18	70.32	79.55
4	21.64	25.08	23.71	20.71	21.88	20.81	33.38	35.53	34.44
5	33.97	37.20	52.12	45.59	49.35	60.05	57.26	61.56	72.65
6	20.58	20.69	20.89	19.85	18.54	18.69	32.24	30.83	31.23
7	33.63	37.76	54.23	45.13	49.96	62.05	56.56	62.42	75.35
8	20.36	21.02	21.79	19.63	18.79	19.36	31.82	31.29	32.49
9	19.75	20.52	18.81	18.98	16.82	15.28	30.29	29.84	28.27
10	36.22	43.03	58.25	34.81	56.67	67.08	60.84	69.12	79.85
11	27.78	32.62	40.17	33.22	37.51	42.63	45.17	50.61	56.20
12	28.17	31.81	38.05	33.69	36.80	40.78	45.95	49.54	53.45
13	27.00	28.51	36.62	32.45	33.51	39.47	44.34	45.71	52.20
14	29.05	35.59	40.59	34.58	40.47	43.05	46.95	53.73	56.08
15	28.00	31.81	38.56	33.49	36.78	41.22	45.62	49.51	54.11

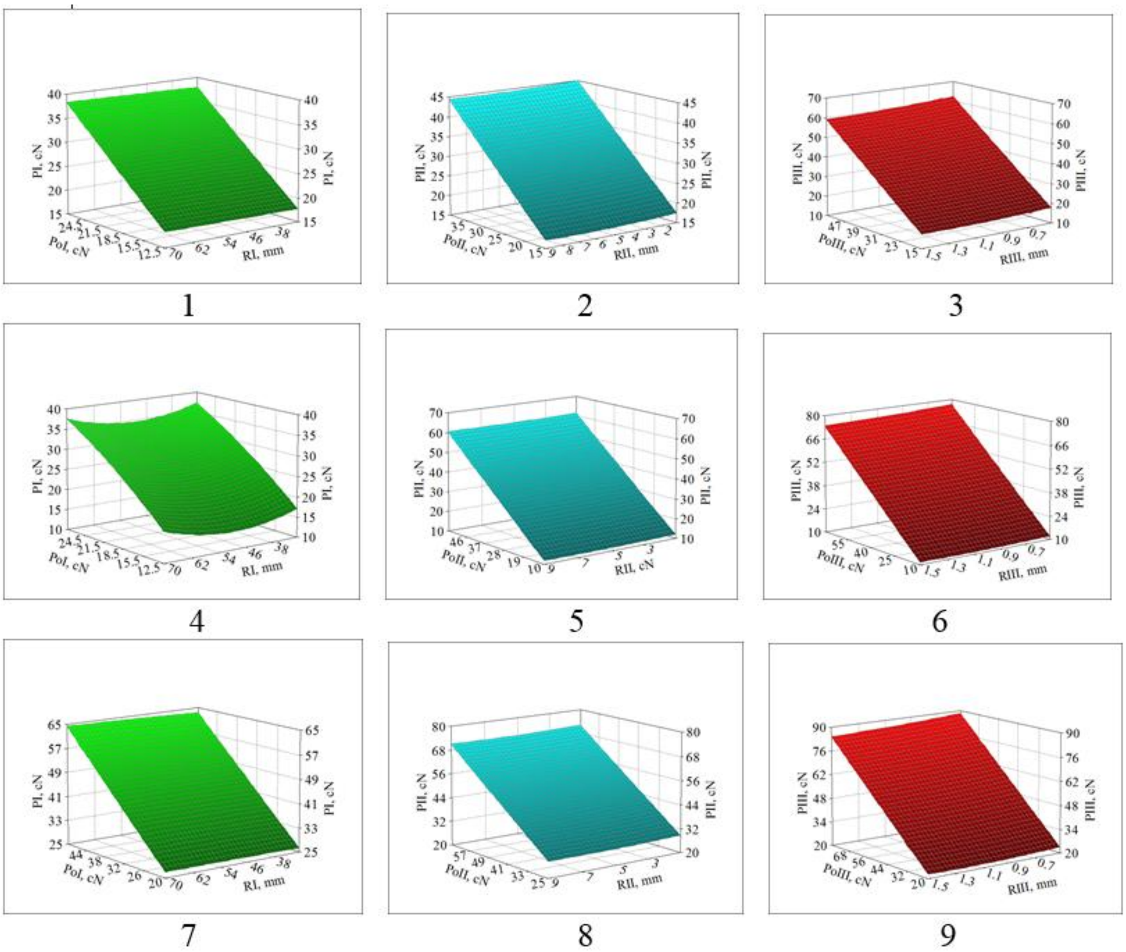

Figure 7 Curve based on warp yarn tension according to loom zones (■ - zone I, ■ - zone II, ■ - zone III): 1, 2, 3 - for series A; 4, 5, 6 - for series B, 7, 8, 9 - for series C

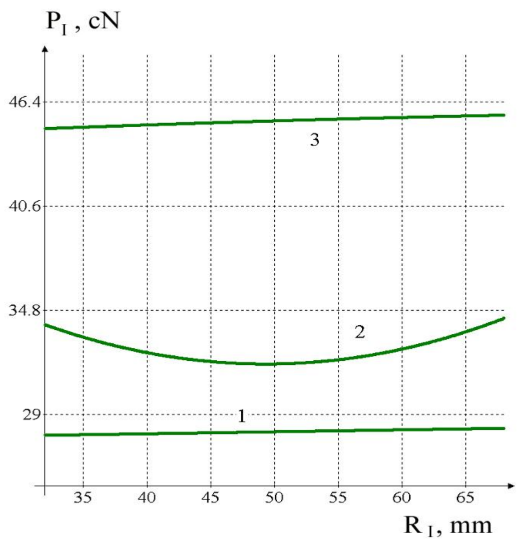

Figure 8 Dependence of the warp yarns tension after I area: 1 - for series A; 2 - for series B; 3 - for series C

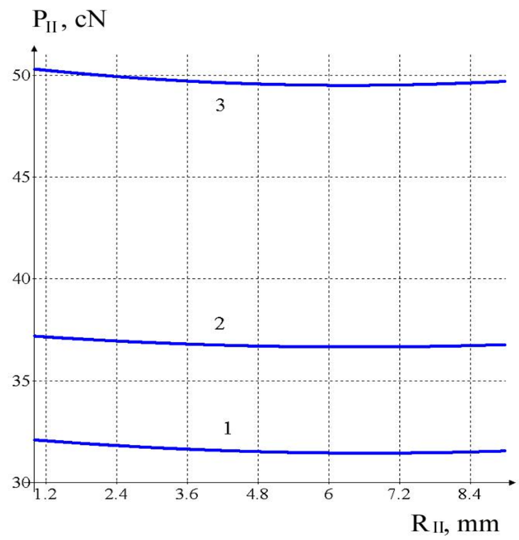

Figure 9 Dependence of the warp yarns tension after II area: 1 - for series A; 2 - for series B; 3 - for series C

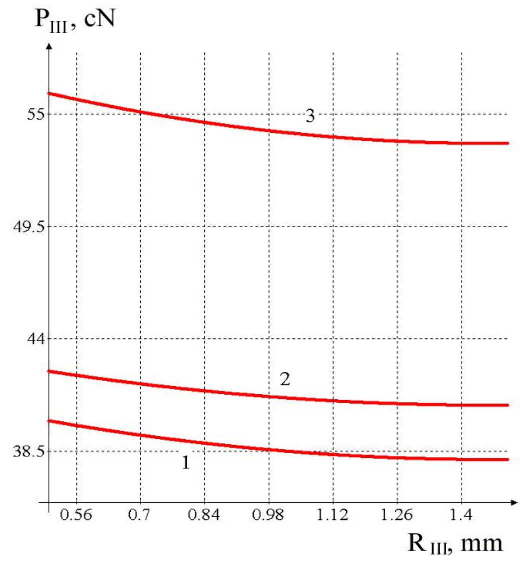

Figure 10 Dependence of the warp yarns tension after III area: 1 - for series A; 2 - for series B; 3 - for series C

From analyse of graphical dependences (Figure 11) allowed to determine that the toughest formation conditions will be for series B during manufacture of sindon; above mentioned is based on bleached flax of wet spun 41 tex. This can be explained by the high value of the rigidity coefficient of the strain and flexure of the warp yarns.

Obtained results can be applied for weaving development to determine the tension at a primary stage when forming fabric.

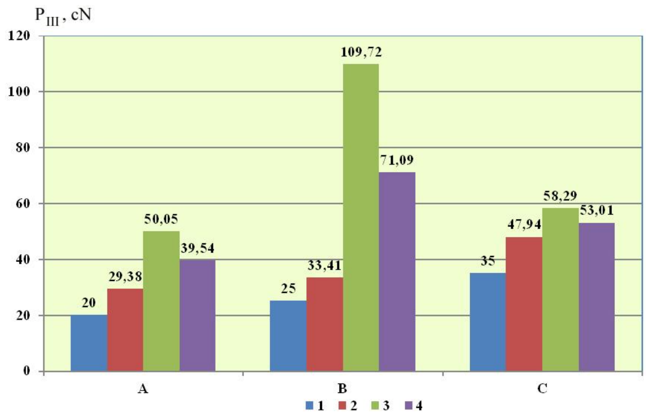

Figure 11 Warp yarns tension P_{III} histogram before fell when forming fabric: A - tartan (warp - carded cotton yarn 18.5x2 tex); B - sindon (warp - bleached flax of wet spun 41 tex); C - boston twill (warp - wool 31.2x2 tex); ■ - threading tension of warp yarns; ■ - warp yarns tension working with closed shed; ■ - tension of warp yarns with fully opened shed; ■ - tension of warp yarns during battening

4 CONCLUSIONS

Resulting from conducted integral experimental research of the interaction process between warp yarns and cylinder guiding surfaces - the latter simulate guiding surfaces and working components of looms - we obtained regression dependences, that allow to determine changes in tension of the warp yarns in the areas from warp beam to the area of fabric formation. Dependences were obtained taking into account types of feedstock processed and construction of the specific looms. Obtained results may be used to optimize weaving process flow in terms of optimizing construction peculiarities, reducing number of yarn breaks, and improving quality of the manufactured fabrics.

ACKNOWLEDGEMENT: We are really grateful to the management of the T-Style Ltd., housed by Rivne "Lyonokombinat" Factory, for supporting our experiments with feedstock and providing us with possibility to test results of the investigation in a production environment. This study could not be completed without LGraph2 program for registring, visualising and processing of the analog signals and technical support in processing of the experiments results provided by the L-Card Company.

5 REFERENCES

1. Shcherban' V.Yu., Khomiak O.N., Shcherban' Yu.Yu.: Thread mechanics, Library of official editions, Kyiv, 2002
2. Shcherban' V.Yu., Kolysko O.Z., Sholudo M.I., Kalashnyk V.Yu.: Algorithmic, software of mathematical components of CAD in industry, Education of Ukraine, Kyiv, 2017
3. Vasilchenko V.N., Shcherban' V.Yu.: Equations of ground warp thread equilibrium in the area of multilayer technical fabric formation, Izvestiya Vysshikh Uchebnykh Zavedenii. Technology of Textile Industry 5, 1986, pp. 44-47
4. Shcherban' V.Yu.: Determination of the geometrical characteristics of the axis form for thread moving along the deformable guiding surface, Izvestiya Vysshikh Uchebnykh Zavedenii. Technology of Textile Industry 6, 1990, pp. 52-55
5. Koo Y., Kim H.: Friction of cotton yarn in relation to fluff formation on circular knitting machines, Textile Research Journal 72, 2002, pp. 17-20
6. Vasconcelos F.B., Marcicano J.P.P., Sanches R.A.: Influence of yarn tension variations before the positive feed on the characteristics of knitted fabrics, Textile Research Journal 85, 2015, pp. 1864-1871
7. Shcherban' V.Yu.: Determination of the technological efforts during the beating process when forming multilayer technical fabric, Izvestiya Vysshikh Uchebnykh Zavedenii. Technology of Textile Industry 3, 1990, pp. 44-47
8. Shcherban' V.Yu.: Determining the technological forces during beating-up in the production of multilayer industrial fabrics, Izvestiya Vysshikh

Uchebnykh Zavedenii. Tekhnologiya Tekstil'noi Promyshlennosti 4, 1990, pp. 41-44

9. Kovar R.: Impact of directions on frictional properties of a knitted fabric, Vlákna a textil (Fibres and Textiles) 2, 2007, pp. 15-20
10. Sodomka L., Chrpová E.: Method of determination of euler friction coefficients of textiles, Vlákna a textil (Fibres and Textiles) 2-3, 2008, pp. 28-33
11. Donmez S., Marmarali A.: A Model for Predicting a Yarns Knittability, Textile Research Journal 74, 2004, pp. 1049-1054
12. Weber M.O., Ehrmann A.: Necessary modification of the Euler-Eytelwein formula for knitting machines, The Journal of The Textile Institute 103, 2012, pp. 687-690
13. Liu X., Chen N., Feng X.: Effect of Yarn Parameters on the Knittability of Glass Ply Yam, Fibres&Textiles in Eastern Europe 16, 2008, pp. 90-93
14. Hammersley M.J.: A Simple Yarn-friction tester for use with knitting yarns, The Journal of the Textile Institute 64, 1973, pp. 108-111

EXPERT SYSTEM TO SELECT THE FABRICS FOR TRANSFORMABLE GARMENTS

Oksana Zakharkevich[1], Tatyana Zhylenko[2], Yulia Koshevko[1], Svetlana Kuleshova[1], Olesya Ditkovska[1] and Galina Shvets[1]

[1]Khmelnitsky National University, Department of Technology and Design of Garments, Institytska str. 11, 29016 Khmelnitskyi, Ukraine
[2]Sumy State University, Department of Mathematical Analysis and Optimization Methods, Rymskogo-Korsakova str. 2, 40007Sumy, Ukraine
zbir_vukladach@ukr.net; t.zhylenko@phe.sumdu.edu.ua; juliakoshevko@gmail.com; kuleshova_lana@ukr.net; o.ditkovska@gmail.com; galyamet@ukr.net

Abstract: *The aim of this study is to develop a prototype of the expert system of the fabrics selection to design transformable clothing with a required level of quality. Based on the final values of the factors the lists of fabrics' properties were formed for any given combinations of garment types. Roughness was selected as a preferable parameter to evaluate the smoothness of the fabric in comparison with the friction coefficient. The ranges of the roughness characteristics for the groups of fabrics were obtained and summarised. Multifractal analysis of the roughness characteristics was performed. Recommended ranges of fabrics properties for transformable garments are obtained as intersections of the uncountable sets, which determine the value ranges of specific parameters of the main fabric properties. As a result of research the expert system knowledge base for solving the subtasks of fabrics selection for the transformable garments in the shell 'Rapana' has been developed. The prototype provides a dialogue with the user as a series of questions and answers of system's user. Thus, the necessary conditions for the further development of artificial intelligence techniques in the design of clothing were created.*

Keywords: *fabric, roughness, multifractal analysis, expert system*

1 INTRODUCTION

Today, fashion industry is facing a huge challenge towards sustainability because fast fashion is dominating the mass market. Fast fashion and consumers' purchasing format are closely linked to each other [1]. The life cycles of fashion items are shortened and the items are being replaced within a very short period to fulfil consumers' needs. Transformable fashion is one of the appropriate alternatives to reduce consumption and reinforce consumers to engage in sustainable lifestyle [2]. The traditional wardrobe is similar in basic functionality and no longer sustained social and consumer needs. It results in the growing need for transformable fashion.

The ability to change its function makes transformable clothes very useful when life conditions are changing as fast as nowadays [3]. These clothes can be worn for longer periods of time and on various occasions, thus minimizing waste generation in two ways by reducing the consumer's need to purchase additional garments, and by decreasing materials consumption in the fashion industry.

2 ANALYSIS OF PUBLISHED DATA AND STATING THE PROBLEM

There is much different information about the appearance of the transformable clothing in literature [2-4], fashion shows, online shops, fashion magazines, online fashion reviews, patents databases, etc. Many researchers investigate the principles of transformation in the clothing design [5].

Transformable fashion or convertible fashion can be defined as a garment that can be comfortably worn in multiple ways. It can be transformed into another shape and able to transform back to the original shape by altering its components. Transformable garments belong to the chains of transformations which usually include at least two different types of garments. Each of them must be made of different fashion fabrics and, besides that, they must meet different quality requirements.

A reversible garment is a type of transformable fashion as well. A reversible garment is a garment that can be worn at least in two different ways. There is no true "inside out" to the reversible garment, since either way, it gives a fashionable appearance. Therefore, each side must have some lining properties. Lining is an inner layer of a fabric, fur, or other material that provides a neat finish; conceals seam allowances, interfacing, and construction details; and allows a garment to slip on and off easily.

High saturation of information environment and the risk of making wrong decisions increase the relevance of information technology as a means to support decision-making [6]. One way to address the informal or weakly formalized problems is the use of artificial intelligence methods and the creation of expert systems (ES).

Nowadays, scientists in the world successfully implement elements of artificial intelligence and the ES at various stages of designing clothes. Among them are expert systems for selection of clothes style according to the constitution features of consumers [7], for the choice of clothes to form a harmonious image of individual consumers [8], to assess the quality of design clothes drawings [9] and for the formation of industrial clothing range [10]. Some of them are aimed for the rapid change in design of women's outerwear [11], for the choice of clothes models based on the assessment of consumers' emotional impressions using the methodology of Kansei Engineering [6]. Development and implementation of interactive systems to select ready-made clothes via the Internet are shown in [12]. Development of ES for the design of special and corporate clothes is presented in [13].

However, none of them considers issues of designing the transformable clothing or selection of fabrics for such garments while usually the chosen fashion fabric defines the quality of clothes.

The aim of this study is to develop a prototype of the expert system for the fabrics selection to design transformable clothing with a required level of quality, which might be achieved by proper fabrics selection.

3 MATERIALS AND METHODS

Recommended ranges of fashion fabrics properties for transformable garments (or garments of the transformational chain) are to be obtained as intersections of the uncountable sets which determine the value ranges of specific parameters of the main fabric properties of the different end uses. If the garment is reversible, then one of the sets reflects the properties of the lining [3].

3.1 Input Data

The following Table 1 gives a summary of all weighting factors for the fabrics of different end uses. Types of garments, which compose typical chains of transformations, determine a number of groups of fabrics in the Table 1 (suit fabrics, raincoat fabrics, coat fabrics, and lining). The weighting factors of lining fabrics' properties were defined on the preliminary stage of the current research.

3.2 Listing the main properties of the fashion fabrics

In the cases when transformable clothing contains more than one garment type, the weighting factors of the main fabrics properties might be computed as arithmetical means of the weighting factors, which are assigned to the fabrics related to the garment types. Based on the final values of the factors the lists of properties were formed for any given combinations of garment types (Table 2).

Values of properties were selected out of the standards with general specifications for the outerwear, lining fabrics, woolen fabrics, semiwoolen fabrics, cotton and mixed fabrics, linen fabrics, waterproof and jacket fabrics, fabrics for waterproofs, and for the fabrics for dresses.

Table 1 Weighting factors of the fabrics properties

Properties	Code	Suit	Jacket	Coat	Lining
Wrinkle resistance [%]	X_1	0.20	0.16	0.05	–
Pilling [pills/cm^2]	X_2	0.15	–	–	–
The number of cycles of abrasion [cycle]	X_3	0.15	0.06	0.25	–
Dimensional stability (shrinkage) [%]	X_4	0.14	0.15	0.05	–
Air permeability [dm^3/(cm^2·s)]	X_5	0.12	–	0.10	0.19
Elasticity: residual strain [%]	X_6	0.12	–	0.12	–
Stiffness [µN·cm^2]	X_7	0.12	–	0.08	–
Water resistance [mm H_2O]	X_8	–	0.24	–	–
Water permeability [g/(m^2·s)]	X_{10}	–	0.22	0.12	–
Thermal resistance [(m^2·K)/W]	X_{11}	–	0.11	0.20	–
Colour fastness [point]	X_{12}	–	0.06	–	0.11
Bursting strength [daN]	X_{13}	–	–	0.03	–
Sewed seam slippage (yarn slippage) [daN]	X_{14}	–	–	–	0.11
Smoothness	X_{15}	–	–	–	0.36
Permeability of water vapour [g/(m^2·hr)]	X_{16}	–	–	–	0.11
Hygroscopicity [%]	X_{17}	–	–	–	0.12

Table 2 Lists of the fabrics properties of different end uses

End use of fabric	Garments types	Number	Revers	Main properties
Suit	Suit jacket	1	–	$X_1, X_2, X_3, X_4, X_5, X_6, X_7$
Raincoat	Jacket	1	–	$X_1, X_3, X_4, X_8, X_9, X_{10}, X_{11}$
Coat	Coat	1	–	$X_1, X_3, X_4, X_5, X_6, X_7, X_9, X_{10}, X_{12}$
Raincoat	Raincoat	1	–	$X_1, X_3, X_4, X_8, X_9, X_{10}, X_{11}$
Suit and raincoat	Suit jacket, jacket	2	–	X_1, X_3, X_4, X_8, X_9
Suit and raincoat	Suit jacket, raincoat	2	–	X_1, X_3, X_4, X_8, X_9
Suit and raincoat	Suit jacket, jacket, raincoat	3	–	X_1, X_3, X_4, X_8, X_9
Suit and coat	Suit jacket, coat	2	–	$X_1, X_3, X_5, X_6, X_7, X_{10}$
Raincoat and coat	Raincoat, coat	2	–	$X_1, X_3, X_4, X_8, X_9, X_{10}$
Raincoat and coat	Jacket, coat	2	–	$X_1, X_3, X_4, X_8, X_9, X_{10}$
Raincoat and coat	Raincoat, jacket, coat	3	–	$X_1, X_3, X_4, X_8, X_9, X_{10}$
Suit, raincoat and coat	Suit jacket, raincoat, coat	3	–	$X_1, X_3, X_4, X_9, X_{10}$
Suit, raincoat and coat	Suit jacket, jacket, coat	3	–	$X_1, X_3, X_4, X_9, X_{10}$
Suit, raincoat and coat	Suit jacket, jacket, raincoat, coat	4	–	$X_1, X_3, X_4, X_9, X_{10}$
Suit and linings	Suit jacket	1	+	X_1, X_5, X_{14}
Raincoat and linings	Raincoat	1	+	$X_5, X_8, X_9, X_{11}, X_{14}$
Raincoat and linings	Jacket	1	+	$X_5, X_8, X_9, X_{11}, X_{14}$
Raincoat and linings	Raincoat, jacket	2	+	$X_5, X_8, X_9, X_{11}, X_{14}$
Coat and linings	Coat	1	+	X_3, X_5, X_{10}, X_{14}
Suit, raincoat and linings	Suit jacket, jacket	2	+	$X_1, X_4, X_5, X_{11}, X_{14}$
Suit, raincoat and linings	Suit jacket, raincoat	2	+	$X_1, X_4, X_5, X_{11}, X_{14}$
Suit, raincoat and linings	Suit jacket, raincoat, jacket	3	+	$X_1, X_4, X_5, X_{11}, X_{14}$
Suit, coat and linings	Suit jacket, coat	2	+	X_3, X_5, X_{14}
Raincoat, coat and linings	Raincoat, coat	2	+	$X_3, X_5, X_9, X_{10}, X_{11}, X_{14}$
Raincoat, coat and linings	Jacket, coat	2	+	$X_3, X_5, X_9, X_{10}, X_{11}, X_{14}$
Raincoat, coat and linings	Raincoat, jacket, coat	3	+	$X_3, X_5, X_9, X_{10}, X_{11}, X_{14}$
Suit, raincoat, coat and linings	Suit jacket, raincoat, coat	3	+	$X_1, X_3, X_5, X_{11}, X_{14}$
Suit, raincoat, coat and linings	Suit jacket, jacket, coat	3	+	$X_1, X_3, X_5, X_{11}, X_{14}$
Suit, raincoat, coat and linings	Suit jacket, jacket, raincoat, coat	4	+	$X_1, X_3, X_5, X_{11}, X_{14}$

4 EXPERIMENTAL PART

According to the information in the Table 2, the most important property of fabric for the reversible garment is its smoothness. Such a property is usually evaluated by the friction coefficient. However, recently more and more often frictional properties of the fabrics are evaluated by roughness characteristics [14-16]. The exact values of them are constant parameters, while the friction coefficient depends on conditions of the measurement. Therefore, roughness is a preferable parameter to evaluate the smoothness of the fashion fabric in comparison with the coefficient of friction.

4.1 Fabrics Roughness

In this way, empirical measurements of the linings roughness will determine a range of fabrics, which might be used for reversible garments. Thus, according to method [16], two parameters (R_a, R_{max}) were used to reflect fabric roughness: R_a – arithmetical mean deviation of the profile [µm]; R_{max} – maximum height of the profile [µm]. The script and scanned images of tissue samples were used in 3D computer graphics software (Rhinoceros) to evaluate the fabrics' roughness [16]. The minimal numbers of measurements were calculated based on the results of the preliminary research: 58 – for the lining, 122 – for the coat fabrics, 73 – for the suit fabrics, and 50 – for the jacket fabrics. Hence, the ranges of the roughness characteristics for the abovementioned groups of fabrics were obtained and summarised in the Table 3.

Table 3 Fabric roughness characteristics

Roughness parameter	R_a [µm]	R_{max} [µm]
Suit and lining	3.2-191.9	10-645
Coat and lining	25-191.9	91-645
Raincoat and lining	1.9-133.5	6-396
Suit, raincoat and lining	3.2-133.5	10-396
Suit, coat and lining	25-191.9	91-645
Raincoat, coat and lining	25-133.5	91-396
Suit, raincoat, coat and lining	25-133.5	91-396

4.2 Multifractal Analysis

Nowadays, scientists of the world successfully implement fractal analysis in clothing design [17]. We suppose that fabrics roughness might be investigated by using multifractal analysis as well.

If we consider a fabric fragment to be a self-similar object and a section profile – a multifractal and regard the series of values of coordinates on the profile as a multifractal set, MFFA can be applied. Recently, we developed a method of MFFA, giving a description of the time series within the framework of a simple numerical procedure [18]. Subsequent optimization of method of MFFA allowed one to carry out the multidimensional analysis of multifractal multiplicities [19-25]. Following [22], we represent a self-athena surface by two-dimensional array $X\ (i,j)$ where the discrete arguments i, j run the values i=1, 2, …, M and j=1, 2, …, N. Then the investigated surface is divided into Ms×Ns nonoverlapping square segments of s×s sizes, where the numbers Ms=[M/s] and Ns=[N/s] represent an integer part obtained after dividing of interval of changing arguments i, j into the segments. Noting the importance of the investigated function in each of its by indices v, w, we present it by the sequence $Xvw(i;j)=X(l_1+i;l_2+j)$, where the arguments $1 \le i$, $j \le s$ are changed in the segment, which is defined by numbers $l_1 = (v\text{-}1)s$ and $l_2 = (w\text{-}1)s$. Then for each segment, we calculate the cumulative sum:

$$u_{vw}(i;j)=\sum_{k_1=1}^{i}\sum_{k_2=1}^{j}X_{vw}(k_1;k_2) \tag{1}$$

where $1 \le l$ and $j \le s$.

From the geometric point of view the dependence $u_{vw}(i;j)$ determines the fractal surface. Like the one-dimensional time series, irregular dependence $u_{vw}(i;j)$ should be measured from the smooth surface $\tilde{u}_{vw}(i;j)$, which takes into account the trend in the changing of original function $u_{vw}(i;j)$ and is called a trend.

$$\widetilde{u}_{vw}(i;j)=ai+bj+c \tag{2}$$

where the parameters a, b, c are determined by the method of least squares.

In the trend interpolation one can use more advanced functions $\tilde{u}_{vw}(i;j)$, however it only slightly improves the accuracy due to the significant spending of computer time. Accounting the trend leads to residual matrix:

$$\widetilde{u}_{vw}(i;j)=u_{vw}(i;j)-\widetilde{u}_{vw}(i;j) \tag{3}$$

~ the use of which provides a specific dispersion of segment:

$$F^2(v;w;s)=\frac{1}{s^2}\sum_{i=1}^{s}\sum_{j=1}^{s}\varepsilon_{vw}^2(i;j) \tag{4}$$

Averaging over all segments leads to total dispersion:

$$F_q(s)=\left\{\frac{1}{M_sN_s}\sum_{v=1}^{M_s}\sum_{w=1}^{N_s}\left[F(v;w;s)\right]^q\right\}^{1/q} \tag{5}$$

which is deformed by parameter q the change of which is limited by the real values. According to (5), the negative values q amplify the contribution of segments corresponding to small fluctuations and positive ones give out large values $F(v; w; s)$. If $q=0$ the definition (5) should be replaced by:

$$F_0(s)=exp\left\{\frac{1}{M_sN_s}\sum_{v=1}^{M_s}\sum_{w=1}^{N_s}ln\left[F(v;w;s)\right]\right\} \tag{6}$$

To obtain statistically reliable data, one should change the value s from $s_{min}\approx 6$ to $s_{max}\approx min(M,N)/4$. For self-similar sets, it leads to the scaling ratio:

$$F_q(s)\sim s^{h(q)} \tag{7}$$

where $h(q)$ is a generic index of Hearst.

In the double logarithmic coordinates the dependence (7) is represented by a straight line whose slope gives the rate $h(q)$ for diverse values of parameter q. The mass index can be found from the dependency $h(q)$:

$$\tau(q)=qh(q)-D \tag{8}$$

where D is the topological dimension of the space containing the investigation object (for the surface D=2).

Multifractal spectrum $f(\alpha)$ is determined by the Legendre transform:

$$f(\alpha)=q\alpha-\tau(q),\ \alpha=d\tau/dq \tag{9}$$

Equations (8) and (9) provide a complete set of multifractal characteristics that describe the self-similar objects [19, 20].

The method of MFFA was applied to two types of fabrics: 1 – the lining and 2 – the coat fabric. The images of fabrics were taken with the digital microscope Sigeta Forward LCD (10-500x). The obtained digital image was cut with the tools for viewing and processing images to the size of 1 mm (using the scale). Then the bitmap image of the fabric profile was scaled to real size and construction lines were applied (Figure 1). In Figure 2 the dependence of variance on the scale s in double logarithmic coordinates for the abovementioned fabrics is demonstrated.

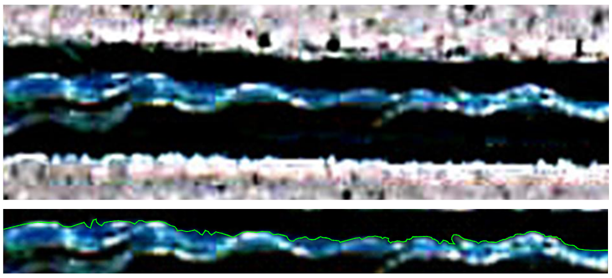

a

b

Figure 1 Arbitrary images of normal fabric sample profiles: lining (a) and coat fabric (b)

The given figures show that a linear type of dependence is evident, and it does not practically change for different values of q. If we pay attention to Figure 2, we can observe significant variance distinctions with the same value q=1 that vividly indicates the differences in fabric roughness.

The negative values of q were disregarded because the method of multifractal analysis is inapplicable when $q<0$. Further application of the method MFFA gave mass indices of the samples under investigation.

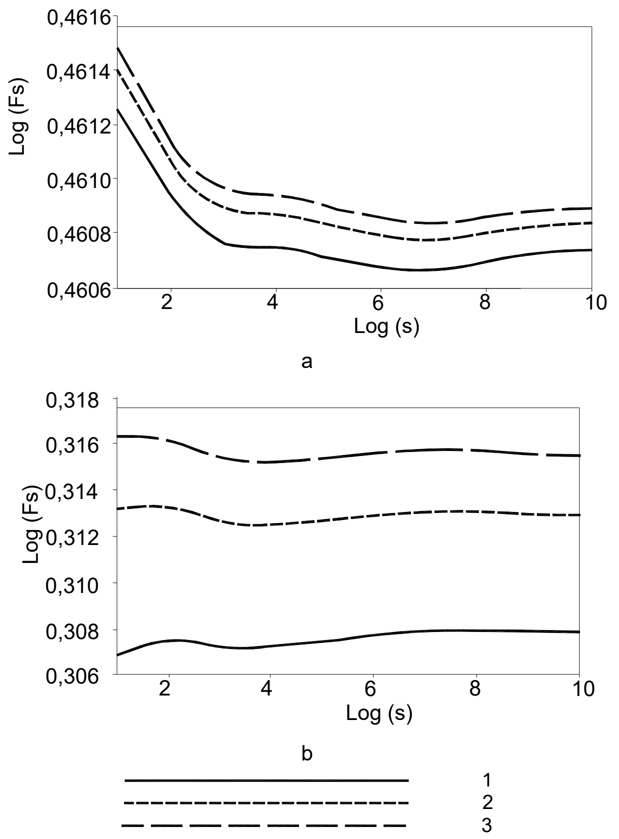

Figure 2 Dependence of dispersion on the scale s; Line 1 corresponds to q=1, Line 2 – q=10, Line 3 – q=15 for the lining (a) and for the coat fabric (b)

The linear dependence in Figures 2 and 3 demonstrates that the error of the method is minimal, i.e. the change of zoom has a little influence on the value of mass index. This proves the existence of a similar-like structure of the fabrics.

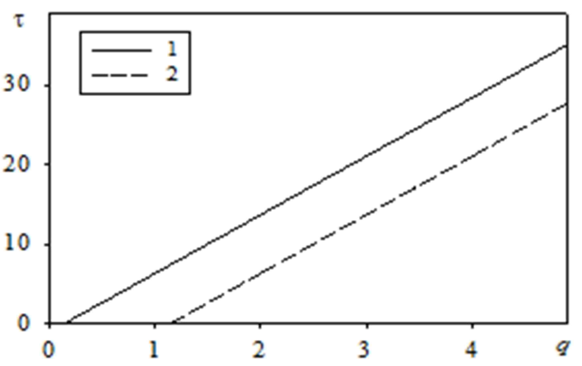

Figure 3 Dependence of mass index:

Line 1 – for the lining, Line 2 – for the coat fabric

5 EXPERT SYSTEM FOR THE FABRICS SELECTION

In order to develop a prototype of ES for subtasks of fabrics selection, we selected 'empty' shell of ES called 'Rapana' [26], which is distributed free of charge via the web-site (http://esrapana.narod.ru/) and is able to solve the problem of different industries. Complex 'Rapana' includes two components: 'Cognitograph' (software for the developers of knowledge base) and 'Expert' (application for users). Using 'Expert' does not require special training, because dialogue is conducted by natural language.

An ES, which is under development, is based on the rules called productions. A production system provides the mechanism necessary to execute productions in order to achieve some goal for the system. In the given situation, the goal is the confirmation of advisability to use the chosen fashion fabric to design the specific garment. Otherwise, the system is supposed to advise which ones of the fabrics properties are to be defined in order to make a well-founded decision. Productions consist of two parts: a sensory precondition ("IF" statements that are represented in the headers rows and columns) and an action ("THEN" statements that are represented in related cells).

The cells, which correspond to the preconditions that are advisable for the given situation, are highlighted in green (Figure 4). The cells highlighted in red represent the properties of fabric that must not be used for the specific garment. White color means that fabric with given properties might be used, but not highly recommended.

Suit and raincoat fabrics		X_1=1				X_1=0			
		X_3=1		X_3=0		X_3=1		X_3=0	
		X_4=1	X_4=0	X_4=1	X_4=0	X_4=1	X_4=0	X_4=1	X_4=0
X_8=1	X_9=1	1.000	0.781	0.841	0.622	0.727	0.508	0.568	0.349
	X_9=0	0.833	0.614	0.674	0.455	0.560	0.341	0.401	0.182
X_8=0	X_9=1	0.818	0.599	0.659	0.440	0.545	0.326	0.386	0.167
	X_9=0	0.651	0.432	0.492	0.273	0.378	0.159	0.219	0

Suit, coat and linings	X_3=1		X_3=0	
	X_5=1	X_5=0	X_5=1	X_5=0
X_{14}=1	1.000	0.651	0.768	0.419
X_{14}=0	0.581	0.232	0.349	0

Suit and linings	X_1=1		X_1=0	
	X_5=1	X_5=0	X_5=1	X_5=0
X_{14}=1	1.000	0.644	0.770	0.414
X_{14}=0	0.586	0.230	0.356	0

Figure 4 A fragment of the production system of the expert system that is developed

Examples of dialogues of the developed expert system, which represent consumer's answers to the system's questions and dialogue results, are shown in Figure 5. The way of decision-making for the given circumstances is presented in the Figure 6. Thus, the necessary conditions for the further development of artificial intelligence techniques in the design of clothing were created.

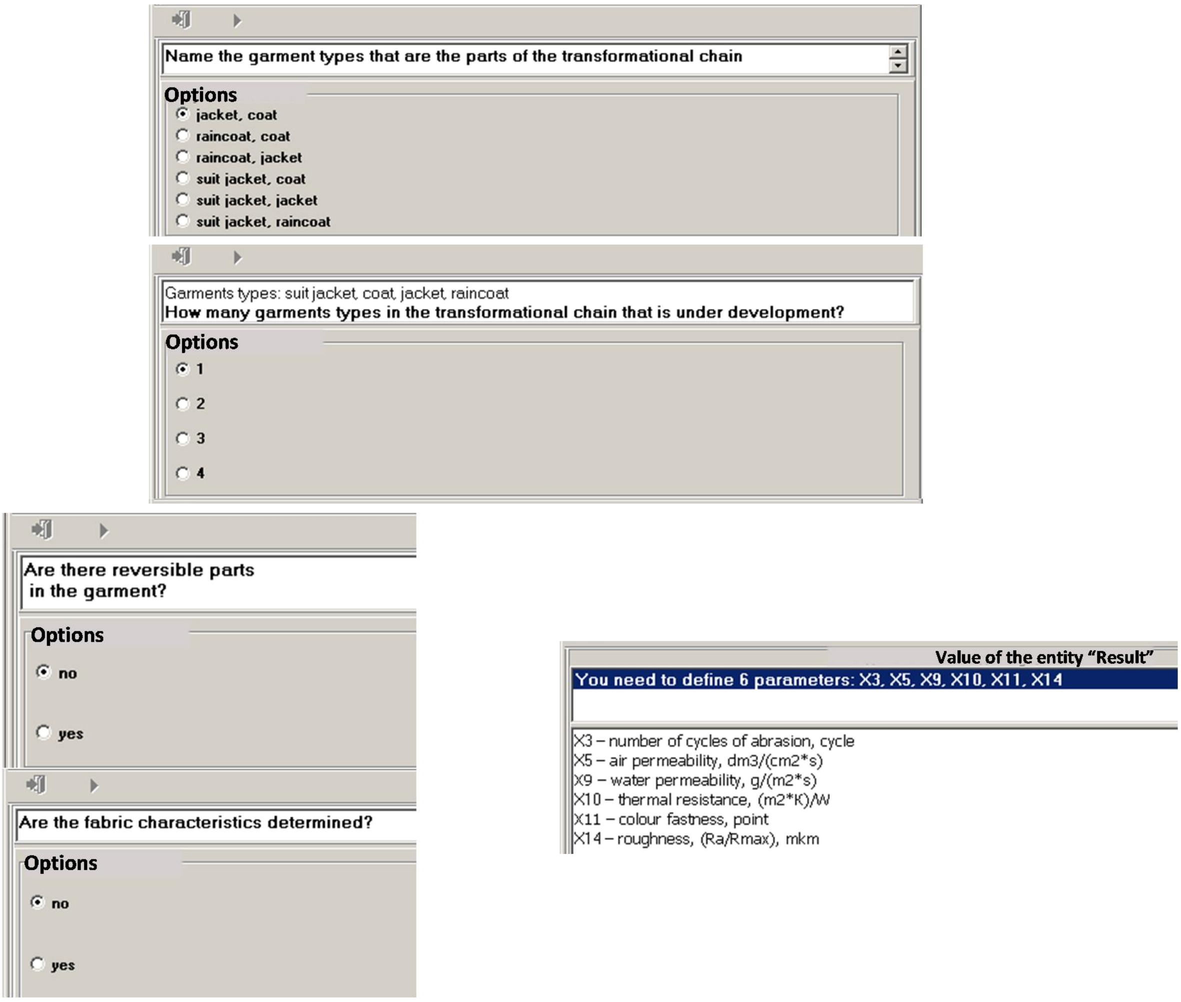

Figure 5 The expert system 'Fabric selection'

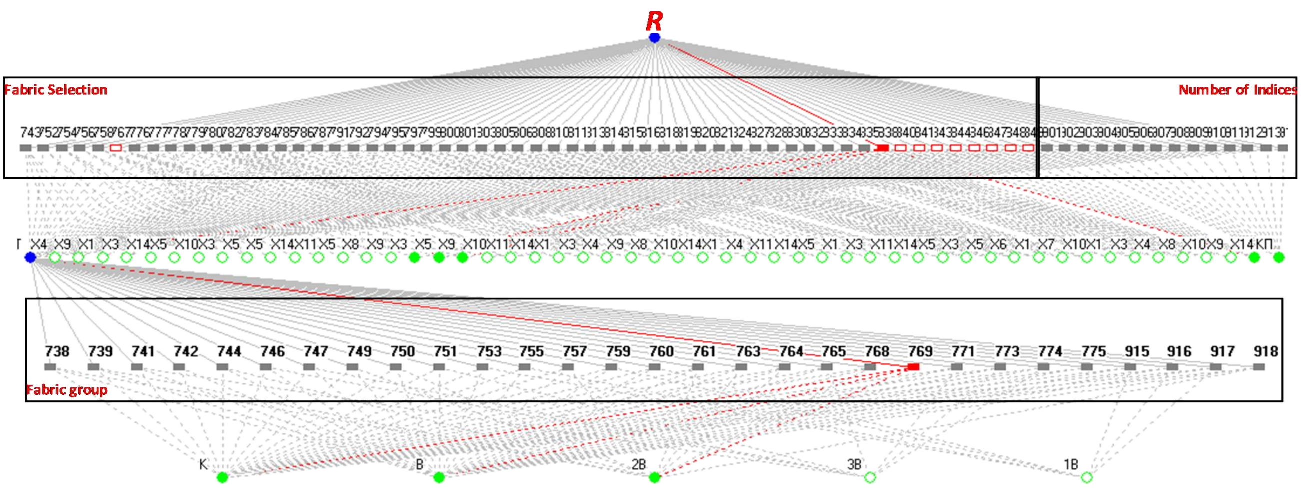

entity that has got the value as a result of the rule applied
entity that has not got a value and depends on the rule applied
entity that has not got a value and does not depend on the rule applied
K number of garments in the transformational chain
3B length of the transformational chain is 3
2B length of the transformational chain is 2
1B length of the transformational chain is 1
B type of the garment

entity that has got a value
applied rule
non applied rule
КП number of indices
R result
Г fabric group
X1-X14 indices of fabrics properties

Figure 6 The way of decision-making of the expert system 'Fabric selection'

The required level of quality of the transformable clothing under development is to be achieved through unmistakable choice of the fashion fabric that is well known as the core of any garment.

6 CONCLUSIONS

As a result of research the ES knowledge base for solving the subtasks of fabrics selection for the transformable garments in the shell 'Rapana' has been developed. The system can be used for the selection of the fabrics for the typical garments that will be designed separately, but successively one after another. Although it is no transformable garment, such chain of designing might be considered as a transformational chain. Therefore, the developed expert system might be considered as a part of the bigger one, which is aimed for the rapid change in apparel design at the specific enterprise.

7 REFERENCES

1. Chouprina N.V.: Characteristics of «fast fashion» concept in fashion industry, Vlakna a textil 21(1), 2014, pp. 31-36
2. Koo H.S., Dunne L., Bye E.: Design functions in transformable garments for sustainability, International Journal of Fashion Design, Technology and Education 7(1), 2014, pp. 10-20, DOI: 10.1080/17543266.2013.845250
3. Zakharkevich O.V., Kuleshova S.G., Shvets G.S.: Determination of fabrics properties for reversible garments, In: Proceedings of TEXTEH 7th International Conference "Creating the future of textiles", 22-23 October 2015, Bucharest, vol. 7. 2015, pp. 78-88
4. Tretiakova L.D., Ostapenko N.V., Kolosnichenko M.V., Pashkevich K.L., Avramenko T.V.: Designing of rational structure of range of insulating protective clothing on the basic of the principles of transformation, Vlakna a textil 23(4), 2016, pp. 27-35
5. Vovk Y.V., Slavinska A.L.: Working out unification of transformation type of the base design of the female skirt in the base design of trousers. Proceedings of higher education institutions, Textile industry Technology 6(354), 2014, pp. 84-89
6. Kuleshova S.G., Zakharkevich O.V., Koshevko J.V., Ditkovska O.A.: Development of expert system based on Kansei Engineering to support clothing design process, Vlakna a textil 24(3), 2017, pp. 30-41
7. Nada Y.A., Meshref H.: Analysis, design and implementation of intelligent expert system for clothes style selection, International Journal of Computer Applications 105(4), 2014, pp. 15-20, DOI: 10.5120/18364-9508
8. Akimochkina I.M., Krivoborodova E.U., Petushkova G.I.: Expert system for choosing preferred clothing to form harmonious appearance of individual consumers, Sewing industry 2, 2007, p. 55
9. Gnidenko A.V., Yudin L.P., Kuzmichev V.E.: Architecting of expert system of quality assessment of clothes' designs, Sewing Industry 5, 2007, pp. 52-54
10. Nigmatova F.W., Alimov H.A.: Formation of industrial range of garments based on expert system, Sewing Industry 2, 2009, pp. 27-28
11. Zakharkevich O.V., Pochuprin A.V.: Development of prototype of expert system for rapid change in production of women's outerwear, Easter-European Journal of Enterprise Technologies 2/2(68), 2014, pp. 50-55, https://doi.org/10.15587/1729-4061.2014.23327
12. Dong A.H., Shan D., Ruan Z., Zhou L.Y., Zuo F.: The design and implementation of an intelligent apparel recommend expert system, Mathematical Problems in Engineering, Article ID 343171, 2013, 8 pages. Retrieved from http://dx.doi.org/10.1155/2013/343171
13. Santos M.: An expert system to support clothing design process, ACM Digital Library, 2007, Retrieved from http://dl.acm.org/citation.cfm?id=1784393
14. Nazanin E., Mohammad A.T., Masoud L., Khosro M.: Modelling of surface roughness based on geometrical parameters of woven fabrics, Indian Journal of Fibre&Textile Research 42(1), 2017, pp. 43-50, http://nopr.niscair.res.in/handle/123456789/40678
15. Vildan Sülar, Eren Öner, Ayşe Okur.: Roughness and frictional properties of cotton and polyester woven fabrics, Indian Journal of Fibre&Textile Research 38(4), 2013, pp. 349-356, http://hdl.handle.net/123456789/24993
16. Zakharkevich O.V.: Method of determination fabrics roughness characteristics, Herald of Khmelnytskyi national university, Technical science 2, 2015, pp. 85-90
17. Kolosnichenko O.V., Baranova A.I., Prykhodko-Kononenko I.O.: Design of concordant forms of modern clothes on the basis of proportional correlations of sacred geometry, Vlakna a Textil, 24(3), 2017, pp. 10-14
18. Kantellhardt J.W., Zschiegner S.A., Koscienly-Bunde E., Havlin S., Bunde A., Stanley H.E.: Multifractal detrended fluctuation analysis of nonstationary time series, Physica A: Statistical Mechanics and its Applications 316(1-4), 2002, pp. 87-114, DOI: 10.1016/S0378-4371(02)01383-3
19. Feder J.: Fractals. Plenum press, New-York and London,1998
20. Halsey T.C., Jensen M.H., Kadanoff L.P., Procaccia I., Sraiman B.I.: Fractal measures and their singularities: the characterization of strange sets, Phys. Rev. A. 33(2), 1986, pp. 1141–1151, https://doi.org/10.1103/PhysRevA.33.1141
21. Chhabra A.B., Sreenivasan K.R.: Negative dimensions: Theory, computation, and experiment, Phys. Rev. A., 4(2)3, 1991, pp. 1114–1117, https://doi.org/10.1103/PhysRevA.43.1114
22. Gao-Feng Gu, Wei-Xing Zhou: Detrended fluctuation analysis for fractals and multifractals in higher dimensions, Phys. Rev. E. 74(6), 061104(8), 2006, https://doi.org/10.1103/PhysRevE.74.061104

23. Olemskoy A.I., Borisyuk V.N., Shuda I.A.: Multifractal analysis of time series (in Russian), Visnyk Of Sumy State University 2, 2008, pp. 70-81

24. Olemskoi A.I., Borisyuk V.N., Shuda I.A., Bagdasaryan A.A.: Multifractal analysis for the time series related to economic systems, J. Nano-Electron. Phys. 1(3), 2009, pp. 82-88

25. Olemskoy A.I., Perekrestov V.I., Shuda I.A., Borisyuk V.N., Mokrenko A.A.: Investigation of multifractal surfaces of condensates deposited by means of magnetron sputtering method (in Russian), Metallofizika i Noveishie Tekhnologi 31(11), 2009, pp. 1505-1518

26. Expert system "Rapana". Retrieved 11. 16. 2016 Available at: http://esrapana.narod.ru/

INSTRUCTIONS FOR AUTHORS

The journal ,,**Vlákna a textil**" (**Fibres and Textiles**) is the scientific and professional journal with a view to technology of fibres and textiles, with emphasis to chemical and natural fibres, processes of fibre spinning, finishing and dyeing, to fibrous and textile engineering and oriented polymer films. The original contributions and works of background researches, new physical-analytical methods and papers concerning the development of fibres, textiles and the marketing of these materials as well as review papers are published in the journal.

Manuscript

The original research papers are required to be written in English language with summary. The advertisements will be published in a language according to the mutual agreement.

The first page of the manuscript has to contain:

The title of the article (16 pt bold, capital letters, centred)

The full *first name* (s) and also *surnames* of all authors (11 pt, bold, centred).

The complete address of the working place of the authors, e-mail of authors (9 pt, italic, centred)

Abstract (9 pt, italic)

Key words (9 pt, italic)

The manuscript has to be written in A4 standard form, in **Arial, 10 pt**.

The text should be in ***double-column format*** *(width 8.1 cm)* ***in single line spacing***.

Page margins: up and down 2.5 cm; left and right 2.0 cm.

Do not number the pages and do not use footnotes. Do not use business letterhead.

Figures, tables, schemes and photos (centered) should be numbered by Arabic numerals and titled over the table and under the figure or picture.

Photos and schemes have to be sufficiently contrastive and insert in text as pictures.

Figures, tables, schemes and photos, please, send in separate file.

Mathematical formulae should be centred on line and numbered consecutively on the right margin.

Physical and technical properties have to be quantified in SI units, names and abbreviations of the chemical materials have to be stated according to the IUPAC standards.

References in the text have to be in square brackets and literature cited at the end of the text. References (9 pt), have to contain names of all authors.

[1] Surname N., Surname N.: Name of paper or Chapter, In Name of Book, Publisher, Place of Publication, YYYY, pp. xxx-yyy

[2] Surname N., Surname N.: Name of paper, Name of Journal Vol. (No.), YYYY, pp. xxx-yyy

[3] Surname N., Surname, N.: Title of conference paper, Proceedings of xxx xxx, conference location, Month and Year, Publisher, City, Surname N. (Ed.), YYYY, pp. xxx-yyy

[4] Surname N., Surname N.: Name of Paper, Available from http://www.exact-address-of-site, Accessed: YYYY-MM-DD

The final template of manuscript is available on **http://www.vat.ft.tul.cz**

Authors are kindly requested to deliver the paper (in Word form) to be published together with information about at least 3 recommended reviewers from institutions others than the parent (name, e-mail, institution, department) by e-mail: marcela.hricova@stuba.sk

After successful review procedure there is charged fee (article processing charge) of EUR 100. All articles after review process are freely available online and this fee helps to cover the costs of taking a manuscript and turning it into a finished article.

Address of the Editor Office:

Marcela Hricová

Faculty of Chemical and Food Technology,

Slovak University of Technology in Bratislava

Radlinskeho 9

812 37 Bratislava,

Slovakia